Adsorbent assisted drying of fine coal

ES Peters
21683883

Dissertation submitted in fulfilment of the requirements for the degree Master of Engineering in Chemical Engineering at the Potchefstroom Campus of the North-West University

Supervisor: Prof M Le Roux
Co-supervisor: Prof QP Campbell

November 2016

It all starts here ™

NORTH-WEST UNIVERSITY
YUNIBESITI YA BOKONE-BOPHIRIMA
NOORDWES-UNIVERSITEIT
®

OVERVIEW OF DOCUMENT

Student identification and information:

Full names and surname:	Elmarie Sunette Peters
Student number:	21683883
Highest qualification:	B.Eng Chemical
Curriculum code:	I103P
Completion year:	2014
Project title:	Adsorbent assisted drying of coal fines
Study level:	M.Eng Chemical
Completion year:	2016
Curriculum code:	I8711P
Institute:	North West University Potchefstroom Campus
Department:	Department of Chemical and Minerals Engineering Coal research group
Study leaders:	Professor M. Le Roux Professor Q.P. Campbell

DELIVERABLES FROM THIS STUDY

- **International conference (Presentation and published conference paper)**

XVIII International Coal Preparation Congress (ICPC 2016).-Saint-Petersburg, Russia. 28 June -01 July 2016.

Van Rensburg, M.J, Le Roux, M., Campbell, Q.P. & Peters, E.S. 2016. Drying of coal fines assisted by ceramic sorbents. XVII *International Coal Preparation Congress* (Published by Springer).

- **Local conference (Presentation)**

Mineral Processing Conference (Minproc 2015).-Cape Town, South Africa. 06 -07 August 2015.

Van Rensburg, M.J, Le Roux, M., Campbell, Q.P. & Peters, E.S. 2015. Drying of coal fines assisted by inorganic material as moisture sorbents.

- **Local conference (Presentation)**

Fossil Fuel Foundation Conference (FFF 2015).-Potchefstroom, South Africa. 25 November 2015.

Peters, E.S., Le Roux, M. & Campbell, Q.P. 2015. Adsorbent assisted drying of coal fines.

SOLEMN DECLARATION

I, **Elmarie Sunette Peters**, declare herewith that the dissertation entitled:

"Adsorbent assisted drying of fine coal"

which I hereby submit, in fulfilment of the requirements set for the degree Masters in Engineering, to the North-West University is my own individual work and has not previously been submitted to another institute.

Elmarie Sunette Peters

ACKNOWLEDGEMENTS

First, I would like to acknowledge my sincere gratitude to the North West University for providing me the opportunity to further my studies. More specifically, I would like to offer my heartfelt appreciation towards the following people for their influences and contributions towards the completion of my study.

- Foremost, I would like to thank my supervisor, Professor Marco Le Roux, for his guidance, support and encouragement throughout the course of my study. Without his vision, knowledge and mentorship, this study would not have been successful.
- Besides my supervisor, I would also like to express thanks to my co-supervisor, Professor Quentin Campbell, for his insight and assistance, especially during the challenging times.
- My mentor, Jana Van Rensburg, for her compassion, advice and devotion towards making this study a success.
- A special thanks to Doctor David Powell, for his assistance in refining this report as well as his words of encouragement when I really needed it.
- The laboratory and workshop personnel at the North West University, for their hard work and contributions towards the research section of my study.
- My dear mother, Gisela Peters, for her constant inspiration, devotion and love, which without I would not have been successful in my studies.
- My parents, Henk and Mitzi Peters, for their guidance, prayers and love, especially during the difficult times.
- A special thanks to my dear friends, Maans Marais, Derrick Goossens and Suzanne Roux, for their sincere understanding and support during my study.
- Finally, with the highest sense of gratitude, I offer my sincere thanks to my Creator and Protector, our God Almighty. To Him I bow down, humbly confiding in His mercy and through Jesus Christ, give thanks for countless great blessings on this path.

"My grace is sufficient for you, for My power is made perfect in weakness."

- 2 Corinthians 12:9 –

Dedicated to

Dewald Diedericks

Thank you for loving me...

For being my eyes, when I could not see...

This achievement would not have been possible without you.

November 2016

ABSTRACT

Coal fines are generated by the increase in mechanization on coal mines, and have the ability to retain large amounts of moisture due to its inherently large surface areas (Reddick *et al.*, 2007). The bulk of the moisture is retained by fine (-1mm+0.1mm) and ultra-fine (-0.15mm+0.1mm) coal fractions, which constitutes about 11% of the nominal product (SANEDI, 2011). This poses a problem for utility companies as moisture retention lowers the effective heating value of the coal. Coal fines are often dewatered, and combined with the coarse coal stream; however, as the coal fines rarely meet the desirable moisture levels, the quality of the final coal product stream suffers (Reddick, 2006).

Commonly, fine coal dewatered by the best mechanised methods is still directed to the coarse coal circuit containing approximately 18%$_{wt}$ moisture (Mohanty and Akbari, 2012). Mohanty and Akbari (2012) remarked that by reducing the initial moisture levels of the fine coal by 50%, the overall turnover of a typically colliery can potentially be improved by ±6%. In the past, whenever mechanical dewatering techniques failed to deliver contract specifications, the solution has leaned towards thermal drying, which is the most effective and expensive drying technique (Bratton *et al*., 2012). Therefore, searches for innovative, cost efficient, and eco-friendly drying techniques have intensified (Bratton *et al*., 2012). One such advanced dewatering process that was developed employs drying media to adsorb remaining surface moisture from the coal fines after mechanical dewatering.

This investigation was primarily focussed on successfully, and feasibly employing adsorbent material to lower the surface moisture content of coal fines. A surface moisture content of 8%$_{wt}$ or 0.08 g(moisture)/g(coal and moisture) was targeted, as dust problems and blending prospects were also considered. During this study, adsorbent assisted drying with integrated fixed-bed and cascading-bed drying techniques were employed to dry mechanically dewatered fine coal. Cascading-bed drying employed motion whilst the fixed-bed drying was operated in motionless state. Laboratory-scale experiments were conducted with various operating parameters and it was found that the surface moisture levels of the fine coal was effectively reduced from ±0.30 g(moisture)/g(coal and moisture) to well-below 0.08 g(moisture)/g(coal and moisture) within 10 minutes. The cascading-bed drying technique proved to be considerably less time consuming than the fixed-bed drying technique, which proves motion is of paramount importance when employing adsorbent assisted drying. The best performing adsorbent to coal mass ratio was found to be 2:1, while the -2mm+1mm fine coal delivered the lowest product moisture levels and the -1mm+0.5mm produced the highest overall initial desorption rates during the cascading-bed drying technique. In addition, it was found that alumina and silica-based adsorbent yielded

similar drying performances, whereas the 3mm adsorbents proved to have increased desorption rates over the 5mm adsorbents.

From an additional set of experiments, it was concluded that the adsorbent material could be reused without regeneration for six sequential cycles, while consistently lowering the moisture content of the fine coal below 0.10 g(moisture)/g(coal and moisture). Both alumina- and silica-based adsorbents were regenerated with ease by employing drying air, conditioned at 25°C and 40%RH. The moisture load of the adsorbents were reduced to between 0.08-0.10 g(moisture)/g(adsorbents and moisture) within 10 minutes, irrespective of particle size. In addition, it was found that adsorbent condition did not influence the final moisture content and drying rates of the fine coal. From an average initial moisture of 0.25 g(moisture)/g(coal and moisture), about 74%, 75% and 72% surface moisture was removed from -1mm+0.5mm coal fines, by the unused, used and air dried (regenerated) 3mm alumina-based adsorbents, respectively.

Although it was concluded that the 2:1 adsorbent to coal mass ratio delivered the best drying performance, the adsorbent to coal mass ratio of 1:1 was selected for investigation of industrial application, as less adsorbent material was required, while respectable drying performances was still reached. The -1mm+0.5mm coal and 3mm alumina-based adsorbents yielded the best drying performance, based on initial desorption rate and final moisture content, at this mass ratio. Therefore, these operating parameters were further investigated for industrial application and energy considerations.

The total amount of energy required to dry the -1mm+0.5mm coal fines (to 0.08 g(moisture)/g(coal and moisture)) with 3mm alumina-based adsorbents was 1637.75 and 1633.33kJ, thereby yielding an energy improvement of 6527.05 and 6531.47kJ/kg at 30%RH and 80%RH (average room temperature and pressure range recorded for South Africa), respectively. In conclusion, it was determined that the minimum and maximum energy required to remove 1kg of moisture from the -1mm+0.5mm coal, by adsorbent assisted drying, was 1012kJ/kg H_2O and 1015kJ/kg H_2O, respectively, which was comparatively lower than existing drying techniques.

Keywords: *Alumina-based adsorbents; silica-based adsorbents, fine coal; moisture content; desorption rate*

TABLE OF CONTENTS

Overview of document ..... **i**

Deliverables from this study ..... **i**

Solemn declaration ..... **i**

Acknowledgements ..... **i**

Abstract ..... **i**

List of figures ..... **i**

List of tables ..... **i**

List of Acronyms ..... **i**

List of symbols ..... **i**

1. General introduction **2**

1.1 Background and motivation 2

1.2 Scope of investigation 4

1.3 Research objectives 5

1.4 Structure of dissertation 6

2. Literature review **8**

2.1 Historic development of coal 8

2.1.1 Coal rank 9

2.1.2 Coal macerals 10

2.1.3 Coal mineralogy 10

2.2 Coal in South Africa 11

2.2.1 Coal preparation in South Africa 11

2.2.2 Classification of coal fines and ultra-fines 12

2.2.3 Problems associated with wet coal 13

2.3 Coal-moisture analogy 14

2.4 Dewatering theory of coal 17

2.4.1 Typical thermal drying rate of coal 17

2.4.2 Phase equilibrium 18

2.5 Conventional fine coal dewatering 19
2.6 Emerging techniques for fine coal dewatering 20
2.7 Adsorption 21
2.7.1 Contact-sorption drying 21
2.7.2 Classification of adsorbents 23
2.7.3 Adsorbent selection 24
2.7.4 Industrial adsorbents 24
2.8 Previous studies 28
2.8.1 Coal drying method and system 28
2.9 Summary and conclusion 31

3. Experimental methods 33

3.1 Overview 33
3.2 Materials used 33
3.2.1 Coal 33
3.2.2 Adsorbents 35
3.3 Variables 37
3.4 Experimental plan 38
3.4.1 Fixed-bed drying technique 38
3.4.2 Cascading-bed drying technique 40
3.4.3 Regeneration of adsorbents 42
3.5 Sample preparation 45
3.5.1 Coal 45
3.5.2 Adsorbents 46
3.6 Supplementary experimental work 47
3.6.1 Adsorbent static moisture capacity 47
3.6.2 Scanning electron microscopy (SEM) and light electron microscopy (LEM) ... 48

4. Fixed-bed drying technique 50

4.1 Variables 50

4.2 General desorption and adsorption curves 50
4.2.1 Desorption rate 52
4.2.2 Moisture transfer mechanism 54
4.3 Operating parameters 58
4.3.1 Influence of adsorbent to coal mass ratio 58
4.3.2 Influence of adsorbent type 63
4.3.3 Influence of adsorbent size 65
4.3.4 Influence of coal particle size range 67
4.4 Statistical significance 70
4.5 Conclusion 73

5. Cascading-bed drying technique 74
5.1 Variables 74
5.2 General adsorption and desorption curves 75
5.3 Operating parameters 79
5.4 Influence of motion 87
5.4.1 General desorption curves 87
5.4.2 Characteristic drying curve 89
5.4.3 Surface moisture and contact time 91
5.5 Statistical significance 96
5.6 Conclusion 98

6. Industrial application and energy considerations 99
6.1 Industrial application 99
6.1.1 Reuse of adsorbents 99
6.1.2 Adsorbent regeneration 101
6.1.3 Adsorbent degradation 106
6.1.4 Prospective continuous process 109
6.2 Energy considerations 112
6.2.1 Energy consumption 113

6.2.2 Energy improvement 114
6.2.3 Coal drying technologies 115
6.3 Conclusions 117

7. Conclusions, recommendations and contributions 118
7.1 Conclusions 118
7.2 Recommendations 120
7.3 Contributions 122

References 123

A Repeatability 126
A.1 Standard deviation and relative standard error 126
A.2 Standard deviation of fixed-bed drying technique 127
A.3 Standard deviation of cascading-bed drying technique 129

B Fixed-bed drying technique 132
B.1 General adsorption-desorption curves 132
B.2 Adsorption rate 134
B.3 Operating conditions 135

C Cascading-bed drying technique 145
C.1 General adsorption and desorption curves 145
C.2 Operating conditions 147
C.3 Influence of motion 157

D Industrial application and energy considerations 161
D.1 Industrial application 161
D.2 Energy considerations 166

LIST OF FIGURES

Figure 1.4.1: Structure of dissertation 7
Figure 2.1.1: Stages of coal maturity adapted from WCI (2009) 9
Figure 2.2.1: Typical colliery coal washing circuit taken from SANEDI (2011) 12
Figure 2.3.1: Types of moisture associated with coal; adapted from Lemley *et al.* (1995) ... 15
Figure 2.3.2: Surface moisture associated with a bed of particles (VICAIRE, 2015) 16
Figure 2.4.1: Typical drying curve of coal, adapted from Mohanty and Akbari (2012) 18
Figure 2.4.2: Phase diagram of water 19
Figure 2.7.1: Mechanism of contact-sorption drying taken from Kudra & Mujumdar (2009) . 22
Figure 2.7.2: Adsorption capacity of silica gel taken from CSGC (2014) 25
Figure 2.7.3: Adsorption capacity of adsorbents taken from Risheng (2014) 27
Figure 2.8.1: Closed-loop drying system of coal fines adapted from Bratton *et al*. (2012) ... 28
Figure 2.8.2: Dewatering repeatability of coal fines taken from Bland & McDaniel (2014) ... 29
Figure 2.8.3: Critical pollutants of thermal drying versus NDT process, taken from Bland & McDaniel (2014) 30
Figure 2.8.4: Relative cost of thermal drying versus NDT process, taken from Bland & McDaniel (2014) 31
Figure 3.2.1: Physical appearance of the alumina and silica-based adsorbents 36
Figure 3.4.1: Top view of fixed-bed vessels 39
Figure 3.4.2: Fixed-bed drying technique experimental procedure 39
Figure 3.4.3: Cascading and cataracting motions, adapted from Henein *et al.* (1983) 40
Figure 3.4.4: Top view of cascading-bed experimental setup 41
Figure 3.4.5: Cascading-bed drying technique experimental procedure 42
Figure 3.4.6: CTS climate test chamber (Type: C-40/100) 43
Figure 3.4.7: Schematic diagram of the packed bed vessel 44
Figure 3.4.8: Packed bed attached to the CTS climate test chamber 45
Figure 3.5.1: Particle size distribution 46
Figure 3.6.1: Static moisture adsorption at 25°C 47
Figure 3.6.2: SEM and LEM micrographs of alumina-based adsorbent particles 48
Figure 3.6.3: SEM and LEM micrographs of silica-based adsorbent particles 49
Figure 4.2.1: Adsorption-desorption curves of -2mm+1mm coal and 3mm adsorbents 51
Figure 4.2.2: Characteristic drying curve of fine coal 53
Figure 4.2.3: Drying mechanism; adapted from ALDACS (2013) 54
Figure 4.2.4: Average and standard deviation of repeats for -1mm+0.5mm coal 56

Figure 4.2.5: Average and standard deviation of repeats for 3mm alumina-based adsorbents 57
Figure 4.3.1: Desorption curves of -2mm+1mm coal and 5mm silica-based adsorbents 59
Figure 4.3.2: Adsorption curves of -2mm+1mm coal and 5mm silica-based adsorbent 60
Figure 4.3.3: Initial desorption rates of -2mm+1mm coal and 5mm silica-based adsorbents 62
Figure 4.3.4: Desorption curves of -2mm+1mm coal and 3mm adsorbents 63
Figure 4.3.5: Initial desorption rates of -2mm+1mm coal with 3mm adsorbents 64
Figure 4.3.6: Desorption rates of -1mm+0.5mm coal and silica-based adsorbents 66
Figure 4.3.7: Desorption curves of coal and 5mm alumina-based adsorbent 67
Figure 4.3.8: Desorption curves of coal and 5mm silica-based adsorbent 68
Figure 4.3.9: Initial desorption rates of fine coal and 5mm adsorbents 70
Figure 5.2.1: Adsorption-desorption curves of -1mm+0.5mm coal and 5mm adsorbents.... 75
Figure 5.2.2: Average and standard deviation of -1mm+0.5mm coal desorption curves 77
Figure 5.2.3: Average and standard deviation of 5mm alumina-based adsorbents adsorption curves 78
Figure 5.3.1: Desorption curves of -1mm+0.5mm coal and 3mm silica-based adsorbents . 79
Figure 5.3.2: Adsorption curves of 3mm silica-based adsorbents and -1mm+0.5mm coal.. 80
Figure 5.3.3: Initial desorption rates of -1mm+0.5mm coal and 3mm silica-based adsorbent 81
Figure 5.3.4: Initial desorption rates of +-1mm+0.5mm coal and 5mm adsorbents 82
Figure 5.3.5: Effect of adsorbent type on the final moisture loads of -1mm+0.5mm coal 83
Figure 5.3.6: Initial desorption rates of -1mm+0.5mm coal 84
Figure 5.3.7: Effect of adsorbent size on final surface moisture content of -1mm+0.5mm coal 84
Figure 5.3.8: Desorption curves of coal in combination with 5mm alumina-based-based adsorbent 85
Figure 5.3.9: Initial desorption rates of coal at an adsorbent to coal mass ratio of 2:1 86
Figure 5.4.1: Desorption curves of -1mm+0.5mm coal and 3mm alumina-based adsorbent 88
Figure 5.4.2: Desorption curves of -1mm+0.5mm coal and 3mm silica-based adsorbent ... 89
Figure 5.4.3: General desorption curve change 90
Figure 5.4.4: Initial desorption rates of -1mm+0.5mm coal and 3mm adsorbents 91
Figure 5.4.5: Final moisture load of -2mm+1mm coal and 3mm alumina-based adsorbent 92
Figure 5.4.6: Alumina-based: Time required to dry -2mm+1mm coal to 0.08 g(moisture)/g(coal and moisture) 93

Figure 5.4.7: Final moisture load of -2mm+1mm coal and 3mm silica-based adsorbent..... 94
Figure 5.4.8: Silica-based: Time required to dry -2mm+1mm coal to 0.08 g(moisture)/g(coal and moisture)..... 95
Figure 6.1.1: Surface moisture content of -2mm+1mmcoal and 5mm alumina-based adsorbent..... 100
Figure 6.1.2: Regeneration curves of alumina-based adsorbents..... 101
Figure 6.1.3: Desorption rates of 3mm and 5mm adsorbents..... 102
Figure 6.1.4: Moisture load of unused, used and air dried 3mm alumina-based adsorbents 103
Figure 6.1.5: Desorption curves of -1mm+0.5mm coal and 3mm alumina-based adsorbents 104
Figure 6.1.6: Initial adsorption and desorption rates of -1mm+0.5mm coal..... 105
Figure 6.1.7: (a) Used and (b) air dried 5mm alumina-based adsorbents..... 107
Figure 6.1.8: (a) Used and (b) air dried 5mm silica-based adsorbents 108
Figure 6.1.9: Effect of motion on adsorbent breakage..... 108
Figure 6.1.10: Continuous process flow of adsorbent assisted drying 110
Figure 6.2.1: Energy process flow diagram 112
Figure 6.2.2: Energy consumption of adsorbent assisted drying compared to other dryers 116
Figure A.2.1: Average and standard deviation of repeats for 3mm alumina-based adsorbents and -2mm+1mm coal..... 127
Figure A.2.2: Average and standard deviation of repeats for -2mm+1mm coal and 3mm alumina-based adsorbents..... 128
Figure A.2.3: Average and standard deviation of repeats for 3mm silica-based adsorbents and -1mm+0.5mm coal 128
Figure A.2.4: Average and standard deviation of repeats for -1mm+0.5mm coal and 3mm silica-based adsorbents 129
Figure A.3.1: Average and standard deviation of repeats for 5mm alumina-based adsorbents and -2mm+1mm coal..... 129
Figure A.3.2: Average and standard deviation of repeats for -2mm+1mm coal and 5mm alumina-based adsorbents..... 130
Figure A.3.3: Average and standard deviation of repeats for 5mm alumina-based adsorbents and -0.5mm+0.25mm coal..... 130
Figure A.3.4: Average and standard deviation of repeats for -0.5mm+0.25mm coal and 5mm alumina-based adsorbents..... 131
Figure B.1.1: Adsorption-desorption curves of -1mm+0.5mm coal and 3mm adsorbents at an adsorbent to coal mass ratio of 2:1 132

Figure B.1.2: Adsorption-desorption curves of -0.5mm+0.25mm coal and 3mm adsorbents at an adsorbent to coal mass ratio of 2:1 133
Figure B.1.3: Adsorption-desorption curves of -2mm+1mm coal and 5mm adsorbents at an adsorbent to coal mass ratio of 2:1 133
Figure B.1.4: Adsorption-desorption curves of -1mm+0.5mm coal and 5mm adsorbents at an adsorbent to coal mass ratio of 2:1 134
Figure B.2.1: Characteristic adsorption curve of adsorbents 134
Figure B.3.1: Desorption curves of -1mm+0.5mm coal and 3mm alumina-based adsorbents 135
Figure B.3.2: Adsorption curves of 3mm alumina-based adsorbents and -1mm+0.5mm coal 136
Figure B.3.3: Initial desorption rates of -1mm+0.5mm coal and 3mm alumina-based adsorbents 136
Figure B.3.4: Desorption curves of -1mm+0.5mm coal and 5mm silica-based adsorbents 137
Figure B.3.5: Adsorption curves of 5mm silica-based adsorbents and -1mm+0.5mm coal 137
Figure B.3.6: Initial desorption rates of -1mm+0.5mm coal and 5mm silica-based adsorbents 138
Figure B.3.7: Desorption curves of -0.5mm+0.25mm coal and 3mm adsorbents at an adsorbent to coal mass ratio of 1:1 138
Figure B.3.8: Initial desorption rates of -0.5mm+0.25mm coal and 3mm adsorbents..... 139
Figure B.3.9: Desorption curves of -1mm+0.5mm coal and 5mm adsorbents at an adsorbent to coal mass ratio of 1:1 139
Figure B.3.10: Initial desorption rates of -1mm+0.5mm coal and 5mm adsorbents..... 140
Figure B.3.11: Desorption rates of -0.5mm+0.25mm coal and silica-based adsorbents.... 140
Figure B.3.12: Desorption rates of -1mm+0.5mm coal and alumina-based adsorbents.... 141
Figure B.3.13: Desorption rates of -0.5mm+0.25mm coal and alumina-based adsorbents 141
Figure B.3.14: Desorption curves of coal and 5mm alumina-based adsorbents at an adsorbent to coal mass ratio of 2:1 142
Figure B.3.15: Desorption curves of coal and 5mm silica-based adsorbents at an adsorbent to coal mass ratio of 2:1 142
Figure B.3.16: Initial desorption rates of coal and 5mm adsorbents at an adsorbent to coal mass ratio of 2:1 143
Figure B.3.17: Desorption curves of coal and 3mm alumina-based adsorbents at an adsorbent to coal mass ratio of 2:1 143
Figure B.3.18: Desorption curves of coal and 3mm silica-based adsorbents at an adsorbent to coal mass ratio of 2:1 144

Figure B.3.19: Initial desorption rates of coal and 3mm adsorbents at an adsorbent to coal mass ratio of 2:1 144
Figure C.1.1: Adsorption-desorption curves of -2mm+1mm coal and 5mm adsorbents at an adsorbent to coal mass ratio of 0.5:1 145
Figure C.1.2: Adsorption-desorption curves of -0.5mm+0.25mm coal and 5mm adsorbents at an adsorbent to coal mass ratio of 1:1..... 146
Figure C.1.3: Adsorption-desorption curves of -1mm+0.5mm coal and 3mm adsorbents at an adsorbent to coal mass ratio of 1:1 146
Figure C.1.4: Adsorption-desorption curves of -0.5mm+0.25mm coal and 3mm adsorbents at an adsorbent to coal mass ratio of 2:1..... 147
Figure C.2.1: Desorption curves of -1mm+0.5mm coal and 3mm alumina-based adsorbents 147
Figure C.2.2: Adsorption curves of 3mm alumina-based adsorbents and -1mm+0.5mm coal 148
Figure C.2.3: Initial desorption rates of -1mm+0.5mm coal and 3mm alumina-based adsorbent..... 148
Figure C.2.4: Desorption curves of -1mm+0.5mm coal and 5mm silica-based adsorbents149
Figure C.2.5: Adsorption curves of 5mm silica-based adsorbents and -1mm+0.5mm coal149
Figure C.2.6: Initial desorption rates of -1mm+0.5mm coal and 5mm silica-based adsorbent 150
Figure C.2.7: Initial desorption rates of -1mm+0.5mm coal and 3mm adsorbents 150
Figure C.2.8: Effect of 3mm adsorbent type on the final moisture loads of -1mm+0.5mm coal 151
Figure C.2.9: Initial desorption rates of -0.5mm+0.25mm coal and 5mm adsorbents 151
Figure C.2.10: Effect of 5mm adsorbent type on the final moisture loads of -0.5mm+0.25mm coal 152
Figure C.2.11: Initial desorption rates of -0.5mm+0.25mm coal and silica-based adsorbents 152
Figure C.2.12: Effect of silica-based adsorbent size on final surface moisture content of -0.5mm+0.25mm coal 153
Figure C.2.13: Initial desorption rates of -0.5mm+0.25mm coal and alumina-based adsorbents 153
Figure C.2.14: Effect of alumina-based adsorbent size on final surface moisture content of -0.5mm+0.25mm coal 154
Figure C.2.15: Desorption curves of coal and 3mm alumina-based adsorbents at an adsorbent to coal mass ratio of 2:1 154

Figure C.2.16: Desorption curves of coal and 3mm silica-based adsorbents at an adsorbent to coal mass ratio of 2:1 155
Figure C.2.17: Desorption curves of coal and 5mm silica-based adsorbents at an adsorbent to coal mass ratio of 2:1 155
Figure C.2.18: Initial desorption rates of coal at an adsorbent to coal mass ratio of 3:1 ... 156
Figure C.2.19: Initial desorption rates of coal at an adsorbent to coal mass ratio of 1:1 ... 156
Figure C.3.1: Desorption curves of -1mm+0.5mm coal and 5mm alumina-based adsorbents at an adsorbent to coal mass ratio of 1:1..... 157
Figure C.3.2: Desorption curves of -1mm+0.5mm coal and 5mm silica-based adsorbents at an adsorbent to coal mass ratio of 1:1 157
Figure C.3.3: Initial desorption rates of -1mm+0.5mm coal and 5mm adsorbents at an adsorbent to coal mass ratio of 1:1 158
Figure C.3.4: Final moisture load of -1mm+0.5mm coal and 3mm alumina-based adsorbent 158
Figure C.3.5: 3mm alumina-based: Time required to dry -0.5mm+1mm coal to 0.08 g(moisture)/g(coal and moisture) 159
Figure C.3.6: Final moisture load of -1mm+0.5mm coal and 3mm silica-based adsorbent 159
Figure C.3.7: 3mm silica-based: Time required to dry -0.5mm+1mm coal to 0.08 g(moisture)/g(coal and moisture) 160
Figure D.1.1: Surface moisture content of -2mm+1mm coal and 5mm alumina-based adsorbent at an adsorbent to coal mass ratio of 2:1 161
Figure D.1.2: Surface moisture content of -2mm+0.25mm coal and 3mm alumina-based adsorbent at an adsorbent to coal mass ratio of 1:1 162
Figure D.1.3: Regeneration curves of silica-based adsorbents..... 162
Figure D.1.4: Regeneration curves of 5mm adsorbents 163
Figure D.1.5: Desorption rates of silica-based and alumina-based adsorbents 163
Figure D.1.6: Desorption curves of -2mm+1mm coal and 3mm alumina-based adsorbents at an adsorbent to coal mass ratio of 1:1 164
Figure D.1.7: Desorption and adsorption rates of -2mm+1mm coal and 3mm alumina-based adsorbents at an adsorbent to coal mass ratio of 1:1 164
Figure D.1.8: Desorption curves of -2mm+1mm coal and 5mm silica-based adsorbents at an adsorbent to coal mass ratio of 1:1 165
Figure D.1.9: Desorption and adsorption rates of -2mm+1mm coal and 5mm silica-based adsorbents at an adsorbent to coal mass ratio of 1:1 165
Figure D.2.1: Energy gain of -1mm+0.5mm coal and silica-based adsorbents at an adsorbent to coal mass ratio of 1:1 170

LIST OF TABLES

Table 2.1: Particle size distribution taken from SANEDI (2011) 13
Table 2.2: Characteristic features of physical adsorption, taken from Dabrowski (2001) 23
Table 3.1: Proximate and ultimate analyses 34
Table 3.2: Typical composition of adsorbents 35
Table 3.3: Physical properties of adsorbents 36
Table 3.4: Set conditions 37
Table 3.5: Manipulated variables 37
Table 3.6: Responses 38
Table 3.7: Grain bulk density and grain apparent porosity results 47
Table 4.1: Mean, standard deviation and relative standard error of initial moisture of coal . 55
Table 4.2: Standard deviation and relative standard error of initial rates 57
Table 4.3: Moisture displacement of -2mm+1mm coal and 5mm silica-based adsorbents... 61
Table 4.4: Moisture displacement of -1mm+0.5mm coal in the presence of 3mm and 5mm silica-based adsorbents 65
Table 4.5: Contact time required to dry coal fines to 0.08 g(moisture)/g(coal and moisture) 69
Table 4.6: ANOVA response of fixed-bed drying technique results 71
Table 4.7: *T*-test response of fixed-bed drying technique results 72
Table 5.1: Mean, standard deviation and relative standard error of initial moisture of coal . 76
Table 5.2: Standard deviation and relative standard error of initial rates 78
Table 5.3: ANOVA response of fixed-bed drying technique results 96
Table 5.4: *T*-test response of fixed-bed drying technique results 97
Table 6.1: Adsorbent grain bulk density and grain apparent porosity 106
Table 6.2: Stream properties 111
Table 6.3: Energy required by various dryers; taken from Karthikeyan *et al*. (2009) and Wilson *et al*. (1992) 115
Table D.2.1: Contact time in rotary dryer (min) 166
Table D.2.2: Energy consumed by rotary dryer (kJ) 167
Table D.2.3: Total energy consumed (kJ/kg load) for -1mm+0.5mm coal and 3mm adsorbents 169

LIST OF ACRONYMS

BET	*Brunauer Emmett Teller*
df	*degrees of freedom*
LEM	*Light Electron Microscopy*
NDT	*Nano Drying Technology*
ROM	*Run Off Mine*
RSE	*Relative Standard Error*
S	*Standard deviation*
SE	*Standard Error*
SEM	*Scanning Electron Microscopy*
WCI	*World Coal Institute*

LIST OF SYMBOLS

Al_2O_3	*aluminium oxide*
cm	*centimeter*
cm^3/g	*cubic centimeter per gram*
CO_2	*carbon dioxide*
Fe_2O_3	*iron (III) oxide*
g	*gram*
H_2O	*water*
kJ/mol	*kilojoule per mole*
kJ/kg	*kilojoule per kilogram*
kg	*kilogram*
kg/m^3	*kilogram per cubic meter*
m^2/g	*square meters per gram*
mm	*millimeter*
Na_2O	*sodium oxide*
SiO_2	*silicon dioxide*
%	*percentage*
°C	*degrees Celsius*
%RH	*percentage relative humidity*
$\%_{wt}$	*percentage by weight*
$\Delta H_{adsorption}$	*enthalpy change*

1

CHAPTER

GENERAL INTRODUCTION

This report is titled "Adsorbent assisted drying of fine coal". Chapter 1 consists of Sections 1.1 to 1.4. Section 1.1 contains a brief background discussion of coal and adsorbents including a short discussion on the motivation for dewatering fine and ultra-fine coal. This is followed by Section 1.2, which details the scope of the investigation. Section 1.3 identifies the main objectives of the study. Lastly, the outline of the project is given in Section 1.4.

1.1 Background and motivation

The World Coal Association (2014) reported that coal meets about 30% of the global energy demand. Although coal is a non-renewable fuel, it is still considered an important energy source worldwide (Eraydin, 2009). South Africa's economy relies largely on coal as a basis of foreign proceeds, and forms a vital national energy source (Reddick, 2006). This reliance, along with the abundant coal reserves still accessible in South Africa, safeguards coal mining for many years to come. Even though this prospect seems promising on an energy basis, mining industries have a large impact on the environment.

Coal fines are generated by the increase in mechanization on coal mines, and have the ability to retain large amounts of moisture due to its inherently large surface areas (Reddick *et al.*, 2007). The bulk of the moisture is retained by fine (-1mm+0.1mm) and ultra-fine (-0.15mm+0.1mm) coal fractions, which constitutes about 11% of the nominal product (SANEDI, 2011). This poses a problem for utility companies as moisture retention lowers the effective heating value of the coal. Coal fines are often dewatered, and combined with the coarse coal stream; however, as the coal fines rarely meet the desirable moisture levels, the quality of the final coal product stream suffers (Reddick, 2006).

Commonly, fine coal dewatered by the best mechanised methods is still directed to the coarse coal circuit containing approximately 18%$_{wt}$ moisture (Mohanty and Akbari, 2012). Mohanty and Akbari (2012) remark that the overall turnover of a typically colliery can potentially be increased by 6% if the initial moisture levels of the fine coal is cut by half. This is discouraging for the coal preparation industry, which caters for a market sector calling for

lower final moisture levels, as in the case of coal-based power stations. In the past, whenever mechanical dewatering techniques failed to deliver contract specifications, the solution has leaned towards thermal drying which is the most effective (and expensive) drying technique (Bratton *et al*., 2012). When implemented properly, this technique is able to achieve coal moisture levels below 6%$_{wt}$, increasing the calorific value of the coal (Bratton *et al*., 2012). However, the coal industry has grown weary of these techniques because of installation, and maintenance cost implications, as well as pollutant emissions (Bratton *et al*., 2012). From an economic standpoint, Rong (1993) reasons that moisture inclusion in coal adds to the weight of coal, and therefore the mass-based transportation costs increase. Consequently, the majority of the fine and ultra-fine coal generated is still disposed of (SANEDI, 2011).

Even though the practice of dumping coal fines into settlement ponds, and coal impoundments is validated to be economical, it is not environmentally friendly (Campbell, 2006). The worldwide abundance of these sites is proof of the longstanding dilemma (Bland and McDaniel, 2014). As coal is a sulphur bearing sedimentary rock, disposal waste management is undesired as it may cause acid rain, and/or acid mine drainage. In response, government enforced legislations have become more stringent, public apprehensions have increased, and rehabilitation ventures, incurred by mining companies, have become progressively more expensive (Reddick, 2006). This points out the need for improved productivity, efficient consumption/utilization of resources, and the reduction of waste production (Reddick, 2006).

In recent years, searches for innovative, cost efficient, and eco-friendly drying techniques have intensified (Bratton *et al*., 2012). One such advanced dewatering process employs drying media to adsorb remaining surface moisture from the coal fines after mechanical dewatering. In a similar study conducted by Bland and McDaniel (2014), it was found that the moisture content of coal fines was trimmed down to single digit values by implementing porous drying media. Yang (2015) conducted a similar study in which it was found that the mechanically dewatered coal product moisture was reduced from 19%wt to 9%wt by contacting with activated alumina adsorbents for ±5 minutes. This moisture reduction in the fine coal circuit will spur a beneficial increase in the fine coal mass, which can be redirected to augment the clean coarse coal circuit (Bratton *et al*., 2012). The dewatered clean fine coal adds to the plant's yield without compromising the plant's original heat content in the final product. Mohanty and Akbari (2012) expect the increase in production revenue to outweigh the installation costs, and elevate the overall profitability of the coal preparation plant within time.

This study investigates the drying performance of coal fines by employing adsorbent ceramic material as a drying agent. It was decided to focus the research on adsorbent assisted drying due to the low pollutant emissions, and the relatively low running costs detailed in literature (Bland and McDaniel, 2014).

1.2 Scope of investigation

The use of ceramic adsorbents in separation processes have been acknowledged worldwide, and the use thereof as an industrial dewatering agent in the beneficiation of coal fines have grown popular in recent years.

The scope of this investigation is primarily focussed on successfully, and feasibly employing adsorbent material to lower the surface moisture content of coal fines. Throughout the investigation, a surface moisture of $8\%_{wt}$ or 0.08 g(moisture)/g(coal and moisture) was targeted. Firstly, the ability of coal fines to release moisture was examined in the presence of various operating parameters in a climate-controlled room, set at 25°C and 40% relative humidity (RH), using fixed-bed (static) vessels. The operating parameters included:

1. Adsorbent to coal mass ratio (3:1, 2:1, 1:1, 0.75:1 and 0.5:1)
2. Adsorbent type (Alumina-based and silica-based adsorbents)
3. Adsorbent size (3mm and 5mm)
4. Coal particle size range (-2mm+1mm, -1mm+0.5mm and -0.5mm+0.25mm)

To further investigate the drying performance of the coal fines, the set of experiments were repeated by employing a cascading-motion. This was done to evaluate the influence of motion on the initial desorption rate of coal fines, the final surface moisture content of coal fines, and contact time required by the coal fines. The results of the best performing drying operating parameters were compared, and the best performing drying technique was identified. Lastly, the framework of industrial application and energy considerations of adsorbent assisted drying was explored. The practicality of the process was investigated, as the technical viability of adsorbent assisted drying is largely reliant on the reuse, and successful regeneration of the adsorbent material. Regeneration can be achieved in various manners, however for the purpose of this study; the adsorbents were air-dried in a packed bed. The drying air was conditioned in the climate chamber to 25°C and 40%RH. The energy consumption of the cascading-bed drying technique was determined in accordance to contact time as well as the energy required by the regeneration process. The overall

energy consumption was compared to the calorific value upgrade of the coal fines to determine whether adsorbent assisted drying is feasible, and whether the venture warrants further research.

1.3 Research objectives

Adsorbent assisted drying was selected for evaluation with the goal of dewatering coal fines to a target surface moisture content of 0.08 g(moisture)/g(coal and moisture). According to Bland and McDaniel (2014), coal fines with a surface moisture content of 0.08 g(moisture)/g(coal and moisture) is considered economically attractive for the coal industry. A sample of sub-bituminous coal, from the Highveld coalfield located in Mpumalanga, South Africa, was collected and crushed for use. The coal fines were drenched in water for 24 hours, and mechanically dewatered by pressure filtration. The initial moisture contents of the coal samples ranged between 0.15 and 0.30 g(moisture)/g(coal and moisture) according to particle size range after filtration. The experiments were conducted in a climate-controlled room on bench-scale by using fixed-bed, and cascading-bed drying techniques. The drying performance of mechanically dewatered coal fines in the presence of two adsorbent types, alumina-based adsorbents (F-200 activated alumina), and silica-based adsorbents (Silsorb N10), were investigated. Therefore, the focus of this project is investigating the drying performance of coal in the presence of adsorbent materials. The specific objectives of the study are listed below:

1. The main objective of this investigative study is to determine whether adsorbent assisted drying is a suitable drying technique for lowering the surface moisture of mechanically dewatered coal fines, in a climate-controlled room at 25°C and 40%RH.

2. To evaluate the ability of adsorbent assisted drying technology to reduce the surface moisture of mechanically dewatered coal fines to a target moisture content of 0.08 g(moisture)/g(coal and moisture).

3. Investigate the effect of various operating parameters on the drying performance of mechanically dewatered coal fines during fixed-bed drying. The operating parameters focussed on in this investigation, includes adsorbent to coal mass ratio, adsorbent type, adsorbent size and coal particle size range.

4. Investigate the effect of various operating parameters such as adsorbent to coal mass ratio, adsorbent type, adsorbent size, and coal particle size range on the drying performance of mechanically dewatered coal fines during cascading-bed drying.

5. Identifying the best performing drying technique in terms of fixed-bed, and cascading-bed, drying techniques.
6. Investigate the prospect of adsorbent regeneration by employing air as drying mechanism in a packed-bed at air temperature and pressure of 25°C and 40%RH, respectively.
7. Briefly evaluate the framework of industrial application in terms of a cyclic reuse of adsorbents, adsorbent condition and adsorbent degradation.
8. Develop a suitable energy balance to investigate the potential energy expenses and returns generated by adsorbent assisted drying. This information is required to evaluate the technical feasibility of adsorbent assisted drying and create a comparative study with other drying technologies.

1.4 Structure of dissertation

Figure.1.4.1 schematically presents the structure the project.

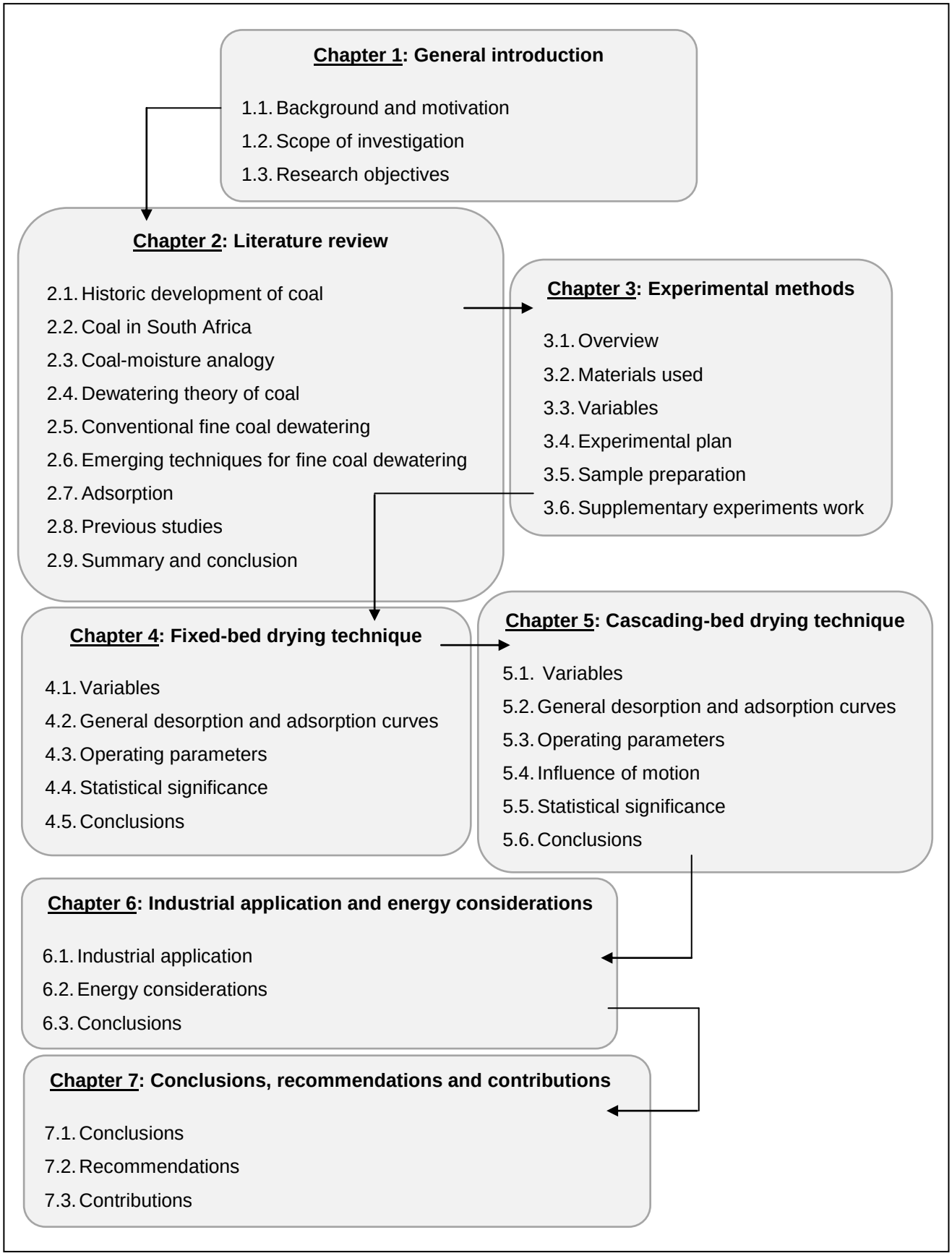

Figure 1.4.1: Structure of dissertation

2

CHAPTER

LITERATURE REVIEW

The information summarised in Chapter 2 is necessary to understand this investigative study. This chapter initiates with an evaluation of the historic development of coal in Section 2.1. Section 2.2 elaborates briefly on coal in South African and includes preparation, size classification and problems associated with the coal. It is essential to understand the active relationship between moisture and coal, as discussed in Section 2.3. Section 2.4 investigates the typical drying curve of coal and phase equilibrium of water to identify the driving forces of moisture adsorption and desorption from coal. Section 2.5 briefly discusses conventional drying techniques of coal, and Section 2.6 examines the new and emerging technologies for drying coal fines. This section aims to formulate a clear understanding of systematic surface moisture desorption and adsorption onto adsorbent media. The adsorption theory discussed in Section 2.7 explains the mechanism of contact-sorption drying in the presence of moisture. Finally, the literature review is concluded in Section 2.8 by considering studies of moisture replacement from one phase to another proving the validity of adsorbent assisted drying of coal.

2.1 Historic development of coal

Coal is physically and chemically altered fragments of prehistoric vegetation (SANEDI, 2011). This sedimentary fossilized rock formed over millennia is rich in carbon. During what is now known as the first coal age, plant residue and other debris along with tectonic movements covered swamps and peat sumps often to considerable depths (Falcon & Ham, 1988). For the duration of the burial stage, the plant remains are subjected to extreme temperatures and pressures which causes physical and chemical changes in the remnant vegetation. These changes lead to transformation from peat into coal (Falcon & Ham, 1988).

2.1.1 Coal rank

The rank of coal is the measure of the degree of alteration during maturation of coal, and can be expressed in the series of lignite to anthracite (Falcon & Ham, 1988). It is helpful to note that coal rank is based mainly on increasing carbon content, and decreasing volatile material. Over time, coal matures in rank as illustrated in Figure 2.1.1 adapted from WCI (2009). This figure shows the stages of maturity through which coal forms during coalification.

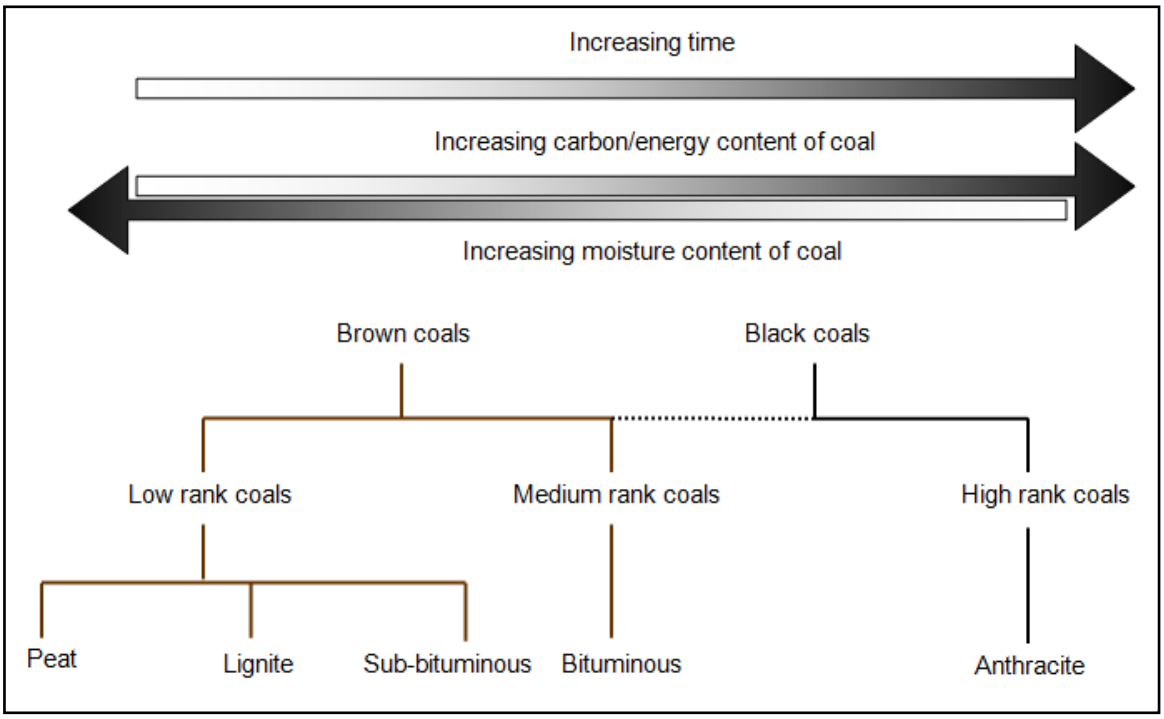

Figure 2.1.1: Stages of coal maturity adapted from WCI (2009)

During coalification, peat is produced from remnants of swamp vegetation, and over time evolves into a soft brown coal known as lignite (WCI, 2009). Falcon & Ham (1988) explains that along with an increase in time, depth of burial, and thermal effects caused the coal to start to blacken, and harder bituminous coals were formed. A further progression in coalification yields a higher rank coal termed anthracite. Together, with a changed appearance, coal matures both on a physical and molecular level. This means that the molecular structure pivots toward a more pure organic material, and a reduced overall porosity fraction (Falcon & Ham, 1988). The more porous structures of low rank coals bring about increased levels of surface moisture, and reduced portions of carbon (Petrick, 1969).

2.1.2 Coal macerals

Macerals are similar in nature to inorganic rock minerals; however they do not possess a crystalline structure (Falcon & Ham, 1988). Macerals are the coalified remnants of vegetation conserved in coal and rock formations. Macerals can be subdivided into three main groups; vitrinite, inertinite and liptinite (Falcon & Ham, 1988).

i. Vitrinite macerals are matured cell wall material (wood tissue) of prehistoric vegetation remnants. Falcon & Ham (1988) noted that the carbon content, and aromaticity, of vitrinite macerals increases diagnostically with rank.
ii. Liptinite macerals originate from waxy and resinous fragments of vegetation. These fragments are resistant to weathering, and include cuticles, spores, and resins. Coalification in its advanced form is rarely seen in liptinite macerals, as they begin to disintegrate in coals of medium volatility, and are rarely present in coals of low volatility. When present in coal, liptinite macerals have a tendency to preserve its original vegetation state, and are often referred to as plant fossils.
iii. Inertinite macerals are formed from remnant vegetation that has endured alteration, and degradation during the peat stage of coal formation. Inertinite macerals undergo minute structural changes with increasing rank. This type of maceral has the highest level of reflectance, and is easily distinguishable from other macerals (SANEDI, 2011).

Surface moisture associated with coal particles are usually held on the surface of macerals. Macerals are further categorized according to their state of reactivity. Vitrinite and liptinite are included in the reactive category, whilst inertinite is branded unreactive (Falcon & Ham, 1988). Reactive semi-fusinite is an

2.1.3 Coal mineralogy

Mineral matter is representative of the fraction of coal occupied by inorganic material. The mineral matter content also establishes the grade of coal. The presence and opulence of coal minerals may well vary according to the area of formation and degree of maturity. Falcon & Snyman (1986) highlighted carbonates, quarts, clays, sulphides, and glauconite as minerals abundantly present in most South African coals. Of these minerals, clays make up about 80% of the mineral suite, and the remaining fraction is constituted of carbonate, and pyrite minerals. Clays are held within the organic matrix of coal as lumps and grainy lenses. Carbonate minerals are attained within the organic matrix, and range from little specks and

nodules, to bulky crystalline formations in wedges and cracks cutting the bed seams through sheets of macerals. Pyrite is usually present in coal as fine or coarse pieces in cleats. The degree of difficulty in removing minerals during beneficiation is determined by their size, shape, and nature (Falcon & Snyman, 1986).

2.2 Coal in South Africa

South Africa is heavily reliant on coal as an energy source. More than 60% of South Africa's major energy supply is provided by coal, and over 90% of the country's electricity demand is met by employment of coal (Burnard & Bhattacharya, 2011). As the energy demand is on a continual escalation rate, the coal production rate in South Africa is expected to remain a pressing situation for years to come.

2.2.1 Coal preparation in South Africa

Raw, run-of-mine (ROM) coal is processed to add to its value. Wet and dry beneficiation is commonly employed in the coal preparation industry to increase the worth of the coal (SANEDI, 2011). Dry beneficiation includes screening, and separation of coal pieces in appropriate categories according to the industrial requirements. Wet coal beneficiation is concerned with washing coal to remove undesired impurities, including a sulphur and ash fraction. Reducing the impurity content provides an improved heating value throughout the coal. The ash and sulphur contents present in coal, which is tolerable by clients, dictates the level of washing required (Reddick, 2006).

Reddick (2006) reported that over 80% of South African ROM coal is washed. Irrespective of efficiency, washing coal remains a water extensive process that involves large volumes of water to operate the beneficiation plant, which can become intensive both in terms of capital and operational expenses (Reddick, 2006). Figure 2.2.1 shows a generalized coal washing circuit of a typical colliery in South Africa.

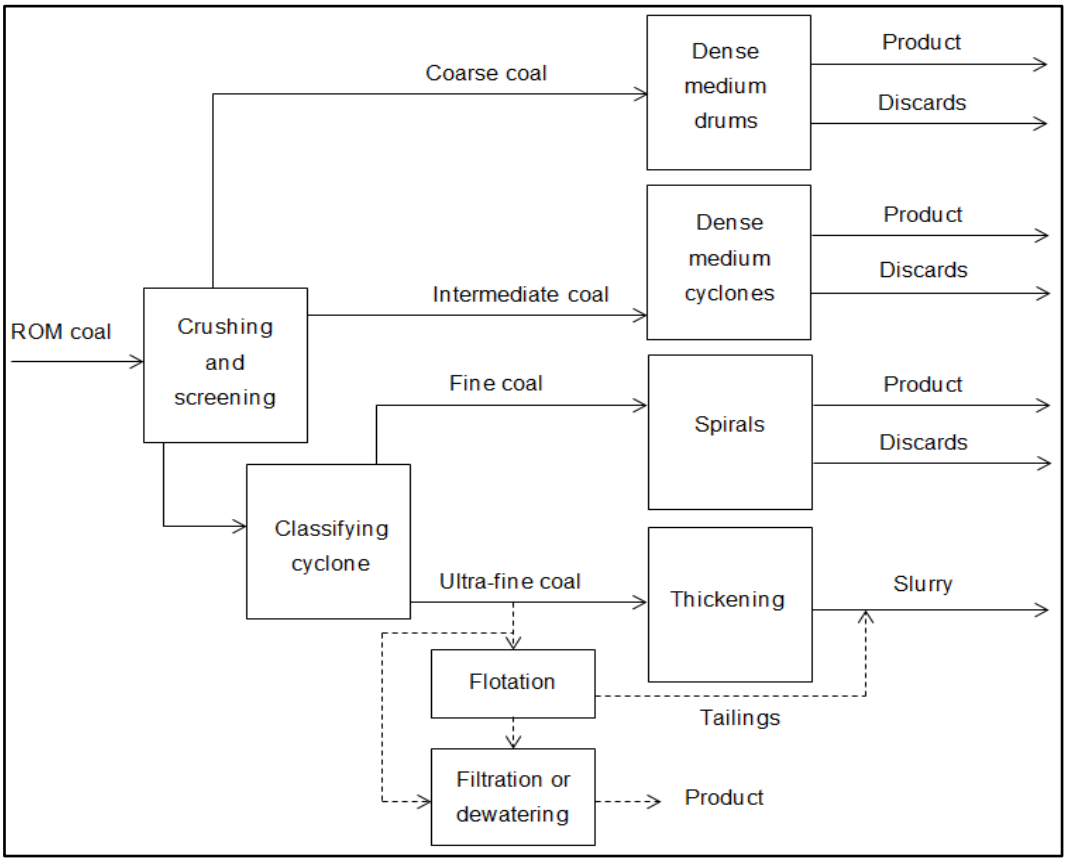

Figure 2.2.1: Typical colliery coal washing circuit taken from SANEDI (2011)

Initially, the ROM coal is crushed, and screened, into various particle size portions after removal of contamination. Classification of size fractions vary according to the need, and the design of each colliery. As shown in Figure 2.2.1, the coarse coal is usually washed in dense medium drums to differentiate between valuable low ash coals, and discardable high ash coals (Reddick, 2000). Dense medium cyclones are employed to wash, and separate, the intermediate sized coal according to density. Fine coal is separated into size fractions in a classifying cyclone, and is beneficiated in spiral concentrators, whereas ultra-fine coal is sent to a flotation unit (Nicol, 1992) or discarded into a slimes dam. Most of the process water is recovered by the overflow of the thickeners, and recycled to the beneficiation plant. The ultra-fines, in thickened slurry form, leave the thickener along with the remaining process water (Reddick, 2000). The water from the slimes dam is also collected and recycled back to the plant.

2.2.2 Classification of coal fines and ultra-fines

Product moisture plays an essential role in the industry. Reddick (2006) noted that a finer coal particle diameter is accompanied by an increased mass surface area to mass volume

ratio, and consequently an increased amount of retained water. Assuming the coal fines, and ultra-fines are washed, Table 2.1 illustrates the representative distribution of the coal mass in the plant along with the total moisture in the coal product.

Table 2.1: Particle size distribution taken from SANEDI (2011)

Description	Coal particle size range (mm)		Mass distribution (% of total product)	Moisture content (%)
	Minimum	Maximum		
Coarse	12-25	100-250	61	5
Small	1	12	28	9
Fine	0.1-0.5	1	7	13
Ultra-fine		0.1-0.15	4	27

The results in Table 2.1 show that the fine, and ultra-fine, coal fractions have comparatively the higher moisture contents in the product circuit. From this, it is understandable that coal fines, and ultra-fines, require further dewatering which leads to additional costs to meet the client's desired moisture levels. Literature from Reddick (2006) supports a report written by De Korte & Mangena (2004), in which it was marked that fine (-0.5mm), and ultra-fine (-0.1mm) coal, can have a moisture content, of 15%$_{wt}$ and 25%$_{wt}$ even after mechanical dewatering.

2.2.3 Problems associated with wet coal

For ages, the solution to dewatering coal fines has eluded the coal industry. The cost of dewatering coal fines, and ultra-fines, are generally perceived by the industry as higher than the value of the dewatered coal, making the dewatering option largely ignored (Reddick, 2006). In general, the fine coal is rather discarded than washed. The economic and environmental implications are discussed briefly in this section.

2.1.1.1 Economic

The energy value of coal is based on its ability to burn (Mohanty and Akbari, 2012). The inclusion of additional moisture reduces the cost-effectiveness of coal, as energy from an external source is required to evaporate this moisture, and expose the exact energy content of the coal. Typically, in industry, coal's worth is measured by its moisture level rating (Bland and McDaniel, 2014). This explains why a portion of the selling price of coal is relative as it is dependent on its moisture content. The price of coal will resultantly decrease along with trimmed down moisture levels. In addition, coal is transported on a weight basis (Rong,

1993). From an economic standpoint, Rong (1993) argues that moisture inclusion in coal adds to the weight of coal, and therefore the mass-based transportation costs increase. The facts are derived; the ability of coal fines to adsorb, and retain excessive volumes of moisture does not vouch well for the coal mining industry.

2.1.1.2 Environmental

Formerly economics sanctioned the practice of dumping coal fines into settlement ponds, and coal impoundments (Campbell, 2006). The worldwide abundance of these sites is proof of the longstanding dilemma (Bland and McDaniel, 2014). Coal is a sulphur-bearing sedimentary rock. In numerous situations, water draining from coal fine impoundments, and waste ponds, is somewhat acidic due to the reaction between the sulphur, water and air. This water usually contaminates streams and rivers in close proximity, which is a source of existence to a range of wildlife.

2.3 Coal-moisture analogy

The process of moisture adsorption onto coal particles is governed by various factors. These factors include the porous nature of coal, as well as the nature of the moisture interaction with the coal particles. Coal remains a porous substance irrespective of the compaction or compression (Petrick, 1969). Du Preez (2012) interprets coal porosity as the total volume fraction of void spaces in a coal particle. The pore size distribution may change according to rank however; mature coals have a much larger internal surface area than external surface area. Petrick (1969) found that this actuality holds true for relatively fine coal particles. The internal surface area of coal is easily accessed by water molecules, or in fact any molecule with a comparable smaller size (Petrick, 1969). Classification of different moisture types associated with coal has been a precarious task in the past (Wakeman, 1984). Considering moisture from a dewatering point of view, Figure 2.3.1 illustrates the types of moisture residing in coal, and its respective locations.

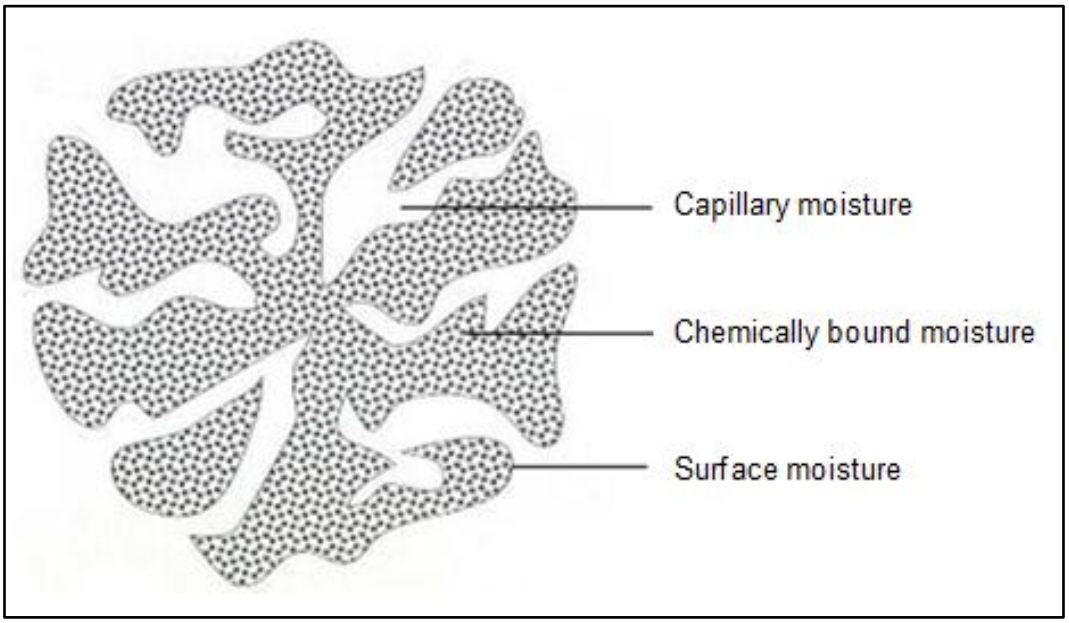

Figure 2.3.1: Types of moisture associated with coal; adapted from Lemley *et al.* (1995)

The various forms of moisture related to coal are described as follows:

I. Surface moisture is located on the surface of the coal particle that includes internal and external surface areas (Petrick, 1969). Additionally, the moisture held between coal particles in a mass or heap also forms part of surface moisture (Le Roux, 2003).
II. Capillary bound moisture, also branded inherent or structural moisture, is moisture that is adsorbed into the capillary matrix (network of small fissures) of the individual coal particle (Du Preez, 2012).
III. Chemically bound moisture of coal refers to moisture that forms part of the structural integrity of the coal, and is found in association with certain minerals present in coal (Campbell, 2006).

Total moisture comprises of “air dry loss free” moisture, and “residual moisture”, as noted by Campbell (2006). Air dry loss free moisture is typically determined as dehydration by drying for 3 hours at 40% relative humidity conditions, and residual moisture is typically determined by drying at 105°C and 110% relative humidity conditions (Campbell, 2006). The equilibrium moisture content can be established at 96%RH and 30°C according to ASTM D-1412 (ISO 1018) (Unsworth *et al*., 1989). Chemically bound moisture is excluded when taking into consideration the total moisture of coal (Le Roux, 2003). Mechanical dewatering is sufficient in removing free moisture to required levels since surface moisture moves relatively free

when subjected to applied pressure gradients (Le Roux, 2003). Moreover, capillary moisture is effectively removed by thermal dewatering techniques. Chemically bound moisture can be removed from coal only by alteration of the chemical structure thereof, e.g. igniting it (Le Roux, 2003).

Water molecules are physically adsorbed with ease onto the surface of coal. Active centres at the surface of the coal may be created by oxygen groupings, which encourage adsorption (Petrick, 1969). When a porous coal particle is placed in an environment containing a higher or lower concentration of water molecules than that present in itself, a concentration gradient is created which promotes movement of water molecules from or to the coal particle (Petrick, 1969). This trend of moisture flow pivots toward maintaining equilibrium with the environment (Petrick, 1969). Figure 2.3.2 shows the presence of moisture in the immediate vicinity of the coal particle's surface.

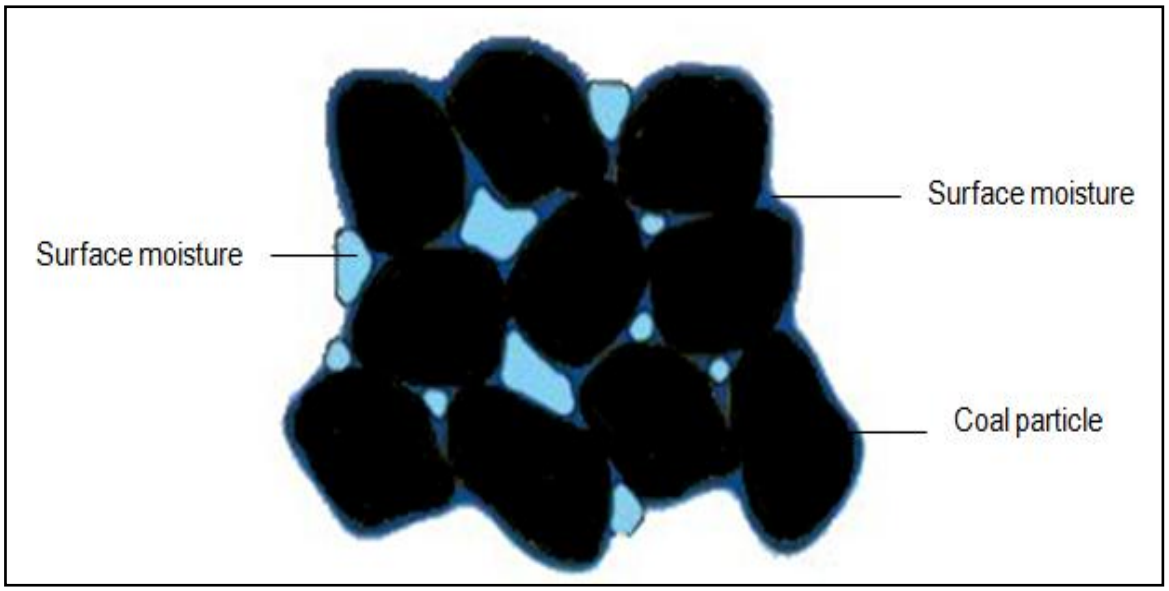

Figure 2.3.2: Surface moisture associated with a bed of particles (VICAIRE, 2015)

Movement of moisture within a bed of coal fines occurs by vapour diffusion, and/or liquid film movement. Liquid moisture is displaced by film movement when particles come into direct contact, however; as the amount of liquid moisture at the surface of the particles decrease, moisture migrates from the capillaries of the coal to the surface, and surface moisture diffusion starts (Kudra and Mujumdar, 2009). Therefore, the rate of adsorption and desorption of capillary moisture is ever dependent on the rate of diffusion between the surrounding air, and the surface of the coal, which means that the rate is proportional to the rapid elimination of water molecules from the direct vicinity of the surface of the coal (Petrick,

1969). Even though it is desirable to distinguish between vapour and liquid movement of moisture, it is impossible to measure the exact phase transformation (Janz, 2000). A further noteworthy fact is that finer coal particles are accompanied by a larger surface area in relation to a similar mass of larger coal particles, which consequently enhances the adsorption rate (Du Preez, 2012).

2.4 Dewatering theory of coal

2.4.1 Typical thermal drying rate of coal

Drying of coal refers to desorption of water molecules from the surface, and capillaries in coal particles, thereby spurring a reduction in the coal's moisture content. Regardless of the drying technique, every type of coal fine is characterised by a drying curve as a function of temperature, relative humidity, and air velocity (Mohanty and Akbari, 2012). The characteristic drying curve of coal particles are divided according to three different periods during the drying process (De Korte and Mangena, 2004).

Figure 2.4.1 shows the characteristic drying curve of coal fines in the presence of temperature change. During the initial drying period, sensible heat is transferred to the moisture located in the fine coal particles (De Korte and Mangena, 2004). As demonstrated in Figure 2.4.1, the fine coal is heated to allow the coal particles to reach the temperature of the evaporation process. The rate at which the moisture is removed increases during the initial drying period, thereby removing the bulk of the surface moisture present (De Korte and Mangena, 2004). The second drying period is considered the constant drying rate as evaporation occurs continuously at a constant rate (Rowan, 2010). The moisture present in pores and capillaries of the coal fines is transferred to the surface of the coal at a rate equivalent to the rate at which the moisture is removed from the surface of the coal. This means that the heat, which is transferred from the warm air, is equal to the heat that is removed from the coal particle's surface by evaporation. This allows the surface temperature of the coal to approach the saturation temperature of the drying air (Rowan, 2010). The factors that govern the constant rate period include the velocity of the drying air as well as the temperature and relative humidity conditions of the air (De Korte & Mangena, 2004).

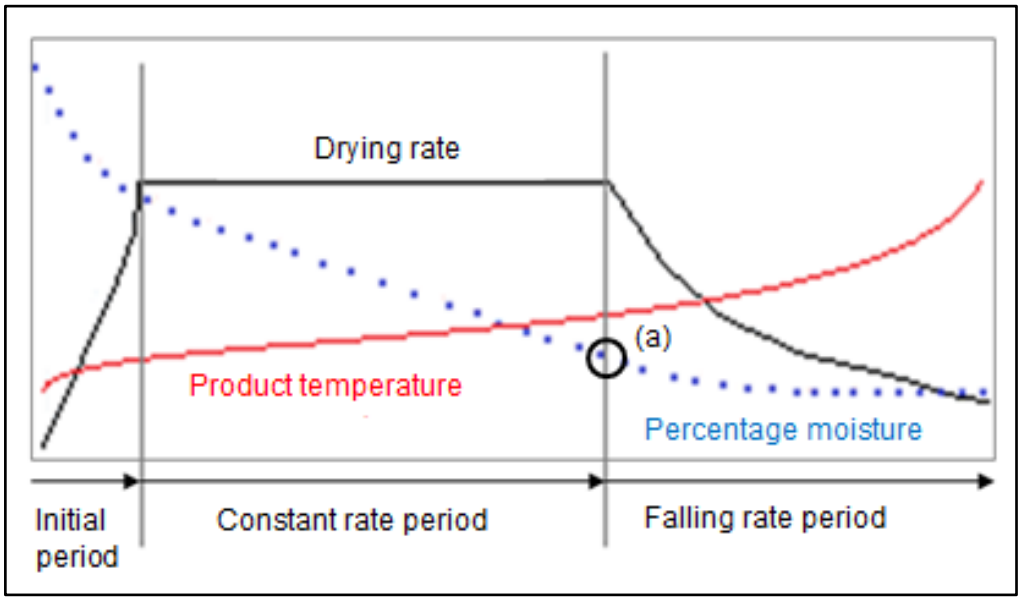

Figure 2.4.1: Typical drying curve of coal, adapted from Mohanty and Akbari (2012)

The last stage of the drying curve, in Figure 2.4.1, is referred to as the falling rate period. The falling rate period is characterised by a decline in the drying rate that continues until the coal particles are nearly dry. The critical surface moisture content (a) of the coal particles is indicated on Figure 2.4.1. The critical moisture content is the point where the drying rate starts to decline (Rowan, 2010). The critical moisture content is reached when the moisture concentration on the surface area is considerably lower than the moisture concentration that was available during the first two periods. In this phase, the controlling factor shifts from the rate of moisture migration to surface area availability (De Korte and Mangena, 2004). In conclusion, the moisture reduction rate demonstrated by the three distinct drying periods in Figure 2.4.1 will vary according to the magnitude of the applied force or drying technique. However, irrespective of the drying time required during each period, the three distinct periods will be ever-present.

2.4.2 Phase equilibrium

Vapour-liquid equilibrium refers to a state of stability reached by the liquid phase of a substance, and its vapour phase where the rate of condensation is in balance with the rate of evaporation, and no net vapour-liquid inter-conversion exists (Le Roux *et al*, 2013). In addition to the various moisture types associated with coal, as described in Section 2.3, particle-water interactions also exists between the moisture and the coal particles (Condie and Veal, 1998). Particle-water interactions can be categorised into various states.

Saturation is achieved by porous particles when the voids and interstitial pores of the particles are entirely occupied by water. The magnitude of capillary forces is largely governed by capillary radii, the angle of contact and the surface tension. If a force (pressure or gravity) that is applied is smaller than the capillary forces, moisture displacement will not occur. However, if the applied force exceeds the capillary forces, moisture displacement from the capillaries and pores to the adjacent air will take place (Condie and Veal, 1998). A vapour-liquid equilibrium substance is usually called a saturated fluid. As indicated on the phase diagram in Figure 2.4.2, the governing factors of the thermodynamic state of water are, vapour pressure and thermal capacity. The phase equilibrium between vapour and liquid may be disrupted when these driving forces are applied (Koretsky, 2004).

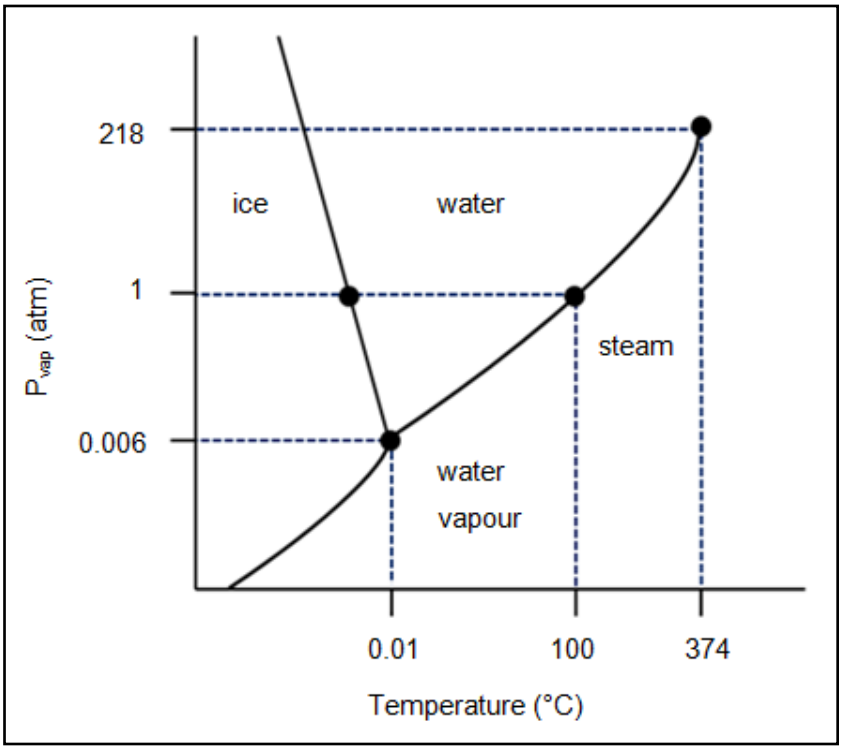

Figure 2.4.2: Phase diagram of water

Therefore, when an applied force disrupts relative humidity equilibrium within the system, water molecules are displaced from cracks, and capillaries of a porous particle by the process of desorption.

2.5 Conventional fine coal dewatering

Conventional drying technologies have been the backbone of the coal industry, and have historically proven its limited effectiveness in the field. However, the coal industry has

become less tolerant of these techniques because of cost implications, and pollutant emissions (Bratton *et al*., 2012). Mechanical dewatering is described kinetically as the outflow process of water, from a mass of particles. As mentioned in Section 2.2.2, mechanical dewatering techniques are able to reduce moisture contents of coal fines, and ultra-fines, to 15%$_{wt}$ and 25%$_{wt}$, respectively. This is discouraging for the coal preparation industry, which caters for a market sector calling for lower final moisture contents, as in the case of coal-based power stations. In the past, whenever mechanical dewatering techniques failed to deliver contract specifications, the solution has leaned towards thermal dewatering which is the most effective (and expensive) dewatering technique (Bratton *et al*., 2012). When implemented properly, this technique may lower moisture levels in coal fines to single digits, increasing the calorific value of the coal (Bratton *et al*., 2012). When considering cost, thermal drying is still considered by many an expensive venture, because the value of the dewatered coal fines does not validate the use of thermal techniques (Bland & McDaniel, 2014). An added disadvantage is the generation of thermal pollutants under stringent government enforced emission restrictions (Bratton *et al*., 2012).

Realizing the pressing need to develop a cost effective alternative dewatering technique to account for the coal fines fraction discarded, researchers have been conducting studies that stretch beyond the field of conventional coal dewatering techniques. Section 2.6 further elaborates on the modern dewatering techniques for coal fines.

2.6 Emerging techniques for fine coal dewatering

Moisture located in the micro-pores, and –capillaries, of coal is expensive to remove due to the time consuming falling rate period discussed in Section 2.4.1 (Mohanty and Akbari, 2012). In recent years, searches for innovative, cost efficient, and eco-friendly drying techniques have intensified (Bratton *et al*., 2012). One such advanced dewatering process that was developed employs drying media to adsorb remaining surface moisture from the coal fines after mechanical dewatering. In a similar study conducted by Bland and McDaniel (2014), it was found that the moisture content of coal fines was trimmed down to single digit values by implementing porous drying media. The moisture reduction in the fine coal circuit will spur a beneficial increase in the heating value of the fine coal, which is redirected to augment the clean coarse coal circuit (Bratton *et al*., 2012). This redirection of clean fine coal adds to the plant's yield without reducing the plant's original heat content. Mohanty and Akbari (2012) expect the increase in production revenue to outweigh the additional capital costs, and elevate the overall profitability of the coal preparation plant within time.

2.7 Adsorption

Separation processes are considered a large contributor to nominal production costs in the industry (Glover, 2008). Glover (2008) interprets the term “adsorption”, as the process of accumulation of molecules on the surface area of the adsorbent material, whereas desorption is defined as the reverse process. During the process of adsorption, water molecules are expected to leave the coal, and relocate to the adsorbent material. This mechanism involves transferal of water molecules from the surface, and capillaries of the coal fines to the surface, and capillaries of the adsorbents by liquid film movement, and moisture diffusion. Employing adsorption as an effective separation tool requires understanding of the operational system as well as the equilibrium, and mass transport interrelation, on a fundamental level (Knaebel, 2006). The mechanism involved with adsorbent assisted drying is known as contact-sorption drying, and is discussed in Section 2.7.1.

2.7.1 Contact-sorption drying

Contact-sorption drying is the process whereby dry adsorbents and a wet material are contacted for a predetermined time period to allow moisture transfer to occur (Kudra & Mujumdar, 2009). The adsorbents are separated by size after sufficient time has elapsed, regenerated, and returned to the process (Bland and McDaniel, 2014). The technical viability of contact-sorption drying relies greatly on adsorbent regeneration, and adsorbent reuse (Knaebel, 2006). The method of contact-sorption drying is complicated, as moisture displacement occurs in distinct phases, and multi-component systems, and is typically helped along by thermal effects (Kudra & Mujumdar, 2009). Figure 2.7.1 shows the various stages of contact-sorption drying taking place in a changing system, where sorbent-material, material-material, and sorbent-sorbent interactions occur.

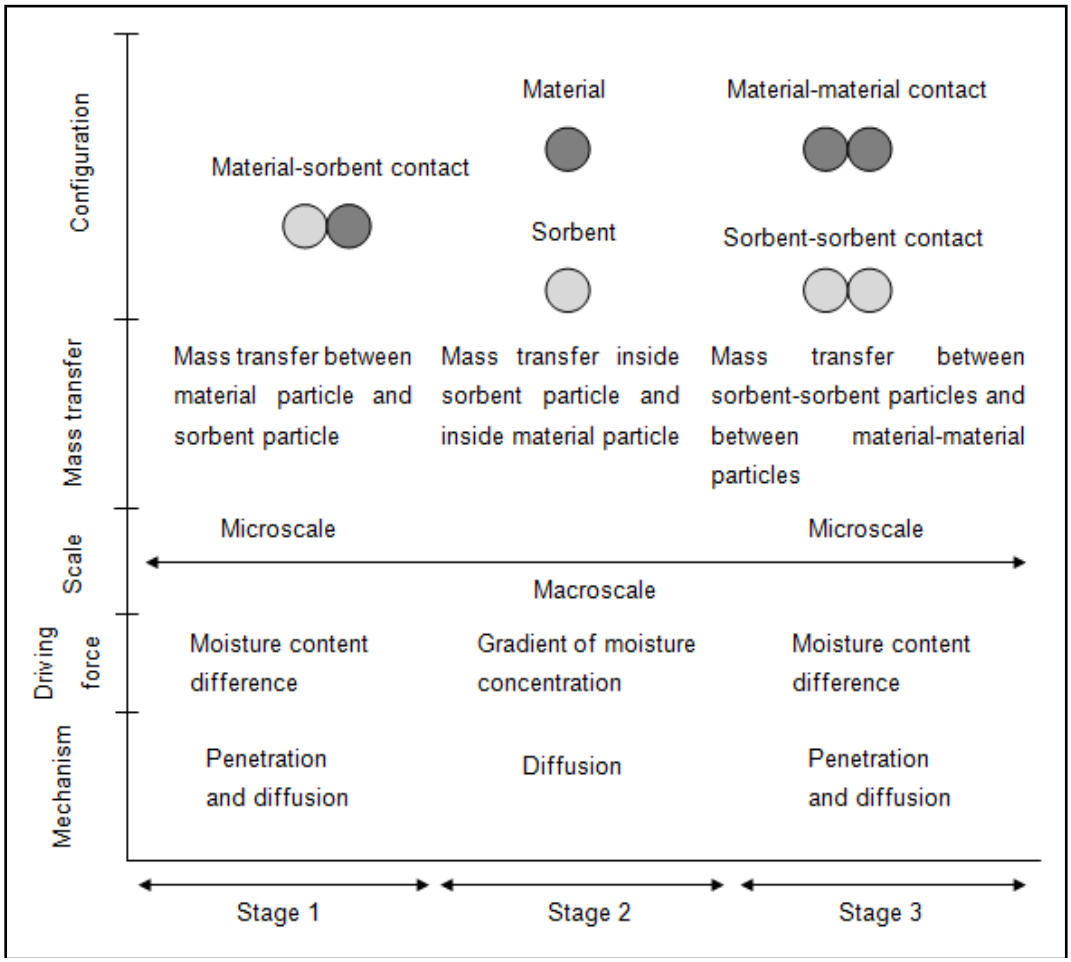

Figure 2.7.1: Mechanism of contact-sorption drying taken from Kudra & Mujumdar (2009)

Stage 1 in Figure 2.7.1 shows that when capillary porous dry adsorbents, and wet material come into contact, the surface layer of the adsorbent initially adsorbs liquid moisture from the surface of the material by capillary flow. As a result, the transfer rate of liquid moisture is reliant on on the area available for contact between the adsorbent, and wet material (Kudra and Mujumdar, 2009). At a certain point, due to the progressive decrease of surface moisture, the suction potential at the material, and adsorbent equals, and moisture transfer through the boundary stops (Kudra & Mujumdar, 2009). Adsorbed moisture migrates from the surface of the adsorbent to its core, and from the material's core to its surface along a concentration gradient in Stage 2, shown in Figure 2.7.1 (Kudra & Mujumdar, 2009). After satisfactory contact time has elapsed, the rate of moisture uptake from the material is minimal, indicating the mass transfer is nearing completion, and the adsorbents can be recovered for regeneration. If the adsorbents are not removed, Stage 3 is likely to occur. Stage 3 is not desired as the process is essentially reversed where the moisture is re-adsorbed onto the surface of the material due to the surface moisture difference established between the adsorbent and material. Contact-sorption drying can be repeated for further

removal of moisture until the desired moisture level in the material is achieved. In actual application, the required time for contact is comparatively less than that necessary to achieve adsorbent-material equilibrium, leading to continual moisture migration after adsorbent-material contact (Kudra & Mujumdar, 2009). Given the alternative of random motion, which is characteristic of fluidised beds, and mixers, adsorbent-adsorbent, and material-material contact is likely to arise, which may encourage further displacement of moisture on a microscopic level.

2.7.2 Classification of adsorbents

Adsorption is typically subdivided into two groups, which include physical adsorption, and chemical adsorption. Physical adsorption is a reversible process that involves intermolecular forces such as van der Waals forces, while chemical adsorption engages valence forces similar to those in the formation process of chemical compounds (Dabrowski, 2001). Physical adsorption is more common, and occurs predominantly during adsorption. Table 2.2 sums up the characteristics by which physical adsorption are usually distinguished.

Table 2.2: Characteristic features of physical adsorption, taken from Dabrowski (2001)

Characteristic feature	Description
Weak bonding (long range)	Van der Waals forces
Adsorption enthalpy	Minimum: 5kJ/mol Maximum: 50kJ/mol
Not specific to surface	Provided the temperature is suitably low, physical adsorption will occur amongst all molecules, regardless of the type of surface.
Reaction	Surface activation does not occur as equilibrium reached relatively rapidly. Surface reactions do not occur.
Adsorption: “multilayer”	Adsorption equilibrium, which is usually demonstrated by means of a BET isotherm.

Inert sorbents can be further classified into porous and nonporous adsorbents. Today adsorbents are mass-produced differing in chemical composition, and structure. Porous adsorbents have countless applications in industry such as gas adsorption, and separation practices (Dabrowski, 2001).

2.7.3 Adsorbent selection

Adsorption refers to water molecules spontaneously gathering at the surface of the individual solid adsorbent rather than the bulk. The degree of adsorption at equilibrium is dependent on temperature, vapour pressure, and the specific surface area of the adsorbent. Prior to adsorption, the gas phase is referred to as adsorptive, whereas in the adsorbed state gas molecules are termed “adsorbate” (Kudra & Mujumdar, 2009).

Knaebel (2006) noted that the success of an adsorbent as a drying agent is reliant on the loading capacity of the adsorbent, the adsorbent compatibility, and the ability of the adsorbent to be regenerated. Adsorbent capacity, or adsorbent loading, is an imperative characteristic of adsorbents, and usually directs the adsorbent selection process (Knaebel, 2006). Adsorption capacity is measured by various means, including surface area available for accumulation (Knaebel, 2006). Adsorption capacity is of chief importance when determining the amount of adsorbents required during the dewatering process. As a result, adsorption capacity also governs the costs associated with installation of the adsorber vessel, as it fixes the volume of this vessel (Knaebel, 2006). After the adsorbent material has reached its full capacity, the adsorbent can either be regenerated or discarded. In order to make the use of adsorbent drying eco-friendly, and cost-effective, adsorbent regeneration is important (Kulkarne and Kaware, 2014). Therefore, the technical viability of employing adsorbents as a drying agent depends on the regeneration ability of the adsorbent material (Knaebel, 2006).

2.7.4 Industrial adsorbents

To date, several types of adsorbents are manufactured for industrial separation processes (Mohanty and Akbari, 2012). Well known industrial adsorbents include silica gel, activated alumina, and molecular sieves.

- Silica gel

Silica gel is produced by the precipitation from acid treated sodium silicate solutions (Knaebel, 2006). This porous, sponge-like adsorbent is rigid in structure. Silica gels have a particularly large inner surface area, with countless microscopic voids, and a large network of interconnecting capillary channels joining the inner voids with the outer surface area (Knaebel, 2006). As the concentration of water vapour in contact with the silica gel increases, so does the adsorptive capacity. Different changing rules apply for different pore sized silica gels, and consequently the adsorptive capacity performances will also vary accordingly. Figure 2.7.2 indicates the adsorption isotherm curves of three types of silica gels with varying pore sizes.

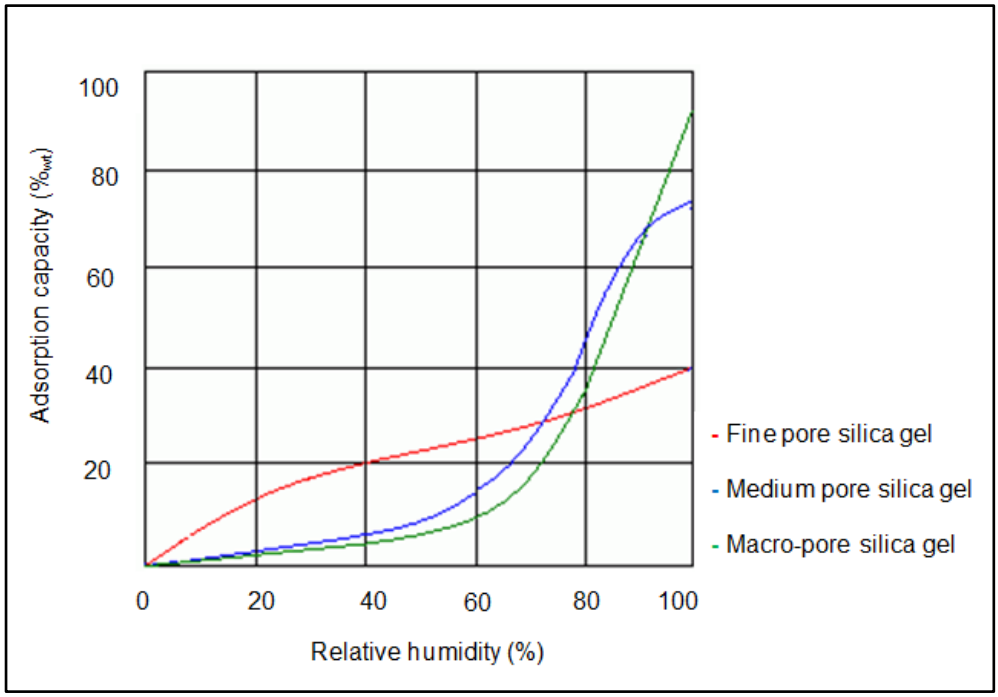

Figure 2.7.2: Adsorption capacity of silica gel taken from CSGC (2014)

Fine, medium, and macro-pored silica gels were used to construct the isotherm curves in the presence of air with various relative humidity conditions (CSGC, 2014). From the fine pore curve in Figure 2.7.2, it is clear that at lower relative humidity conditions the adsorptive capacity is higher; while the macro pore curve is indicative of a high adsorptive capacity under high relative humidity conditions (CSGC, 2014). Silica gels are usually chosen according to the environment, and conditions it best suits.

- Molecular sieves

Industrial ceramics are commonly referred to as molecular sieves. Porous glasses, zeolites, activated carbon, alumina-silicate minerals, clays, and other synthetic compounds are some well-known adsorbents classified under molecular sieves (Bland & McDaniel, 2014). Alumina-silicates are the mineral constituent that is most commonly present in molecular sieves, and can be classified on a weight basis ranging from $10\%_{wt}$-$100\%_{wt}$ (Bland and McDaniel, 2014). In some cases the sieves are strengthened by enhancing the chemical composition with minerals such as titanium and zirconium oxides. Molecular sieves contain precise, and uniform sized pores, and can adsorb gasses or liquids during separation processes (Knaebel, 2006). A range of molecular sieves can be employed, either alone or in combination, to dewater coal fines. Small molecules such as water and nitrogen can diffuse into molecular sieves with ease due to their open pore structures, but are small enough to prevent coal fines from entering. Bland and McDaniel (2014) remarked that molecular sieves could effectively be dewatered to permit reuse, as they are sturdy, and are not easily degraded.

- Activated alumina

Activated alumina is an aluminium oxide material that is activated at elevated temperatures, and primarily implemented for capturing moisture from gas streams such as air, industrial gasses, and CO_2 gas (Milton and Buffalo, 1962). This durable, hard ceramic compound is highly porous, and can adsorb liquids and gasses (Milton and Buffalo, 1962). Relative to using molecular sieves, activated alumina proves to be more advantageous in a number of ways including hydroxylated surfaces that draw water molecules strongly, and adheres with water by hydrogen bonding (Bland and McDaniel, 2014). Activated alumina is comprised primarily of aluminium oxide, and can have surface areas exceeding $200m^2/g$ (Knaebel, 2006). The surface area to weight ratio is significantly high, and the porous nature displays channels forming a network throughout the particle allowing for adsorption of significant moisture volumes to porous surface distributions. Activated alumina has pores that are large enough to draw water molecules into its channel network, but small enough to prevent coal fines from moving into the porous bead (Knaebel, 2006). Activated alumina is typically white in colour, and manufactured in spheres that has the ability of enduring substantial abrasion and wear (Bland and McDaniel, 2014). Additional materials may be introduced in this ceramic compound in an aid to enhance certain properties, such as adsorption capacity, and strength. The high crushing strength sanctions very slow destruction, and so increases its service life (Bland and McDaniel, 2014).

The curve shown in Figure 2.7.3 shows the water adsorption on three of the discussed adsorbents. The curve demonstrates the weight percentage water adsorbed onto the adsorbents at 25°C in the presence of an air stream.

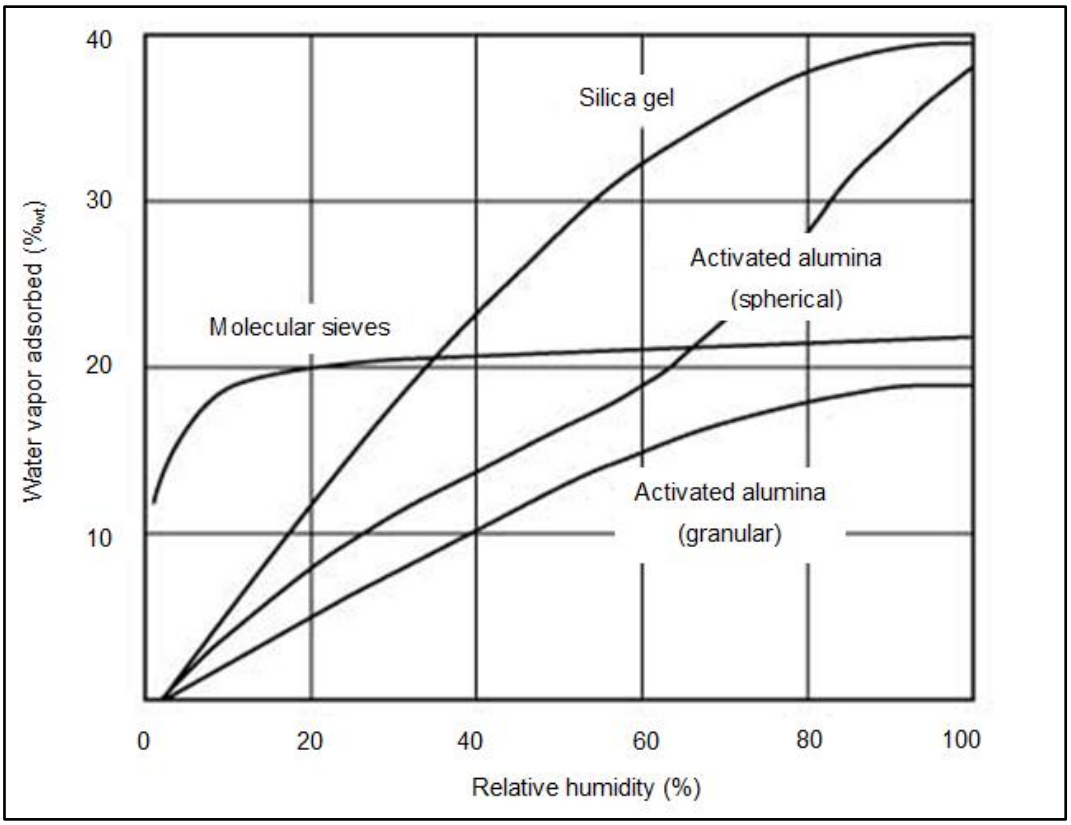

Figure 2.7.3: Adsorption capacity of adsorbents taken from Risheng (2014)

Figure 2.7.3 shows that the percentage water adsorbed by silica gels grows in a linear tendency to the relative humidity up to about 60%. As the air stream approaches 100% relative humidity, the curve plateaus. On the other hand, molecular sieves show a strong affinity to water adsorption up to 20%RH, after which it plateaus quickly (Risheng, 2014). This explains why molecular sieves are popular for industrial regeneration applications, for example in dehumidification systems, in which the relative humidity of process air streams must be reduced.

2.8 Previous studies

2.8.1 Coal drying method and system

In a recent study, the effect of adsorbent drying was investigated by combining adsorbent material with saturated coal fines. Bland & McDaniel (2014) found that by combining coal fines of ≤0.7mm with an adsorbent effectively reduced the moisture load of the fines to an economically attractive ≤8%$_{wt}$. This process entailed continually agitating the coal fines, and adsorbent material to ensure maximum surface area exposure (Bland & McDaniel, 2014). Following a sufficient agitation period, the coal fines, and adsorbents were separated based on particle size difference. Most adsorbents have the ability to endure agitation for a number of cycles in a bed of fine coal particles without flaking or splintering (Bland and McDaniel, 2014). The adsorbent media were capable of removing large capacities of water from the coal fines, and the mixture was separated readily by screening. Regeneration of these adsorbent can be achieved by thermal swing, pressure swing or a combination of thermal and pressure swing (Knaebel, 2006). The process of adsorbent assisted drying is referred to as nano-drying technology (NDT) process (Bratton *et al*., 2012).

Coal fines can be dried using molecular sieves in a closed loop system as shown in Figure 2.8.1.

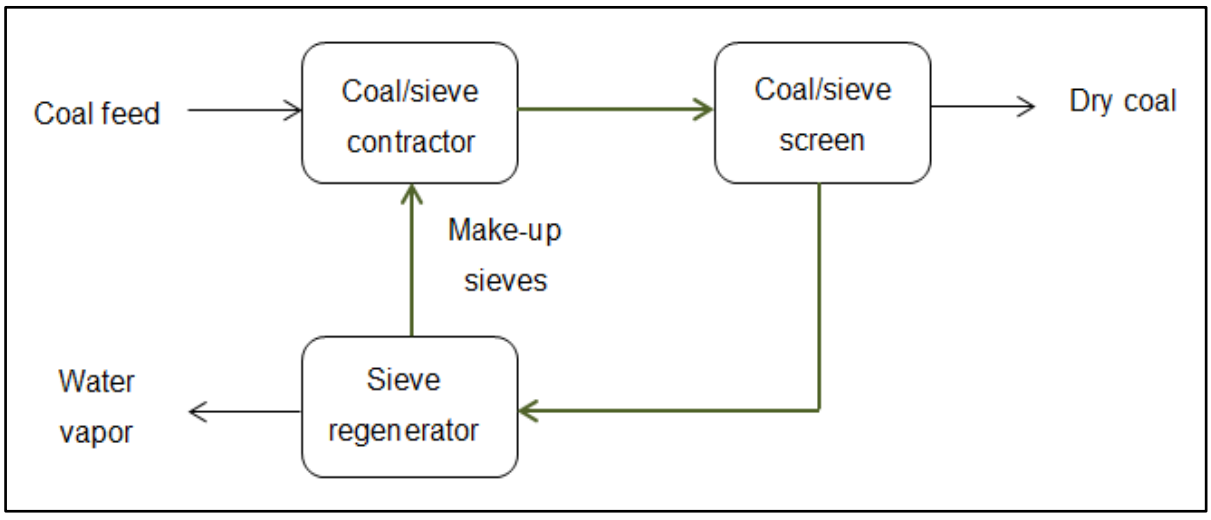

Figure 2.8.1: Closed-loop drying system of coal fines adapted from Bratton *et al*. (2012)

The mixing section in Figure 2.8.1 is illustrative of the molecular sieves and coal fines that are mixed, and continually agitated, to ensure adequate contact. After sufficient drying time has elapsed, the molecular sieves, and coal fines are separated according to size by screening. The coal fines are usually the underflow of the screen while the molecular

sieves are the overflow of the screen (Mohanty and Akbari, 2012). The molecular sieves carry minute amounts of coal dust along on their outer surface (Bland and McDaniel, 2014). The saturated sieves are regenerated by heating during which minimal agitation is required. After regeneration, the molecular sieves are introduced into the mixing stage by a make-up stream. As mentioned in Section 2.7.1, the economic feasibility of contact-sorption drying is fully reliant on the ability of the adsorbent to be regenerated and reused (Bland and McDaniel, 2014).

Bland and McDaniel (2014) concluded that this closed-loop system outperforms conventional dewatering techniques such as Centribaric^{TM}, and screenbowl centrifuge systems. Moreover, NDT processes reduce moisture load of coal fines to below 10%$_{wt}$ irrespective of the particle size variations in the feed stream (Bratton *et al*., 2012). Repeatability tests shown in Figure 2.8.2 show the predictability, and controllability, of adsorbent assisted drying (Bland & McDaniel, 2014).

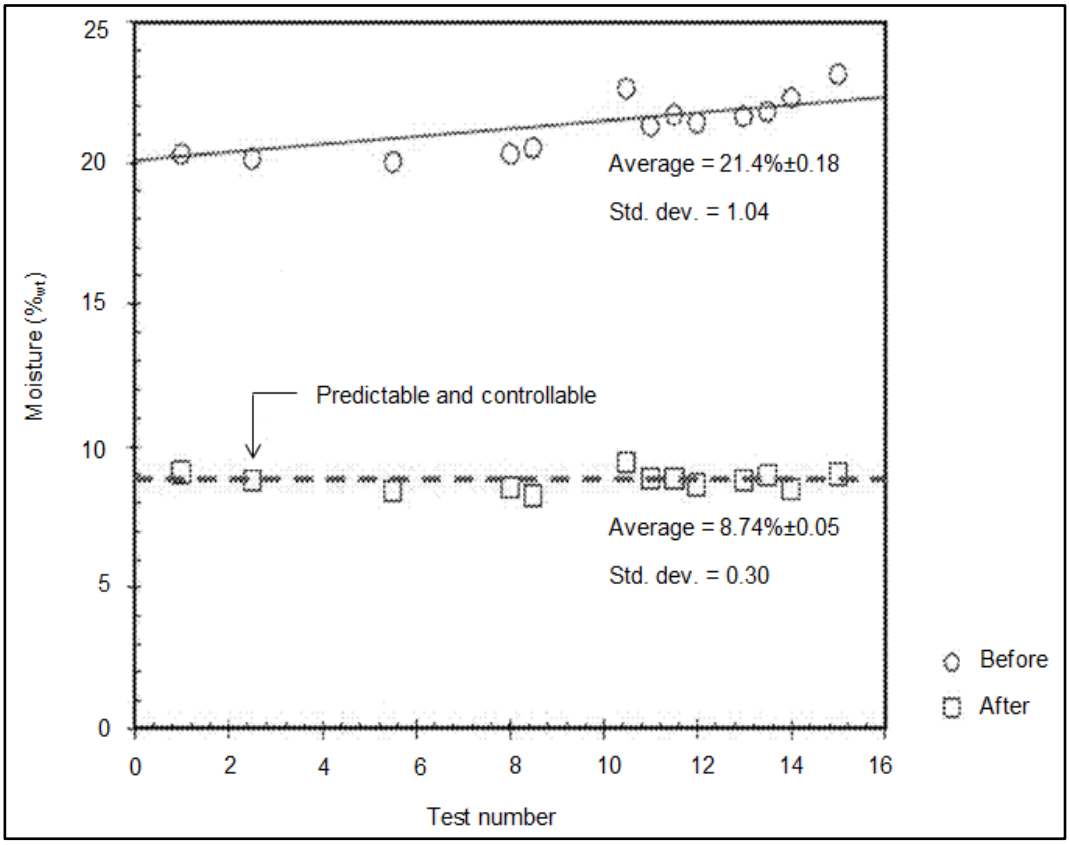

Figure 2.8.2: Dewatering repeatability of coal fines taken from Bland & McDaniel (2014)

An average coal fines moisture reduction of ±12.66%$_{wt}$ was achieved by using this technique as presented in Figure 2.8.2. Moreover, Figure 2.8.2 also shows the consistent final moisture content of the coal fines was obtained for 13 batch tests after a predetermined time

period of contacting (Bland and McDaniel, 2014). Additionally, batches of coal fines (±15 grams) with an initial moisture load of ±30%$_{wt}$ were mixed with molecular sieves for 60 minutes to achieve a final moisture load below 5%$_{wt}$. After screening, the molecular sieves were placed in an oven at 100°C, and weighed periodically. The aim of this periodic weighing scheme was to govern the time frame required for driving off water adsorbed from the coal fines (Bland and McDaniel, 2014).

Figure 2.8.3 provides a comparison of the relative pollutant emissions of NDT processes and thermal drying techniques.

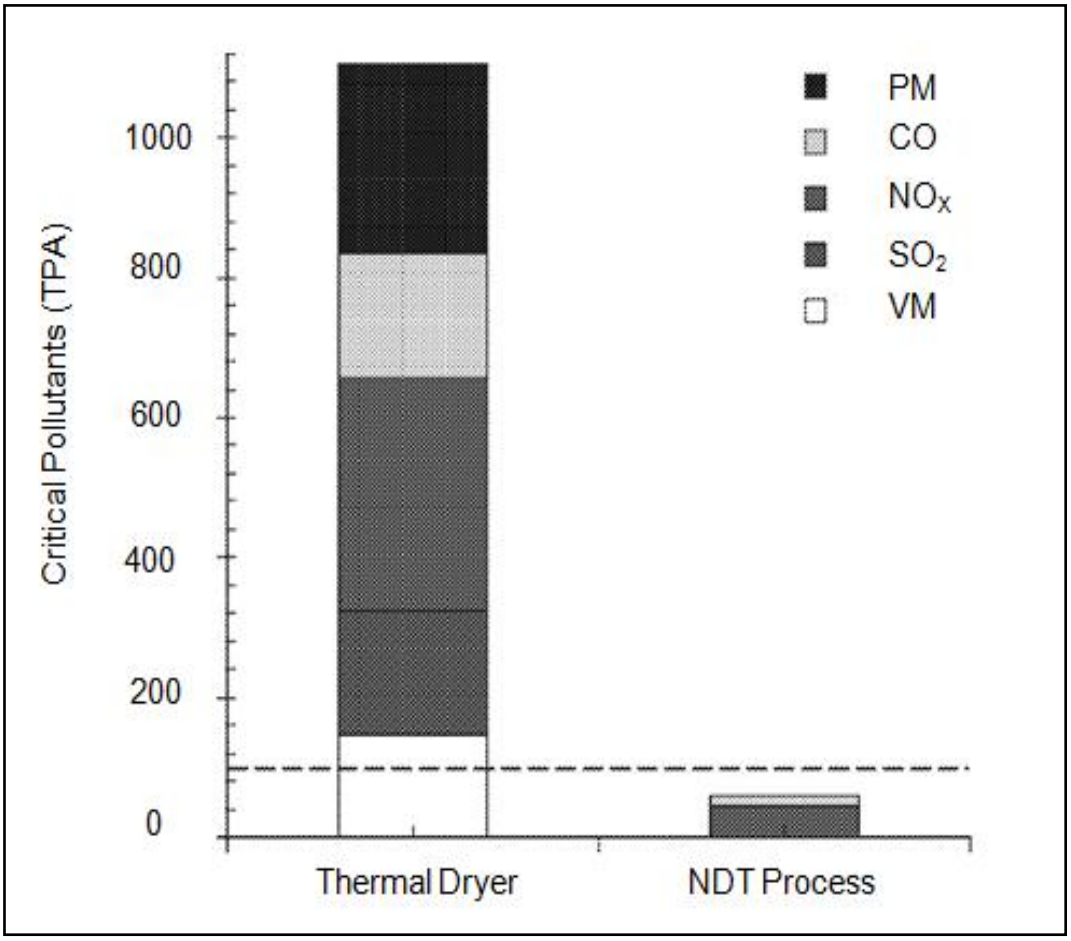

Figure 2.8.3: Critical pollutants of thermal drying versus NDT process, taken from Bland & McDaniel (2014)

From Figure 2.8.3, it was apparent that the NDT process is immensely cleaner when compared to thermal dryers (Bland & McDaniel, 2014). A significant reduction in particulate matter emissions, including aerosolized coal dust, provides a considerable advance above thermal drying. Furthermore, combustion by-products, NO_X, SO_2, CO, and volatile matter, are significantly reduced by implementing NDT processes (Bland & McDaniel, 2014).

Figure 2.8.4 shows the relative drying cost of coal by implementing the NDT process, compared to conventional thermal drying methods (Bland & McDaniel, 2014).

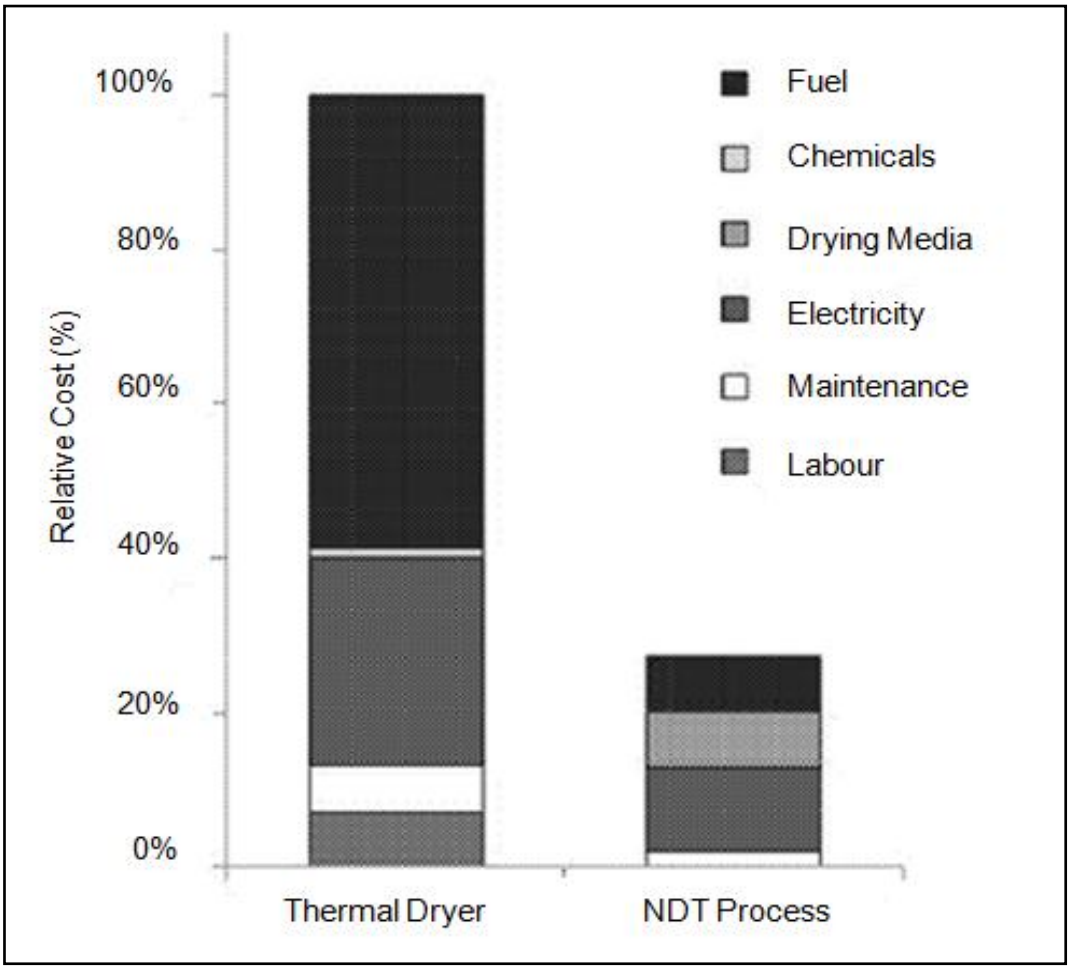

Figure 2.8.4: Relative cost of thermal drying versus NDT process, taken from Bland & McDaniel (2014)

The largest portion of the thermal drying relative cost, fuel and electricity, was saved by drying coal fines using the NDT process, as indicated in Figure 2.8.4. The nominal cost of the NDT process is about one third of that required to dry coal fines by employing existing thermal drying methods (Bland & McDaniel, 2014). From an economical view, the closed-loop system provides a significant reduction in coal fines drying expenditure compared to thermal drying.

2.9 Summary and conclusion

The solution to dewatering fine coal to moisture levels in line with contract specifications has long eluded the coal industry. As discussed in Section 2.5, the coal industry has become

less tolerant of thermal drying because of cost implications, and pollutant emissions. Adsorbent assisted drying, also referred to as “contact-sorption” or “nano-drying technology (NDT)”, have grown increasingly popular over recent years due to its cost effectiveness and environmentally friendly advantage. Adsorbent assisted drying employs porous drying media to lower the surface moisture of mechanically dewatered fine coal. Various studies were conducted in which porous drying media was successfully implemented to trim down the moisture content of fine coal to single digit values. This moisture reduction in the fine coal circuit will spur a beneficial increase in the fine coal heating value, which is redirected to supplement the clean coarse coal circuit and adds to the plant’s overall yield. The drying performance of fine coal in the presence of adsorbent material will be examined during this study, by employing fixed-bed and cascading-bed drying techniques, while the regeneration of adsorbents will also be investigated by employing an air-drying technique instead of microwave drying.

3

CHAPTER

EXPERIMENTAL METHODS

To study the process of surface moisture displacement between coal particles and capillary-porous adsorbent material, the nature of the coal fines and adsorbent material used should be inspected. Chapter 3 details the experimental strategy followed throughout this investigative study. Chapter 3 commences with Section 3.1, which gives a brief overview of the process under investigation. Section 3.2 introduces the materials used, and Section 3.3 elaborates on the variables, and subsequent parameters implemented during the experimental procedure. The experimental plan is detailed in Section 3.4, the sample preparation is summarised in Section 3.5. Lastly, the supplementary experimental work is discussed in Section 3.6.

3.1 Overview

The purpose of this study is investigating the drying performance of moist coal fines (-2mm+1mm, -1mm+0.5mm, -0.5mm+0.25mm) in the presence of an adsorbent material. This was done by monitoring the desorption of moisture from coal, and the adsorption of moisture onto adsorbents at 25°C and 40%RH. The effect of alterations on manipulated variables such as adsorbent to coal mass ratio, adsorbent type, adsorbent size, and mass coal particle size range were observed and finally, the effect of motion on the drying performance of the coal fines was investigated by implementing fixed-bed and cascading-bed drying techniques. The used adsorbents were recovered, and a set of regeneration experiments were investigated.

3.2 Materials used

3.2.1 Coal

The coal used for this study is sub-bituminous coal originating in the Highveld coalfield located in Mpumalanga, South Africa. The coal was stored in plastic bags to prevent the

inherent moisture equilibrium of the coal to be disturbed by the ambient air conditions whilst in storage. Table 3.1 contains the results of the proximate and ultimate analysis as well as the total sulphur of the coal used on both air dried and dry bases.

Table 3.1: Proximate and ultimate analyses

Sample Identification		Coal fines		Test method standard
		Air dry basis result	Dry basis result	
Proximate Analysis	% Inherent moisture content	3.6	-	ACT-TPM-010 based on ISO11722: 1999
	% Ash content	14.9	15.5	ACT-TPM-011 based on ISO 1171: 2010
	% Volatile Matter	29.6	30.7	ACT-TPM-012 based on ISO 562: 2010
	%Fixed carbon *(by calculation)*	51.9		(by difference)
	% Total sulphur	0.97	-	ACT-TPM-013 based on ISO 19579: 2006
Ultimate Analysis	% Carbon Content	63.20	-	ACT-TPM-027 based on ISO 29541: 2010
	% Hydrogen Content	4.04	-	
	% Nitrogen Content	1.57	-	
	% Oxygen Content *(by calculation)*	11.71	-	

The inherent moisture content in Table 3.1 indicates the initial amount of moisture present in the coal in situ. According to Rodrigues and Lemos de Sousa (2002), sub-bituminous coals have macro pores that enhance the permeability of the coal to certain liquids. The value of the inherent moisture content of coal depends on the porosity of the coal sample (Gupta, 2010). This relatively high inherent moisture in Table 3.1 is indicative of a relatively high degree of porosity, which is useful when studying the drying performance of the coal.

3.2.2 Adsorbents

Two types of adsorbents were selected for the experimental investigation. For purposes of this study, spherically shaped alumina and silica-based ceramic adsorbents were selected. These adsorbents are composed primarily of fractional compositions of Al_2O_3 and SiO_2. The selection was mainly based on the commercial availability, the working capacity of the adsorbent, and its porous nature.

The first adsorbent selected for investigation was F-200 activated alumina adsorbent consisting predominantly Al_2O_3 with trace amounts of SiO_2, Fe_2O_3 and Na_2O. For descriptive purposes, the F-200 adsorbent will be referred to as an alumina-based adsorbent. The second adsorbent material selected for investigation is Silsorb N10 adsorbent. The Silsorb N10 adsorbent is known for predominantly SiO_2 component; however, a low proportion of Al_2O_3 was incorporated into the blend during manufacture. From this point onward, the Silsorb N10 adsorbent will be referred to as a silica-based adsorbent. Table 3.2 contains the main components present in the alumina-based and silica-based adsorbents respectively.

Table 3.2: Typical composition of adsorbents

Component	Adsorbent type	
	Alumina-based (F-200)	**Silica-based (Silsorb N10)**
Al_2O_3 content (%)	92.70	3.0
SiO_2 content (%)	0.02	97.0
Fe_2O_3 content (%)	0.02	-
Na_2O content (%)	0.30	-
Loss on ignition: 250-1100°C (%)	6.96	-

Figure 3.2.1 displays the (a) alumina-based and (b) silica-based adsorbents used during this investigation. The spherically shaped adsorbents have a white colour as can be seen in Figure 3.2.1.

Figure 3.2.1: Physical appearance of the alumina and silica-based adsorbents

The physical properties of the alumina-based and silica-based adsorbent are summarized in Table 3.3. It useful to note the total pore volume and package moisture as these give an indication of the porosity of the material.

Table 3.3: Physical properties of adsorbents

Physical properties	Adsorbent type	
	Alumina-based (F-200)	Silica-based (Silsorb N10)
Surface area (m^2/g)	350	750
Total pore volume (cm^3/g)	0.5	0.4
Packed bulk density (kg/m^3)	769	800
Package moisture ($\%_{wt}$)	1.80	1.69

The total pore volume of the silica-based is less than the alumina-based adsorbents however; the effective surface area of the silica-based adsorbent is almost double that of the alumina based adsorbents. Based on this, the porosity and surface area of the adsorbents were investigated further, and the results are discussed in Section 3.6.2.

3.3 Variables

The set conditions considered in this study are summarised in Table 3.4. The set conditions include coal type and atmospheric conditions (temperature and relative humidity).

Table 3.4: Set conditions

Set conditions	
Constant	**Description**
Coal type	Highveld sub-bituminous coal
Temperature	25°C
Relative humidity	40% RH

A set of manipulated variables were investigated during this study, each consisting of a set of operating parameters. The manipulated variables are provided in Table 3.5.

Table 3.5: Manipulated variables

Manipulated variables	
Variable	**Operating parameters**
Adsorbent type	Alumina based adsorbent Silica based adsorbent
Adsorbent to coal mass ratio	3:1 2:1 1:1 0.75:1 0.5:1
Adsorbent size	3mm 5mm
Coal particle size ranges	-2mm+1mm -1mm+0.5mm -0.5mm+0.25mm
Adsorbent condition	Unused adsorbents Used adsorbents Air dried adsorbents
Drying technique	Fixed-bed Cascading-bed

The responses in Table 3.6 were measured to determine the dependence of the final moisture content, dewatering time of coal, and the moisture transfer rate on the manipulated variables given in Table 3.5.

Table 3.6: Responses

Responses	
Description	**Unit**
Inherent surface moisture	g(moisture)/g(adsorbent and moisture) g(moisture)/g(coal and moisture)
Moisture transfer rate	(g[moisture]/g[adsorbent and moisture])/min (g[moisture]/g[coal and moisture])/min
Drying time of coal	minutes

Loading is a key property of an adsorbent, and is described as the quantity of moisture taken up by the adsorbent per unit mass of adsorbent (Knaebel, 2006). This definition also applies for porous coal particles. The surface moisture of both the coal and adsorbents measured at various time intervals was categorized as a response. The adsorption rate (g[moisture]/g[adsorbent and moisture]/min), and desorption rate (g[moisture]/g[coal and moisture]/min), of moisture as well as the total drying time of the coal (min) was investigated during this study to determine the best performing operating parameters according to initial rate, final surface moisture contents, and optimum contact time.

3.4 Experimental plan

The experimental plan was subdivided into three sections according to the drying techniques and regeneration experiments conducted.

3.4.1 Fixed-bed drying technique

Cylindrical vessels, with an inner diameter of 5cm and a length of 5.5cm, were used during the experimental procedure of the fixed-bed drying technique. A wet coal sample of 10g, and a predetermined mass of adsorbent material was placed in the cylindrical vessels and sealed. Figure 3.4.1 shows the top view of the fixed-bed vessels containing the combined coal and adsorbent sample.

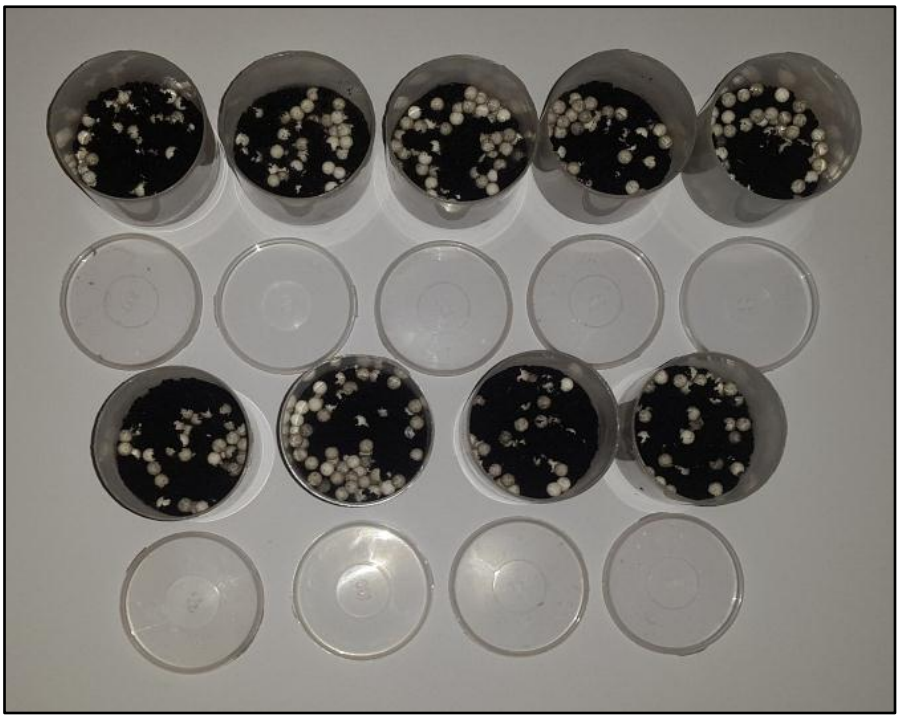

Figure 3.4.1: Top view of fixed-bed vessels

The mass of adsorbent material was determined in accordance with the adsorbent to coal mass ratio selected for investigation. The vessels were shaken promptly to promote uniform distribution of adsorbent particles (adsorbent/adsorbents) throughout the coal bed. The closed cylindrical vessels were set aside to rest and allow moisture transfer to occur. Figure 3.4.2 schematically represents the experimental procedure of the fixed-bed drying technique.

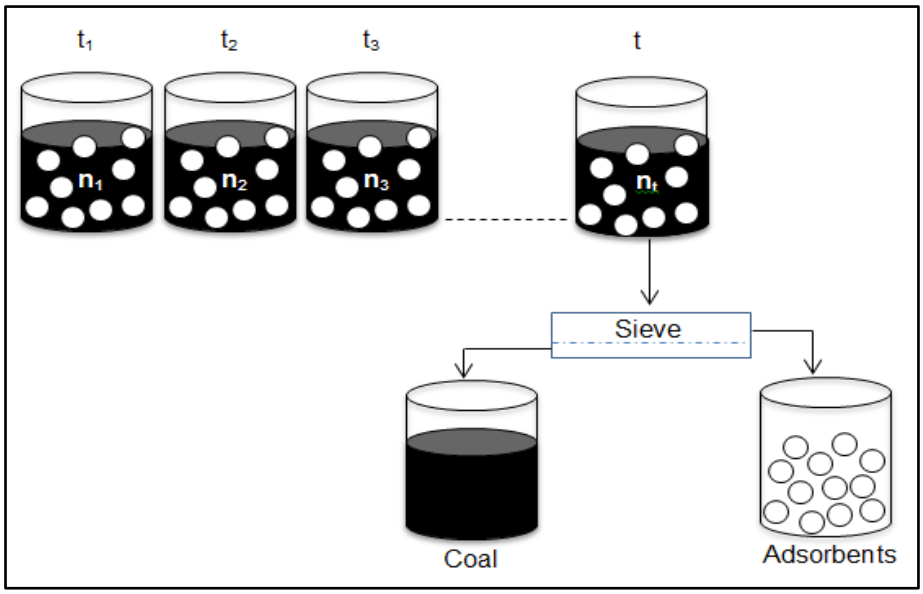

Figure 3.4.2: Fixed-bed drying technique experimental procedure

As illustrated in Figure 3.4.2, samples were prepared to ensure uniformity and reproducibility of each experimental run. The moisture content of the coal and adsorbent sample n_1 to sample n_4 was tested at 2.5-minute intervals and the moisture content of the coal and adsorbent samples n_5 and n_6 was tested at 5-minute intervals, respectively. From this point onwards, the time intervals were increased to 10 minutes until the moisture transfer became negligibly small. As shown in Figure 3.4.2, the combined coal and adsorbent samples were separated after each time interval has elapsed, and weighed to determine the amount of moisture displaced. In addition to weighing, the coal and adsorbent samples were analysed in a vacuum oven to determine the moisture content. This was done to determine the time required to lower the moisture content of the coal fines to 0.08 g(moisture)/g(coal and moisture). Sub-sampling was avoided to prevent the possibility of moisture or mass loss from the sample during sampling and improve experimental accuracy.

3.4.2 Cascading-bed drying technique

A dynamic variable was introduced into the system to enhance the contact area between the adsorbent and coal, thereby evaluating the effect of contact area on the drying performance. The cascading-bed experiments were conducted in cylindrical vessels with an inner diameter of 5cm and a length of 5.5cm, similar to the vessels used during the fixed-bed drying technique. The particles in the cylindrical vessels may adopt various patterns of flow when motion is introduced. A cascading and a cataracting motion may be created according to the rotational speed applied. The crescent section formed by the particle bed during rotation is termed “cascading”. Cataracting refers to particles that are projected into the free region of the vessel and showers back to the toe of the particle bed (Henein *et al*., 1983). Figure 3.4.3 shows the basic cascading and cataracting motions, respectively.

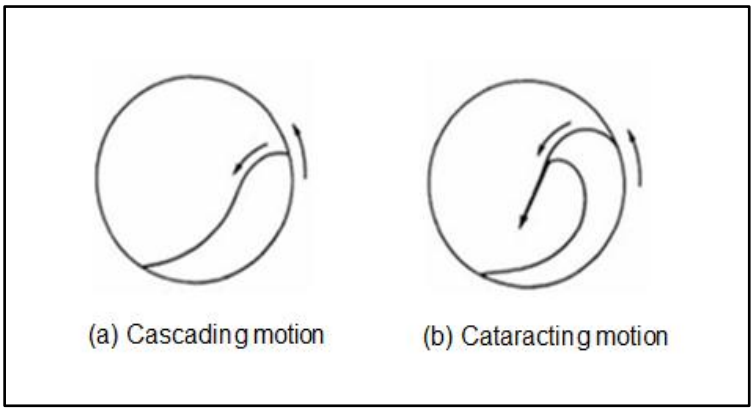

Figure 3.4.3: Cascading and cataracting motions, adapted from Henein *et al.* (1983)

An experimental setup was designed for the cascading-bed experiments were conducted. The cascading-bed experimental setup is shown in Figure 3.4.4. The components labelled A, B and C, in Figure 3.4.4, represents the electrical motor, horizontal rollers and steel frame respectively. The setup was designed to accommodate numerous individual cylindrical vessels that rotate horizontally on the electrically powered rollers. The cylindrical vessels, labelled D in Figure 3.4.4, were placed horizontally on the experimental setup, and continually rotate in a cascading motion on the rollers.

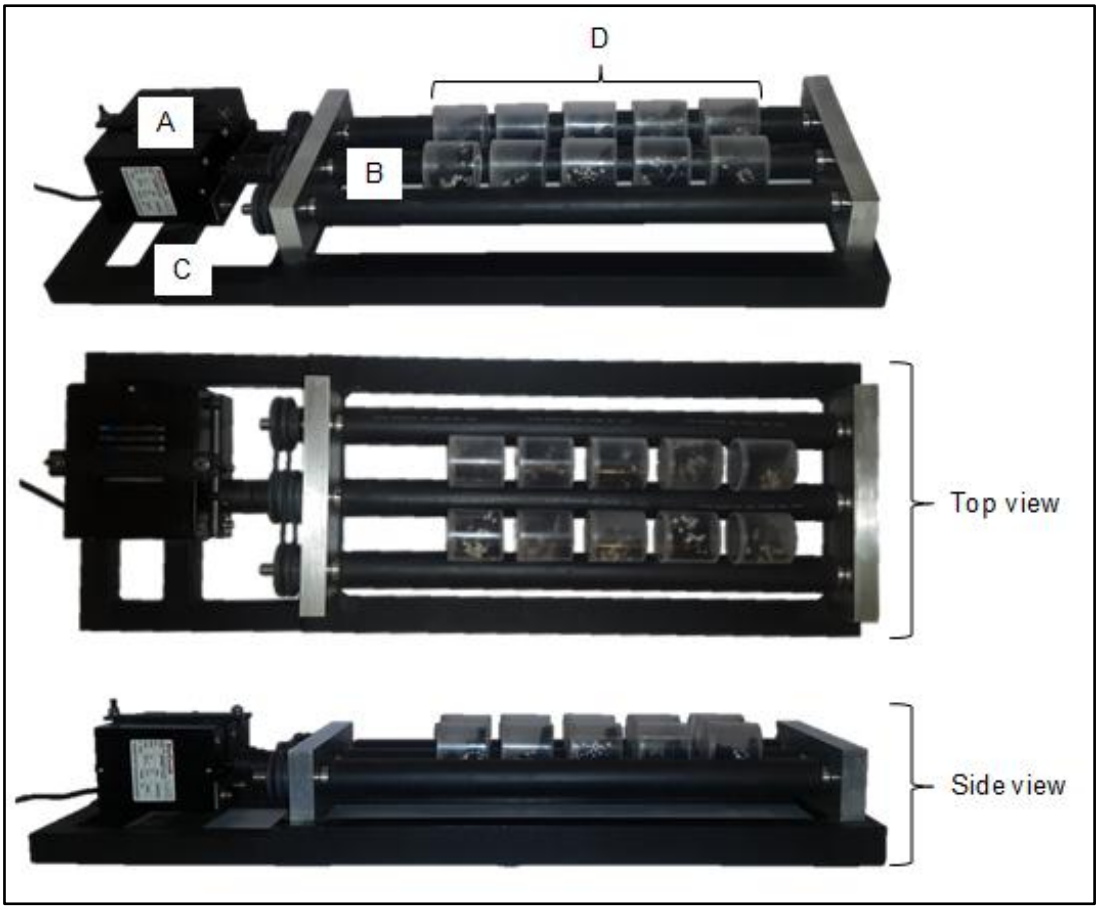

Figure 3.4.4: Top view of cascading-bed experimental setup

The rotational speed of the cylindrical vessels was kept constant at 3 revolutions per minute to maintain a gradual cascading motion, and minimize particle breakage. The operating speed was found to be 9.6% of the theoretical critical speed. The cascading-bed experimental procedure is demonstrated in Figure 3.4.5.

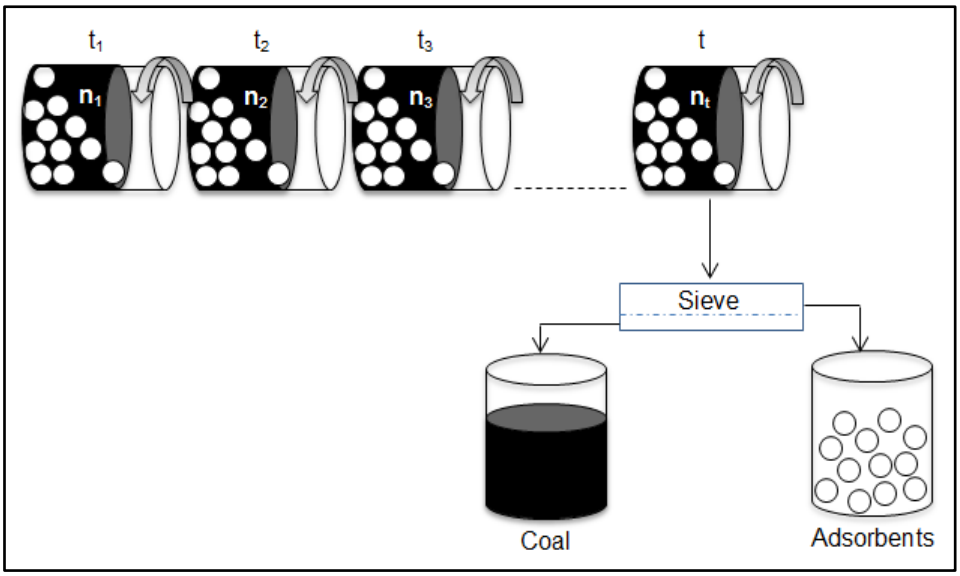

Figure 3.4.5: Cascading-bed drying technique experimental procedure

Once the desired contact time had elapsed, the cylindrical vessel was removed from the experimental setup, and the coal and adsorbents were recovered as shown in Figure 3.4.5. Similar to the method used during the fixed-bed experiments in Section 3.4.2, the individual coal and adsorbent samples were weighed, to determine the moisture displacement between the coal and adsorbents. In addition to weighing, the coal and adsorbent samples were analysed in a vacuum oven to determine the moisture content. This method of testing was followed to monitor the displacement of surface moisture between the coal and adsorbents over time.

3.4.3 Regeneration of adsorbents

The technical viability of adsorbent assisted drying is largely dependent on the ability of the adsorbent material to be regenerated. For purposes of this study, an air-drying technique that incorporates drying air, conditioned at 25°C and 40%RH, was selected as the regeneration procedure. The regenerator assembly consisted of a packed-bed vessel attached to a climate chamber.

The air required for drying the adsorbents was conditioned in a CTS climate test chamber (Type: C-40/100). The climate chamber, designed to simulate climatic conditions, was used to obtain the required temperature and relative humidity. Figure 3.4.6 shows the CTS climate test chamber used during regeneration.

Figure 3.4.6: CTS climate test chamber (Type: C-40/100)

The climate chamber in Figure 3.4.6 consists of two integrated sections, a top section and a bottom section. The bottom section of the machine contains heating coils, a water tank as well as the refrigeration gas, which is responsible for maintaining the temperature and relative humidity conditions of the air.

Figure 3.4.7 shows a schematic representation of the packed bed setup. Adsorbents are loaded into the packed bed vessel and conditioned air, drawn from the climate chamber, is introduced into the bottom of the packed bed vessel.

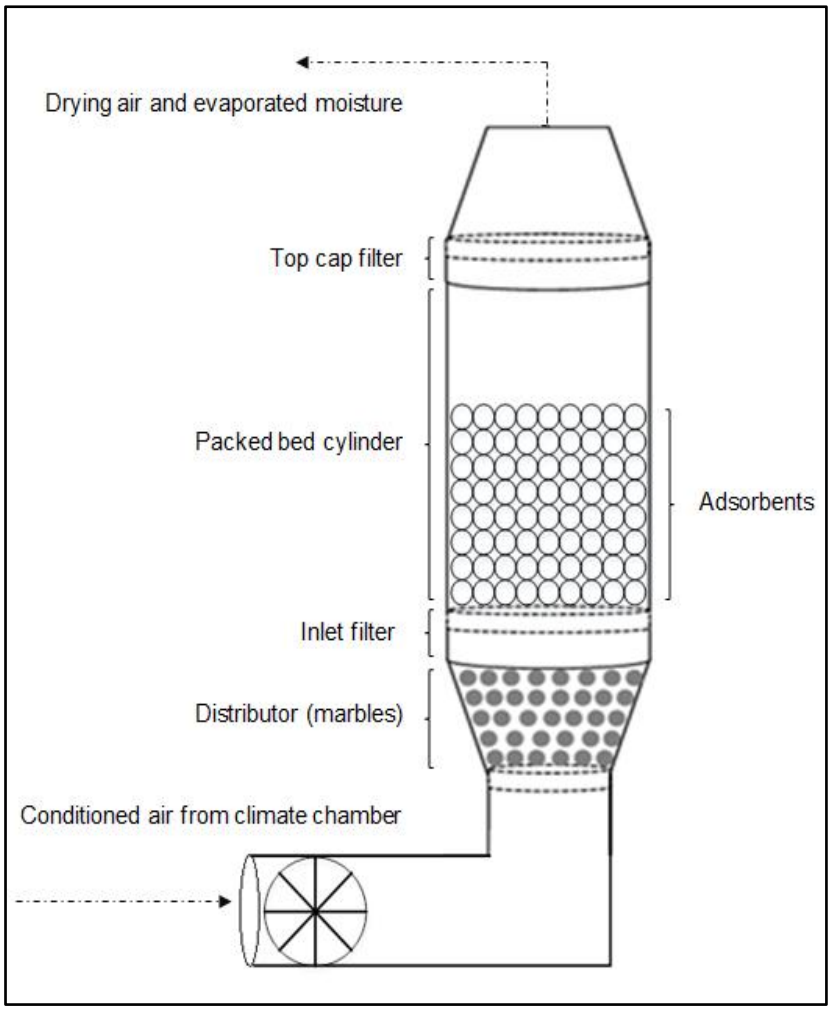

Figure 3.4.7: Schematic diagram of the packed bed vessel

The marble distributor indicated in Figure 3.4.7, acts as a dispersion mechanism that distributes the drying air evenly across the diameter of the vessel. The drying air, that enters the bottom of the packed-bed vessel, percolates the adsorbents, capturing moisture and carrying it away from the adsorbents. The moist air that leaves the top of the packed bed vessel is returned to the climate chamber for re-conditioning. The top and bottom sections of the vessel are covered with sieves, thereby preventing small particles from escaping the cylinder along with the humid air. The adsorbents were weighed periodically to monitor the moisture loss. The adsorbent mass was removed from the packed bed vessel when moisture displacement stopped, and a moisture analysis was conducted on the adsorbents to determine the final moisture load.

As previously mentioned, the actual packed bed vessel was attached to the side of the climate chamber and the assemblage is illustrated in Figure 3.4.8.

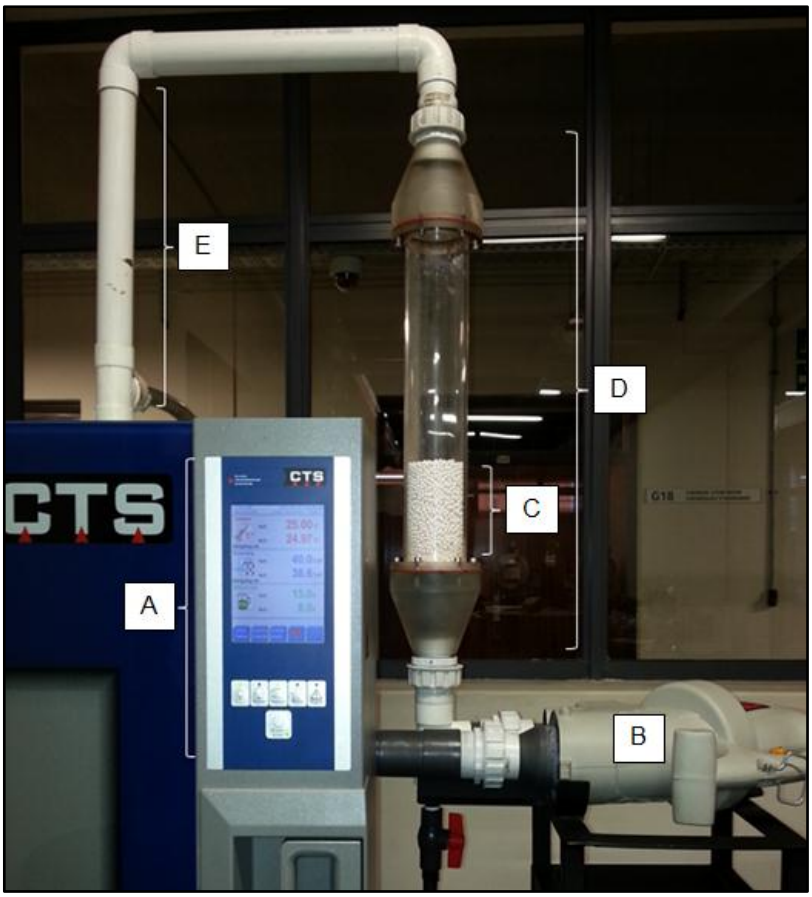

Figure 3.4.8: Packed bed attached to the CTS climate test chamber

The instruction manual and screen of the climate chamber is labelled A in Figure 3.4.8. The screen allows the operator to monitor the condition of the air inside the climate chamber. The blower (B) is connected to the port from which conditioned air was extracted from the climate chamber. Label C shows the adsorbents loaded inside the packed bed cylinder. The packed bed setup (D) was connected to the blower and climate chamber. Lastly, the section of the pipes that redirect the drying air back to the climate chamber is labelled E.

3.5 Sample preparation

3.5.1 Coal

Run-of-Mine (ROM) (as received) coal was crushed in a cone crusher to smaller size fractions. The coal was subsequently separated into various particle size ranges by sieving. Three coal size ranges were selected, -2mm+1mm, -1mm+0.5mm, -0.5mm+0.25mm. Figure 3.5.1 shows the particle size distribution curves for each of the three selected size ranges (ACT-TPM-003 based on SABS ISO 1953 – 1994 (Not a SANAS Accredited test method at the testing laboratory)).

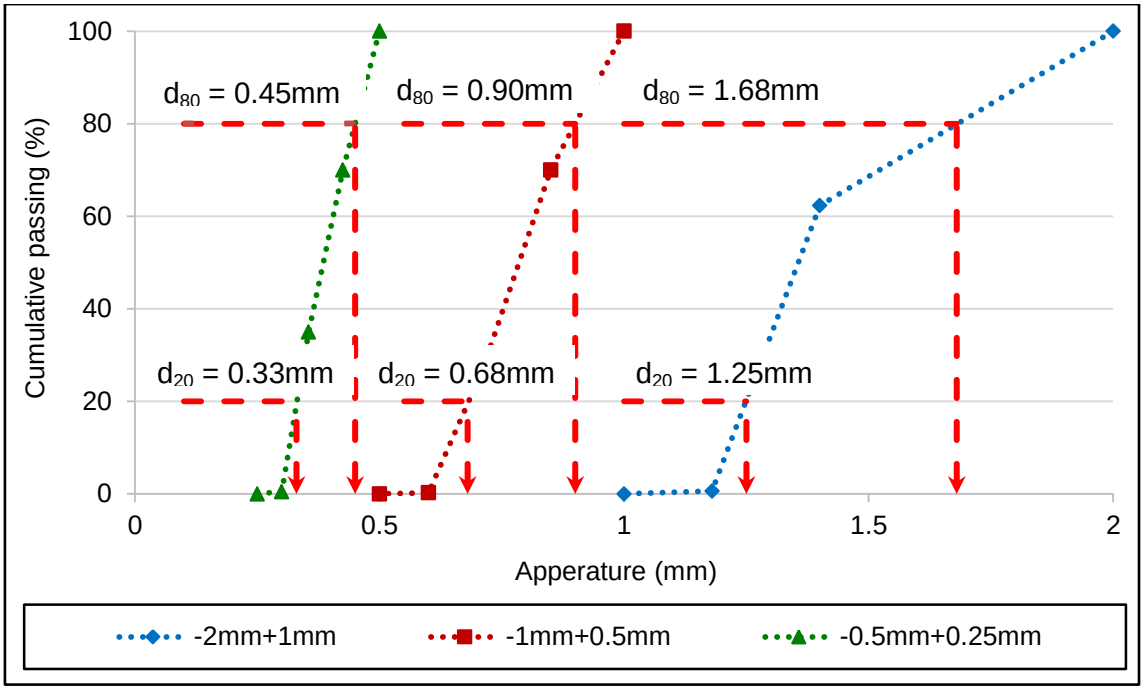

Figure 3.5.1: Particle size distribution

The d_{20} and d_{80} values for each particle size range can be seen in Figure 3.5.1. From Figure 3.5.1 it was concluded that 80% of the -2mm+1mm particle size range will pass through a screen or sieve with an aperture size of approximately 1.68mm. Moreover, the d_{20} value of the -2mm+1mm was approximately 1.25mm. . Additionally, the values for -1mm+0.5mm and -0.5mm+0.25mm are also indicated on Figure 3.5.1. The d_{20} and d_{80} sizes acted as indicators of the mass of coal fines present in each particle size range.

Once sieving was completed, the coal was drenched in water for 24 hours to ensure complete saturation. Samples were portioned on a wet basis for each experiment. Excess moisture was removed from the coal fines by pressure filtration. Each coal sample contains 10g wet coal.

3.5.2 Adsorbents

The adsorbents were stored in sealed containers in the climate controlled room at 22°C and 40%RH. The adsorbents were taken out of the sealed containers, and left exposed in the climate controlled room for 24 hours. This allowed the adsorbents to draw moisture, and reach equilibrium moisture content in the climate controlled room which ensured a similar starting moisture load for each sample. A sub-sample was taken from which the initial moisture content was determined.

3.6 Supplementary experimental work

3.6.1 Adsorbent static moisture capacity

To determine the moisture adsorption capacity of the adsorbents, a simple experiment was conducted. The inherent moisture content of the adsorbents was determined after which the adsorbents were submerged into water for 24 hours. The moisture load of the adsorbents was determined after the submersion period, giving an indication of the maximum amount of water that the adsorbents were able to adsorb. Figure 3.6.1 shows the static moisture adsorption of alumina-based and silica-based adsorbents at 25°C.

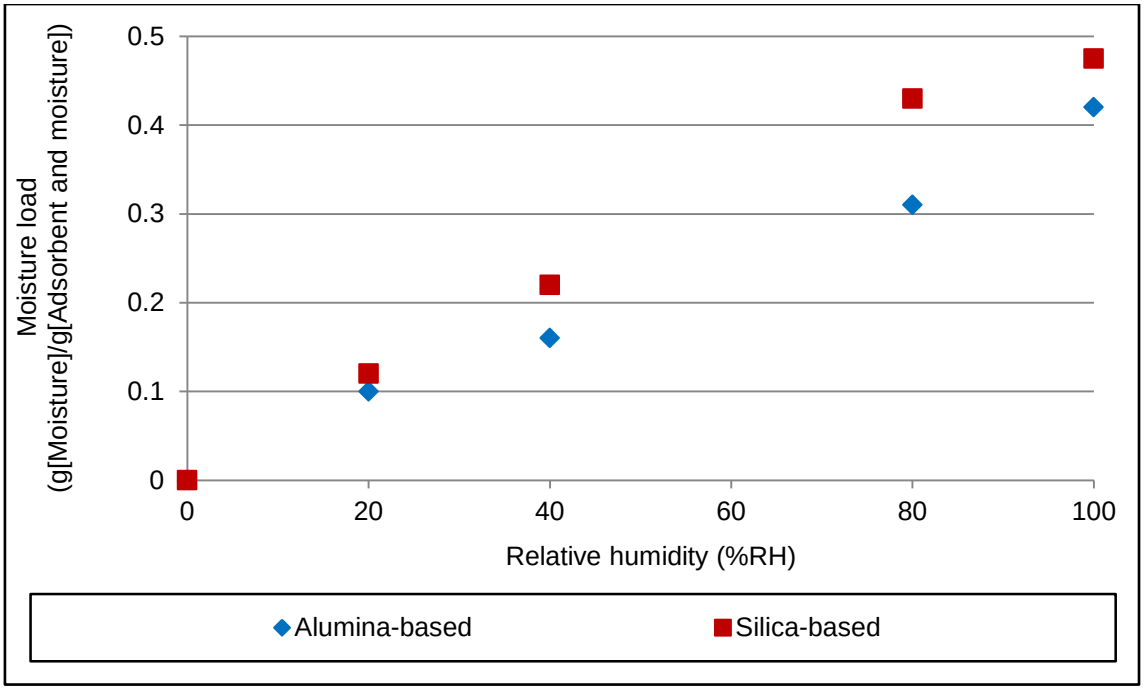

Figure 3.6.1: Static moisture adsorption at 25°C

The adsorption capacity seen in Figure 3.6.1 is suggestive of a high degree of porosity. Grain bulk density and grain apparent porosity analyses were determined as a further investigative measure. The grain bulk density and grain apparent porosity results are summarized in Table 3.7.

Table 3.7: Grain bulk density and grain apparent porosity results

Sample identification	Grain bulk density (g/cm^3)	Grain apparent porosity (%)
Alumina based adsorbent	1.37	50.7
Silica based adsorbent	1.11	47.7

From Table 3.7 it is noted that the alumina-based adsorbent had a markedly higher bulk density, and was also somewhat more porous than the silica based adsorbent.

It is evident from Figure 3.6.1 that the silica-based adsorbent has adsorbed more moisture than the alumina-based adsorbent; however, the porosity of the silica-based adsorbents in Table 3.7 is lower than its counterpart. The reason for this may be that silica-based adsorbents are manufactured with layers, whereas alumina-based adsorbents are not manufactured in the same manner. It is believed that when the adsorbents were submerged in water, the moisture was adsorbed into the pores of both of the adsorbents; however one must take into account the spaces between the layers of the silica-based adsorbent particles which is essentially absent from the alumina-based adsorbents. Moisture is gathered between the layers of the silica-based adsorbent particle, which explains the higher moisture load retained in Figure 3.6.1.

3.6.2 Scanning electron microscopy (SEM) and light electron microscopy (LEM)

Scanning Electron Microscopy (SEM) and Light Electron Microscopy (LEM) were employed to visually investigate the surface area and porosity of the adsorbent material to better understand the adsorption capabilities of the adsorbents. Figure 3.6.2 shows the SEM and LEM micrographs of the alumina-based adsorbent respectively.

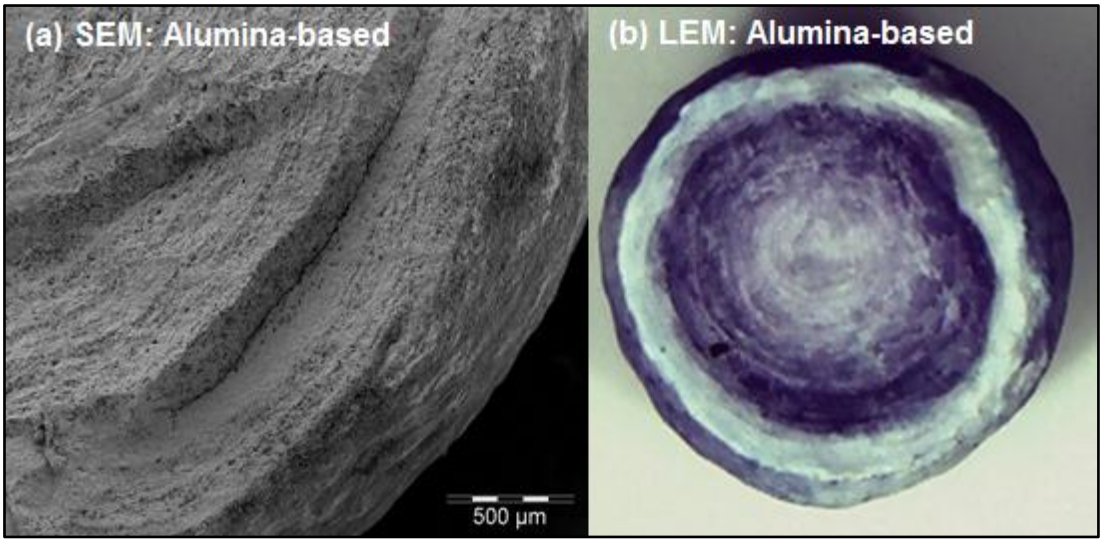

Figure 3.6.2: SEM and LEM micrographs of alumina-based adsorbent particles

The SEM micrograph of the alumina-based adsorbent in Figure 3.6.2(a) showed that the adsorbent is permeable as pores were visible in the structure at 500µm magnification.

Additionally, the adsorbents were submerged for 48 hours in water, prepared with gentian violet, to investigate the magnitude of the pores of the alumina-based adsorbents visible in Figure 3.6.2. It is evident in Figure 3.6.2(b) that the alumina-based adsorbents allowed molecules larger than water to penetrate the surface, and infiltrate the adsorbent, as the core of the adsorbent material is violet coloured.

The SEM micrograph of the silica based adsorbent particle can be seen in Figure 3.6.3(a) and less pores are visible than the alumina based adsorbent in Figure 3.6.2(a).

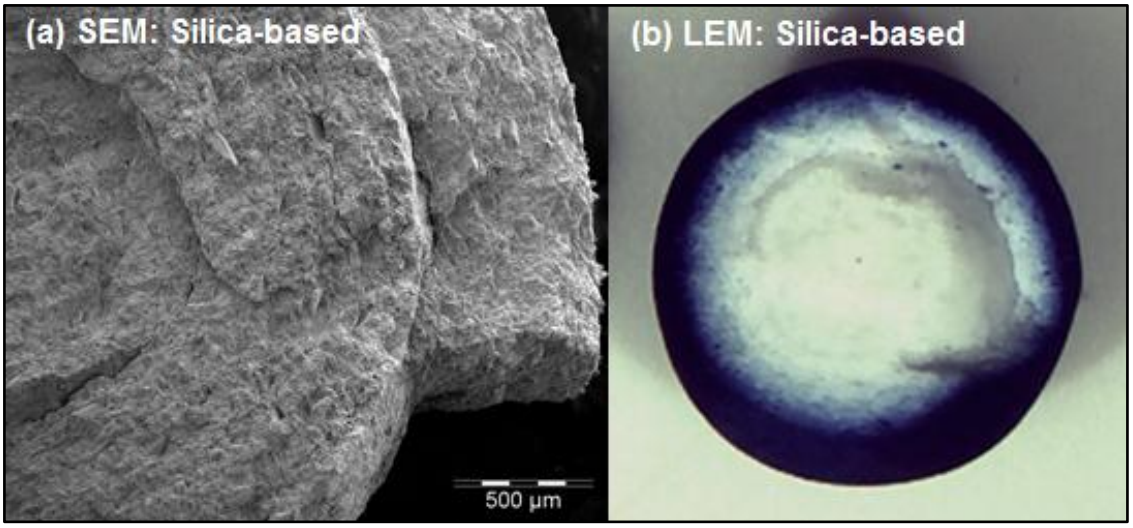

Figure 3.6.3: SEM and LEM micrographs of silica-based adsorbent particles

The silica-based adsorbent shown illustrated by the SEM micrograph in Figure 3.6.3(a) is constructed in layers, each composed of the same material as the seed material. In Figure 3.6.3(b), the silica-based adsorbent is evidently denser as the coloring of the gentian violet was only able to penetrate its external surface without infiltrating the core of the adsorbent. It is presumed that the water adsorbed by the silica-based adsorbents is therefore likely to accumulate between the individual layers of construction, and may pose a breakage risk as the layers could peel off when subjected to agitation.

The SEM and LEM micrographs show that the pore size of the alumina-based adsorbent is consistently larger throughout the adsorbent structure, whereas the silica-based adsorbents have smaller pores. These findings are in agreement with the physical properties of the adsorbents summarized in Table 3.3 of Section 3.2.2. This is noteworthy information as it helpful in describing the adsorption processes experienced by the adsorbent types.

4

CHAPTER

FIXED-BED DRYING TECHNIQUE

Chapter 4 summarizes the results obtained during the fixed-bed experimental runs. Section 4.1 summarizes the variables under investigation as discussed in Section 3.1.2. The description of the general moisture adsorption and desorption curves is found in Section 4.2. Furthermore, Section 4.3 elaborates on the influence of various operating conditions on the final moisture load of the coal as well as the initial adsorption and desorption rates. The statistical significance of the fixed-bed experimental runs is discussed in Section 4.4 and Section 4.5 contains conclusions on the findings.

4.1 Variables

A number of fixed-bed experimental procedures were conducted in order to observe the moisture reduction in coal fines. The variables and operating parameters tested during experiments are discussed in detail in Section 3.3 of Chapter 3. Wet coal, at predetermined set size ranges, were combined to a specific type and size of adsorbent according to selected mass ratios. The effect of each variable on the drying performance of the coal fines was monitored in order to identify the best operating parameters. The fixed-bed experiments were conducted at 25°C and 40%RH.

4.2 General desorption and adsorption curves

The experiments were conducted in a climate controlled room, set at 25°C and 40%RH, using fixed-bed cylindrical vessels as demonstrated in Chapter 3. The drying performance of two adsorbent types, an alumina-based adsorbent (F-200 activated alumina) and a silica-based adsorbent (Silsorb N10) were evaluated during this study. The coal and adsorbent types were discussed in detail in Section 3.2.1 and 3.2.2 of Chapter 3. The adsorbents were left exposed to the surrounding air in the climate-controlled room for 24 hours in order to reach a similar equilibrium starting point when added to the coal fines. Samples of the coal and adsorbents were collected during the experiment at set time intervals, and the surface moisture for each sample was analysed in a vacuum oven, respectively. Surface

moisture is discussed in Section 2.3 of Chapter 2. Surface moisture refers to the moisture that is located on the surface of the coal particle that includes internal and external surface areas (Petrick, 1969). Additionally, the moisture held between coal particles in a mass or heap also forms part of surface moisture (Le Roux, 2003).

General desorption and adsorption curves were constructed from the surface moisture results, and essentially illustrated the surface moisture exchange between wet coal and dry porous adsorbents. Figure 4.2.1 shows the desorption and adsorption curves of -2mm+1mm coal and 3mm alumina-based and silica-based adsorbents. The desorption curves of the coal samples dried by the (a) alumina-based adsorbents and the (b) silica-based adsorbents is indicated in Figure 4.2.1 by (a) coal and (b) coal, respectively. The average initial surface moisture content of the -2mm+1mm coal fines were 0.18 g(moisture)/g(coal and moisture) with a standard deviation of 2.20 percentage points, and a relative standard error of 2.78%. The results in Figure 4.2.1 was obtained for an adsorbent to coal mass ratio of 1:1, and the dashed black line represents the target surface moisture selected for the study. According to Bland and McDaniel (2014), coal fines with a surface moisture of 0.08 g(moisture)/g(coal and moisture) is economically attractive for the coal industry. Elevated moisture levels in fine coal may compromise prospective blending benefits. Moreover, coal dusting may occur when the moisture levels of fine coal is reduced below 0.08 g(moisture)/g(coal and moisture), and when reduced even more, the risk of dust explosions should be considered (Bratton *et al*., 2012).

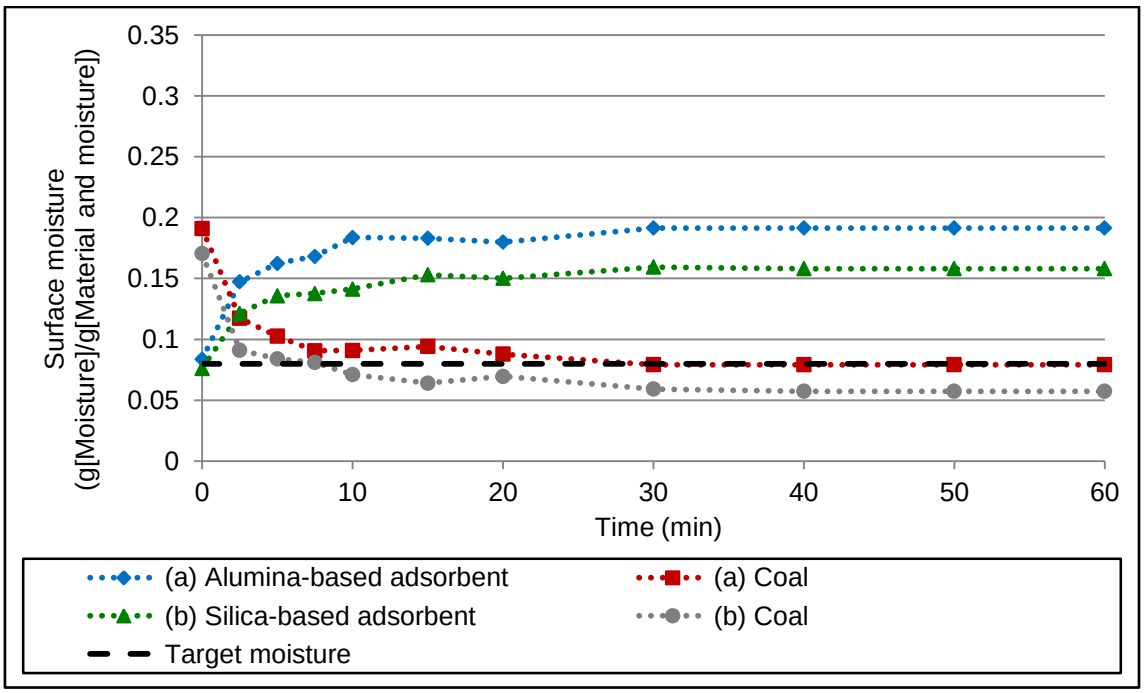

Figure 4.2.1: Adsorption-desorption curves of -2mm+1mm coal and 3mm adsorbents

In Figure 4.2.1, the desorption curve indicates the displacement of surface moisture from wet coal in g(moisture)/g(coal and moisture) over time (minutes) while the adsorption curve illustrates the moisture gained by the adsorbent in g(moisture)/g(adsorbent and moisture) over time (min). After 10 minute of drying, the respective adsorbent types were able to reduce the surface moisture content of the coal fines by (a) 52% and (b) 58%. The experimental runs continued for 60 minutes to ensure that equilibrium between the moisture in the coal, the adsorbents, and the surrounding air was reached. At (a) 25 minutes, and (b) 8 minutes, the target surface moisture was achieved. After 30 minutes of drying, the equilibrium surface moisture for both coals was reached as shown in Figure 4.2.1. The adsorbents gained (a) 0.10 g(moisture)/g(adsorbent and moisture), and (b) 0.08 g(moisture)/g(adsorbent and moisture), while the coal displaced (a) 0.12 g(moisture)/g(coal and moisture), and (b) 0.11 g(moisture)/g(coal and moisture) respectively for the two experiments.

When studying the mass balance of moisture displacement between the coal and adsorbents masses only, an imbalance may be observed. However, when conducting the mass balance, one must account for the fraction of moisture retained in the air surrounding the coal and adsorbent masses. The process therefore also alters the relative humidity equilibrium of the surrounding air. This explains the reduced moisture uptake by the adsorbents in comparison to the moisture loss by the coal. A detailed discussion of the moisture transfer mechanism follows in Section 4.2.2.

4.2.1 Desorption rate

The desorption curves for the -2mm+1mm coal in Figure 4.2.1 exhibited similar drying trends. The experimental results obtained for the -1mm+0.5mm and -0.5mm+0.25mm coal were examined as well, and a characteristic drying curve was identified. The desorption curves in Figure 4.2.1 were plotted in Figure 4.2.2 to demonstrate this characteristic drying curve. Three distinct drying phases were recognised from the drying curves as indicated in Figure 4.2.2 by A, B and C.

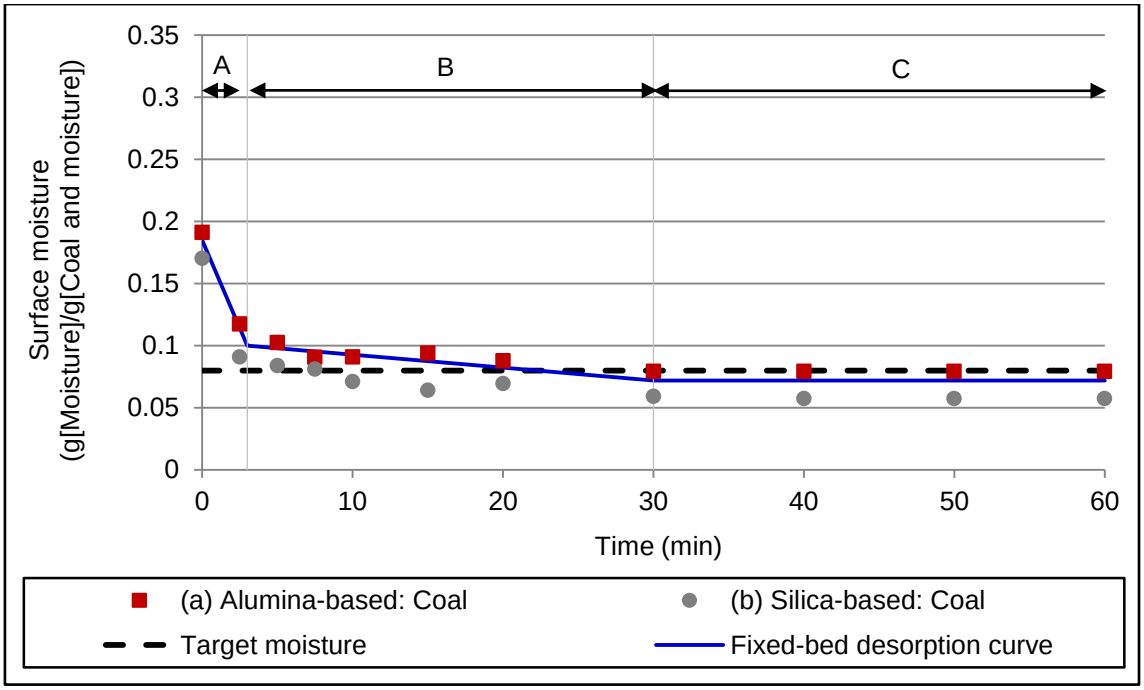

Figure 4.2.2: Characteristic drying curve of fine coal

The phases on the drying curve in Figure 4.2.2 represents; (A) a rapid initial desorption phase, (B) a secondary desorption phase, and (C) the equilibrium moisture on the coal samples. The largest fraction of the surface moisture located on the coal is transferred onto the adsorbents during the initial liquid-liquid desorption phase. The desorption rate slows down during the secondary desorption phase as the surface moisture displacement from the internal capillaries of the individual coal particles begins. This phase is largely characterized by both liquid-liquid desorption and liquid-vapour desorption. The characteristic desorption curve in Figure 4.2.2 shows that the amount of surface moisture removed during the initial slope (A) is considerably larger than the amount of surface moisture removed during the secondary slope (B). As a result, the initial desorption rate was a focus point during this investigation. The initial desorption rate is defined as the load of moisture removed from the coal per unit mass of coal over time. The initial desorption rate is expressed in Equation 4.1,

$$Initial\ desorption\ rate = \frac{Initial\ moisture\ reduction}{\Delta time}$$

Equation 4.1

where the initial moisture load reduction refers to the surface moisture lost during phase A, and is measured in g(moisture)/g(coal and moisture), and the time recorded in minutes.

In addition to the initial desorption rates, the initial adsorption rates of the experiments were calculated to investigate the rate at which moisture is initially adsorbed by the adsorbents. Annexure B.2 details the procedure followed for calculating the initial adsorption rates.

4.2.2 Moisture transfer mechanism

The experiments were conducted in cylindrical vessels that were conditioned at 25°C and 40%RH. Originally, the air that surrounds the surface of the wet coal fines in the vessel is in relative humidity equilibrium with the air. When dry adsorbents are introduced into the system, the relative humidity equilibrium is disturbed, and a moisture concentration gradient is created due to the moisture levels of the coal and the adsorbent particles. Moisture is displaced from the coal by capillary flow and diffusion processes to the adsorbent material and the proposed drying mechanism is demonstrated in Figure 4.2.3.

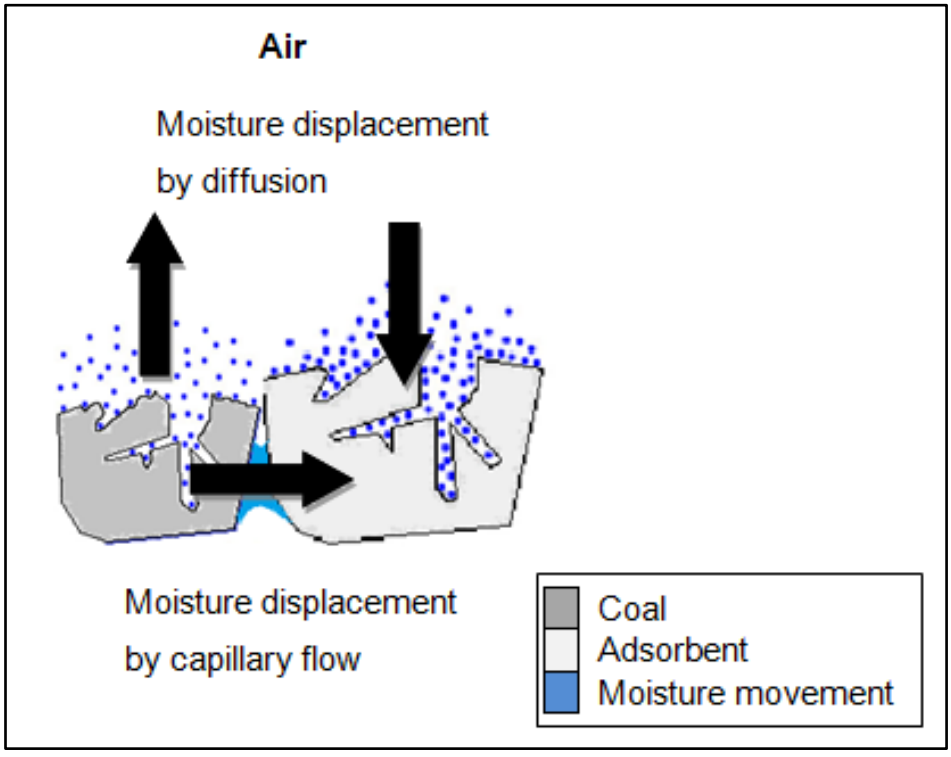

Figure 4.2.3: Drying mechanism; adapted from ALDACS (2013)

Liquid surface moisture held on the external surface and larger interconnecting pores between coal particles is transferred to the adsorbents by capillary flow through the interphase between the coal and the adsorbents. As the amount of liquid moisture on the coal's surface decreases, moisture displacement by capillary flow becomes negligibly small

(Kudra and Mujumdar, 2009). As the surface moisture is being removed, moisture located in the capillaries of the coal particles migrates to the surface of the coal at a sufficient rate to compensate for the deficit. The moisture proceeds to diffuse through the interstitial air between the particles along the concentration gradient. The point of equilibrium depends largely on the relative humidity conditions of the air surrounding the particles (Le Roux et al., 2015). The starting moisture in the surrounding air contributes to the initial 40%RH, and adds to the amount of moisture adsorbed by the adsorbents. The moisture difference is retained in the air surrounding the coal and adsorbent particles as inherent moisture equilibrium is reached by the system.

The reliability of the experimental procedure was evaluated by repeating a series of fixed-bed experiments. The method followed for determining the standard deviation and relative standard error is discussed in detail in Annexure A.1. Additional repeatability data can be found in Annexure A.2. The mean, standard deviation and relative standard error of the initial moisture content was determined for the -2mm+1mm, -1mm+0.5mm and -0.5mm+0.25mm coal and the obtained results are given in Table 4.1.

Table 4.1: Mean, standard deviation and relative standard error of initial moisture of coal

Description	Mean (g[Moisture]/g[Coal and moisture])	Standard deviation (%)	Relative standard error (%)
-2mm+1mm	0.18	2.20	2.78
-1mm+0.5mm	0.25	0.85	0.75
-0.5mm+0.25mm	0.29	0.75	0.60

The results listed in Table 4.1 shows that the initial moisture contents of the various coal particle size ranges fall within a narrow margin from one another. Keeping the initial moisture content of coal close to constant will minimise the experimental error. Figure 4.2.4 and Figure 4.2.5 shows repeatability data of the desorption and adsorption curves of the -1mm+0.5mm coal and 3mm alumina-based adsorbents, respectively. In both Figure 4.2.4 and Figure 4.2.5, the upper and lower limits represent the standard deviation from the average of the repeats.

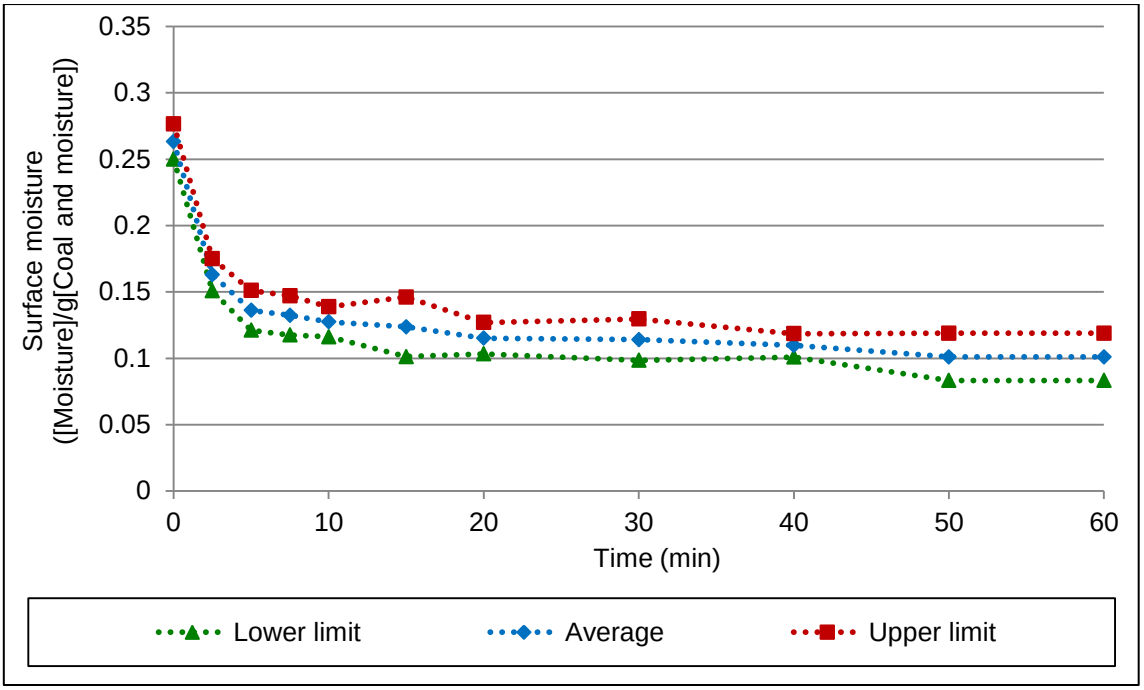

Figure 4.2.4: Average and standard deviation of repeats for -1mm+0.5mm coal

The minimum and maximum standard deviation of the desorption curves were 0.88 percentage points and 2.24 percentage points, respectively. Additionally, the relative standard error (RSE) was calculated for the set of experimental runs to determine the magnitude of the deviation between the survey mean and the true population. The minimum and maximum relative standard errors of the desorption curve were 2.91% and 10.46%, respectively. Figure 4.2.5 shows the repeatability data of the adsorption curves for 3mm alumina-based adsorbents.

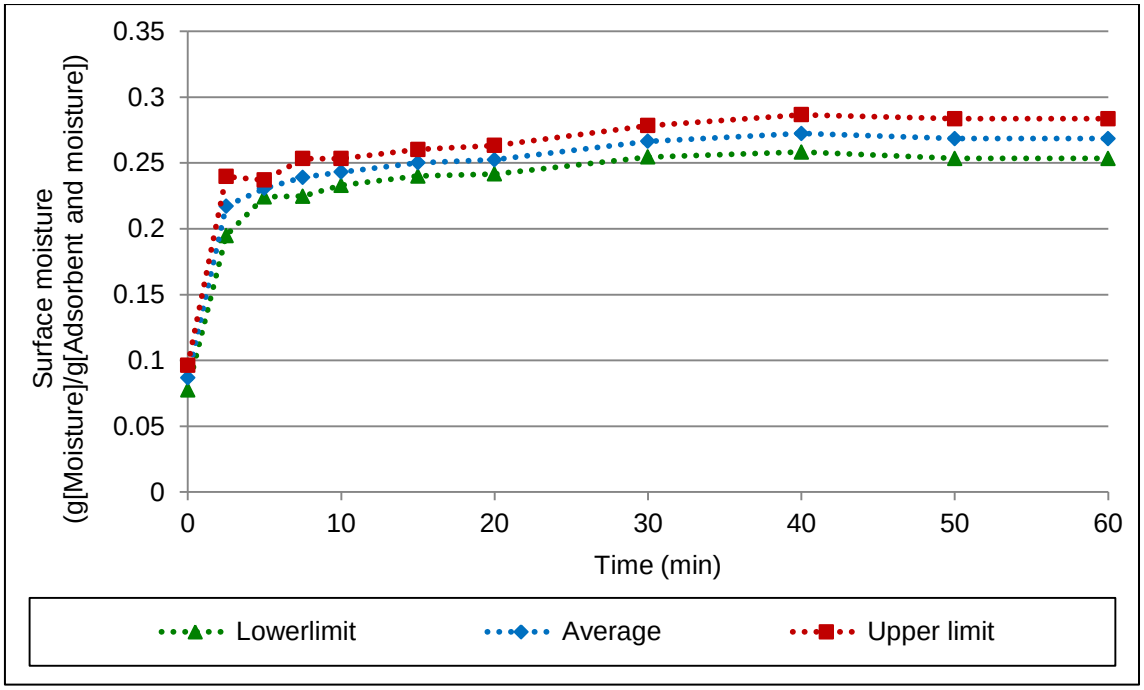

Figure 4.2.5: Average and standard deviation of repeats for 3mm alumina-based adsorbents

The minimum standard deviation obtained for the adsorption curves shown in Figure 4.2.5 were 0.90percentage points and the maximum standard deviation was 2.25 percentage points. The minimum and maximum relative standard errors for the adsorption curve were 2.77% and 10.34%, respectively. To further verify the reliability of this drying technique, the repeatability data for the initial desorption and adsorption rates of the -1mm+0.5mm coal and 3mm alumina-based adsorbents were determined and the corresponding results is presented in Table 4.2.

Table 4.2: Standard deviation and relative standard error of initial rates

Description	Initial desorption rates	Initial adsorption rates
Standard deviation (%)	0.37	0.57
Relative standard error (%)	5.72	6.36

The initial desorption rates in Table 4.2 has a standard deviation of 0.37 percentage points. Similarly, the initial adsorption rates showed a standard deviation of 0.57 percentage points. The relative standard error for the initial desorption rates were 5.72%. The desorption rates obtained for the experimental runs proved to be highly reproducible. The marginal standard

deviations were also an indication that the experimental procedure followed was reliable. The results found for the repeats tests apply to all the experimental results obtained.

4.3 Operating parameters

The fixed-bed experiments evaluated in Section 4.3 focussed on identifying the set of operating parameters that was best suited for drying coal fines. The operating parameters that were investigated include adsorbent to coal mass ratio, adsorbent type, adsorbent size, and coal size range as discussed in Section 3.3 of Chapter 3. The operating parameters were assessed and conclusions were drawn from the results.

4.3.1 Influence of adsorbent to coal mass ratio

The influence of adsorbent to coal mass ratio is studied in this section. The adsorption and desorption curves obtained assisted in determining the best operating adsorbent to coal mass ratio required for effective coal drying. Coal fines of various particle size ranges was tested with adsorbent to coal mass ratios of 3:1, 2:1, 1:1, 0.75:1 and 0.5:1 as given in Table 3.6. For the 60 fixed-bed experiments conducted, 5 experiments conducted with the same adsorbent type, same adsorbent size, same coal particle size range, and different adsorbent to coal mass ratios were selected, and plotted in Figure 4.3.1. Figure 4.3.1 shows the effect of varying adsorbent to coal mass ratios on the surface moisture of -2mm+1mm coal with an average initial surface moisture content of 0.18 g(moisture)/g(coal and moisture). The surrounding air conditions were maintained at 25°C and 40%RH to enhance experimental accuracy. From the curves shown in Figure 4.3.1, one can see that the coal reached inherent moisture equilibrium after 10 minutes of drying.

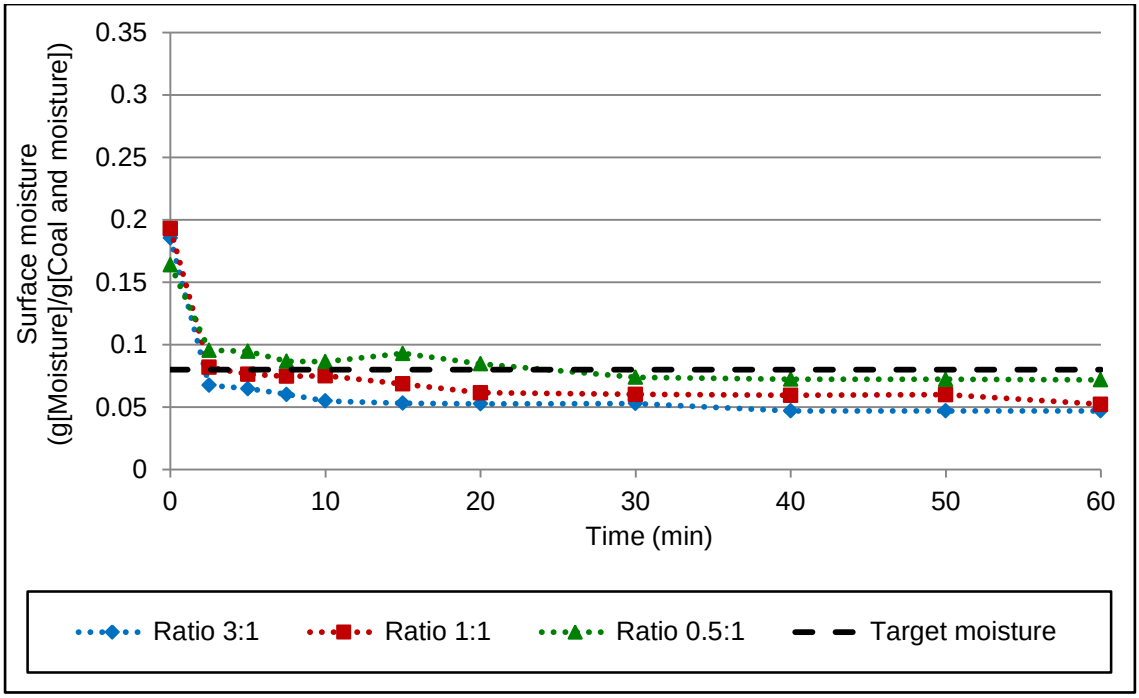

Figure 4.3.1: Desorption curves of -2mm+1mm coal and 5mm silica-based adsorbents

The moisture curves plotted in Figure 4.3.1 shows that the surface moisture of the coal was reduced by 64% at an adsorbent to coal mass ratio of 3:1 during the initial desorption phase, whereas at 0.5:1 the surface moisture of the coal was reduced by 42%. After 10 minutes of drying, the coal fines reached inherent moisture equilibrium at 0.055 and 0.087 g(moisture)/g(coal and moisture) for the 3:1 and 0.5:1 mass ratios, respectively. Bratton *et al*. (2012) stated that the final moisture load of the coal fines could be "dialled in" by varying the adsorbent to coal mass ratio. Adsorption equilibrium is the constraint that limits adsorption capacity (Knaebel, 2006). When the adsorbent to coal mass ratios is altered, adsorption equilibrium is disrupted. By increasing the amount of adsorbents, the adsorbent volume will attempt to perform to its full capacity, and draw more moisture from the surrounding air. The relative humidity of the surrounding air will continue to oscillate as moisture diffuses from the coal fines into the air, until adsorption equilibrium is reached. Although the moisture desorption rate is greatly dependent on contact area between the adsorbent and the coal, Kudra and Mujumdar (2009) states that moisture displacement will continue until the "pull power" of the coal mass is equal to that of the adsorbent volume.

Figure 4.3.2 shows the corresponding adsorption results of 5mm silica-based adsorbents in combination with -2mm+1mm coal, over time. The moisture loads were recorded at regular time intervals to monitor the moisture uptake in accordance with time. The initial surface

moisture of the adsorbents were 0.087 g(moisture)/g(adsorbent and moisture) at 25°C and 40%RH with a standard deviation of 1.01%.

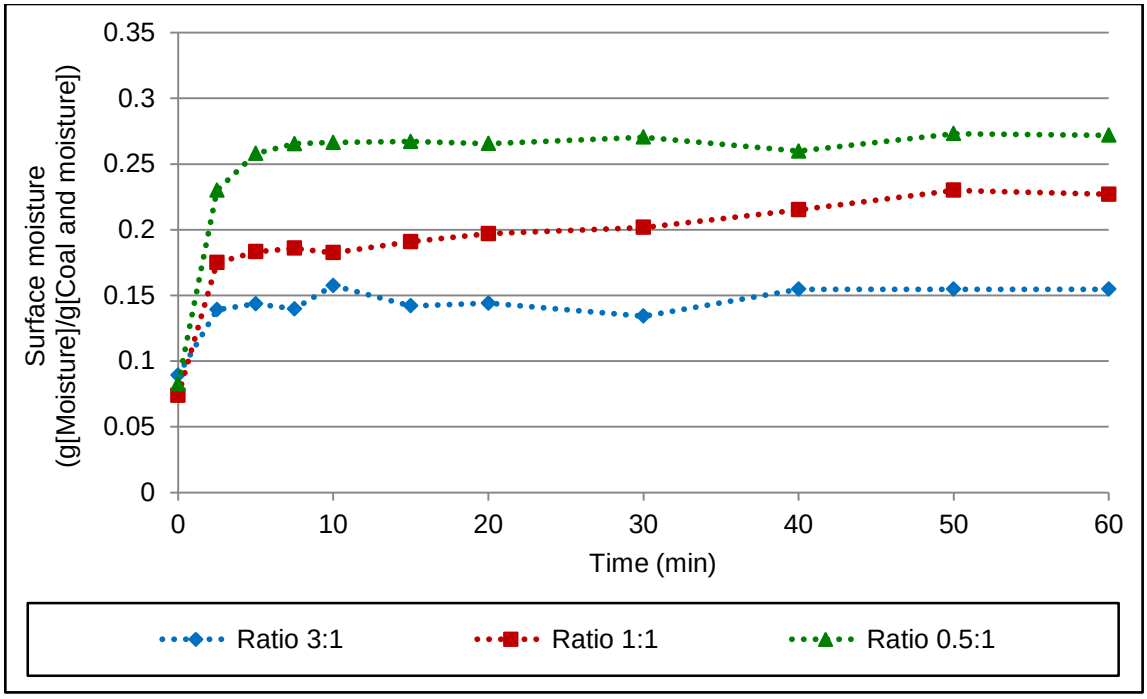

Figure 4.3.2: Adsorption curves of -2mm+1mm coal and 5mm silica-based adsorbent

In Figure 4.3.2, it may seem the moisture load of the adsorbents increase with decreasing adsorbent to coal mass ratios; however, this is not the case. After 10 minutes of drying, the results in Figure 4.3.2 shows the 0.5:1 adsorbent to coal mass ratio adsorbed 25% more moisture than the adsorbent to coal mass ratio of 3:1. Adsorption load is defined as the amount of moisture taken up by the adsorbent per unit mass of the adsorbent (Knaebel, 2006). The initial surface moisture available within the coal fines are fixed, the adsorbents will therefore continue to adsorb moisture until inherent equilibrium is achieved. As the amount of adsorbent is increased, the amount of surface moisture adsorbed by the adsorbent will be redefined as per unit mass of adsorbent present in the system. The mass of adsorbent to coal is less at 0.5:1 than at 3:1, therefore the percentage of surface moisture adsorbed per unit mass at 0.5:1 will be more. Since the initial moisture available is fixed, the amount of moisture uptake per unit mass of adsorbent will decrease as the adsorbent mass increase.

The moisture uptake for the adsorbent to coal mass ratios was summarized in Table 4.3. The surface moisture and percentage moisture displacement of the -2mm+1mm coal fines and silica-based adsorbents were recorded after 10 minutes of drying. The results obtained

for adsorbent to coal mass ratios of 3:1, 2:1, 1:1, 0.75:1 and 0.5:1 are also summarized in Table 4.3.

Table 4.3: Moisture displacement of -2mm+1mm coal and 5mm silica-based adsorbents

Ratio	Adsorbent		Coal	
	Moisture load (g[Moisture]/g[Adsorbent and moisture])	**Moisture gain** (%)	**Moisture content** (g[Moisture]/g[Coal and moisture])	**Moisture removed** (%)
3:1	0.16	43.31	0.05	70.39
2:1	0.16	43.76	0.06	67.25
1:1	0.18	59.56	0.08	61.12
0.75:1	0.22	54.46	0.10	48.48
0.5:1	0.27	69.02	0.09	47.26

The results in Table 4.3, show lower moisture contents were obtained at higher adsorbent to coal mass ratios after 10 minutes of contacting. At this time, the initial moisture of the coal fines were reduced by 70.39% at an adsorbent to coal mass ratio of 3:1 whereas at 0.5:1 only a 47.26% moisture reduction was achieved within the same time frame. Contact time is a governing factor of drying performance, and extended periods allows the adsorbents to perform to its full capacity (Yang, 2015). After 10 minutes of drying, the 3:1 ratio was able to remove more moisture than the 0.5:1 ratio, which indicated that the available contact time was sufficient for the 3:1 ratio to perform well, while the time was not sufficient for the 0.5:1 ratio to reduce the moisture content of the coal fines by 50%. It was also noted that the percentage moisture removed from the coal fines increased with increasing adsorbent to coal mass ratios. This is due to the increased surface area available for moisture accumulation at higher adsorbent to coal mass ratios (Hand, 2000).

The initial moisture desorption rates from coal were calculated to identify the adsorbent to coal mass ratio that performed the best. This was calculated by using Equation 4.1. Figure 4.3.3 shows the initial desorption rates for the desorption curves discussed in Figure 4.3.1 for varying adsorbent to coal mass ratios. The trend followed in Figure 4.3.3 shows the initial desorption rate decreased with decreasing adsorbent to coal mass ratios, especially below a 1:1 ratio.

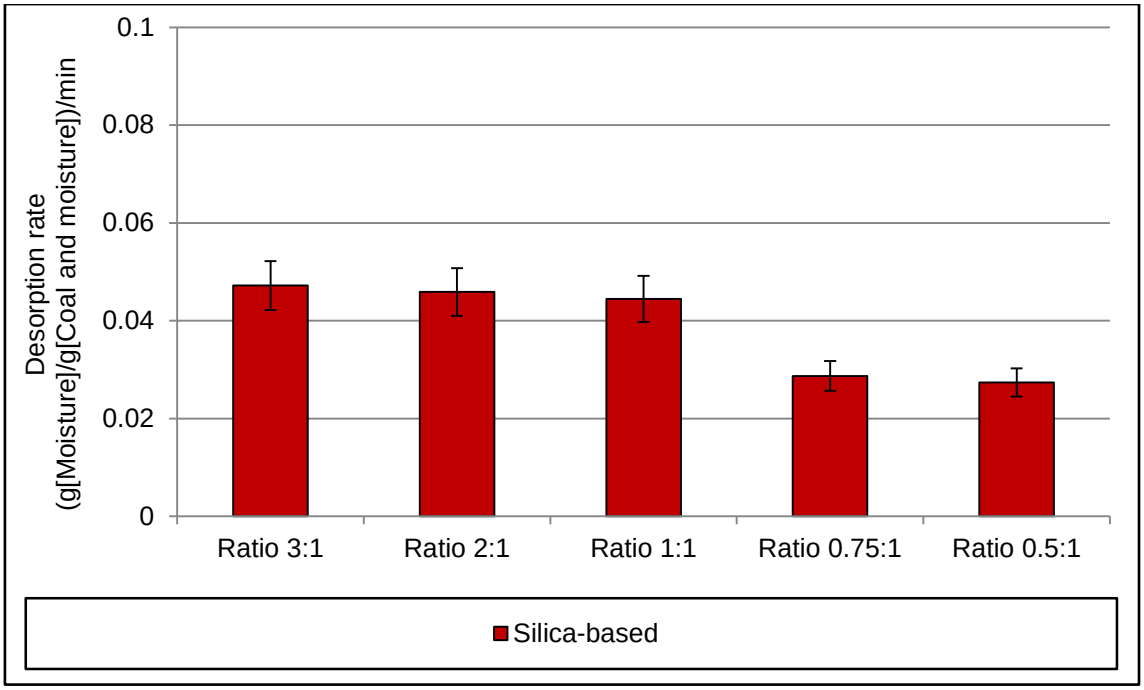

Figure 4.3.3: Initial desorption rates of -2mm+1mm coal and 5mm silica-based adsorbents

According to Kudra and Mujumdar (2009), the rate at which mass is transferred is largely dependent on the available contact area between the adsorbent and the coal. The increased adsorbent to coal mass ratio allows for a larger load of adsorbents per unit mass of coal, and therefore the surface area for moisture accumulation is increased. The adsorbents are able to draw moisture at an increased rate, as more surface area is available to accommodate the moisture. This explains the elevated desorption rates at higher adsorbent to coal mass ratios. The relative standard error of the desorption rates is indicated by the bars in Figure 4.3.3, where it is apparent that the results for adsorbent to coal mass ratios of 3:1, 2:1 and 1:1, fall within experimental error from each other. The relative standard error for the desorption rates of -2mm+1mm coal and silica-based adsorbents was determined as 10.59%.

It was concluded from the results in this section that the best drying performance was achieved by the adsorbent to coal mass ratio of 3:1. However, for industrial performance, a ratio down to 1:1 can still achieve the desired moisture content within the set time frame of 10 minutes. The adsorption and desorption curves, and initial adsorption and desorption rates, for the remaining experiments were also constructed and are provided in Annexure B.3.1.

4.3.2 Influence of adsorbent type

Alumina-based and silica-based adsorbents were selected for investigation in this study. The composition of the alumina-based adsorbents and the silica-based adsorbents were given in Table 3.6 and Table 3.9 in Chapter 3 as provided by the manufacturer. The physical properties of the adsorbents are given in Table 3.7 and Table 3.10. The adsorbent type was varied to identify the adsorbent that was best suited for this drying technique. Knaebel (2006) notes that the success of an adsorbent as a drying agent is reliant on the loading capacity of the adsorbent, the adsorbent density, and the adsorbent compatibility. Both adsorbent types were able to reduce the surface moisture of the -2mm+1mm coal by 57% to below the target surface moisture during the initial desorption phase as shown in Figure 4.3.4. The mass ratio was selected for discussion was identified in Section 4.3.1 as the best performing adsorbent to coal mass ratio. The coal fines and adsorbents shown in Figure 4.3.4 are for the best operating adsorbent to coal mass ratio of 3:1.

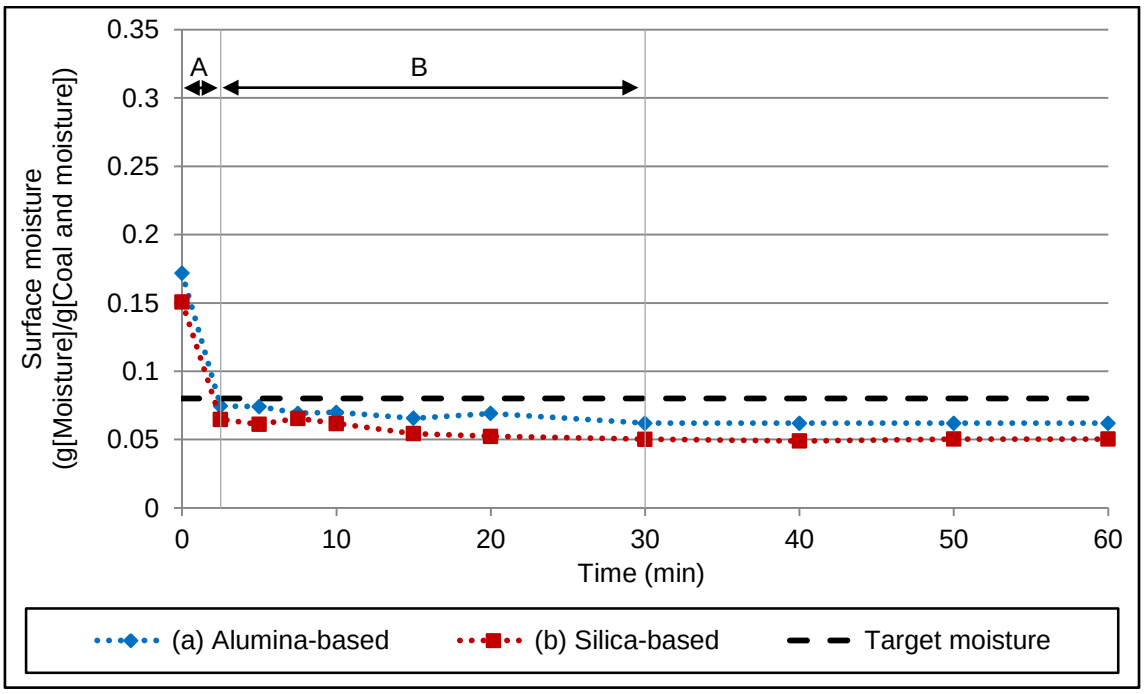

Figure 4.3.4: Desorption curves of -2mm+1mm coal and 3mm adsorbents

Figure 4.3.4 shows the surface moisture desorption curves of -2mm+1mm coal fines in combination with (a) alumina-based and (b) silica-based adsorbents. The initial desorption phase and secondary desorption phase is also indicated in Figure 4.3.4, and are labelled A and B, respectively. The desorption curves in Figure 4.3.4 show that the bulk of the surface moisture was displaced during the (A) initial desorption phase, thereby removing 57% of the total (a) 64% and (b) 66% surface moisture present in the coal samples. After 2.5 minutes,

the (B) secondary desorption phase starts, as indicated in Figure 4.34Figure 4.3.4, and moisture displacement from the pores and capillaries of the coal particles start. The secondary desorption phase is time consuming, and only (a) 7% and (b) 9% of the total amount of surface moisture present was removed during this phase. Final inherent surface moisture of the coal samples was reached at (a) 0.06 g(moisture)/g(coal and moisture) and (b) 0.05 g(moisture)/g(coal and moisture). The difference in final surface moisture content of the coal samples is insignificant. The grain apparent porosity of the alumina-based and silica-based adsorbents is 50.7% and 47.7%, respectively, and the marginal difference in final surface moisture contents of the coal may be a result of small variation in porosity between the two adsorbent types.

Figure 4.3.5 displays the initial desorption rates for -2mm+1mm coal in the presence of both 3mm alumina based adsorbent and 3mm silica based adsorbent. The experimental runs were conducted at 25°C and 40%RH, and the adsorbent to coal mass ratios selected for discussion were 3:1, 2:1, 1:1, 0.75:1 and 0.5:1.

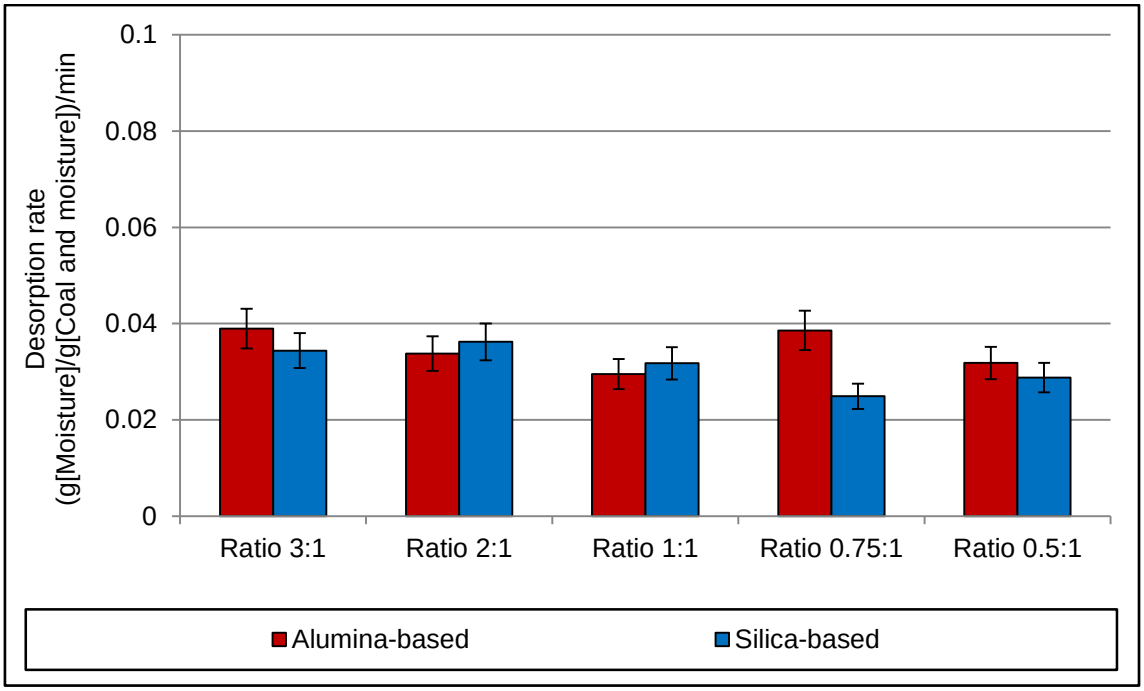

Figure 4.3.5: Initial desorption rates of -2mm+1mm coal with 3mm adsorbents

The results in Figure 4.3.5 shows only a significant difference in initial desorption rates of the coal at the adsorbent to coal mass ratio of 0.75:1. The relative standard error bars indicated on the other desorption rates in Figure 4.3.5 overlap, indicating the difference between desorption rates is insignificant. According to Farag *et al*. (2011), the amount of moisture removed is governed by the inlet moisture concentration. The initial desorption rate is

largely dependent on the amount of initial moisture present therefore; the significant deviance at ratio 0.75:1 in Figure 4.3.5 may be a result of a larger variance in initial moisture contents of the coal fines and classified as an outlier.

More adsorbent type results are summarized in Annexure B.3.2.

4.3.3 Influence of adsorbent size

Adsorbent sizes of 3mm and 5mm were chosen for the fixed-bed experiments based on the commercial availability thereof, and accounting for the screening separation process. By varying the diameter of the adsorbents, the influence of adsorbent size on the adsorbent drying performance was studied. A set of tests were conducted in which the surface moisture content of -1mm+0.5mm coal was examined after 10 minute of drying with 3mm and 5mm silica-based adsorbents. Table 4.4 shows the operating parameters and the corresponding results obtained.

Table 4.4: Moisture displacement of -1mm+0.5mm coal in the presence of 3mm and 5mm silica-based adsorbents

Ratio	**Moisture content** (g[Moisture]/g[Coal and moisture])		**Moisture removed** (%)	
	3mm	**5mm**	**3mm**	**5mm**
3:1	0.075	0.055	69.81	77.38
2:1	0.089	0.066	64.40	73.33
1:1	0.113	0.096	57.44	61.28
0.75:1	0.122	0.097	54.41	60.27
0.5:1	0.120	0.098	52.63	62.56

The results in Table 4.4 show the largest standard deviation was achieved after 10 minutes of drying at an adsorbent to coal mass ratio of 0.75:1. The surface moisture content of the coal fines shown in Table 4.4 differs marginally from each other, which indicated that adsorbent size was not a significant factor for lowering the surface moisture of the coal. Yang (2015) found that adsorbent size played a significant part in lowering the surface moisture content of the coal. Although this was true for the particular study, one must keep in mind that different materials and parameters were investigated. Prairie Eagle coal was used with a particle size range of -1mm, and the adsorbent to coal ratios investigated ranged from 0.88 to 0.70 (Yang, 2015).

The initial desorption rates were examined to determine whether the difference was substantial enough to warrant further investigation into adsorbent size. Figure 4.3.6 displays the initial desorption rates obtained for the 3mm and 5mm alumina-based adsorbents for all the adsorbent to coal mass ratios, individually. Figure 4.3.6 shows some differences between the initial rate responses for -1mm+0.5mm coal in the presence of 3mm and 5mm silica-based adsorbents.

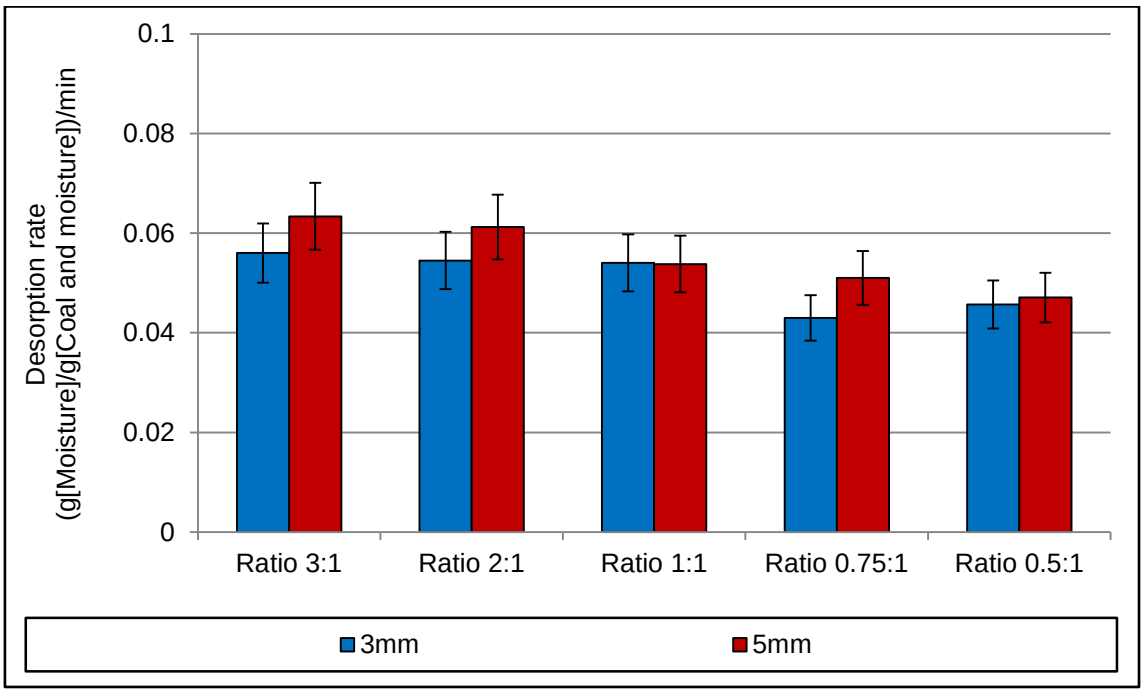

Figure 4.3.6: Desorption rates of -1mm+0.5mm coal and silica-based adsorbents

Figure 4.3.6 shows that the coal in combination with the 3mm silica-based adsorbent yielded lower initial desorption rates than the coal in combination with the 5mm silica-based adsorbents. The relative standard error bars displayed for the rates in Figure 4.3.6 show that variance between the initial desorption rates of the adsorbent sizes is insignificant. Yang (2015) found that adsorbent size had a significant effect on lowering the final moisture content of fine coal. One must keep in mind that the experiments conducted by Yang (2015) included mixing, whereas the fixed-bed experiments conducted during this study did not include mixing.

More adsorbent size results can be found in Annexure B.3.3.

4.3.4 Influence of coal particle size range

In order to examine the effect of coal particle size distribution on drying performance, three coal particle size ranges were selected and varied while the adsorbent to coal mass ratios, adsorbent type and adsorbent size were kept constant. The coal particle size ranges chosen for investigation were -2mm+1mm, -1mm+0.5mm, and -0.5mm+0.25mm. It is well-known that the degree in difficulty for reducing moisture levels in coal fines intensifies as the coal particle diameter decreases (Hand, 2000). The average initial surface moisture content of the -2mm+1mm, -15mm+0.5mm, and -0.5mm+0.25mm coal were 0.18, 0.25 and 0.29 g(moisture)/g(coal and moisture), respectively. The best performing adsorbent to coal mass ratio of 3:1 was determined in Section 4.3.1 and selected for discussion in this section. Figure 4.3.7 shows the surface moisture response of the various coal fine size ranges. The adsorbent used in Figure 4.3.7 was the 5mm alumina-based adsorbents, and the adsorbent to coal mass ratio selected for discussion was the best operating ratio of 3:1.

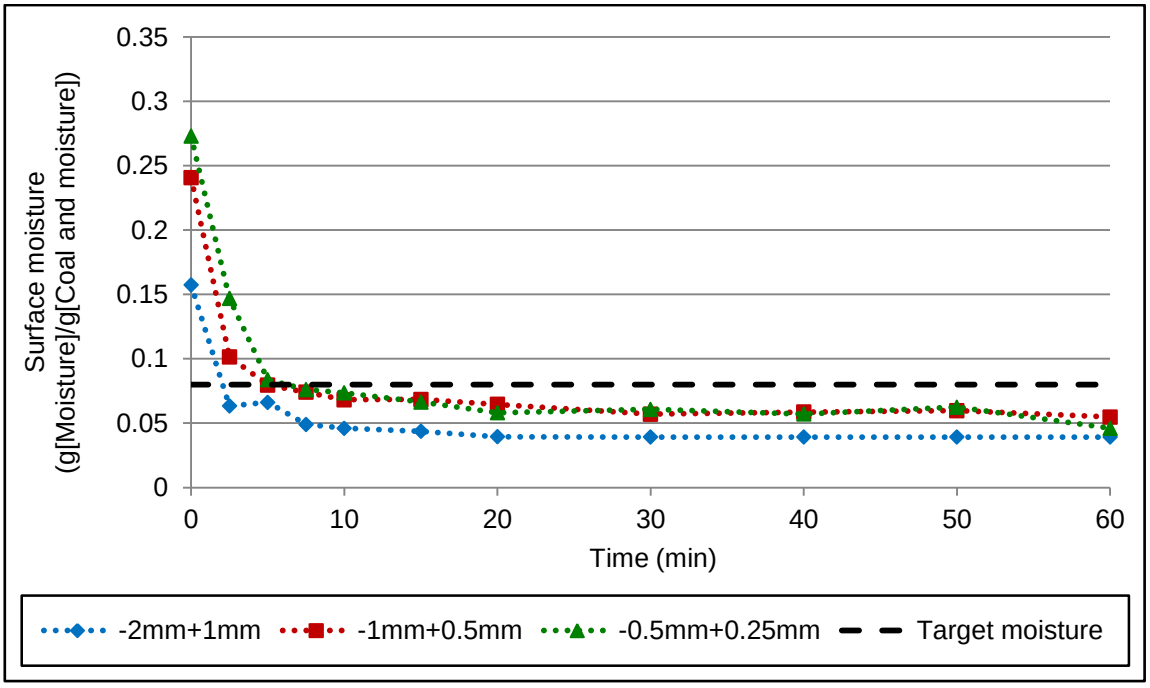

Figure 4.3.7: Desorption curves of coal and 5mm alumina-based adsorbent

The results in Figure 4.3.7 shows that the coal particle size range did not have a significant effect on the final surface moisture content of the coal fines however, sufficient contact time was crucial for best adsorbent performance. The results in Figure 4.3.7 show that only 2 minutes was required to reduce the surface moisture of the -2mm+1mm coal to approximately 0.08 g(moisture)/g(coal and moisture), compared to the 5 minutes required by the -0.5mm+0.25mm coal to reach the same surface moisture content. Fine coal is more

difficult to dewater than coarse coal since the particle surface area is considerably larger for equivalent masses. While surface moisture is generally defined as the moisture located on the internal and external surface areas of the coal particle, Le Roux (2003) adds that the moisture held between adjacent coal particles in a mass also forms part of surface moisture. This means that reduced particle diameters is accompanied by an increased surface area, which retains more surface moisture. Therefore it is more time consuming to remove the surface moisture of the -0.5mm+0.25mm coal.

Figure 4.3.8 shows the comparison of the drying performance of -2mm+1mm, -1mm+0.25mm, and -0.5mm+0.25mm coal in the presence of 5mm silica-based adsorbents at an adsorbent to coal mass ratio of 3:1.

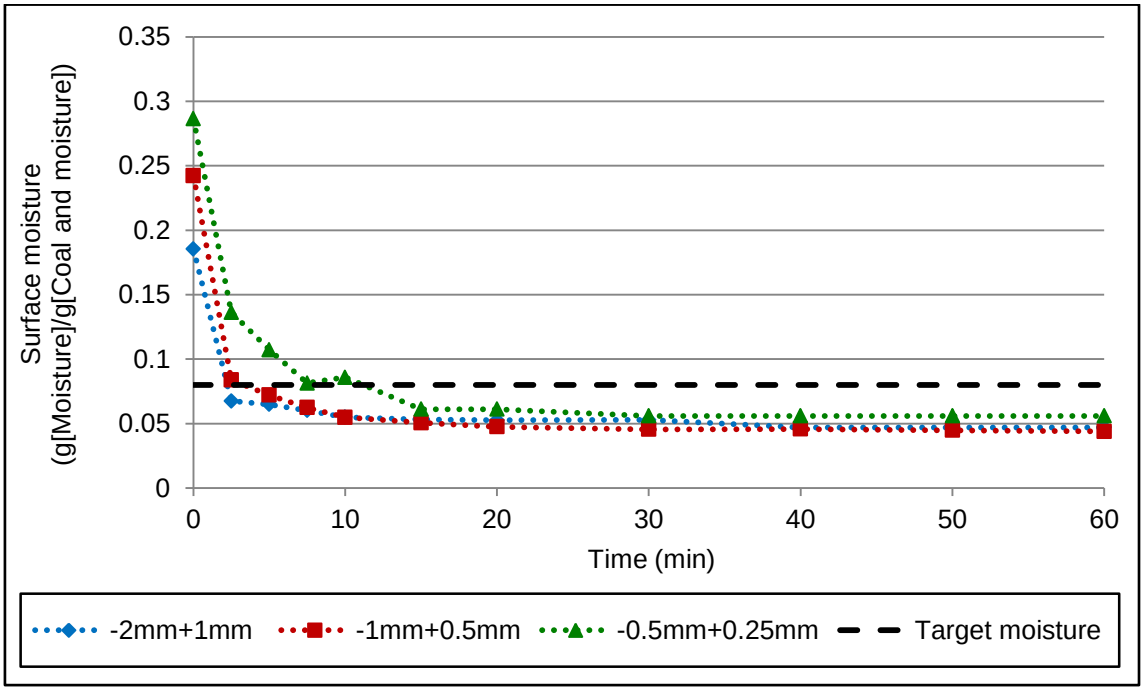

Figure 4.3.8: Desorption curves of coal and 5mm silica-based adsorbent

The results in Figure 4.3.8 shows that more time is required to reduce the surface moisture content of the -0.5mm+0.25mm coal particle size range than the time required to reduce the moisture load of the larger coal particles. From Figure 4.3.8, one can see that only 3 minutes is required to reduce the surface moisture of the -2mm+1mm coal size range to 0.08 g(moisture)/g(coal and moisture), and about 10 minutes is required to achieve the same surface moisture for the -0.5mm+0.25mm coal size range. The difference in drying times may be due to the extended surface area of the -0.5mm+0.25mm coal size range (Hand, 2000). The filter cakes of -2mm+1mm, -1mm+0.5mm, and -0.5mm+0.25mm coal reached the same equilibrium surface moisture content within 10 minutes, 10 minutes, and 15

minutes of drying, respectively. Bratton *et al*. (2012) found that the particle size distribution of the feed stream did not influence the final surface moisture content of the coal fines, provided sufficient contact time between the adsorbents and coal fines was allowed. Therefore, contact time was the controlling factor in reducing the surface moisture of the coal fines. Sufficient contact time allows the adsorbents to perform to full capacity (Yang, 2015).

From an economical perspective, the ideal drying time needs to be identified. In response, the drying time required to reach the target surface moisture content were investigated for the desorption curves shown in Figure 4.3.7 and Figure 4.3.8. The target moisture that was investigated throughout this study was 0.08 g(moisture)/g(coal and moisture). Table 4.5 shows the drying parameters and the corresponding residence times to dry coal to 0.08 g(moisture)/g(coal and moisture).

Table 4.5: Contact time required to dry coal fines to 0.08 g(moisture)/g(coal and moisture)

Coal particle size range	**Contact time** (minutes)	
	Alumina-based adsorbent	**Silica-based adsorbent**
-2mm+1mm	2.0	2.5
-1mm+0.5mm	5.0	3.5
-0.5mm+0.25mm	8.0	11.0

The results in Table 4.5 show that the lowest residence time was required for drying the -2mm+1mm coal fines to the target moisture load, while the most time was required by the -0.5mm+0.25mm coal. This shows that the contact time increases as the coal particle size diameter decreases. Small particles retain more moisture due to the increase surface area created. The difficulty in dewatering coal fines is increased as the particle diameter decreases (Hand, 2000). When the particle size range of the coal decrease, more surface moisture is present, and has to be removed to reach the target surface moisture content. Yang (2015) found that longer contact time allows the adsorbents to perform to its full capacity, and sufficiently remove moisture from coal fines. Therefore, it can be concluded that the contact time required increases as the initial surface moisture content increase.

The initial desorption rates were determined for the desorption curves in Figure 4.3.7 and Figure 4.3.8, and the corresponding results are shown in Figure 4.3.9.

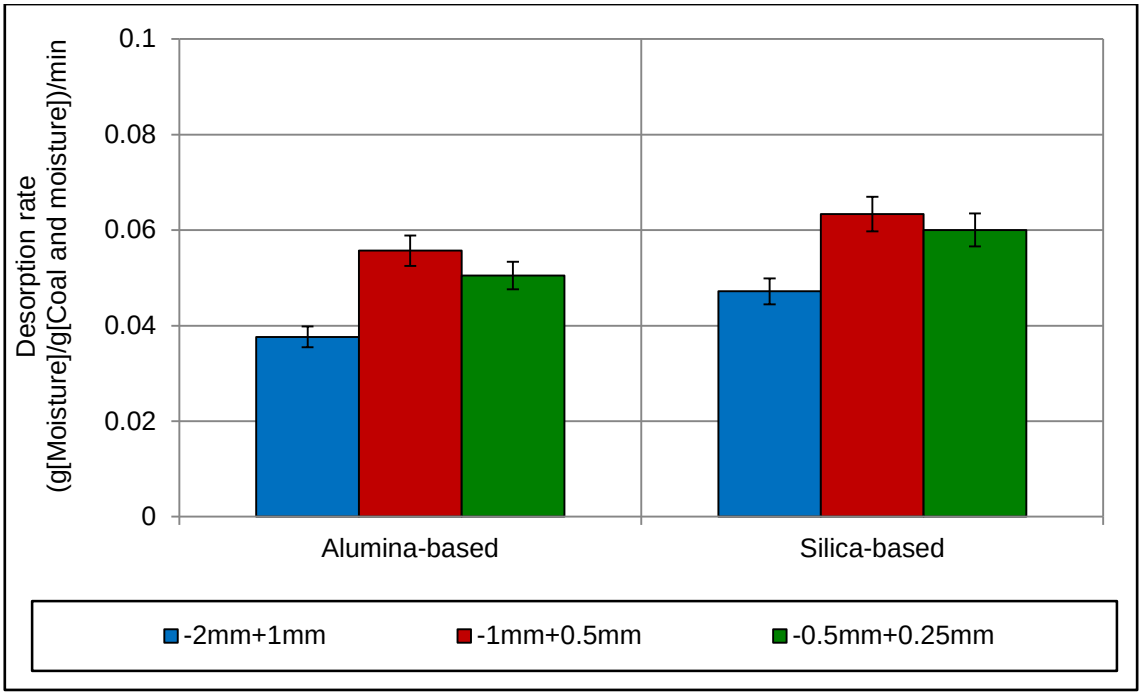

Figure 4.3.9: Initial desorption rates of fine coal and 5mm adsorbents

The initial desorption rates in Figure 4.3.9, shows minimal variance between the -1mm+0.5mm and -0.5mm+0.25mm particle sizes. However, the desorption rates of the -2mm+1mm deviates more significantly from the desorption rates of the -1mm+0.5mm and -0.5mm+0.25mm particle sizes. This indicated that particle size range is a limiting factor for initial drying rate. The initial rates in Figure 4.3.9 show that the rate at which moisture is released from the coal increase with decreasing particle diameter. The rate at which mass is transferred is governed by the contact area (Kudra & Mujumdar, 2009). According to Hand (2000), the surface area of a volume of particles increases with decreasing particle diameter, which in turn increases the surface area for moisture accumulation. Therefore, if there is a large amount of surface moisture available, which is indicated by the coal moisture levels at time zero, the desorption rate of the surface moisture will be swift. The larger contact area created by the -1mm+0.5mm and -0.5mm+0.25mm particle sizes increases the rate at which moisture is initially displaced from the coal.

More data collected for coal particle size ranges can be found in Annexure B.3.4.

4.4 Statistical significance

Statistical significance is a term that refers to the probability that a random sample chosen from a population is not representative of that population. As the level of significance

decrease, one can become more confident in reproducing results. One-way analysis of variance (ANOVA), and significance testing (*t*-test), was performed on the results obtained by the fixed-bed drying technique. The ANOVA was used in cases where the parameters of the measured variables found in Table 3.6 of Chapter 3 were equal to or more than three, and *t*-tests were conducted in cases where there were only two parameters. ANOVA results were generated for the adsorbent to coal mass ratio and coal particle size range parameters. The *t*-tests were applied to describe the outcomes of the adsorbent type and adsorbent size parameters. The p-value (statistical significance) is a criterion of the statistical testing techniques, and is determined by the following probabilities (Ellis and Steyn, 2003):

- $p < 0.05$, statistically significant
- $p > 0.05$, statistically insignificant

The final surface moistures for the coal fines and adsorbents were investigated for 20 minutes of drying to ensure inherent equilibrium moisture was achieved. The ANOVA results generated for the final surface moisture and initial rates of the coal and adsorbents is shown in Table 4.6.

Table 4.6: ANOVA response of fixed-bed drying technique results

Manipulated variable	Measured variable	Sum of squares	df	Mean square	F-value	p-value
Adsorbent to coal mass ratio	Surface moisture: Coal	0.036	4	0.009	12.877	1.83E-07
	Desorption rate	0.003	4	0.001	4.552	3.01E-03
	Surface moisture: Adsorbent	0.117	4	0.029	20.384	2.41E-10
	Adsorption rate	0.010	4	0.003	14.679	3.21E-08
Coal particle size range	Surface moisture: Coal	0.016	2	0.008	7.876	9.55E-04
	Desorption rate	0.004	2	0.002	21.200	1.31E-07
	Surface moisture: Adsorbent	0.051	2	0.025	10.075	1.79E-04
	Adsorption rate	0.005	2	0.003	10.700	1.13E-04

The F-value (F statistic), shown in Table 4.6, measures the variability between groups compared to the variability within groups. The results in Table 4.6 validate the findings in Section 4.3.1 and 4.3.4. The adsorbent to coal mass ratios and the coal particle size ranges were found to be governing factors in reducing the final surface moisture content of the coal as the p-values were less than 0.05. The measured variables listed in Table 4.6 also had a significant effect on increasing the surface moisture load of the adsorbent, the initial adsorption rates of the adsorbents as well the initial desorption rates of the coal.

The response of the *t*-tests for the adsorbent type and the adsorbent size is given in Table 4.7.

Table 4.7: *T*-test response of fixed-bed drying technique results

Manipulated variable	Measured variable	Mean	Standard deviation	t	df	p-value
Adsorbent type	Surface moisture: Coal	0.09	0.035	1.073	58	4.24E-01
	Desorption rate	0.04	0.013	-0.035	58	4.08E-01
	Surface moisture: Adsorbent	0.20	0.058	0.361	58	4.54E-01
	Adsorption rate	0.04	0.018	0.177	58	7.61E-01
Adsorbent size	Surface moisture: Coal	0.09	0.035	0.456	52	1.79E-01
	Desorption rate	0.04	0.013	-0.186	56	4.70E-01
	Surface moisture: Adsorbent	0.21	0.058	0.415	58	5.20E-02
	Adsorption rate	0.04	0.018	0.796	58	4.70E-02

From Table 4.7 is apparent that the p-values of the adsorbent type variable were more than 0.05. This indicated that the final moisture content and initial transfer rates of moisture between the coal and adsorbent, respectively, are independent from adsorbent type. The *t*-tests generated p-values for adsorbent size that exceeded 0.05 for the final surface moisture and initial desorption rates of coal as shown in Table 4.7. Moreover, the p-values obtained for the adsorbent surface moisture and initial adsorption rate were less than 0.05, indicating the adsorbent size was a significant factor increasing the surface moisture load of the adsorbents and the initial adsorption rate.

4.5 Conclusion

From the variables tested, it was found that the adsorbent to coal mass ratio played a significant role in lowering the final moisture content of the coal. Similarly, the adsorbent to coal mass ratio was a significant factor in increasing the product moisture of the adsorbents as well as increasing the adsorption and desorption rates. It was further concluded that adsorbent type did not have a significant effect on the product moisture and the initial rates of the coal and adsorbents. The adsorbent size had a small effect on the adsorption product moisture, and the initial adsorption rate whereas the adsorbent size did not influence the coal product moisture and initial desorption rate. The initial adsorption and desorption rates were largely dependent on the coal particle size range, as was the product moistures of both the adsorbent and coal.

The best performing adsorbent to coal mass ratio was 3:1. Moreover, the coal particle size range that delivered the best initial desorption rate and final moisture content was the -1mm+0.5mm and -2mm+1mm coal, respectively. The initial desorption rate standard deviation was found to be 0.37 percentage points for the -1mm+0.5mm coal and the standard deviation of the -2mm+1mm coal was found to be 1.47 percentage points.

5

CHAPTER

CASCADING-BED DRYING TECHNIQUE

Similar to the fixed-bed experiments investigated in Chapter 4, a set of cascading-bed bench-scale experiments were carried out. Cascading motion was added by slowly rotating the cylindrical vessels about its axis on a bench-scale rotary dryer, to study the effect of improved particle contact on the drying performance of coal and adsorbents. Chapter 5 evaluates and conclude on the findings for the set of cascading-bed experimental runs. Chapter 5 starts by outlining the variables and parameters that were tested during the cascading-bed experiments in Section 5.1. The general adsorption and desorption curves were discussed in Section 5.2. Section 5.3 summarises the influences of various operating parameters on the drying performance of coal and adsorbents. The effect of motion on the drying performance of coal and adsorbents is detailed in Section 5.4, while Section 5.5 holds the statistical significance of the tested variables. Section 5.6 concludes on the findings of Chapter 5.

5.1 Variables

The cascading-bed experimental runs were performed in a climate-controlled room at 25°C and 40%RH. The apparatus consisted of a cascading-bed rotary dryer and laboratory sieves as demonstrated in Section 3.4.2 of Chapter 3. Numerous lab-scale experiments were conducted on Highveld coal using alumina-based (F-200) and silica-based (Silsorb-N10) adsorbents. The surface moisture content and initial moisture transfer rates of both the coal and adsorbents were monitored. Adsorbent to coal mass ratio, adsorbent size and coal particle size range formed part of the test matrix investigated to achieve the desired target coal moisture. The target moisture investigated during this study was 0.08 g(moisture)/g(coal and moisture). Section 3.3 in Chapter 3 contains the variables that were investigated during the cascading-bed experimental test runs.

5.2 General adsorption and desorption curves

Similar to the fixed-bed experiments, the cascading-bed experiments were conducted in a climate-controlled room at 25°C and 40%RH. Prior to experiments, the coal fines were submerged in water for 24 hours while the adsorbent material was left exposed in the climate-controlled room for 24 hours. During cascading-bed experiments, wet coal and a predetermined amount of adsorbent material was contacted in cylindrical vessels on a bench-scale rotary dryer for defined time intervals, as discussed in Chapter 3. After sufficient contact time has elapsed, the mixture was separated and the coal and adsorbent samples were analysed for surface moisture contents. In this manner, the displacement of surface moisture between wet coal fines and capillary-porous dry adsorbent material is observed. The purpose of the desorption and adsorption curves in this section is to illustrate surface moisture displacement between the coal fines and adsorbents. Figure 5.2.1 demonstrates the general desorption and adsorption curves of -1mm+0.5mm coal fines and 5mm (a) alumina-based and (b) silica-based adsorbents in a adsorbent to coal mass ratio of 1:1. The average initial surface moisture content of the coal fines were 0.25 g(moisture)/g(coal and moisture) with a standard deviation of 0.92%.

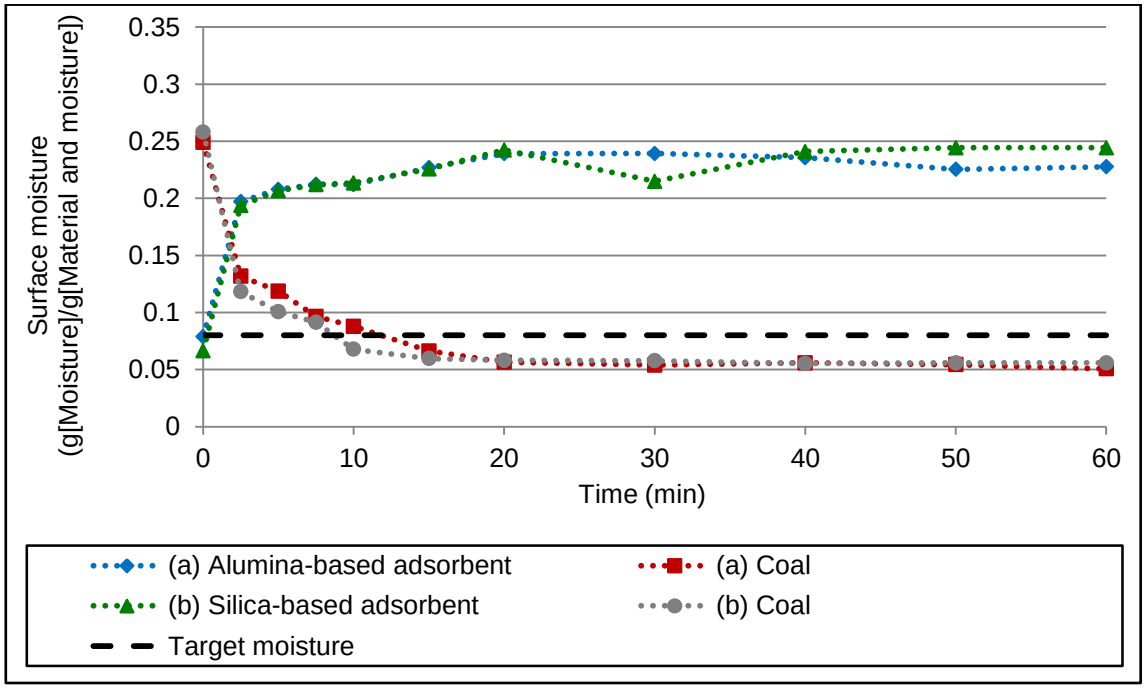

Figure 5.2.1: Adsorption-desorption curves of -1mm+0.5mm coal and 5mm adsorbents

The surface moisture removed from the coal fines was measured in g(moisture)/g(coal and moisture) and the surface moisture adsorbed by the adsorbent material in g(moisture)/g(adsorbent and moisture). The coal fines in Figure 5.2.1 reached inherent

moisture equilibrium when about 80% of the surface moisture present was removed. After 10 minute of contacting, the surface moisture content of the coal fines was reduced by (a) 0.16 and (b) 0.19 g(moisture)/g(coal and moisture), which is (a) 80% and (b) 95% of the total amount of surface moisture removed. The adsorbents in Figure 5.2.1 gained roughly (a) 0.14 and (b) 0.15 g(moisture)/g(adsorbent and moisture) after 10 minutes of contacting and equilibrium adsorption loading was reached after a further (a) 3% and (b) 4% surface moisture was adsorbed. The moisture transfer mechanism associated with adsorbent assisted drying of coal fines was discussed in detail in Section 4.2.2 of Chapter 4. Initially moisture is transferred by capillary flow through an interphase between the adsorbent and coal particles (Kudra and Mujumdar, 2009). As the amount of moisture on the coal's surface decrease, moisture displacement through the interphase stops and moisture from the pores and capillaries of the coal particles starts to diffuse through the interstitial air between the particles along a concentration gradient. Inherent moisture equilibrium is directed by the relative humidity conditions of the air adjacent to the particles surfaces (Le Roux et al., 2015). Therefore, when moisture diffuses into interstitial air spaces between the particles, the relative humidity of the air surrounding the particles is affected and the drying kinetics change. The unequal surface moisture at inherent moisture equilibrium noticed in Figure 5.2.1 is a result of the moisture difference suspended in the surrounding air.

In order to test the reproducibility of the experimental procedure, a series of cascading-bed experiments with the same operating parameters were selected at random and repeated. The method followed for determining the standard deviation and relative standard error is discussed in detail in Annexure A.1. The mean, standard deviation and relative standard error of the initial surface moisture content was determined for the (-2mm+1mm, -1mm+0.5mm and -0.5mm+0.25mm coal used during the cascading-bed experiments and the corresponding results are given in Table 5.1.

Table 5.1: Mean, standard deviation and relative standard error of initial moisture of coal

Description	Mean (g[Moisture]/g[Coal and moisture])	Standard deviation (%)	Relative standard error (%)
-2mm+1mm	0.17	1.18	1.80
-1mm+0.5mm	0.25	0.92	0.80
-0.5mm+0.25mm	0.30	0.95	0.70

It is important to ensure the initial surface moisture content of the individual coal particle size ranges lie within close proximity from one another. Maintaining the initial moisture content of the coal steady will increase experimental accuracy and ensure that the experimental results are comparable. The results summarised in Table 5.1 shows that the initial moisture contents of the various coal particle size ranges differs marginally.

Figure 5.2.2 presents the repeatability data of the desorption curves of -1mm+0.5mm coal and 5mm alumina-based adsorbents in an adsorbent to coal mass ratio of 2:1. The upper and lower limits represent the standard deviation from the average of the repeats. The minimum and maximum standard deviations calculated for the desorption curves in Figure 5.2.2 were 0.83 and 1.98 percentage points, respectively.

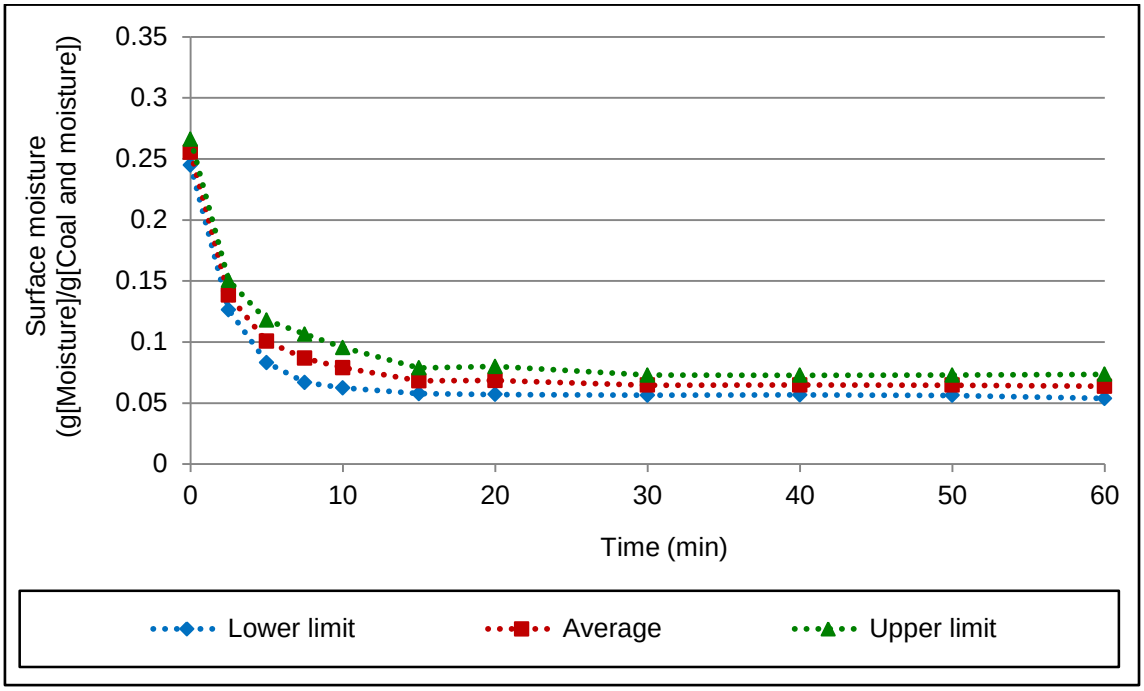

Figure 5.2.2: Average and standard deviation of -1mm+0.5mm coal desorption curves

The relative standard error (RSE) was also calculated to determine the magnitude of variance between the mean and the experimental runs. The minimum relative standard error was found to be 2.40% and the maximum relative standard error was 13.21%. Figure 5.2.3 represents the repeatability data of the general adsorption curves of 5mm alumina-based adsorbents at an adsorbent to coal mass ratio of 2:1.

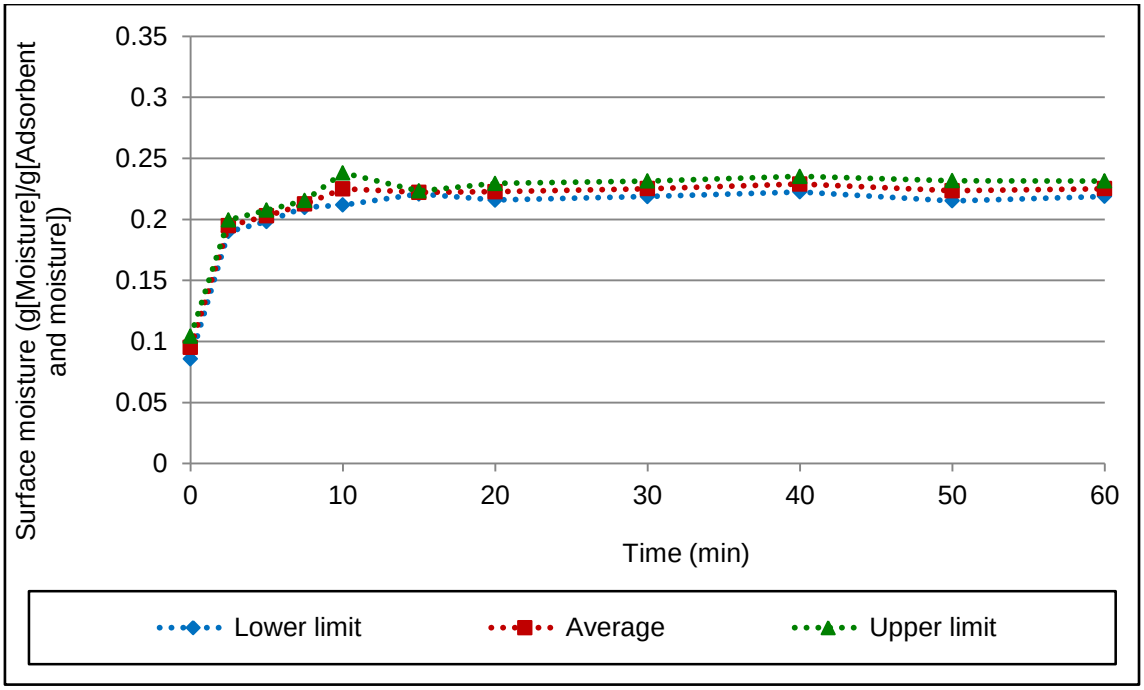

Figure 5.2.3: Average and standard deviation of 5mm alumina-based adsorbents adsorption curves

The minimum and maximum standard deviation was 0.12 and 1.31 percentage points, respectively. The minimum and maximum relative standard error for the adsorption curve was 0.32% and 5.62%, respectively. The reliability of the cascading-bed experiments was further investigated by determining the standard deviation and relative standard error for the initial desorption and adsorption rates of the -1mm+0.5mm coal and 5mm alumina-based adsorbents. Initial desorption and adsorption rates of the general desorption, and adsorption curves in Figure 5.2.2 and Figure 5.2.3 were then summarised in Table 5.2.

Table 5.2: Standard deviation and relative standard error of initial rates

Description	Initial desorption rates	Initial adsorption rates
Standard deviation (%)	0.20	0.35
Relative standard error (%)	2.22	4.99

The standard deviation for the initial desorption rates and adsorption rates in Table 5.2 is 0.20 and 0.35 percentage points, respectively. The relative standard error for the initial desorption rate was 2.22% and the relative standard error calculated for the initial adsorption rate was 4.99%. The repeatability data determined for the experimental runs proved that the

experimental procedure was accurate and the data was reproducible. The marginal standard deviations were an indication that a consistent experimental procedure was followed. The repeatability data applies to all the cascading-bed experiments. Additional repeatability data for the cascading-bed drying technique can be found in Annexure A.3.

5.3 Operating parameters

This section describes the effect of varying operating parameters on the drying performance of coal. Similar to the fixed-bed drying technique, adsorbent to coal mass ratio, adsorbent type, adsorbent size and coal particle size range was selected as main variables under investigation. The effect of the operating parameters on the drying performance of the cascading-bed experiments was similar to the effect of the fixed-bed experiments however, the extent of the effect increased.

Laboratory-scale cascading-bed experiments were conducted at adsorbent to coal mass ratios of 3:1, 2:1, 1:1, 0.75:1 and 0.5:1 as listed in Table 3.5. Figure 5.3.1 displays the coal desorption curves for -1mm+0.5mm coal contacted with 3mm silica-based adsorbents. The air condition in the climate-controlled room was 25°C and 40%RH.

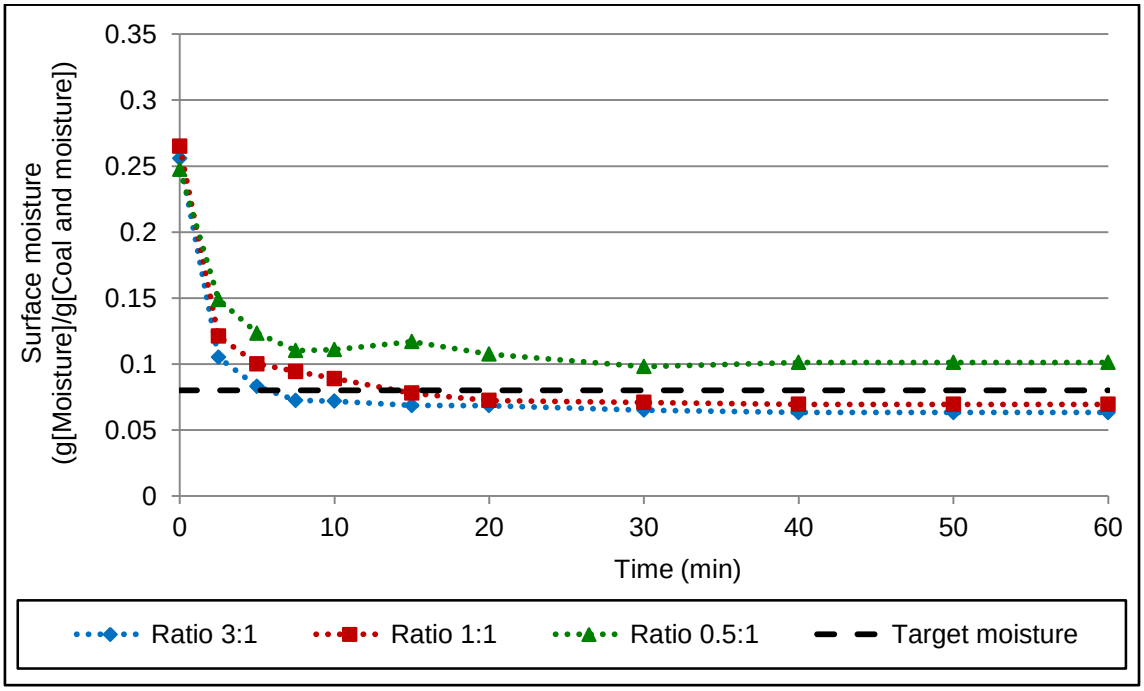

Figure 5.3.1: Desorption curves of -1mm+0.5mm coal and 3mm silica-based adsorbents

The -1mm+0.5mm coal particle size range had an average initial moisture content of 0.25 g(moisture)/g(coal and moisture) with a standard deviation of 0.92 percentage points and a

relative standard error of 0.80%. The results in Figure 5.3.1 show that after 10 minutes of contacting, the surface moisture of the adsorbent to coal mass ratio 3:1 and 0.5:1 was reduced by 72% and 55%, respectively. The -1mm+0.5mm coal, dried in an adsorbent to coal mass ratio of 3:1, reached inherent moisture equilibrium after 8 minutes at 0.070 g(moisture)/g(coal and moisture). The -1mm+0.5mm coal that were contacted in an adsorbent to coal mass ratio of 0.5:1 reached inherent moisture equilibrium after 20 minutes at 0.011 g(moisture)/g(coal and moisture). Similar to the fixed-bed drying technique, the inherent moisture content of the coal fines dried by the cascading-bed drying technique could be "dialled in" by varying the adsorbent to coal mass ratio (Bratton *et al*., 2012). Adsorption equilibrium governs the amount of surface moisture adsorbed (Knaebel, 2006). When increasing the amount of adsorbents present, the adsorbents will attempt to reach full capacity by drawing moisture from the surrounding air. This will cause the relative humidity of the surrounding air to fluctuate as moisture continues to diffuse between the coal fines, air and adsorbents. Inherent moisture equilibrium is achieved when surface moisture displacement stops. Moisture displacement will continue until the "pull power" of the coal mass is equal to that of the adsorbent volume (Kudra and Mujumdar, 2009).

Figure 5.3.2 shows the corresponding adsorption curves of 3mm silica-based adsorbents in combination with -1mm+0.5mm coal, over time. The surface moisture loads were recorded at fixed time intervals to observe surface moisture uptake of the adsorbents over time. The silica-based adsorbents have an average initial moisture load of 0.081 g(moisture)/g(coal and moisture) and a standard deviation of 0.42 percentage points.

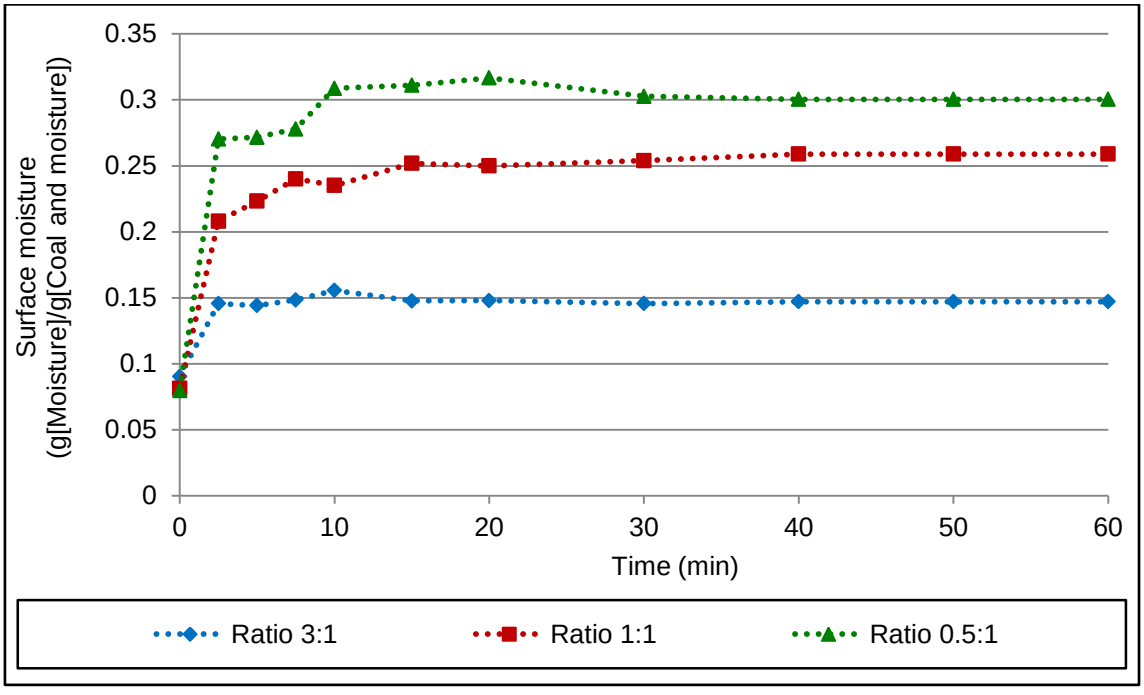

Figure 5.3.2: Adsorption curves of 3mm silica-based adsorbents and -1mm+0.5mm coal

The adsorption curves of 3:1and 0.5:1 in Figure 5.3.2 shows an increase of surface moisture load of 42% and 72% after 10 minutes of contacting. Knaebel (2006) defines adsorption load as the amount of surface moisture taken up by the adsorbent per unit mass of the adsorbent. The adsorbents will continue to adsorb surface moisture until adsorption equilibrium is achieved based on the initial surface moisture concentration available. As the quantity of adsorbents is increased, the mass of surface moisture adsorbed by the adsorbents will be redefined as per unit mass of adsorbents present in the system. The mass of adsorbent to coal is less at 0.5:1 than at 3:1, therefore the percentage of surface moisture adsorbed per unit mass at 0.5:1 will be more.

The initial desorption rates of the -1mm+0.5mm coal in combination with the 3mm silica-based adsorbents were determined and the results are presented in Figure 5.3.3. The initial desorption rates shown in Figure 5.3.3 decrease as the adsorbent to coal mass ratio decrease. This is due to the increased volume of adsorbents present at high adsorbent to coal mass ratios.

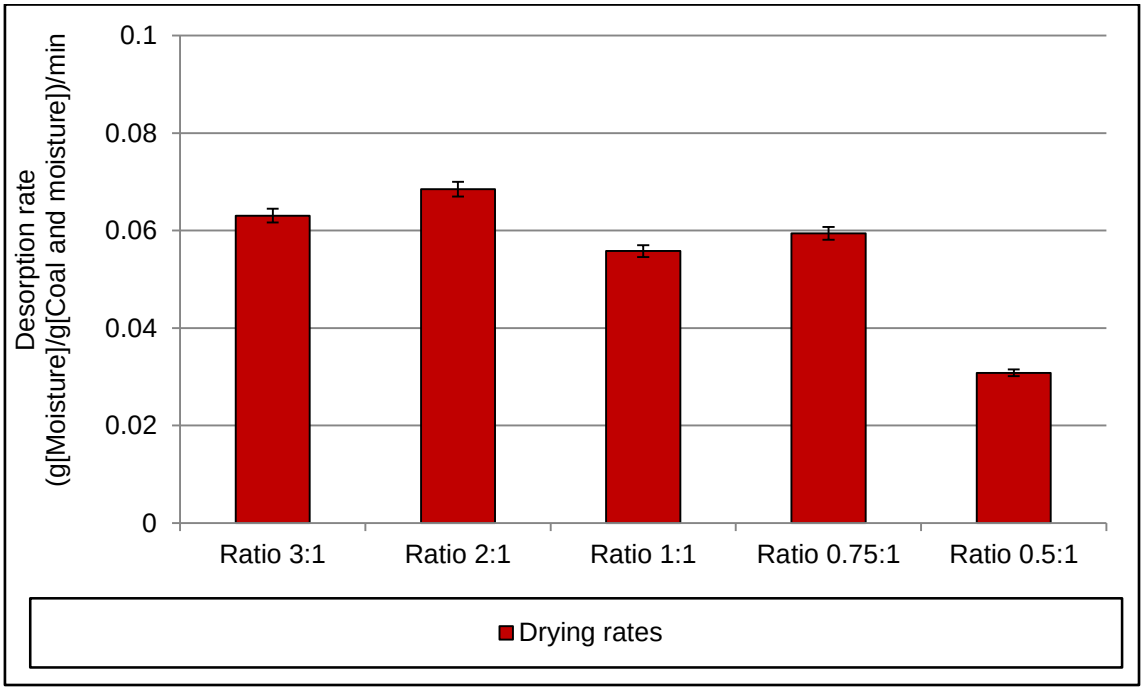

Figure 5.3.3: Initial desorption rates of -1mm+0.5mm coal and 3mm silica-based adsorbent

Bratton *et al*. (2012) conducted a study in which it was concluded that the drying performance of coal could be regulated by adjusting the adsorbent to coal mass ratio. Larger contact areas create favourable conditions for moisture transferal (Kudra and

Mujumdar, 2009). The surface moisture was displaced at an elevated rate from the coal onto the adsorbent surface because of the stronger "pull" experienced by larger adsorbent volumes as well as the increased surface area available for surface moisture adhesion. The relative standard error for the initial desorption rates were 2.22% and is indicated in Figure 5.3.3. More adsorbent to coal mass ratio results can be found in Annexure C.2.1.

Adsorbent type was also investigated for the cascading-bed drying technique and alumina-based (F-200) and silica-based (Silsorb-N10) adsorbents were selected for investigation. This was done to determine which adsorbent material was best suited for the cascading-bed drying technique. The success of adsorbent assisted drying is largely dependent on the adsorbent loading, adsorbent density and the compatibility of the adsorbent (Knaebel, 2006). Figure 5.3.4 illustrates the initial desorption rates determined for -1mm+0.5mm coal in the presence of 5mm alumina-based adsorbents and 5mm silica-based adsorbents.

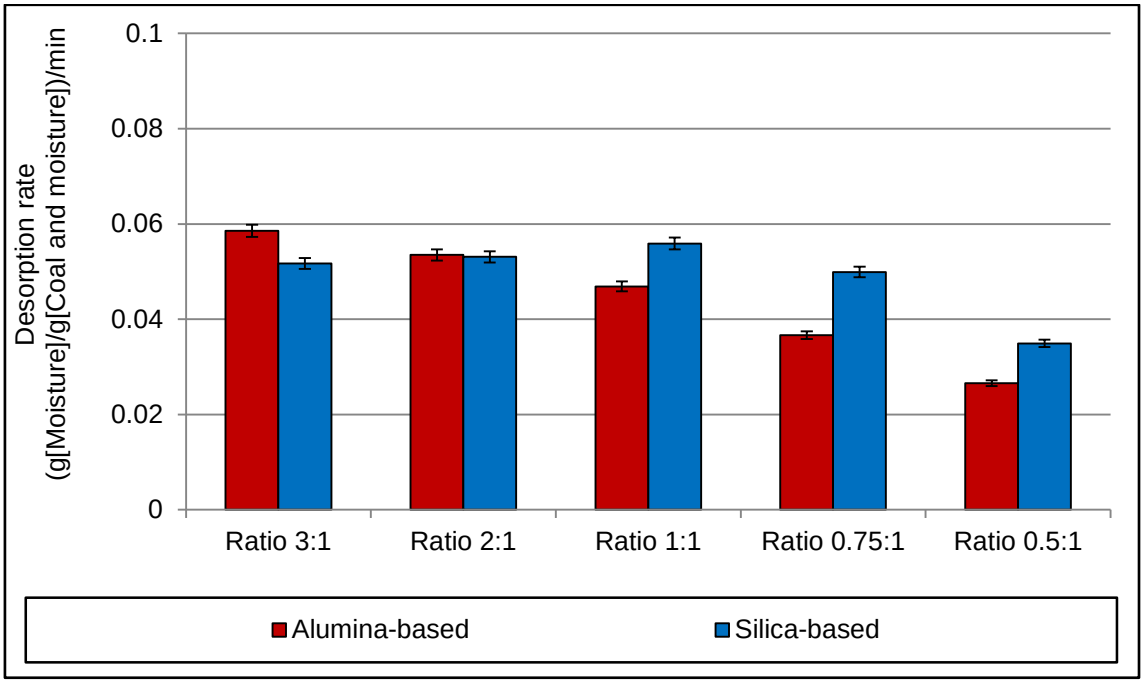

Figure 5.3.4: Initial desorption rates of +-1mm+0.5mm coal and 5mm adsorbents

From Figure 5.3.4 it was evident that the initial desorption rates of the silica-based adsorbents varies marginally from the initial desorption rates of the alumina-based adsorbents. The relative standard error for the initial desorption rates was 2.22% and is indicated in Figure 5.3.4. The grain apparent porosity of the alumina-based and silica-based adsorbents is 50.7% and 47.7%, respectively. This suggests that the surface area available for moisture adsorption is similar and as previously stated; the rate at which surface moisture is displaced from the surface of the coal is largely dependent on the contact area available

(Kudra and Mujumdar, 2009). The surface moisture content of -1mm+0.5mm coal in contact with 5mm adsorbents is shown in Figure 5.3.5. Figure 5.3.5 showed both adsorbents were able to reduce the final moisture content of the coal to 0.08g (moisture)/g (coal and moisture) (Bland and McDaniel, 2014).

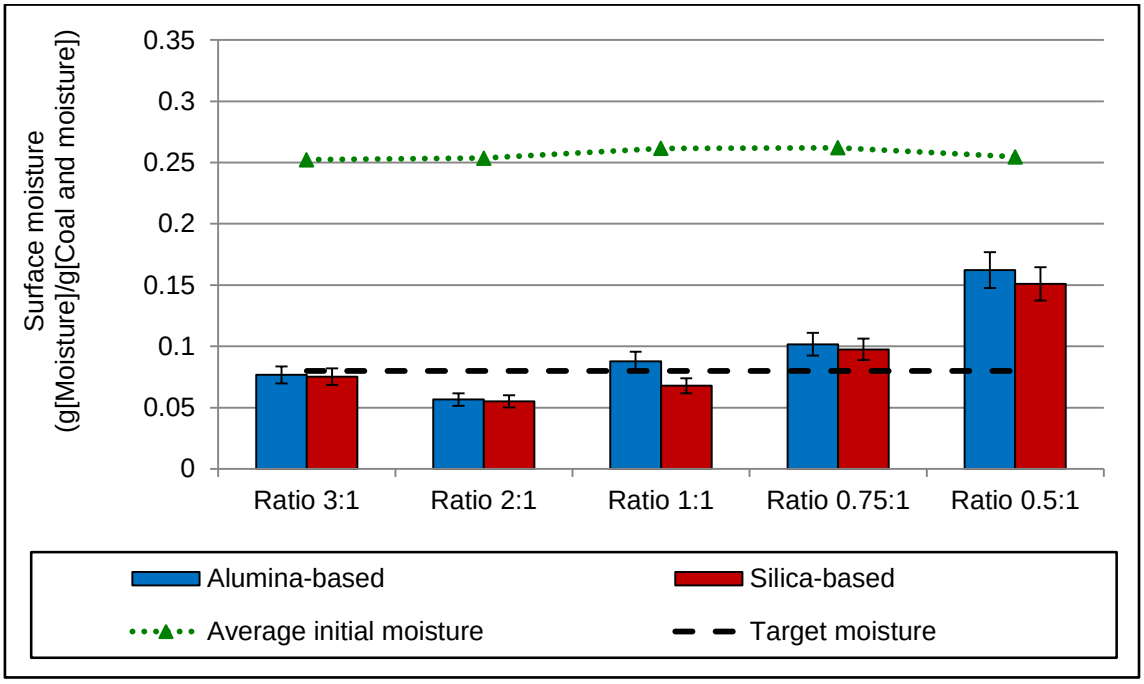

Figure 5.3.5: Effect of adsorbent type on the final moisture loads of -1mm+0.5mm coal

The surface moisture contents obtained validated that adsorbent type did not play a significant part in lowering the surface moisture content of the coal. The marginal difference in final surface moisture contents of the coal may be a result of small variation in grain apparent porosity between the adsorbent types. Annexure C.2.2 contains additional adsorbent type results.

By varying the diameter of the adsorbents, the influence of adsorbent size on the drying performance of the coal was determined. Adsorbent sizes of 3mm and 5mm were selected for investigation. The influence of alumina-based adsorbent size on the initial desorption rate of -1mm+0.5mm coal at an adsorbent to coal mass ratio of 2:1 is presented in Figure 5.3.6. It is evident from Figure 5.3.6 that the adsorbent diameter has an effect on the initial desorption rates of moisture. Contrary to the findings in Section 4.3.3 of Chapter 4, Figure 5.3.6 indicated that an increase in adsorbent diameter resulted in a decrease in initial desorption rates. This was a result of a decreased surface area for adsorption and a reduced concentration of adsorbent particles throughout the coal mass. Hand (2000) addresses this occurrence, by stating the surface area of a volume of particles increases per cube as the diameter as of the particle decreases. Therefore, a larger surface area of the

3mm adsorbent particles was exposed per unit of coal, prompting faster initial transferal rates of moisture from the coal.

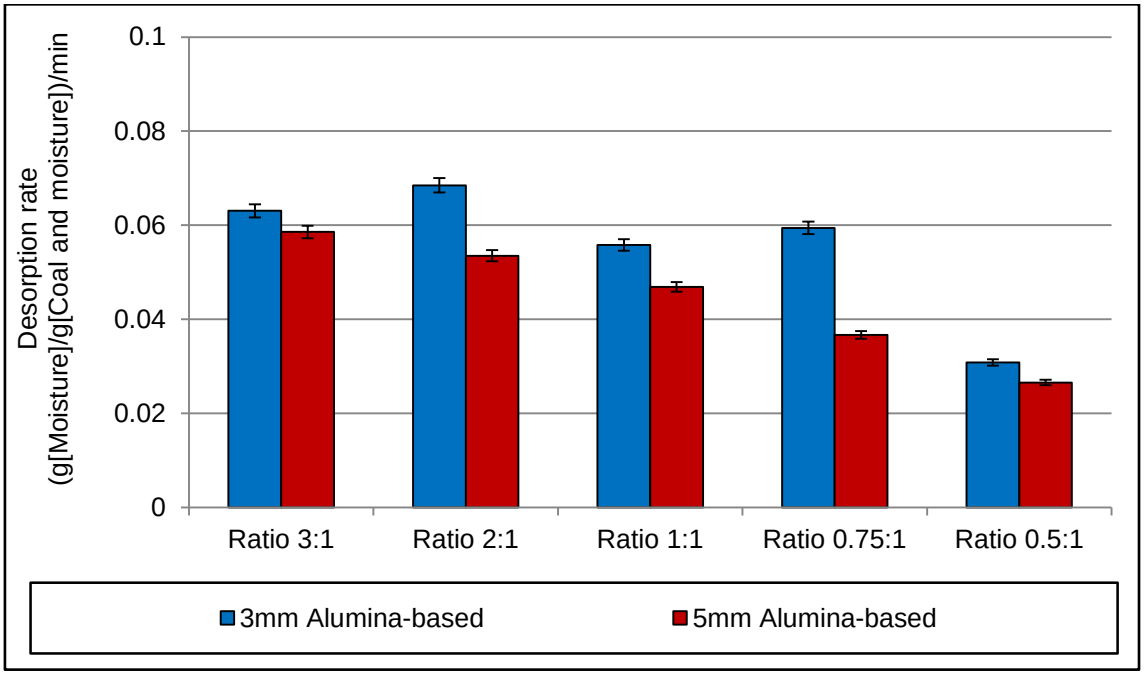

Figure 5.3.6: Initial desorption rates of -1mm+0.5mm coal

A set of tests were conducted in which the surface moisture content of -1mm+0.5mm coal was analysed after 10 minute of drying with 3mm and 5mm silica-based adsorbents and the corresponding results are shown in Figure5.3.7.

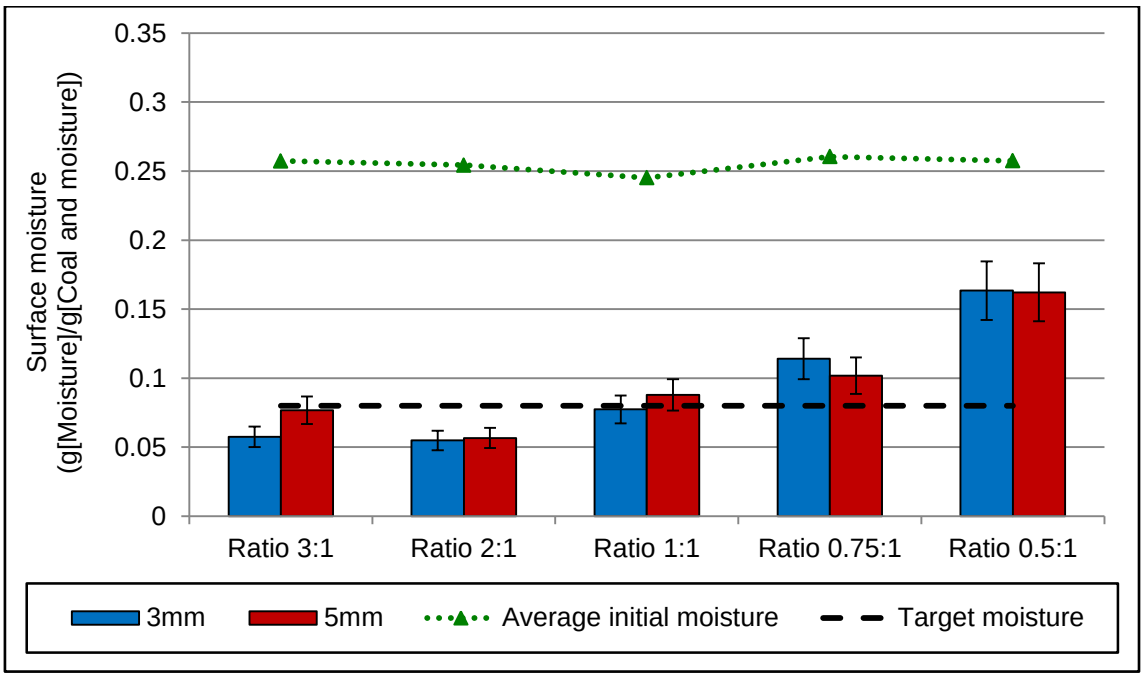

Figure 5.3.7: Effect of adsorbent size on final surface moisture content of -1mm+0.5mm coal

The results in Figure 5.3.7 show that adsorbent size does not influence the final surface moisture of the coal, as 10 minutes was sufficient contact time for the adsorbents to perform to its full capacity. Therefore, the adsorbents will perform at full capacity irrespective of adsorbent size, provided the inlet conditions are the same and sufficient contact time is available. Bratton *et al*. (2012) found that the particle size distribution in the feed stream did not influence the surface moisture content of the product stream. Additional results of this nature is available in Annexure C.2.3.

The influence of coal particle size range was investigation for the cascading-bed drying technique. Figure 5.3.8 shows the response of -2mm+1mm, -1mm+0.5mm and -0.5mm+0.25mm coal to 5mm alumina-based adsorbents at an adsorbent to coal mass ratio of 2:1.

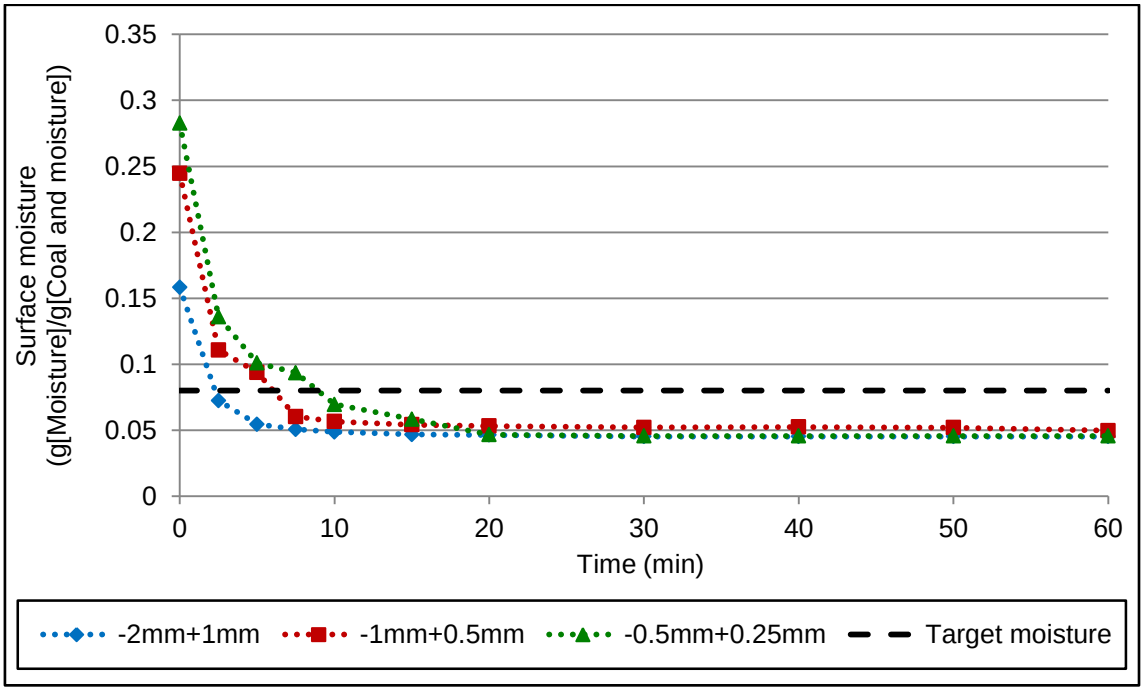

Figure 5.3.8: Desorption curves of coal in combination with 5mm alumina-based-based adsorbent

The coal particle size ranges in Figure 5.3.8 reached the same inherent surface moisture content after 20 minutes, however it is evident the controlling factors are initial surface moisture content and contact time. From an economical perspective, the amount of time consumed to reduce the surface moisture of the coal fines regulates the revenue generated by the coal fines. More than 3 minutes of drying time is commercially unattractive (Yang, 2015). Therefore, Figure 5.3.8 shows that the -0.5mm+0.25mm coal size range reached

0.13 g(moisture)/g(coal and moisture) after 3 minutes residence time whereas the -2mm+1mm coal size range reached final surface moisture content of 0.06 g(moisture)/g(coal and moisture) within the same time frame. The -0.5mm+0.25mm coal size range had smaller particle diameters than the -2mm+1mm, that provides an increased surface area for moisture accumulation (Hand, 2000). Additionally, moisture has difficulty moving through the interstitial voids and pores as the coal particle diameter decrease (Hand, 2000), which explains the prolonged drying time required for the smaller coal particles.

Figure 5.3.9 shows the -2mm+1mm, -1mm+0.5mm and -0.5mm+0.25mm coal particle size ranges' average initial surface moisture contents of 0.17, 0.25 and 0.30 g(moisture)/g(coal and moisture), respectively, compared to the initial desorption rates of the various coal particle size ranges. It is evident from Figure 5.3.9 that the desorption rate increases as the initial moisture concentration is increased. This is a result of the increased concentration gradient as the initial surface moisture content of the coal increases.

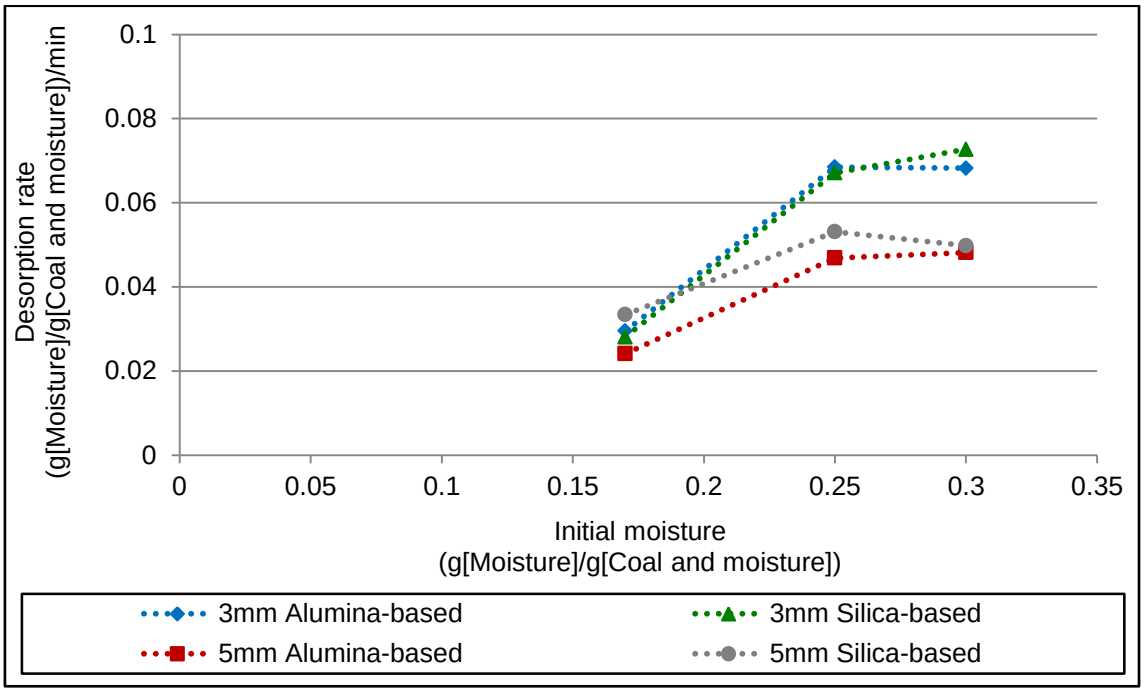

Figure 5.3.9: Initial desorption rates of coal at an adsorbent to coal mass ratio of 2:1

The initial desorption rate is determined by the initial slope of the desorption curves and is defined as the amount of initial surface moisture removed of coal per unit mass of coal over time. Since the amount of surface moisture present increases as the coal particle diameter decreases, the initial desorption rates increase (Hand, 2000). Therefore, from Figure 5.3.9, it can be concluded that coal particle size range has a significant influence on the initial desorption rates and therefore the contact time.

Further coal particle size range results can be found in Annexure C.2.4.

5.4 Influence of motion

The rate at which surface moisture is transferred between particles is greatly dependent on the amount of surface area available for contact. According to Bratton *et al*. (2012), surface contact between adsorbent material and coal fines is maximised by introduction of motion. Motion provides regular inter-particle contact, which improves moisture association between the adsorbent and coal particles. Therefore, motion was introduced as a secondary drying technique for investigation. Motion was created by rotating the cylindrical vessels containing the coal and adsorbents along its length on a cascading-bed rotary dryer. The rotary dryer was operated at 3rpm to ensure a cascading motion was maintained as opposed to a cataracting motion. In this way, inter-particle contact is stimulated without affecting the structural integrity of the coal or adsorbent particles. The fixed-bed results discussed in Section 4.3 of Chapter 4 were reviewed and compared to the cascading-bed results that were discussed in Section 5.3. To demonstrate the influence of motion, the general desorption curves, characteristic drying curve and surface moisture is discussed in Section 5.4.

5.4.1 General desorption curves

The influence of motion on the general desorption of moisture is discussed in this section. The adsorbent to coal mass ratio, adsorbent type, adsorbent size and coal particle size range was kept constant, while the drying technique was varied. The results obtained for two of the experimental test comparisons are shown in Figure 5.4.1 and Figure 5.4.2. Figure 5.4.1 shows the fixed-bed and cascading-bed desorption curves of -1mm+0.5mm coal contacted with 3mm alumina-based adsorbents in an adsorbent to coal mass ratio of 1:1.

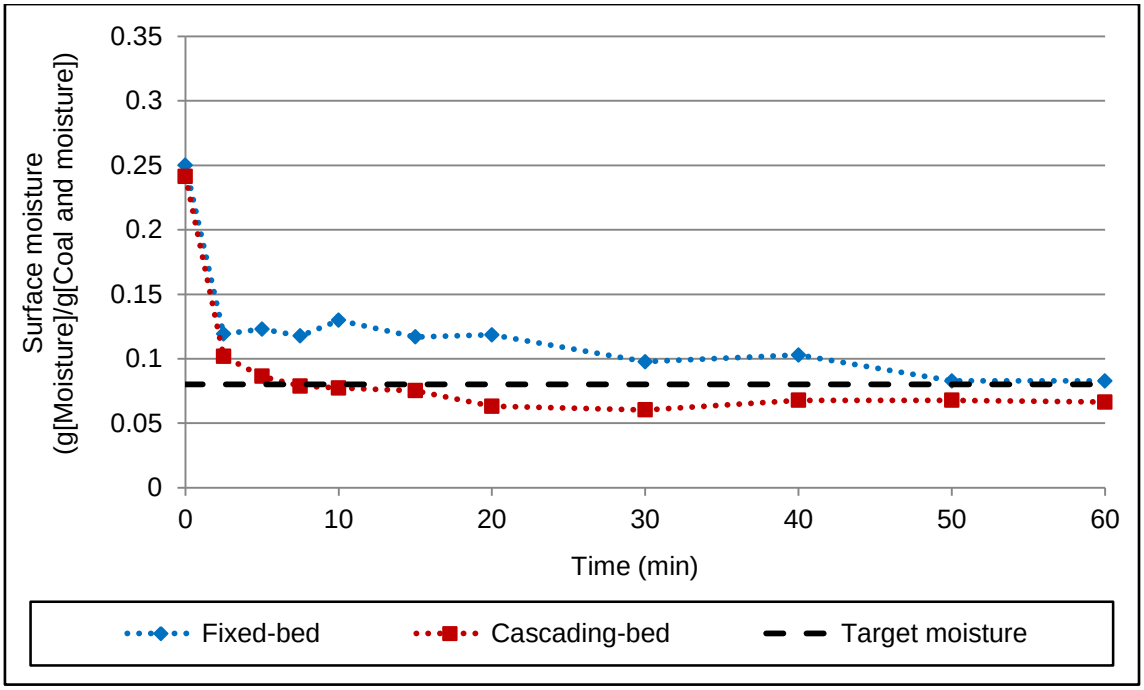

Figure 5.4.1: Desorption curves of -1mm+0.5mm coal and 3mm alumina-based adsorbent

The desorption curves in Figure 5.4.1 shows no significant difference between the initial desorption rates of the fixed-bed and cascading-bed drying techniques. Note the surface moisture contents after 10 minutes differ by 0.05 g(moisture)/g(coal and moisture), with the lowest final surface moisture obtained by the cascading-bed technique. The target surface moisture is reached in15 minutes when the cascading-bed drying technique was applied, whereas 35 minutes more was required by the fixed-bed drying technique to achieve the same surface moisture content.

Figure 5.4.2 shows the desorption curves of -1mm+0.5mm coal in contact with 3mm silica-based adsorbents, at an adsorbent to coal mass ratio of 1:1, for the fixed-bed and cascading-bed drying techniques. The desorption curves in Figure 5.4.2 exhibited similar desorption trends to the curves in Figure 5.4.1. The difference in initial desorption rates for the fixed-bed and cascading-bed drying techniques shown in Figure 5.4.2 were insignificant. However, the cascading-bed technique reached a surface moisture content of 0.09 g(moisture)/g(coal and moisture) within 10 minutes of commencing while the fixed-bed drying technique required 40 minutes to reach the same surface moisture content.

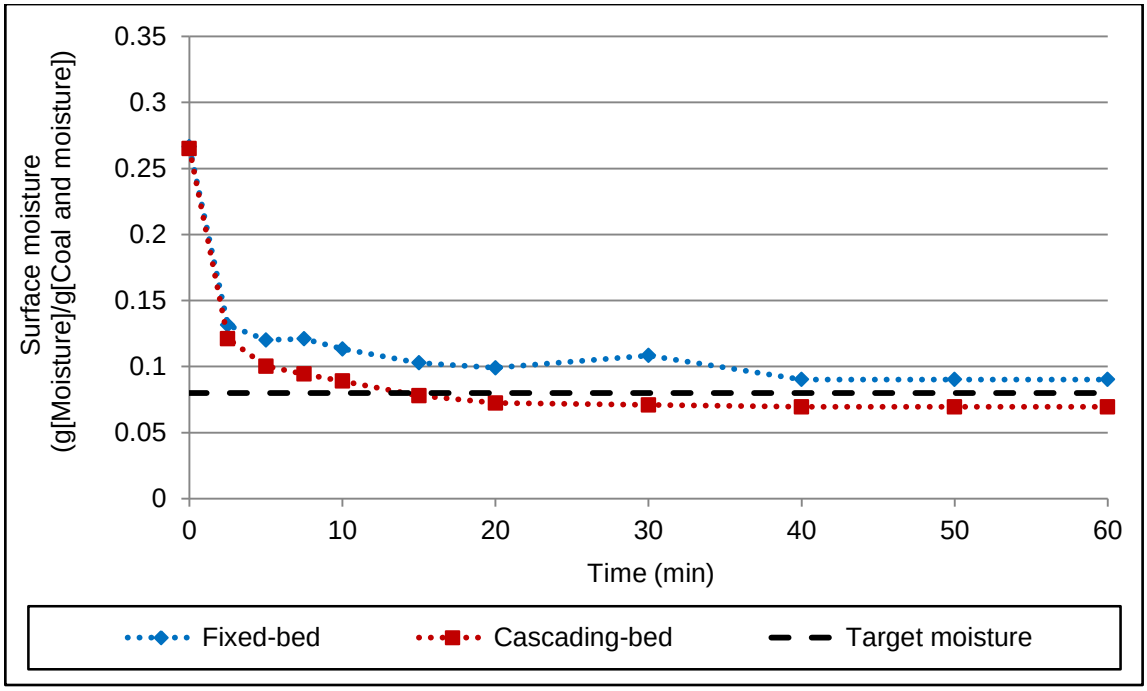

Figure 5.4.2: Desorption curves of -1mm+0.5mm coal and 3mm silica-based adsorbent

The results in Figure 5.4.1 and Figure 5.4.2 showed that motion enhances the contact area, which in turn increases the secondary desorption rate. The increase in secondary desorption rate results in a reduced amount of contact time required. Introduction of motion increases the inter-particle contact, which maximises the portion of surface area available for moisture exchange (Bland and McDaniel, 2014). As the surface moisture of the fine coal is removed at an increased rate, the rate at which the moisture is replaced at the surface (secondary desorption phase) also increases.

More drying technique comparison curves are provided in Annexure C.3.1.

5.4.2 Characteristic drying curve

The characteristic drying curve was discussed in detail in Section 4.2 of Chapter 4. The desorption curves observed for the cascading-bed drying technique showed an initial desorption phase, a secondary desoprtion phase and an inherent surface moisture content phase that was similar to the desorption phases observed for the fixed-bed drying technique. Although the desorption curves offer the same distinct desorption phases, a difference in the secondary desoprtion phase was observed. The characteristic desorption curves of the cascading-bed drying technique and fixed-bed drying technique is collectively illustrated in Figure 5.4.3.

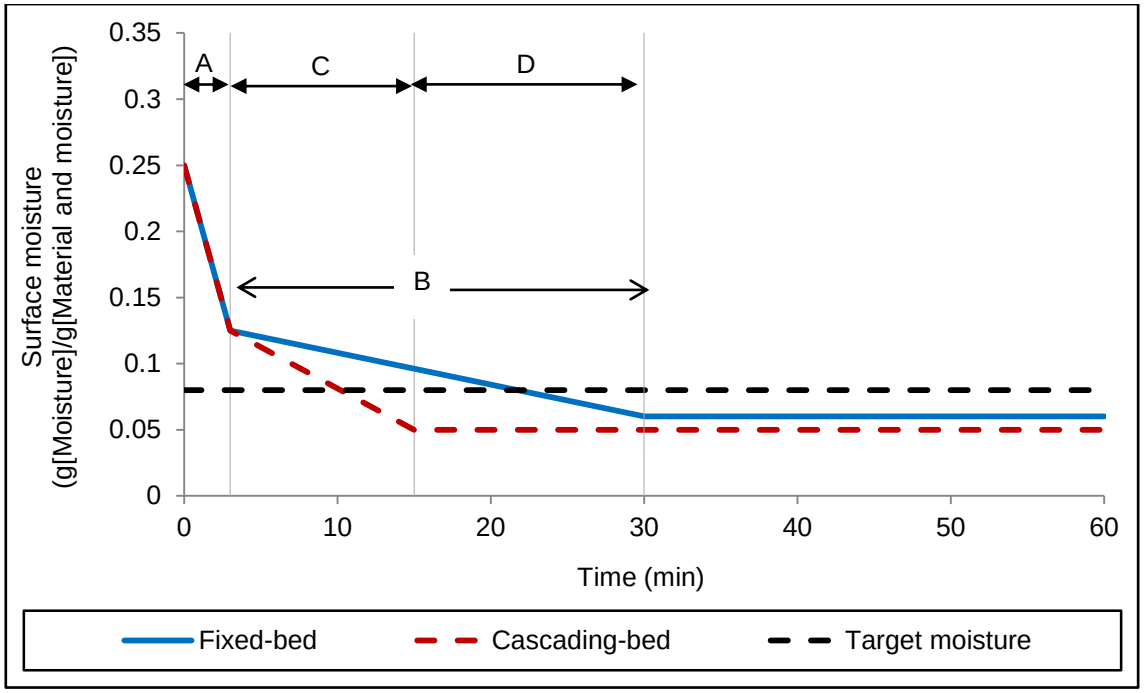

Figure 5.4.3: General desorption curve change

The sections labelled A, B, C, and D in Figure 5.4.3, represents (A) the rapid initial desorption phase, (B) the fixed-bed secondary desorption phase, (C) the cascading-bed secondary desorption phase and (D) the difference in drying time, respectively. The fixed-bed and cascading-bed data collected during this investigation shows that the initial desorption rates does not have a significant effect in lowering the surface moisture content, however a distinct difference is observed between the secondary desorption rates of the curves. As discussed in Section 4.2, the secondary desorption phase is time consuming as surface moisture displacement from pores and capillaries occur by diffusion. When moisture is removed from the surface of the coal fines, inherent moisture equilibrium is disturbed and moisture from the core of the coal fines migrates to the surface of the coal fines to restore equilibrium. By introducing motion into the system, inter-particle contact is enhanced and the rate at which moisture is removed from the surface of the coal is increased. Therefore, the rate at which moisture is replaced at the surface of the coal, during the secondary desorption phase, is also increased.

The initial desorption rate is calculated from the slope of the (A) initial desorption phase shown in Figure 5.4.3. Irrespective of the minimalistic initial desorption rate deviance visible in Figure 5.4.1 and Figure 5.4.2, the initial desorption rates were calculated for the fixed-bed and cascading-bed drying techniques. The initial desorption rates for the -1mm+0.5mm coal

and 3mm alumina-based adsorbent and 3mm silica-based adsorbent is shown in Figure 5.4.4.

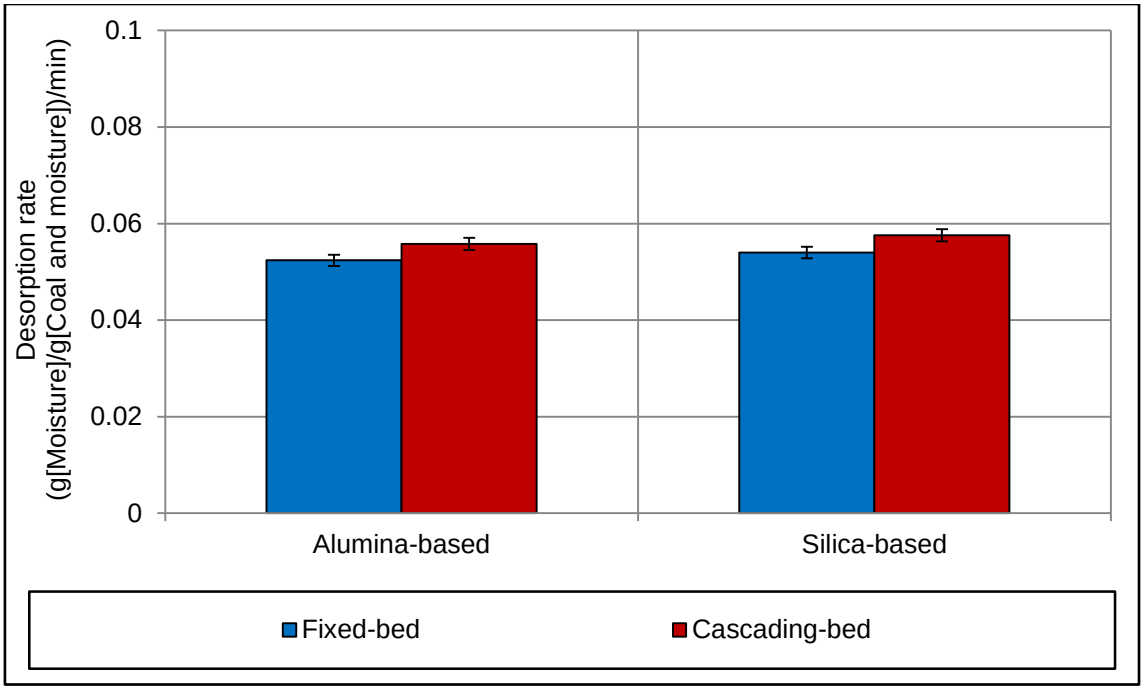

Figure 5.4.4: Initial desorption rates of -1mm+0.5mm coal and 3mm adsorbents

The difference in initial desorption rates in Figure 5.4.4 fall within the experimental error of 2.22%. Therefore, it is apparent that the drying technique does not influence the rate at which moisture is transferred from the coal fines during the initial desorption phase. Additional initial desorption rates were summed up and is provided in Annexure C.3.1.

5.4.3 Surface moisture and contact time

The surface moisture and contact time associated with the drying performance of coal was investigated during this section of the study. It was concluded that the target surface moisture was achieved by employing adsorbents as drying agent however; the drying technique had an influence on the contact time required during the secondary desorption phase. Longer contact time offers the adsorbent material adequate time to perform to its full capacity (Yang, 2015). However, from an economical perspective, the best performing drying technique needs to be identified with regards to time consumption and final surface moisture content. The surface moisture and drying times were studied by keeping the operating parameters constant while varying the drying technique. The surface moisture content of -2mm+1mm coal in combination with 3mm alumina-based adsorbents was

recorded after 10 minutes of contact and the corresponding results for the fixed-bed and cascading-bed drying techniques are provided in Figure 5.4.5.

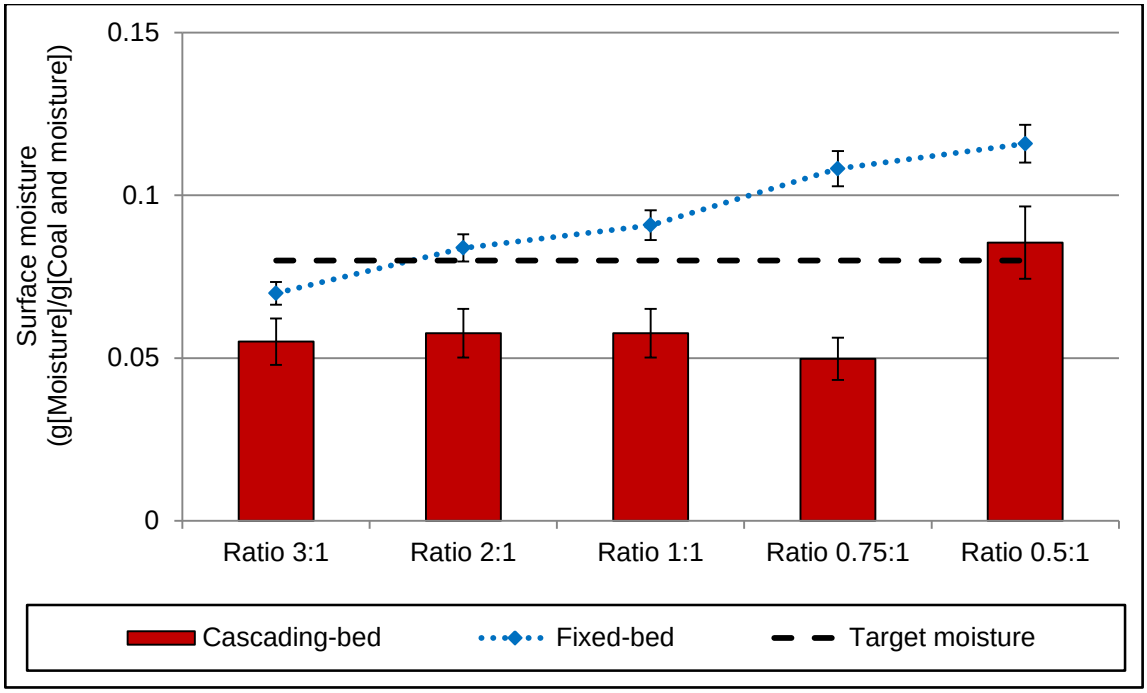

Figure 5.4.5: Final moisture load of -2mm+1mm coal and 3mm alumina-based adsorbent

The results obtained by using the fixed-bed drying technique yielded higher surface moisture contents for all the adsorbent to coal mass ratios when compared to the cascading-bed drying technique. The target surface moisture of 0.08 g(moisture)/g(coal and moisture) is indicated by a dashed line on Figure 5.4.5. After 10 minutes of contact, the surface moisture achieved by the cascading-bed technique was well under 0.08 g(moisture)/g(coal and moisture) whereas at the fixed-bed drying technique managed to bring about promising results for only the adsorbent to coal mass ratio of 3:1. Bland and McDaniel (2014) remarked that motion enhances the area of contact between the adsorbent material and coal fines.

Figure 5.4.6 was constructed to determine the time needed to dry -2mm+1mm coal with 3mm alumina-based adsorbents to the target moisture of 0.08 g(moisture)/g(coal and moisture). The coal fines had an average initial surface moisture of 0.17 g(moisture)/g(coal and moisture) and a standard deviation of 1.18 percentage points. The results in Figure 5.4.6 show that the adsorbent to coal mass ratios of 0.75:1 and 0.5:1 did not reach the target surface moisture when fixed-bed drying was employed.

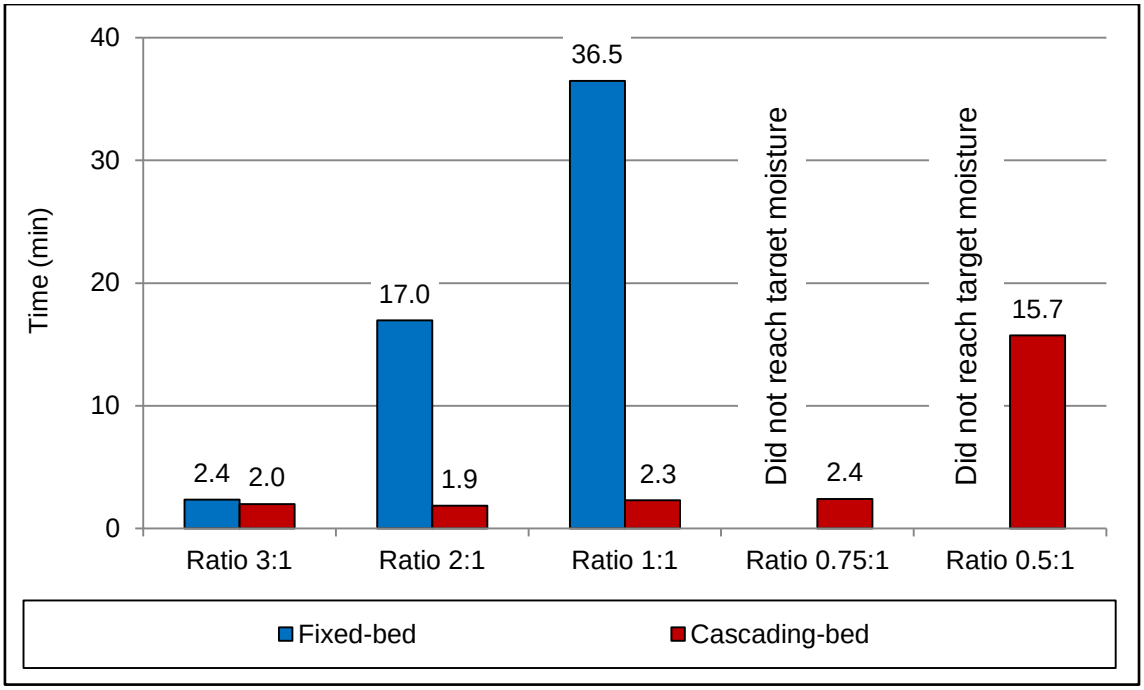

Figure 5.4.6: Alumina-based: Time required to dry -2mm+1mm coal to 0.08 g(moisture)/g(coal and moisture)

In Figure 5.4.6, the time consumption increases as the adsorbent to coal mass ratio decreases. When implementing motion, the drying times required to achieve 0.08 g(moisture)/g(coal and moisture) was reduced considerably. At an adsorbent to coal mass ratio of 1:1, more than 30 minutes was saved by using the cascading-bed drying technique rather than the fixed-bed drying technique. The cascading-bed drying technique was able to dry the coal fines in 2.4 minutes at an adsorbent to coal mass ratio, whereas the fixed-bed drying technique was only able to achieve target moisture within 2.4 minutes at a mass ratio of 3:1, as shown in Figure 5.4.6. The drying time of the fixed-bed drying technique does not validate the use of excess adsorbent material. Yang (2015) stated more than 3 minutes of contact time is less desirable for commercial use.

The set of experiments discussed in Figure 5.4.5 was repeated for the -2mm+1mm coal and 3mm silica-based adsorbents and the surface moisture content of the coal fines are shown in Figure 5.4.7. The fixed-bed drying technique results shown in Figure 5.4.7 was able to deliver surface moisture contents below the 0.08 g(moisture)/g(coal and moisture) when using 3mm silica-based adsorbents, although the cascading-bed drying technique performed better.

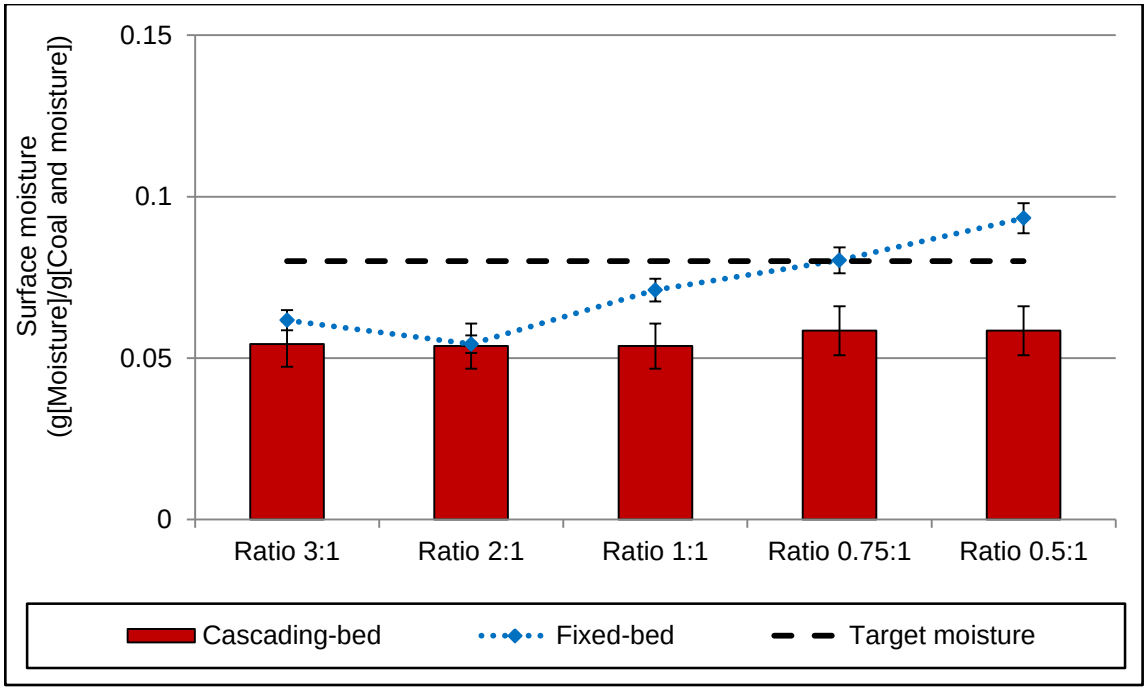

Figure 5.4.7: Final moisture load of -2mm+1mm coal and 3mm silica-based adsorbent

Returns generated by addition of the fine coal fraction, into the course coal circuit, depends greatly on the time required to dry the coal fines to moisture levels in line with contractual specifications. Therefore, the drying time needs to be investigated to determine whether the difference in final surface moisture, shown in Figure 5.4.7, is significant enough to employ cascading-bed drying technique. Similar to the discussion of Figure 5.4.5, the adsorbent to coal mass ratios were selected and the time required to reduce the surface moisture content of the coal to 0.08 g(moisture)/g(coal and moisture) are shown in Figure 5.4.8.

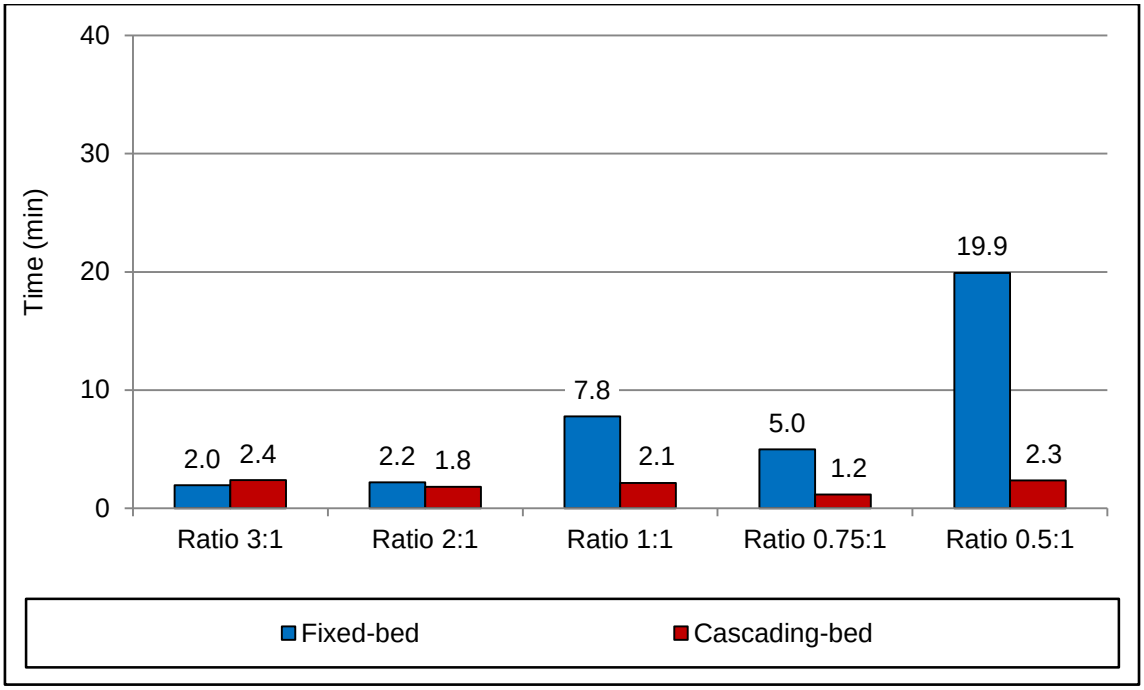

Figure 5.4.8: Silica-based: Time required to dry -2mm+1mm coal to 0.08 g(moisture)/g(coal and moisture)

The results in Figure 5.4.8 provide sufficient evidence that the cascading-bed drying technique delivers superior drying times. The time consumption is kept low and constant throughout al of the adsorbent to coal mass ratios in the case of the cascading-bed technique in Figure 5.4.8. When applying the fixed-bed technique, one can see in Figure 5.4.8 the process becomes more timely and time consumotion increases with decreasing adsorbent to coal mass ratios. This is a result of an increased area for contact between the adsorbent and coal mass when motion was introduced. Bratton *et al*. (2012) stated that the adsorbent and coal combination was agitated to enhance the surface area for contact.

In conclusion, the experimental results revealed that the boundaries restricting the drying process during fixed-bed drying was overcome by implementing motion. Additional surface moisture and contact time results can be found in Annexure C.3.2.

5.5 Statistical significance

The ANOVA and *t*-tests are discussed in detail in Section 4.4 of Chapter 4. The ANOVA results generated for the final surface moisture and initial rates of the coal and adsorbents is shown in Table 5.3. It should be noted that the surface moistures of the coal fines and adsorbent material was investigated after 20 minutes of contacting.

Table 5.3: ANOVA response of fixed-bed drying technique results

Manipulated variable	Measured variable	Sum of squares	df	Mean square	F-value	p-value
Adsorbent to coal mass ratio	Surface moisture: Coal	0.049	4	0.012	13.009	1.61E-07
	Desorption rate	0.003	4	0.001	3.743	9.17E-03
	Surface moisture: Adsorbent	0.122	4	0.031	12.041	4.26E-07
	Adsorption rate	0.011	4	0.003	9.334	7.87E-06
Coal particle size range	Surface moisture: Coal	0.024	2	0.012	8.840	4.53E-04
	Desorption rate	0.007	2	0.003	29.542	1.57E-09
	Surface moisture: Adsorbent	0.096	2	0.048	16.450	2.29E-06
	Adsorption rate	0.007	2	0.003	29.542	1.57E-09

The results in Table 5.3 validate the findings in Section 5.3. The adsorbent to coal mass ratios and the coal particle size ranges were found to be governing factors in reducing the inherent surface moisture of the coal as the p-values obtained were less than 0.05. The manipulated variables listed in Table 5.3 also had a statistically significant effect on increasing the product moisture of the adsorbent, the initial adsorption rates of the adsorbents as well the initial desorption rates of the coal.

The response of the *t*-tests for the adsorbent type and the adsorbent size is given in Table 5.4. The results show that adsorbent type had a significant effect on the inherent surface moisture of the adsorbents as well as the initial adsorption rate of the adsorbents as the p-values are less than 0.05. However, it is evident that the adsorbent type had no effect on the drying performance of the coal. The results in Table 5.4 indicate that the inherent surface moisture and initial rates of the coal and adsorbent, respectively, are independent from adsorbent type.

Table 5.4: *T*-test response of fixed-bed drying technique results

Manipulated variable	Measured variable	Mean	Standard deviation	t	df	p-value
Adsorbent type	Surface moisture: Coal	0.084	0.044	0.559	58	2.88E-01
	Desorption rate	0.042	0.016	-0.792	58	1.78E-01
	Surface moisture: Adsorbent	0.219	0.048	0.428	58	3.00E-04
	Adsorption rate	0.040	0.016	0.175	58	9.05E-04
Adsorbent size	Surface moisture: Coal	0.080	0.040	-0.187	58	8.90E-01
	Desorption rate	0.047	0.017	2.029	58	1.61E-03
	Surface moisture: Adsorbent	0.212	0.073	-0.396	58	1.62E-01
	Adsorption rate	0.040	0.024	0.001	58	8.39E-02

Moreover, the p-values obtained for adsorbent size shown in Table 5.4 was a significant factor for increasing the initial desorption rate. Additionally, it was found that the type of drying technique had a significant influence on lowering the inherent surface moisture content of the coal fines as the p-value obtained was less than 0.05.

5.6 Conclusion

The best initial adsorption and desorption rates were investigated during this chapter in addition to the final surface moisture content of the coal. Moreover, the time required to reduce the moisture content of the coal fines to an economically attractive 0.08g (moisture)/g (coal and moisture) were also investigated. Finally, the fixed-bed results and cascading-bed results were compared to determine the influence of motion on the drying performance of the fine coal.

The best performing adsorbent to coal mass ratio was 2:1. The adsorbent to coal mass ratio of 2:1 yielded the best overall initial desorption rates and the lowest coal final surface moisture contents. The lowest drying times required was found to be at an adsorbent to coal mass ratio of 2:1. It was also found that the adsorbent type did not exhibit a significant influence on the drying performance of coal. The 3mm adsorbent generated the fastest initial desorption rates, while the -1mm+0.5mm coal yielded the highest overall desorption rates. The -2mm+1mm coal produced the lowest overall final surface moisture contents.

In addition to these operating parameters, the difference between the initial adsorption and desorption rates of the drying techniques were found to be minimal. However, the contact time required to reduce the surface moisture content of the coal to an economically attractive value was influenced greatly by the drying technique. The fixed-bed drying technique is much more time consuming compared to the cascading-bed drying technique during the secondary desorption phase. Conclusively, it was also determined that the cascading-bed drying technique yielded the lowest final coal moisture content, making this drying technique more beneficial than the fixed-bed drying technique.

6

CHAPTER

INDUSTRIAL APPLICATION AND ENERGY CONSIDERATIONS

It is known that excess amounts of moisture retained in coal are considered a contaminant (Hand, 2000). The moisture retained in the coal decreases the heating value of the coal, adds to the mass based transportation costs and increase the difficulty in handling-ability of the coal. This moisture has to be removed; however, current processes of moisture removal are either energy intensive or ineffective. Based on contract specifications, penalties may be given to excess moisture retained in the coal or in some cases the coal may be rejected (Hand, 2000). For this reason, the energy use of the drying process must be justified. A preliminary industrial application is introduced in Section 6.1. Section 6.2 elaborates on the basic energy considerations of the drying process. Lastly, the findings in Section 6.1 and 6.2 is summarised and concluded on in Section 6.3.

6.1 Industrial application

Considering the promising results obtained by the cascading-bed drying technique on laboratory-scale, the decision was made to further investigate the prospect of implementing a pilot scale unit in continuous mode. Although the basic process was validated by laboratory-scale testing, various factors should be taken into account when operating the process on larger scale in continuous mode. The adsorbent cyclic reuse, adsorbent regeneration retention time and the influence of adsorbent condition need to be taken into consideration, prior to implementation of a continuous pilot scale process.

6.1.1 Reuse of adsorbents

When considering an industrial application, various key operating factors need to be taken into account. One of these factors, that require evaluation, is effective reuse of adsorbent material prior to regeneration. Therefore, adsorption capacity or adsorption loading is one of the most important characteristics to consider when selecting an adsorbent, as discussed in Section 2.7 of Chapter 2. The adsorption capacity of adsorbents dictates the amount of runs

that the setup can do before adsorbents reach its full capacity and needs to be regenerated. In order to investigate the sequential reusability of adsorbent material, a set of cascading-bed experimental runs was conducted on -2mm+1mm coal and 5mm adsorbents. The experiments were repeated using the same adsorbent material through numerous batches of coal. Figure 6.1.1 demonstrates that the 5mm alumina-based adsorbents can be effectively reused at an adsorbent to coal mass ratio of 3:1.

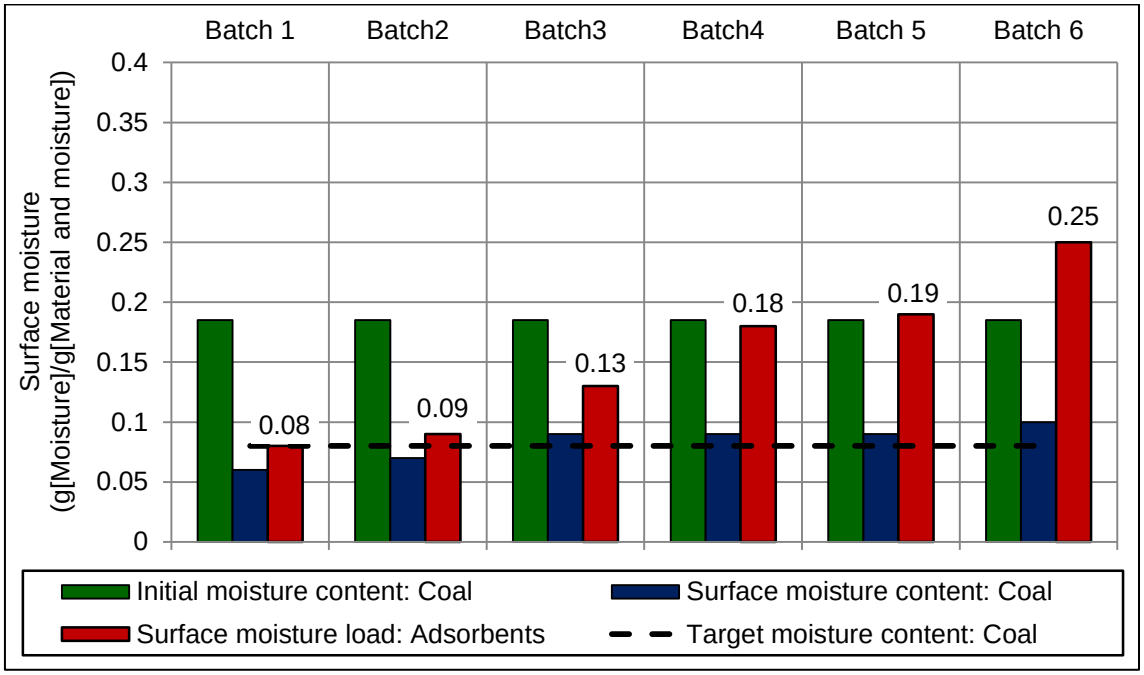

Figure 6.1.1: Surface moisture content of -2mm+1mmcoal and 5mm alumina-based adsorbent

It is evident from Figure 6.1.1 that the adsorbent material was able to lower the final moisture contents of six batches of -2mm+1mm coal to between 0.06 to 0.10 g(moisture)/g (coal and moisture). The first two batches of coal produced moisture contents below the 0.08 g(moisture)/g(coal and moisture) target moisture and the subsequent batches produced moisture contents below 0.10 g(moisture)/g(coal and moisture). The adsorbent moisture load, presented by the red bars in Figure 6.1.1, shows that the moisture load of the adsorbents increased throughout the batches while effectively reducing the moisture content of the coal fines. Although the target moisture was reached after two sequential cycles of reuse, the adsorbent material has not yet performed to its full capacity and the final moisture load of the adsorbent was reached after the sixth sequential cycle of drying at approximately 0.25 g(moisture)/g(adsorbent and moisture). These experiments showed that the adsorbent material could be reused effectively in sequential cycles whilst continually delivering favourable final moisture contents for the coal fines. The results may vary according to the different drying techniques and operating parameters applied.

Additional results of this nature are provided in Annexure D.1.1.

6.1.2 Adsorbent regeneration

In order to make the use of adsorbent drying eco-friendly and cost-effective, adsorbent regeneration is of utmost importance (Kulkarne and Kaware, 2014). Regeneration enables active adsorbent operation in sequential cycles with uniform performance (Knaebel, 2006). During this study, the used adsorbents were regenerated in a packed bed with drying air, conditioned to 25°C and 40%RH. The regeneration procedure was discussed in detail in Section 3.4.3 of Chapter 3. A set of experimental runs were performed to determine whether the adsorbents could be successfully regenerated. Figure 6.1.2 shows the moisture load response of 3mm and 5mm alumina-based adsorbents regenerated in a packed-bed with drying air conditioned at 25°C and 40%RH. The results in Figure 6.1.2 show that surface moisture can be removed successfully from the adsorbent material by airflow.

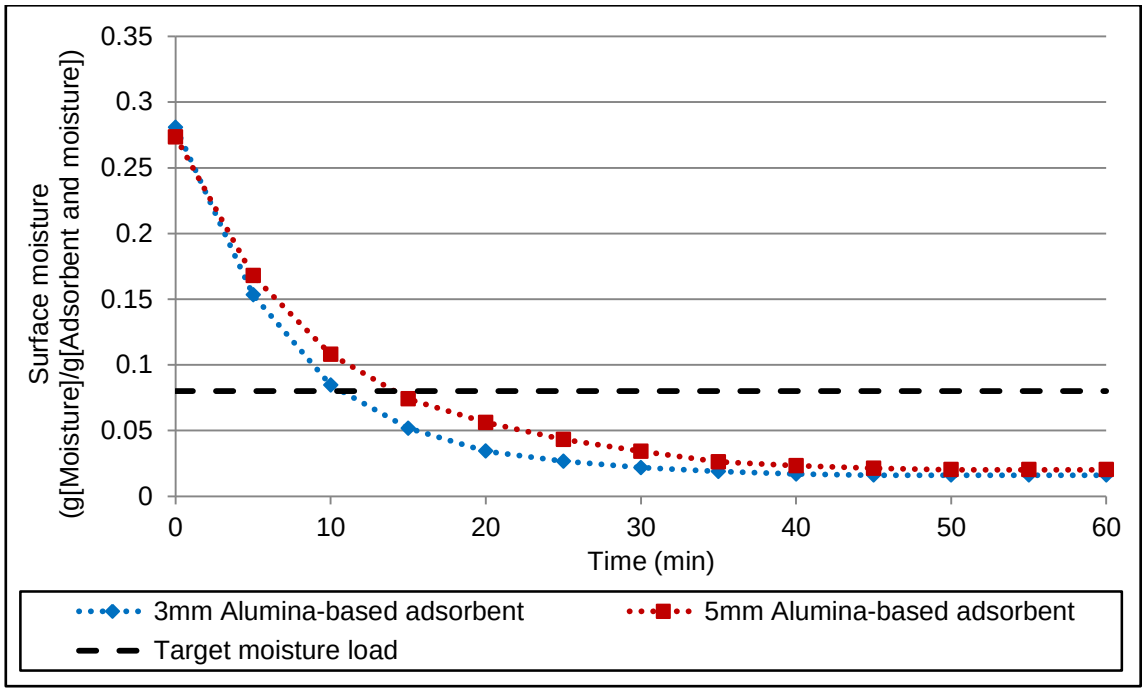

Figure 6.1.2: Regeneration curves of alumina-based adsorbents

The starting moisture load of the adsorbents when combined with the coal fines were approximately 0.08-0.10 g(moisture)/g(adsorbent and moisture), therefore this was the target moisture load investigated during regeneration. The regeneration curves in Figure 6.1.2 illustrates that the 3mm and 5mm alumina-based adsorbents reached 0.08

g(moisture)/g(adsorbent and moisture) after 10 minutes and 13 minutes of drying, respectively. Therefore, a retention time of 10 minutes within the regeneration section of the pilot plant is sufficient for regenerating the adsorbent material to the desired starting point. Even though the initial desorption rates of the 3mm and 5mm adsorbents in Figure 6.1.2 differ somewhat from each other, both adsorbent sizes eventually reach the same final moisture load of 0.020 g(moisture)/g(adsorbent and moisture) after 40 minutes.

Figure 6.1.3 shows the initial desorption rates of moisture from 3mm alumina and silica-based adsorbents as well as 5mm alumina and silica-based adsorbents.

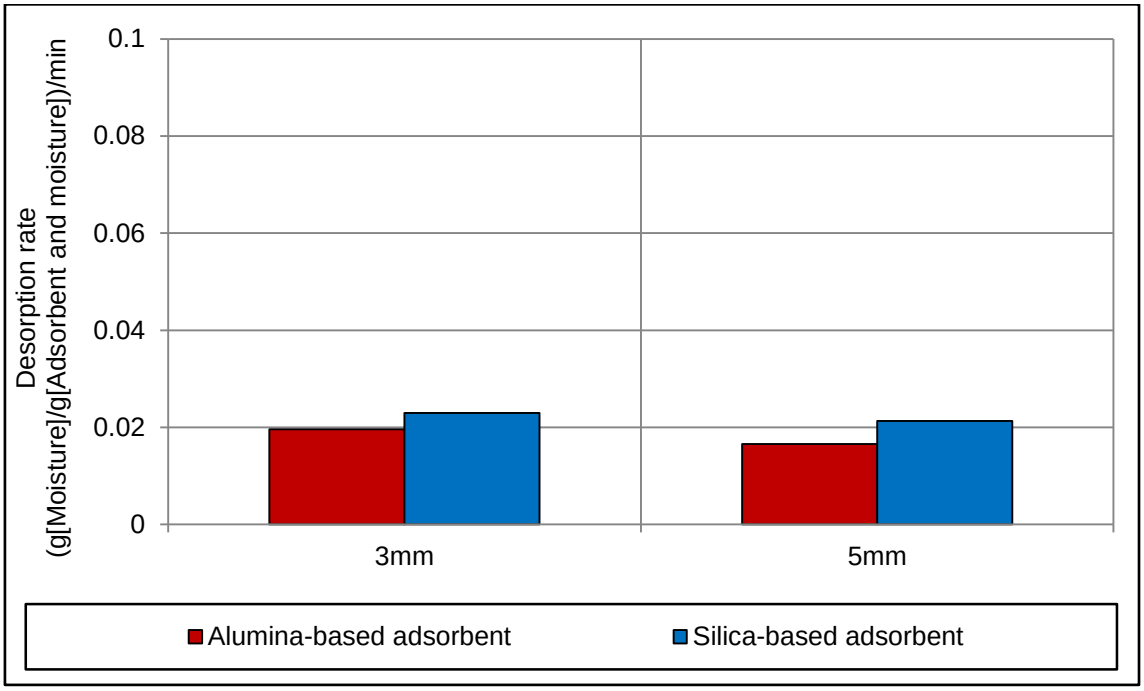

Figure 6.1.3: Desorption rates of 3mm and 5mm adsorbents

The rates in Figure 6.1.3 show that the silica-based adsorbents initially desorb moisture at a slightly faster rate than alumina-based adsorbents; however, the difference is minimal. The grain apparent porosity of the alumina-based was found to be 50.7% and the apparent grain porosity of the silica-based adsorbent was found to be 47.7%. This suggests that the surface area available for moisture displacement within the grain differs by 2%, hence the rate at which surface moisture is displaced from the pores fall within a narrow range from each other. However, the results obtained from this section indicate that regeneration of the adsorbent material is possible by employing drying air, set at 25°C and 40% RH, in a packed bed.

Former results substantiate reuse of adsorbents and regeneration of adsorbents; therefore, it was decided to investigate the influence of employing unused, used and air dried (regenerated) adsorbents on the adsorption capabilities thereof. This was done by submerging 3mm alumina-based adsorbents in water for 1 hour. The procedure was repeated and the results obtained are provided in Figure 6.1.4.

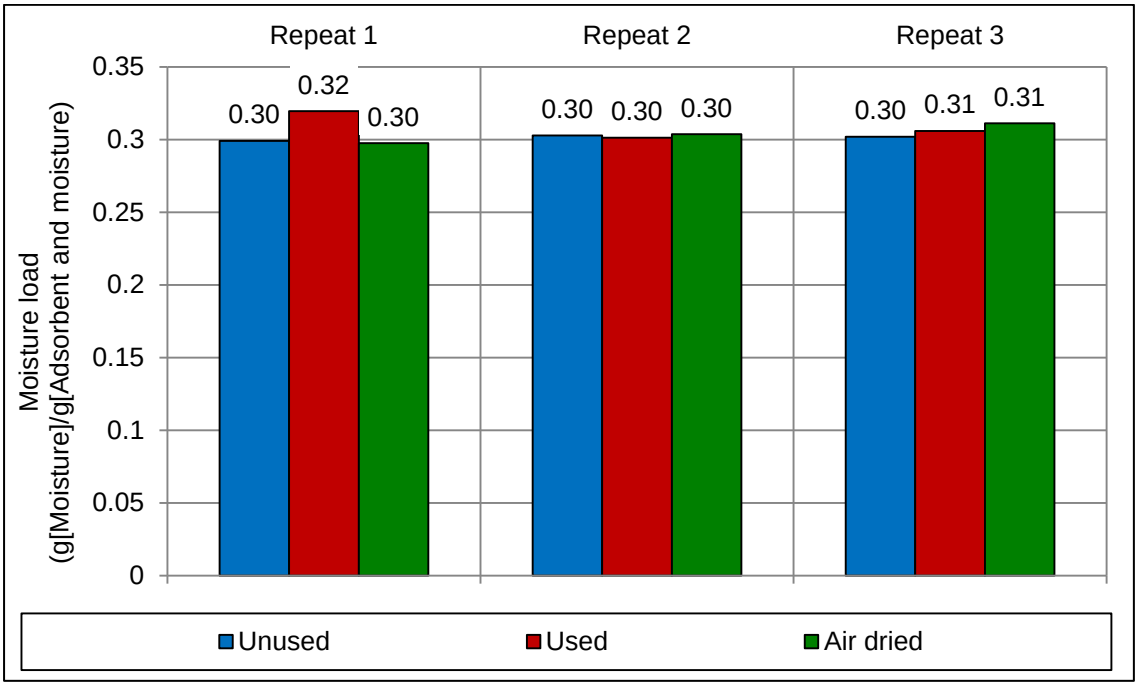

Figure 6.1.4: Moisture load of unused, used and air dried 3mm alumina-based adsorbents

The results in Figure 6.1.4 show that the potential moisture uptake of the 3mm alumina-based adsorbents remained constant for the repeats. More importantly, the unused, used and air dried adsorbents produced consistent moisture loads after 1 hour of submersion, indicating the adsorption capabilities of the adsorbents were not compromised after use. Bratton *et al*. (2012) reported similar findings, noting that no substantial difference in effectiveness of the adsorbents was detected after regeneration. The moisture loads of the unused, used and air dried adsorbents remained within a 0.02 g(moisture)/g(adsorbent and moisture) range from one another.

In order to examine the effectiveness of the adsorbent material, the drying performance of -1mm+0.5mm coal was investigated in the presence of unused, used and air dried (regenerated) adsorbents. Figure 6.1.5 shows the moisture reduction of -1mm+0.5mm coal in the presence of 3mm alumina-based adsorbents at an adsorbent to coal mass ratio of 1:1. The results show that moisture desorption from coal was not influenced by the condition of the adsorbents.

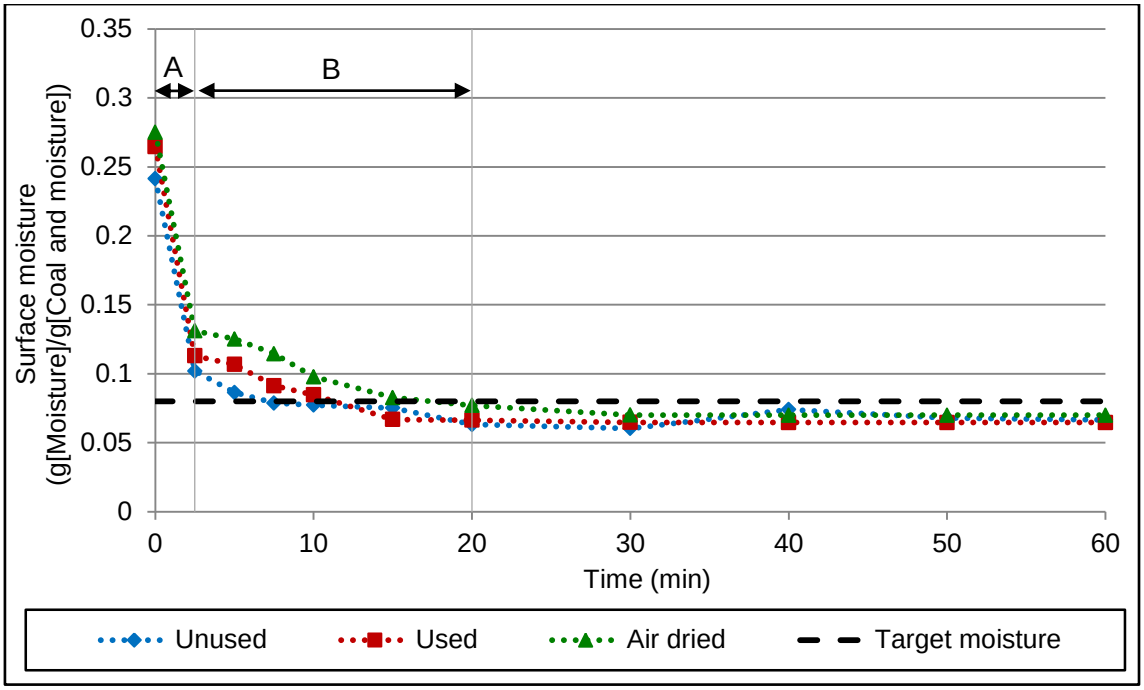

Figure 6.1.5: Desorption curves of -1mm+0.5mm coal and 3mm alumina-based adsorbents

The results in Figure 6.1.5 shows that the target moisture content was reached within 10 minutes, 12 minute and 15 minutes of contacting with unused, used and air dried 3mm alumina-based adsorbents, respectively. Bratton *et al*. (2012) found that the adsorbents can be successfully regenerated and reused, without affecting the amount of moisture removed from coal fines. In addition, it is evident from the initial desorption (A) phase in Figure 6.1.5 that the initial desorption rates varies only marginally and that the majority of the surface moisture retained by the coal fines was removed during this phase. About 58%, 57% and 52%, of the total amount of surface moisture removed from the coal fines, was removed during the initial desorption phase (A), while 16%, 18% and 20% was removed during the secondary desorption phase (B) by the unused, used and air dried adsorbents, respectively. The initial desorption rates were further investigated in Figure 6.1.6.

Figure 6.1.6 shows the initial desorption and adsorption rates of 3mm alumina-based adsorbents and -1mm+0.5mm coal at an adsorbent to coal mass ratio of 1:1. It was marked that the adsorption rates of the used and air dried (regenerated) adsorbents was lower than the initial adsorption rate of the unused adsorbents however, the difference is marginal.

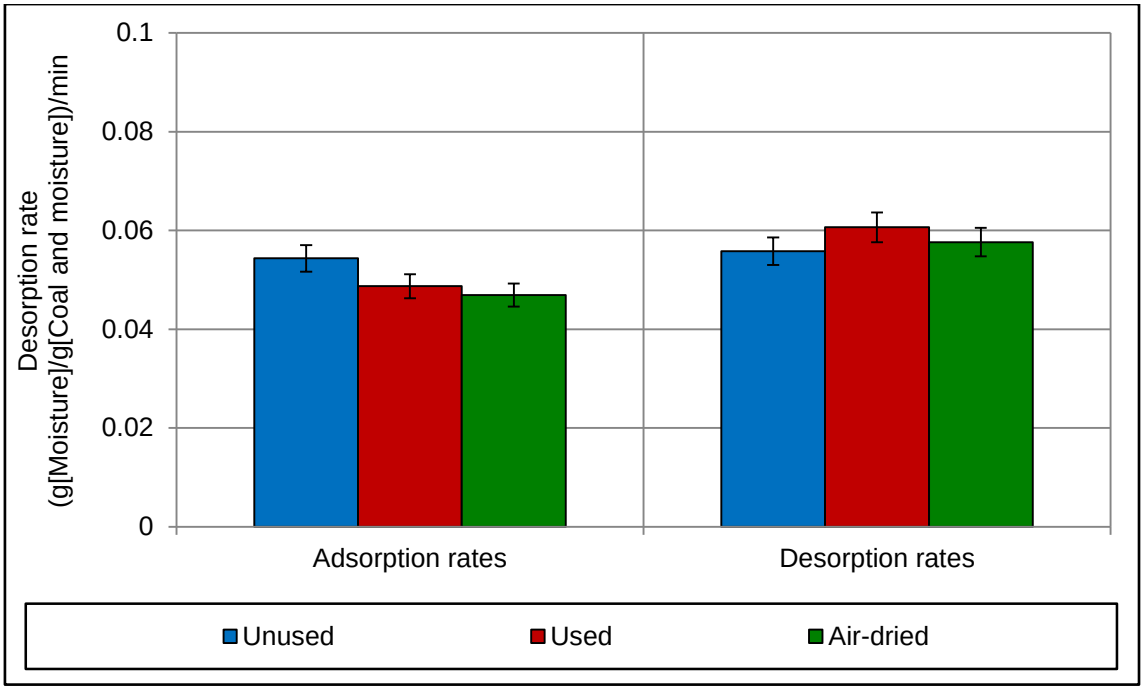

Figure 6.1.6: Initial adsorption and desorption rates of -1mm+0.5mm coal

The initial desorption rates in Figure 6.1.6 differs marginally from one another. The relative standard error was 5 percentage points and is indicated on the rates in Figure 6.1.6. Knaebel (2006) remarked that the technical viability of adsorbent assisted drying relies largely on the ability of the adsorbent material to be regenerated. From an industrial point of view, the results in Figure 6.1.4, Figure 6.1.5 and Figure 6.1.6 are promising as the adsorbents performed uniformly for all the adsorbent conditions. Knaebel (2006) mentioned that the drying performance of the adsorbent material is of paramount importance, as the adsorbents form a major part of the plant's capital investment. Therefore, reusing and regenerating adsorbents with consistent results will guarantee a technical viable process.

Moreover, the grain bulk density and grain apparent porosity change throughout the adsorbent conditions was also investigated. The grain bulk density and grain apparent porosity is summarised in Table 6.1. The grain bulk density and grain apparent porosity was performed based on works procedure MSM-LM-WP-300 (Rev 03), employing large volume pycnometers and the procedure is SANAS accredited.

Table 6.1: Adsorbent grain bulk density and grain apparent porosity

Adsorbent type	Adsorbent condition	Grain bulk density (g/cm3)	Grain apparent porosity (%)
Alumina-based adsorbent	Unused	1.37	50.7
	Used	1.41	50.4
	Air dried	1.37	52.4
Silica-based adsorbent	Unused	1.11	47.7
	Used	1.05	44.6
	Air dried	1.03	50.6

It can be seen from Table 6.1 that the air dried alumina-based adsorbents and silica-based adsorbents had the highest porosity. The unused alumina-based adsorbents vary with about 0.3% from the used alumina-based adsorbents. Upon receiving the unused adsorbents, a whitish powder-like substance was observed on the adsorbents' surface. The powder, generated by the adsorbents brushing against one another during storage, blocked the unused adsorbent pores, hence reducing its porosity. Furthermore, the lowest porosity in Table 6.1 was observed for the used adsorbents. Fine coal dusting remained on the adsorbents after separation. This is not preferred because the coal dust particles block the pores of the adsorbent material and reduce the porosity.

Additional regeneration and adsorbent condition results can be found in Annexure D.1.2.

6.1.3 Adsorbent degradation

The life expectancy or service life of adsorbents refers to the sequential cycles of employment of the adsorbent without undergoing intensive structural decay (Knaebel, 2006). When increased portions of the original adsorption capacity are degraded, failure in successful moisture removal from coal fines will be experienced, as the effective surface area for moisture accumulation is compromised. Adsorbent reuse, regeneration and condition were previously discussed and the results obtained were encouraging. However, structural degradation remains a possibility and Section 6.1.3 is focussed on investigating the structure of the adsorbents used during this study. According to Bland and McDaniel (2014), the adsorbent material selected for use in a continuous industrial process should be

capable of being successfully regenerated and recycled without suffering intensive degradation. In order to examine possible structural decay of the adsorbent particle, LEM micrographs of the adsorbent particles were taken after contacting with coal fines as well as after the regeneration process. In addition to the LEM micrographs, the adsorbents were cascaded in a steel mill with coal fines (-2mm+0.25mm) for a predetermined time to investigate the influence of contact on the structural decay of the adsorbents.

Figure 6.1.7 presents LEM micrographs of (a) used and (a) air dried 5mm alumina-based adsorbent particles. The used 5mm alumina-based adsorbent particle in Figure 6.1.7 (a) clearly shows that the coal dusting only influences the external surface of the particle and does not enter the internal structure of the particle as the dust particles are too large to pass. From the surface of the air dried 5mm alumina-based adsorbent particle in Figure 6.1.7 (b), it is apparent that the majority of the coal dusting on the external surface of the particle is removed by regeneration.

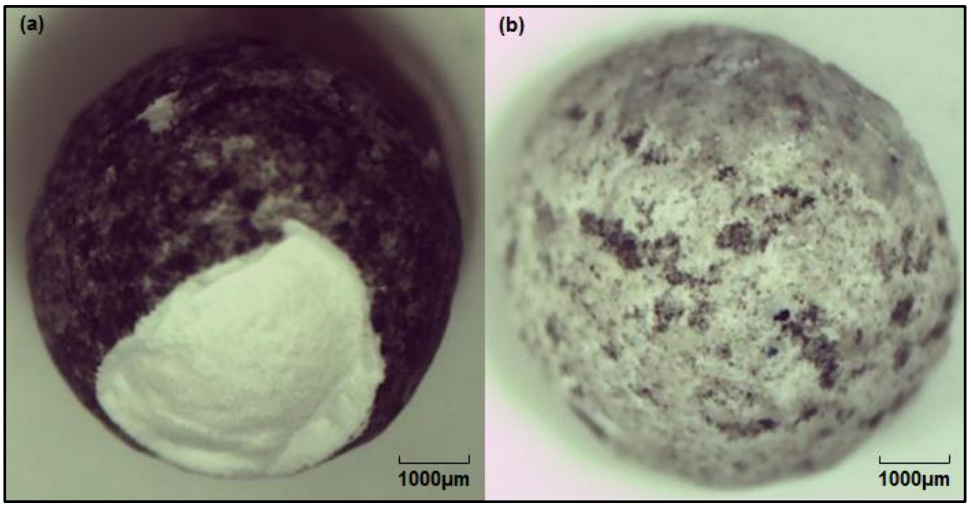

Figure 6.1.7: (a) Used and (b) air dried 5mm alumina-based adsorbents

The LEM micrographs of the 5mm silica-based adsorbents in Figure 6.1.8 show similar results for the (a) used and (b) air dried adsorbents as the micrographs of the alumina-based adsorbents in Figure 6.1.7. A crack is visible on the surface of the air dried 5mm silica-based adsorbent in Figure 6.1.8 (b). It was observed during the experimental runs that the silica-based adsorbent was more brittle than the alumina-based adsorbents and that is evident in Figure 6.1.8 (b). The formation layers of the silica-based adsorbents, discussed in Section 3.6.2 of Chapter 3, are unstable and tend to peel off when experiencing excessive contact, while the alumina-based adsorbents proved to be hard, durable drying agents.

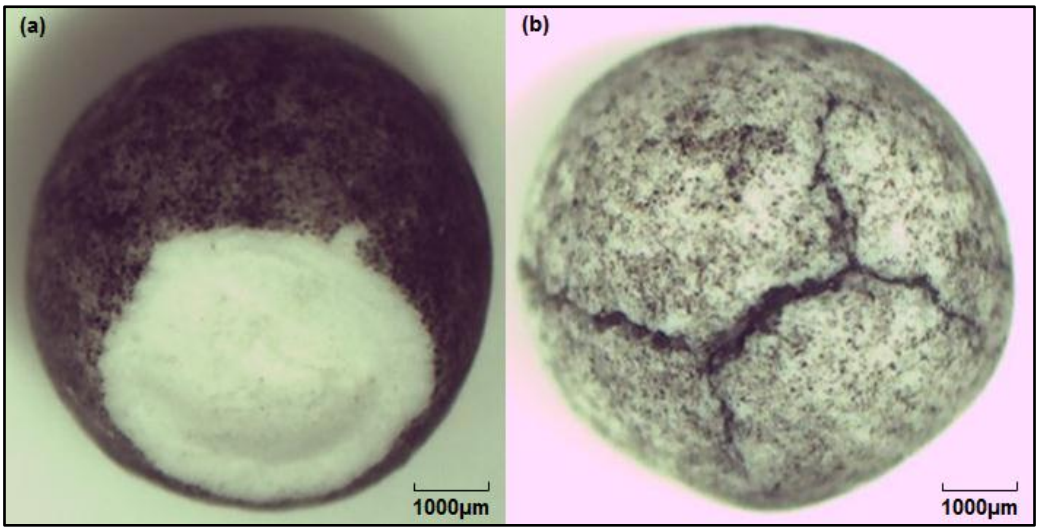

Figure 6.1.8: (a) Used and (b) air dried 5mm silica-based adsorbents

In order to investigate the effect of particle-contact on adsorbent degradation, a series of breakage experiments were conducted in a steel mill. Adsorbents and coal were combined in an adsorbent to coal mass ratio of 1:1 and placed into a steel mill that was operated at a rotational speed of 12 rpm. A particle size distribution analysis was conducted on the adsorbents and coal to identify breakage, if any. The top size of the adsorbents was monitored over a period of time to monitor any mass reduction. Figure 6.1.9 shows the results of the top size 5mm alumina-based and silica-based adsorbents for 120 minutes of milling.

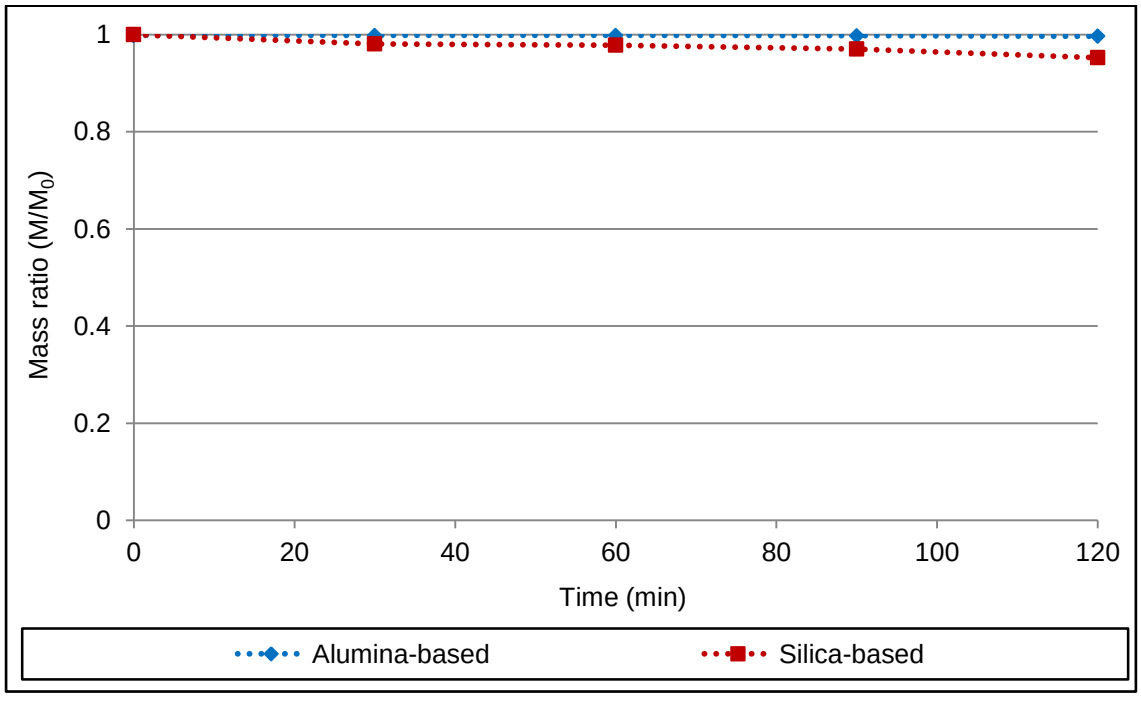

Figure 6.1.9: Effect of motion on adsorbent breakage

From the results in Figure 6.1.9, it was noted that the silica-based adsorbents experienced more breakage than the alumina-based adsorbent, as the initial top-size fraction decreases with increasing milling time. However, the breakage experienced by the top size of the alumina and silica-based adsorbents remained insignificant. After 120 minutes of milling, the mass ratio of the top size has decreased by 0.05 g(adsorbent)/g(adsorbent)$_0$, while the top size of the alumina-based adsorbent remained consisted.

The minimal breakage experienced by the adsorbent material is a promising prospect for industrial application as this shows that adsorbent-coal contact as well as the introduction of motion does not have a significant influence on the structure of the adsorbents. Alumina and silica-based adsorbents are hard and durable even though the silica-based adsorbents exhibited some breakage tendencies.

6.1.4 Prospective continuous process

A target surface moisture content of 0.08 g(moisture)/g(coal and moisture) was selected for all calculations in this section. The target moisture was selected as when the moisture content is lowered too much, dust problems and explosion hazards should be considered. If the moisture content of the coal fines is not lowered to the target moisture and remain above 0.10 g(moisture)/g(coal and moisture), the prospective blending benefits are compromised (Bratton *et al*., 2012). As seen in Section 5.4 of Chapter 5, when implementing the cascading-bed setup, less contact-time was required to reduce the moisture content of the coal fines to the target moisture. Therefore, it was decided to select the cascading-bed drying technique for further investigation as constant motion ensures optimal contact area.

When evaluating the capital investment of a plant, adsorbent to coal mass ratio needs to be considered, as it fixes the amount of adsorbent material required as well as the volume of the dryer vessel. In Chapter 5, it was concluded that the 2:1 adsorbent to coal mass ratio delivered the best drying performance, however the adsorbent to coal mass ratio of 1:1 was selected for investigation of industrial application. The mass ratio of 1:1 was selected, as less adsorbent material was required (lowers capital costs), while respectable drying performances was achieved (shown in Section 6.1.2). The -1mm+0.5mm coal and 3mm alumina-based adsorbents yielded the best drying performance, based on initial desorption rate and final moisture content, at this mass ratio. A prospective continuous closed loop process for drying fine coal by adsorbent assisted drying was designed. Figure 6.1.10

shows the continuous process, consisting of a drying section and a regeneration section. The drying section consists of a cascading-bed rotary dryer with an integrated separation trommel screen, while the regeneration section consists of a packed bed and a blower. The total mass flow rate of the coal (stream 1) and adsorbents (stream 2) fed to the drying section, in Figure 6.10, is 200kg/hr, while the adsorbent mass flow rate fed to the regeneration section is 117.3kg/hr (stream 4).

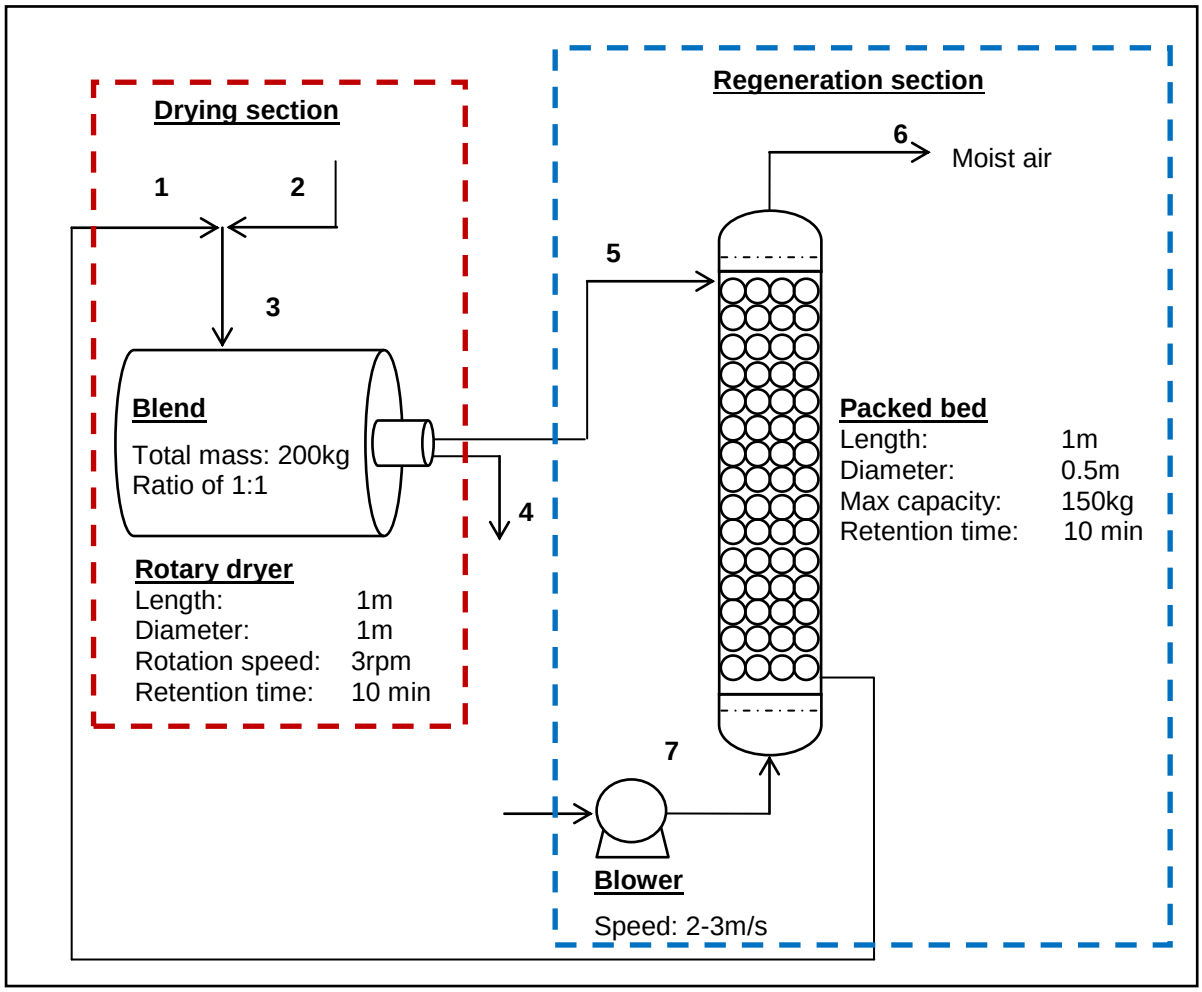

Figure 6.1.10: Continuous process flow of adsorbent assisted drying

Stream 1 and 2, in Figure 6.1.10, represents the fresh adsorbent and coal streams that are being fed to the cascading-bed rotary dryer. The retention time for the adsorbents and coal fines in the rotary dryer was maintained at 10 minutes to ensure sufficient time is provided to allow the fine coal to reach the target moisture content. The cascading-bed vessel is operated at 1/3 of its total volume. As the coal and adsorbents are contacted in the cascading-bed rotary dryer, the coal fines are dried. When the contact time has elapsed, the coal fines and adsorbents exit the cascading-bed and are separated into stream 3 and 4,

respectively. A sample is collected from the coal fines and is analysed to determine the moisture content of the coal product. The adsorbents are sent to the regeneration unit where the adsorbents were regenerated and recycled into the system by stream 6. The drying air is indicated by stream 7 in Figure 6.1.10. The description and properties of streams 1-7 illustrated in Figure 6.1.10 are given in Table 6.2.

Table 6.2: Stream properties

Stream	Description	Properties
1.	Adsorbent feed	Feed rate: 100kg/h Density: 769kg/m^3 Starting moisture load: 0.08 g(Moisture)/g(Adsorbent and moisture) Size: 3mm
2.	Coal feed	Feed rate: 100kg/h Density: 800kg/m^3 Initial surface moisture content: 0.25 g(Moisture)/g(Coal and moisture) Size: -1mm+0.5mm
3.	Combined feed	Feed rate: 200kg/h
4.	Dry coal product	Flow rate: 82.7kg/h Final surface moisture load: 0.077 g(Moisture)/g(Coal and moisture)
5.	Adsorbent recovery	Flow rate: 117.3kg/h Surface moisture content: 0.253g(Moisture)/g(Adsorbent and moisture)
6.	Moisture removed	17.3L/h (without taking efficiency into account)
7.	Air	Ambient air conditions

6.2 Energy considerations

Conventional methods used to dry coal beyond mechanical dewatered moisture levels usually employ heaters or blowers that are capital- and energy intensive (Bland and McDaniel, 2014). Therefore, in order to determine the energy consumed by adsorbent assisted drying, it is crucial to identify the various key energy-consuming factors of the process. In Section 6.1.1, it was concluded that the most suitable adsorbent to coal mass ratio, both from an economical and effectiveness point of view, was 1:1. As the cascading-bed drying technique delivered optimum results, the energy consumed by adsorbent assisted drying was determined for the adsorbent to coal mass ratio of 1:1, based on adsorbent type, adsorbent particle size and coal particle size range .

The energy requirements of the process were divided into two processes:

- Drying process
- Regeneration process

For this energy study, the energy consumption was determined for drying the fine coal to an arbitrary value of 0.08 g(moisture)/g(coal and moisture), which is accepted to be in line with most contractual specifications. The energy consuming factors the form part of the drying and regeneration processes are summarised in Figure 6.2.1.

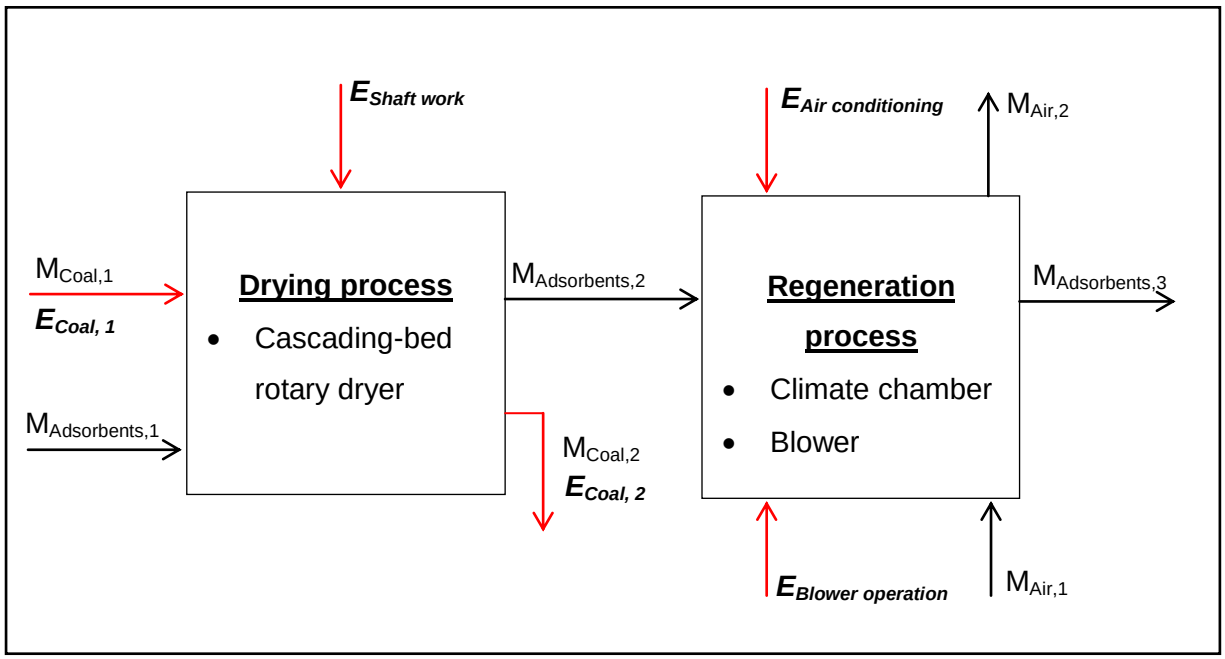

Figure 6.2.1: Energy process flow diagram

The total energy consumed during the processes was compared to the net calorific energy gained by the coal fines due to the lower moisture content. Accordingly, one can determine whether the process of adsorbent assistant drying is net energy positive and if so, to what extent. Finally, the total energy consumption of the process was compared to that of current existing fine coal dewatering techniques.

The energy study focussed on the best drying performance obtained at the adsorbent to coal mass ratio of 1:1, which proved to be the-1mm+0.5mm coal and 3mm alumina-based adsorbents, as concluded in Section 6.1.1.

6.2.1 Energy consumption

In this section, the energy consumed by the drying and regeneration processes is briefly discussed. Firstly, the energy consumed by operating the cascading-bed rotary dryer during the drying process, labelled $E_{Shaft\ work}$ in Figure 6.2.1, was determined. The regeneration energy requirements was then calculated for conditioning the drying air inside the climate chamber and running the climate chamber ($E_{Climate\ chamber}$) as well as for running the blower ($E_{Blower\ operation}$). The results were compared to the nett calorific value upgrade of the coal fines and the most energy efficient operating condition was determined.

During the drying process, the cascading-bed rotary dryer was operated for 2 minutes to reach the target moisture of 0.08 g(moisture)/g(coal and moisture), consuming 17.04kJ. Similarly, the energy consumed for conditioning the air inside the climate chamber as well as the energy required for operating the blower during the regeneration process was determined.

The drying air, required to regenerate the adsorbents, was conditioned in the climate chamber set at 25°C and 40%RH. The climate chamber was operated for the duration of the regeneration experiments to maintain consistent air conditions. The average room temperature and pressure range recorded for South Africa in the summer are 25°C and 30-80%RH. The enthalpies obtained for the minimum and maximum relative humidity values of 30-and 80%RH were 41.5-and 66.5kJ/kg, respectively. The temperature and pressure of the regeneration drying air was set at 25°C and 40%RH with an enthalpy of 45.50 kJ/kg. Therefore, firstly, the change in enthalpy that was required to condition the air to these conditions was determined. By using the change in enthalpy, the energy needed to condition the drying air from the average room temperature and pressure range to 25°C and 40%RH was calculated. The climate chamber consumed a total amount of energy of

1200.71kJ and 1196.26kJ for the minimum and maximum relative humidity 30%RH and 80%RH, respectively. The blower was operated at high airflow (700J/s) for approximately10 minutes, consuming 420kJ, to reduce the moisture of the 3mm alumina-based adsorbents to the starting moisture load of 0.08 g(moisture)/g(adsorbent and moisture). Equation 6.1 was used to determine the total amount of energy consumed (E_{Total}) by the process:

$$E_{Total} = E_{Shaft\ work} + E_{Climate\ chamber} + E_{Blower\ operation}$$

Equation 6.1

Where $E_{Shaft\ work}$ is the energy required by the cascading-bed rotary dryer, $E_{Climate\ chamber}$ is the energy consumed by the climate chamber and $E_{Blower\ operation}$ is the energy required to operate the blower. The total amount of energy required to dry the -1mm+0.5mm coal fines with 3mm alumina-based adsorbents was 1637.75 and 1633.33kJ at 30%RH and 80%RH, respectively.

Annexure D.2.1 and D.2.2 contains a detailed description of the calculations followed to determine the total energy consumed during the drying and regeneration processes.

6.2.2 Energy improvement

In order to determine whether the process was energy efficient, the energy improvement of the fine coal ($E_{Coal,2}$) was calculated. The calorific values of the coal fines before and after drying were determined to calculate the calorific value upgrade of the coal. The -1mm+0.5mm coal filter cake had average initial moisture content of 0.25 g(moisture)/g(coal and moisture) and a calorific value of 16836.00kJ/kg. By drying the -1mm+0.5mm coal fines to 0.08 g(moisture)/g(coal and moisture), the calorific value of the -1mm+0.5mm fine coal was effectively upgraded by 8164.80 kJ/kg. Even though there was an increase in calorific value of the coal fines, the energy required by the drying and the regeneration processes still needs to be taken into account. As a result, the energy improvement was determined by deducting the total amount of energy consumed by the drying and regeneration processes from the calorific value upgrade of the coal fines. The energy improvement achieved by drying the fine coal was calculated by using Equation 6.2:

$$Energy\ improvement = (E_{Coal,2} - E_{Coal,1}) - E_{Total}$$

Equation 6.2

Where $E_{Coal,1}$ and $E_{Coal,2}$ is the calorific value of the fine coal before and after drying, respectively. E_{Total} represents the total amount of energy required by the process. The

energy improvement of drying -1mm+0.5mm coal fines to 0.08 g(moisture)/g(coal and moisture), by employing 3mm alumina-based adsorbents, was 6527.05 and 6531.47kJ/kg at 30%RH and 80%RH, respectively.

6.2.3 Coal drying technologies

Over the past century, numerous drying processes were developed for lowering coal moisture levels, which directly yields an improved heating value (Karthikeyan *et al*., 2009). This section elaborates on the energy consumption per kilogram of moisture removed from coal, by comparing the energy consumption of various existing drying technologies to that of adsorbent assisted drying. Karthikeyan *et al*. (2009) and Wilson *et al*. (1992) conducted a study on the energy consumption of various types of coal dryers and the energy consumption of these dryers are summarised in Table 6.3. The minimum and maximum energy requirements for drying -1mm+0.5mm coal with 3mm alumina-based adsorbents are also provided in Table 6.3.

Table 6.3: Energy required by various dryers; taken from Karthikeyan *et al*. (2009) and Wilson *et al*. (1992)

Type of dryer	**Energy consumption per mass of water removed (kJ/kg H_2O)**	
Moisture level	**Minimum**	**Maximum**
Kinetic disintegration system (KDS) micronex dryer		2020
Rotary dryer	2950	3700
Rotary tube dryer		3150
Chamber dryer		3100
Pneumatic dryer	3100	3100
Fluid-bed dryer		3100
Fleissner process		1750
Air fluidised-bed dryer		4000
Adsorbent assisted drying	**1012**	**1015**

Felder and Rousseau (2005) remarked that at 100°C and atmospheric pressure, 2256.9kJ/kg is consumed to vaporise 1kg of water. It was evident from Table 6.3 that only two of the existing drying techniques achieved values below 2256.9kJ/kg. Furthermore, the minimum and maximum energy required to dry the -1mm+0.5mm coal with 3mm alumina-

based adsorbents was 1012kJ/kg and 1015kJ/kg, respectively. The energy consumed by employing adsorbent assisted drying was comparatively lower than the existing drying techniques listed in Table 6.3.

Figure 6.2.2 illustrates the energy usage of adsorbent assisted drying compared to other drying techniques currently in operation.

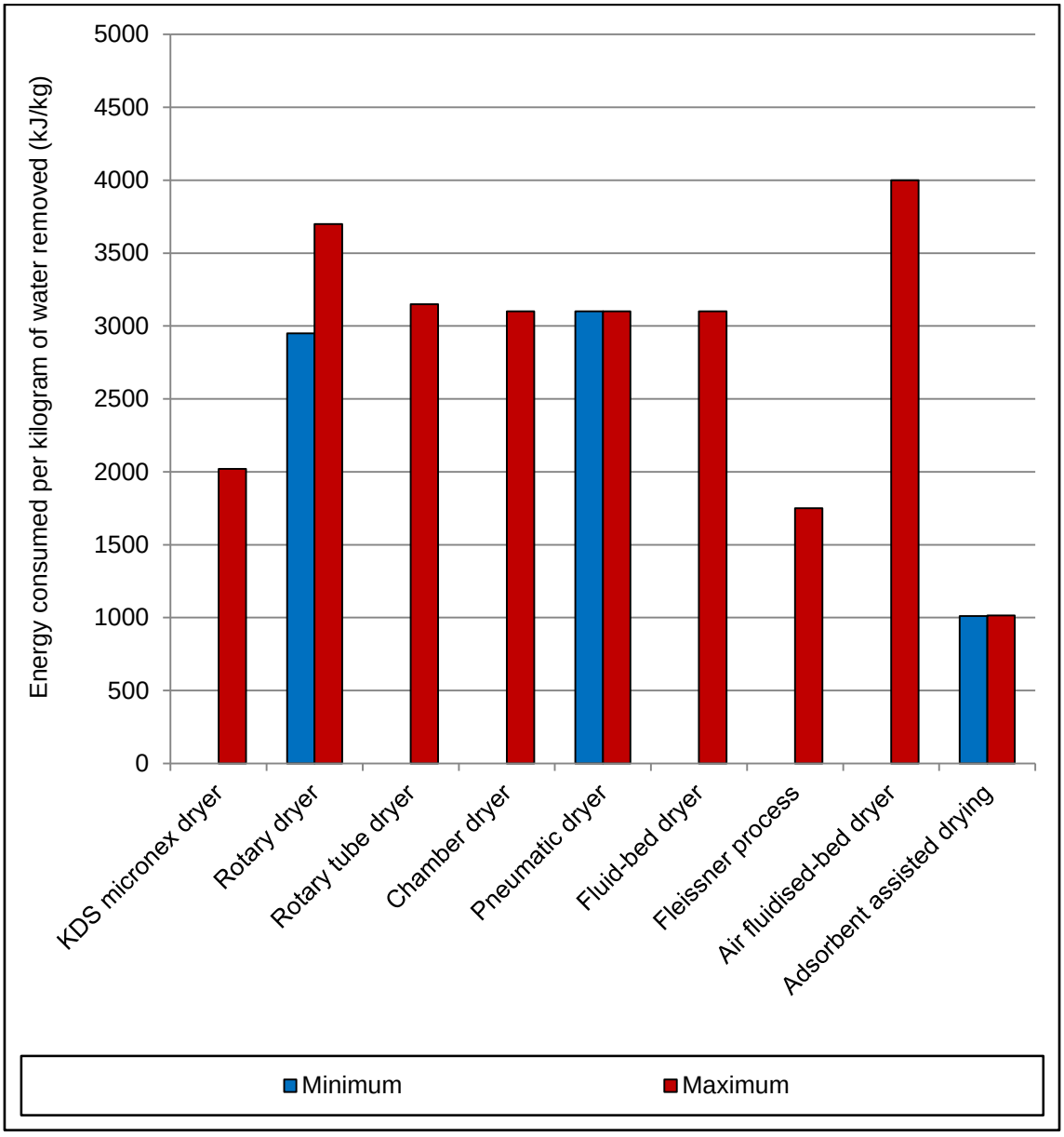

Figure 6.2.2: Energy consumption of adsorbent assisted drying compared to other dryers

Adsorbent assisted drying, presented in Figure 6.2.2, proved the most energy efficient drying technique compared to the existing drying techniques. The correlation in Figure 6.2.2 was also investigated and compared for the remaining adsorbent type, adsorbent particle sizes and coal particle size ranges and the results are provided in Annexure D.2.3.

6.3 Conclusions

The results in Section 6.1.1 showed that the adsorbent material could be reused effectively in sequential cycles whilst continually delivering favourable final moisture contents for the coal fines. The 3mm and 5mm alumina-based adsorbents reached 0.08 g(moisture)/g(adsorbent and moisture) after 10 minutes and 13 minutes of drying, respectively. Therefore, it was concluded that a 10-minute retention time within the regenerator is satisfactory for regenerating the adsorbent material to the desired starting point. In addition, the results in Section 6.1.2 further showed that adsorbent condition did not influence the effectiveness of the adsorbent material. About 58%, 57% and 52%, of the total amount of surface moisture removed from the coal fines, was removed during the initial desorption phase, while 16%, 18% and 20% was removed during the secondary desorption phase by the unused, used and air dried (regenerated) adsorbents, respectively.

The adsorbent material experienced minimal breakage, which was promising for industrial application as it showed that adsorbent-coal contact as well as the introduction of motion did not have a significant influence on the structure of the adsorbents. Both the alumina and silica-based adsorbents proved to be hard and durable, even though the silica-based adsorbents exhibited some breakage tendencies.

The total amount of energy required to dry the -1mm+0.5mm coal fines (to 0.08 g(moisture)/g(coal and moisture)) with 3mm alumina-based adsorbents was 1637.75 and 1633.33kJ, thereby yielding an energy improvement of 6527.05 and 6531.47kJ/kg at 30%RH and 80%RH, respectively. In Section 6.1.4, it was concluded that the minimum and maximum energy required to dry the -1mm+0.5mm coal by adsorbent assisted drying was 1012kJ/kg H_2O and 1015kJ/kg H_2O, respectively. In conclusion, the energy consumed by employing adsorbent assisted drying was comparatively lower than the existing drying techniques.

7

CHAPTER

CONCLUSIONS, RECOMMENDATIONS AND CONTRIBUTIONS

Conclusions, recommendations and contributions on the research covered in this dissertation are provided in Chapter 7. The conclusions, provided in Section 7.1, were constructed in response to the research objectives listed in Section 1.3 of Chapter 3 and are numbered accordingly. Certain recommendations were made, in Section 7.2, regarding adsorbent assisted drying technology for future reference and further research on the topic. Finally, the contributions that were made to the general research field and beneficiation industry are summarised in Section 7.3.

7.1 Conclusions

In response to the research objectives listed in Section 1.3 of Chapter 1, the following conclusions were assembled:

1. It was found that the surface moisture levels of the mechanically dewatered coal fines were effectively lowered by 50-80%, after only 10 minutes of contacting with adsorbent material, in a climate-controlled room at 25°C and 40%RH. The amount of moisture removed from the coal fines varied according to the operating parameters that were applied and contact time provided.

2. The surface moisture content of the fine was effectively reduced to 0.08 g(moisture)/g(coal and moisture) within 2.5 minutes of drying with 3mm alumina and silica-based adsorbents during the cascading-bed drying technique.

3. The results obtained from the fixed-bed experiments indicated that the coal fines achieved lower final surface moisture contents and elevated initial desorption rates upon increasing adsorbent to coal mass ratio. Additionally, the fixed-bed results showed that adsorbent type and adsorbent particle size did not play a significant role on lowering the surface moisture of the coal fines. The initial desorption rate was also not influences by the adsorbent type and adsorbent particle size. However, coal particle size range proved to be a key factor in lowering the final moisture content of the coal fines.

Reduced particle diameters are accompanied by an increased surface area, which retains more surface moisture and therefore it was more time consuming to remove the surface moisture of the -0.5mm+0.25mm coal. It was also found that the initial desorption rate was increased when the coal particle size range was decreased, which was due to the inlet surface moisture concentrations. The -2mm+1mm coal fines and 5mm alumina-based adsorbents, at an adsorbent to coal mass ratio of 3:1,achieved the lowest coal final moisture content, with a 73.83% moisture reduction after 10 minutes of drying.

4. The cascading-bed experimental results largely resembled the fixed-bed experimental results, indicating the final moisture content of the mechanically dewatered coal fines could be dialled in by varying the adsorbent to coal mass ratio. By increasing the adsorbent to coal mass ratio, the initial desorption rate of the fine coal was increased and the final moisture content of the coal was lowered. The adsorbent type did not influence the final moisture content and initial desorption rate of the coal fines during the cascading-bed experiments. The 3mm adsorbents provided increased initial desorption rates over the 5mm adsorbents, while the final surface moisture content of the coal fines were not influenced by adsorbent size. The coal particle size range played a significant part in lowering the final moisture content of the coal fines and it was more time consuming to lower the surface moisture of the -1mm+0.5mm and -0.5mm+0.25mm coal than the -2 mm+1mm. The -2mm+1mm coal fines and 5mm silica-based adsorbents, in an adsorbent to coal mass ratio of 2:1, delivered the lowest coal moisture content, with a 68.35% moisture reduction after 10 minutes of drying.

5. The target moisture was not easily reached by the fixed-bed drying technique, due to the lack of motion. By introducing motion, a rise in the secondary desorption rate of the coal was detected, resulting in an overall reduction in the required contact time and final surface moisture. The surface moisture of the -2mm+1mm coal fines, in an adsorbent to coal mass ratio of 1:1, was able to reach the target moisture in less than 2.5 minutes during cascading-bed experiments, while the fixed-bed experiments was only able to deliver the same results after 7.5 minutes.

6. Adsorbent regeneration by air drying in a packed bed proved to be effective and consistent for the 3mm and 5mm alumina and silica-based adsorbents. The surface moisture of the 3mm and 5mm alumina-based adsorbents was reduced from an average of 0.28 g(moisture)/g(adsorbent and moisture) to 0.016 g(moisture)/g(adsorbent and moisture) and 0.02 g(moisture)/g(adsorbent and moisture), respectively. The silica-based adsorbents yielded similar results by reducing the surface moisture of 3mm and

5mm silica-based adsorbents from an average of 0.32 g(moisture)/g(adsorbent and moisture) to 0.03 g(moisture)/g(adsorbent and moisture) and 0.006 g(moisture)/g(adsorbent and moisture), respectively.

7. It was found that the adsorbent material could be reused for up to 6 cycles, at an adsorbent to coal mass ratio of 3:1, without regeneration and still produce a final coal moisture content below 0.10 g(moisture)/g(coal and moisture). However, the adsorbent to coal mass ratio of 1:1 was selected for industrial application investigation as less adsorbent material was required (lowers capital costs), while respectable drying performances was achieved. The results obtained by comparing the unused, used and air dried adsorbents indicated no significant difference in the effectiveness of surface moisture reduction of coal fines. Although the adsorbents showed visible cracks after operation, the adsorbents showed insignificant degradation when milled for 2 hours.

8. The total amount of energy required to dry the -1mm+0.5mm coal fines (to 0.08 g(moisture)/g(coal and moisture)) with 3mm alumina-based adsorbents was 1637.75 and 1633.33kJ/kg, thereby yielding an energy improvement of 6527.05 and 6531.47kJ/kg at 30%RH and 80%RH, respectively. The minimum and maximum energy required to dry 1 kilogram of -1mm+0.5mm coal by adsorbent assisted drying was 1012kJ/kg H_2O and 1015kJ/kg H_2O, respectively. In conclusion, the energy consumed by employing adsorbent assisted drying was found to be comparatively lower than the existing drying techniques.

7.2 Recommendations

In response to the conclusions drawn from the study, a number of recommendations were made for prospective future studies. The recommendations are listed below:

1. In order to further investigate the adsorbent assisted drying process, it is recommended to construct a pilot scale unit, with an integrated air drying regeneration section, in continuous mode. This will be especially useful when investigating the optimum residence time and operating parameters required for drying an increased amount of fine coal and adsorbent material. This will produce a set of data that will aid in better understanding the limitations of the drying technology.

2. For purposes of this study, the drying performance of mechanically dewatered fine coal was investigated, only. The highest average initial surface moisture content of

the mechanically dewatered fine coal was 0.29 g(moisture)/g(coal and moisture) with a standard deviation of 0.75 percentage points. The prospect of dewatering fine coal by adsorbent assisted drying, in continuous mode, before mechanical dewatering should be considered in order to identify the limitations of the drying technology.

3. Investigate the pore network of coal particles and adsorbents and the effect of pore network distribution on moisture desorption and adsorption processes within the coal-adsorbent system. This will result in a better understanding of the desorption and adsorption rates of moisture related to coal and adsorbents, as well as provide insight into the sorption kinetics of the system.

4. It may be useful to investigate the porosity of the adsorbent material in terms of pore size in addition to the pore volume, as examined during this study. At similar pore volume, finer pore diameters will result in higher levels of moisture retained, however reduced pore diameters will make it more difficult for moisture to desorb.

5. Adsorbent assisted drying should be investigated beyond the coal particle size ranges considered during this study, as finer coal particles (-0.25mm) requires drying the most.

6. Conduct further test runs on a wider range of temperatures and relative humidity conditions as key factors identified at 25°C and 40%RH may change with changing air conditions. In addition, investigation into the drying performance of fine coal with adsorbent material in ambient air conditions as well as the time required to reach inherent moisture equilibrium is required. This will give insight into the effectiveness of the process when employing air at ambient conditions that is readily available as an alternative to conditioning air, which is an energy consuming process.

7. Adsorbent degradation during adsorbent assisted drying operation should be further investigated on pilot scale, in continuous mode by employing utilities on site. Minimal degradation of adsorbent material was observed during laboratory scale experiments however, cracks were evident on a number of adsorbent particles and may escalate when the process is scaled up. The degradation evidence observed during the experiments warrants further research into adsorbent attrition and breakage, on pilot scale in continuous mode. This will provide further insight into the service life of the adsorbents.

8. For purposes of industrial application, it might be useful to investigate the prospect of implementing a cold trap for water knock-off, after the regeneration section on a pilot

scale unit. Since South Africa's current water status is unstable, it is of immense importance to optimise water usage in an aid to safeguard water resources for the future. By including a cold trap in the regeneration section, water recovery from the adsorbents during regeneration may be possible. It is also necessary to determine whether the water recovered from the adsorbent material, if any, is potable and without contamination.

9. A prospective energy balance and economic evaluation should be considered on pilot scale to provide a more detailed understanding of the energy consumed, operating costs and capital expenditures associated with the process.

7.3 Contributions

It was concluded from this study that it is possible to dry fine coal with adsorbent material to a target moisture of .08 g(moisture)/g(coal and moisture) or 8%$_{wt}$. The findings showed that various certain factors, such as adsorbent to coal mass ratio and coal particle size range, are key when lowering the surface moisture of mechanically dewatered fine coal. In addition, it was determined that by introducing motion, the process was made more time efficient. Adsorbent assisted drying compared well to the drying technologies, however it was evident that the cascading-bed drying technique delivered the more energy efficient conditions, in general. In conclusion, adsorbent assisted drying yielded

results, making the process energy efficient. Therefore, this technology is a feasible, energy efficient technology for dewatering fine coal.

REFERENCES

Bland, W. & McDaniel, B. 2014. Coal drying method and system. (Patent: US 2014/0144072).

Bratton, R., Ali, Z., Luttrell, G., Bland, R. & Mcdaniel, B. 2012.Nano drying technology. Coalage, pp50-57. June.

Burnard, K., & Bhattacharya, S. 2011. Power generation from coal. International Energy Agency. Paris, France: IEA Publishers.

Campbell, Q.P. 2006. Dewatering of fine coal with flowing air using low pressure drop systems. Potchefstroom: NWU. (Philosophiae Doctor thesis). 130pp.

Condie, D. & Veal, C., 1998. Improved fine coal dewatering via modelling of cake desaturation. Australia: CSIRO. Apr:1-34.

Dabrowski, A. 2001. Adsorption – from theory to practice. Advances in colloid and interface science. M. Curie-Sklodowska University: Faculty of chemistry. Lublin, Poland. 93: pp135-224.

De Korte, G.J. & Mangena, S.J. 2004.Thermal Drying of Fine and Ultra-fine Coal. Report No. 2004 - 0255, Division of Mining Technology, CSIR.pp.5-24.

De Korte, G.J. 2006. Senior Coal Preparation Engineer, CSIR, Pretoria; Personal communication. July.

Du Preez, S.M. 2012. Influence of minerals on the moisture adsorption and desorption properties of South African fine coal. Potchefstroom: NWU. (M.Eng. dissertation). 111pp.

Ellis, S.M. & Steyn, H.S. 2003. Practical significance (effect sizes) versus or in combination with statistical significance (p-values), *Management Dynamics,* 12(4): 51-53.

Falcon, R. & Ham, A.J.1988.The characteristics of Southern African coals. *Journal of the South African institute of mining and metallurgy*, 88(5):145-161. May.

Felder, R.M. & Rousseau, R.W. 2005. Elementary Principles of Chemical Processes. 3rd edition. United States of America: John Wiley & Sons Inc.

Glover, T.G. 2008. Novel adsorbent synthesis, diffusion in nanoporous materials, and adsorption system optimization. Nashville: Vanderbilt University. (Masters dissertation).153p.

Gupta.R.C. 2010. Theory and Laboratory Experiments in Ferrous Metallurgy. First edition.p.99

Karthikeyan, M., Zhonghua, W. &Mujumdar, A.S. 2009. Low-rank coal drying technologies – Current status and new developments. *Drying technology: An international journal*, 27(3): 403-415. 25Feb.

Knaebel, K.S. 2006. Adsorbent selection. Adsorption Research Inc. Dublin: Ohio. pp1-21. Oct. 07.

Koretsky, M.D. 2004. Engineering and Chemical Thermodynamics. 2nded. Hoboken, NewJersey, USA: John Wiley & Sons Inc.

Kudra, T. & Mujumdar, A.S. 2009. Advanced drying technologies. Second edition.pp.169-184.

Kulkarni, S. & Kaware, J. 2014. Regeneration and Recovery in Adsorption- a Review. *IJISET - International Journal of Innovative Science, Engineering & Technology*, Vol. 1 Issue 8: 61-64.

Lemley, A., Wagenet, L. & Kneen, B. 1995. Activated Carbon Treatment of Drinking Water. http://www.sswn.info/sites/default/files/toolbox/LEMLEY%20et%20al%201995%20a%20Typical%20Carbon%20Particle.jpg Date of access: 06 Jun 2014.

Le Roux, M.& Campbell, Q.P. 2003. An Investigation into an Improved Method of Fine Coal Dewatering. *Minerals Engineering*, 16(10):999-1003.

Le Roux, M., Campbell, Q.P. & Van Rensburg, M.J .2013. Fine coal dewatering using high airflow. *International journal of coal preparation and utilization*, pp1-18. 02 Dec.

Mohanty, M.K. & Akbari, H. 2012. Fine coal dewatering and plant profitability. Department of mining and mineral resources engineering. Illinois. pp.1-14.

Nicol, S.K., (1992); *Fine coal beneficiation*, in Swanson, A.R., and Partridge, A.C. (Ed.); Advanced Coal Preparation Monograph Series; Volume IV; Part 9

Petrick, A.J.1969. Moisture in coal. Report No. 1969 - 16, Fuel Research Institute of South Africa. pp.1-12.

Reddick, J.F., Von Blottnitz, H. & Kothuis, B. 2007. A cleaner production assessment of the ultra-fine coal waste generated in South Africa. *The Journal of The South African Institute of Mining and Metallurgy*, 107:811-816.

Risheng. 2014.Adsorption drying. http://www.risheng.com/tech/adsorption-drying--16.html. Date of access: 10 June 2015.

Rodrigues, E.F. & Lemos de Sousa, M.J. 2002. The measurement of coal porosity with different gases. International Journal of Coal Geology, 48:245-251.

Rong, R.X. 1993. Literature review on fine coal and tailings dewatering. Advances in coal preparation technology, (2) Project P239A. Brisbane. Australia:JKMRC, University of Queensland. Nov. 120pp.

Rowan, S.L. 2010. Analysis and scaling of a two-stage fluidized bed for drying of fine coal particles using Shannon entropy, thermodynamic exergy and statistical methods. Morgantown: West Virginia University.(Philosophiae Doctor - thesis). 154pp.

SANEDI.2011.http://www.sanedi.org.za/coal-roadmap/.Date of access: 25 Jun 2014.

Unsworth, J.F., Fowler, C.S. & Jones, L.F. 1989. Moisture in coal: Maceral effects on pore structure. Fuel, pp. 18-26. Jan: Vol 68

VICAIRE (Virtual campus in hydrology and water resources management). 2015. http://echo2.epfl.ch/VICAIRE/mod_3/chapt_4/main.htm .Module 3 Chapter 4: Water potential in porous media. Date of access: 15 September 2015.

Wakeman, R.J. 1984. Residual saturation and dewatering of fine coals and filter cakes. Powder Technology, (40):53-63.

World Coal Institute (WCI). The coal resource: A comprehensive overview of coal. A2009. http://www.worldcoal.org/.Date of access: 5 Mar 2015.

Yang, X. 2015. Suitability evaluation of emerging drying technologies for fine clean coal drying. Southern Illinois University at Carbondale. (Philosophiae Doctor - thesis). 101pp.

A

ANNEXURE

REPEATABILITY

Annexure A contains additional repeatability results that validate the reproducibility of the experimental procedure followed.

- A.1 Standard deviation and relative standard error
- A.2 Standard deviation of fixed-bed drying technique
- A.3 Standard deviation of cascading-bed drying technique

A.1 Standard deviation and relative standard error

A series of repeats were completed to quantify the precision of the fixed-bed experimental runs. The fixed-bed experiments delivered results in a narrow range from one another. The average for each data point was determined with Equation A.1.1 where x_i is a data point, n is the amount of runs and $\bar{x}$ is the average of the data points.

$$\bar{x} = \frac{\sum_1^n x_i}{n}$$

Equation A.1.1

The standard deviation (S) was determined by using the average for every data point Equation A.1.2.

$$S = \sqrt{\frac{1}{n-1}\sum_1^n (x_i - \bar{x})^2}$$

Equation A.1.2

The average and standard deviation was determined per time interval.

It was decided to calculated the relative standard error in order to obtain a representative error for the experimental results that are not normally distributed. The standard error (SE) was calculated by using Equation A.1.3:

$$SE = \frac{S}{\sqrt{n}}$$

Equation A.1.3

Where S is the standard deviation and n is the amount of runs.

The relative standard error (RSE) was calculated by using Equation A.1.4, where SE is the standard error and $\bar{x}$ is the average of the data points.

$$RSE = \frac{SE}{\bar{x}}$$

Equation A.1.4

A.2 Standard deviation of fixed-bed drying technique

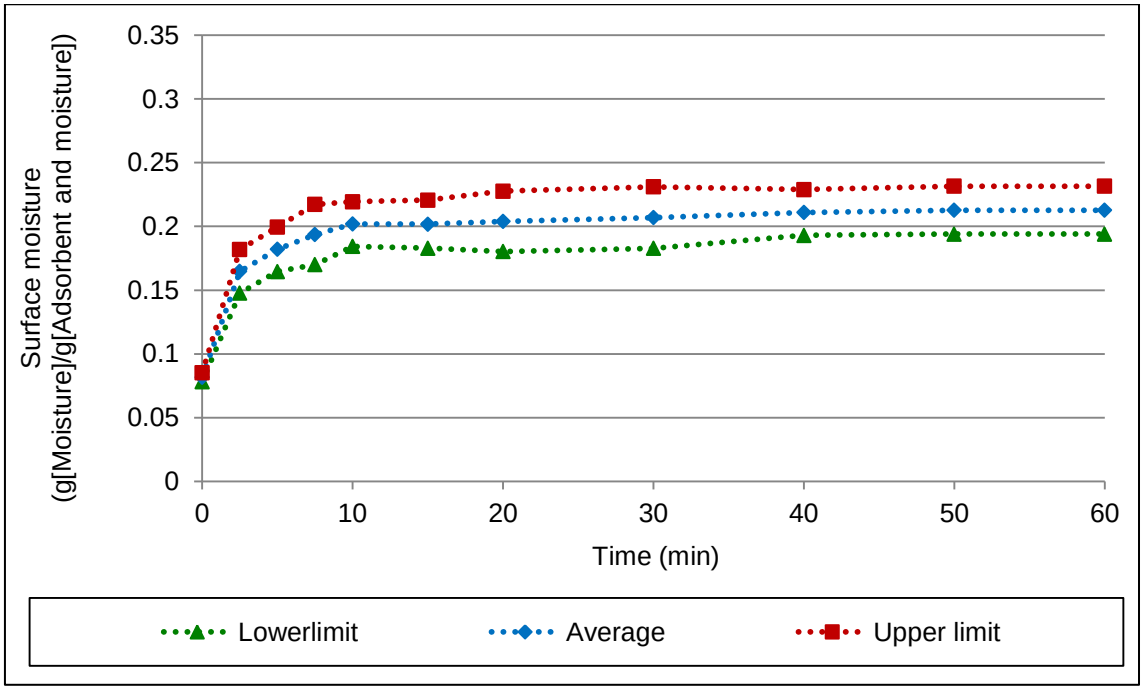

Figure A.2.1: Average and standard deviation of repeats for 3mm alumina-based adsorbents and -2mm+1mm coal

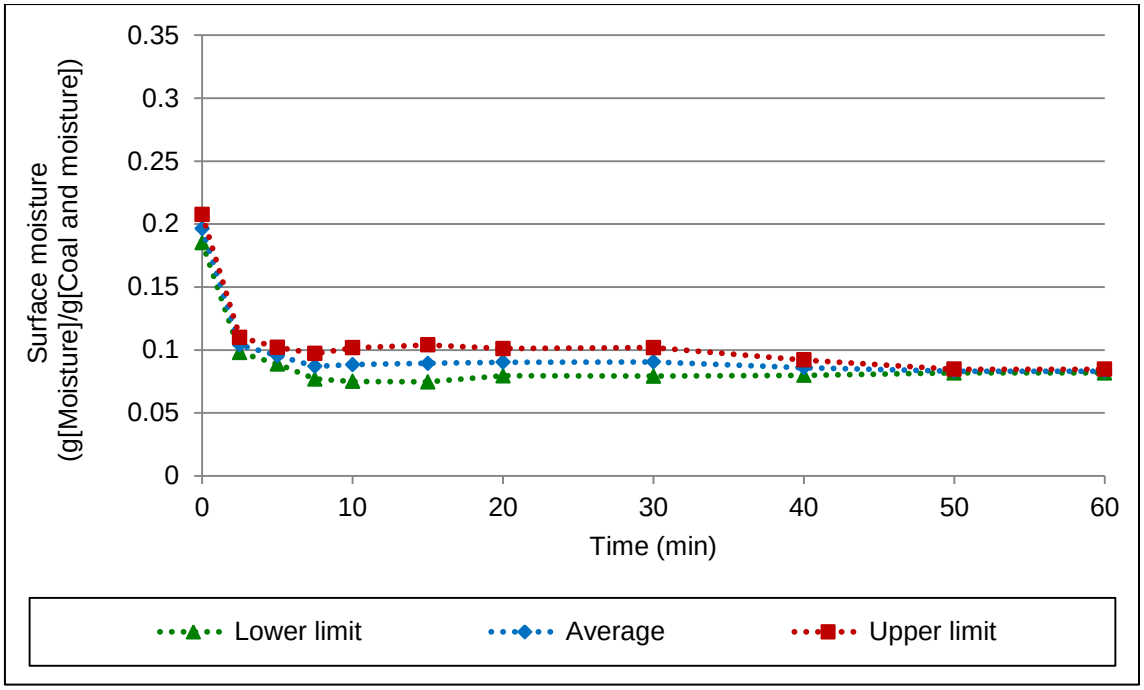

Figure A.2.2: Average and standard deviation of repeats for -2mm+1mm coal and 3mm alumina-based adsorbents

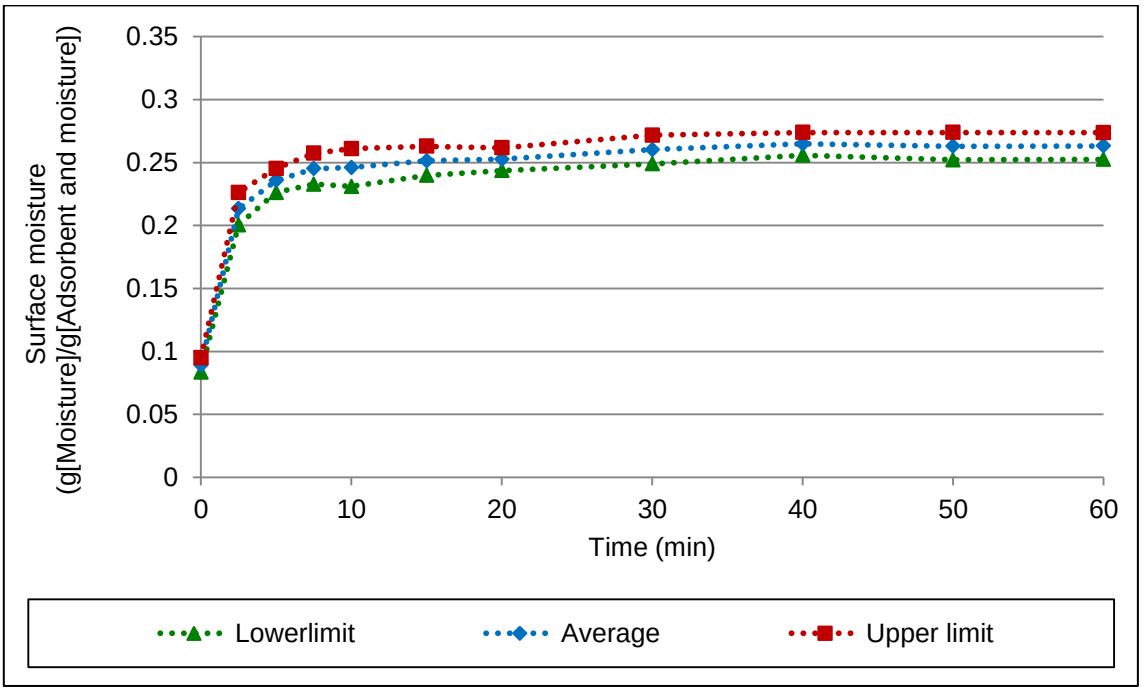

Figure A.2.3: Average and standard deviation of repeats for 3mm silica-based adsorbents and -1mm+0.5mm coal

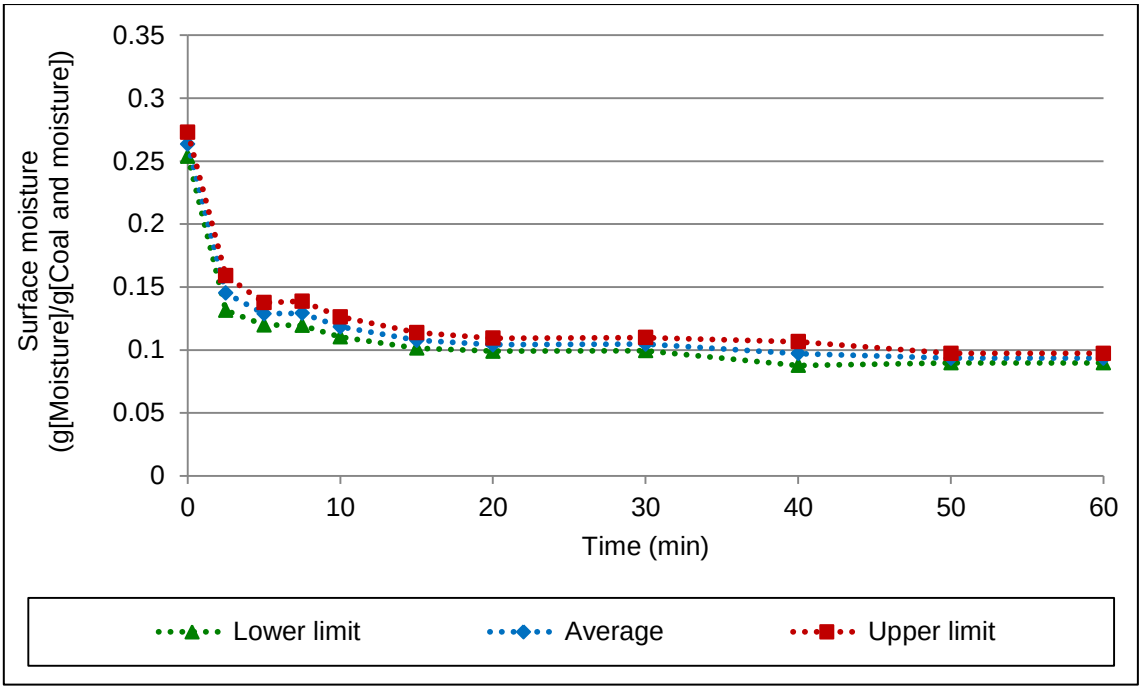

Figure A.2.4: Average and standard deviation of repeats for -1mm+0.5mm coal and 3mm silica-based adsorbents

A.3 Standard deviation of cascading-bed drying technique

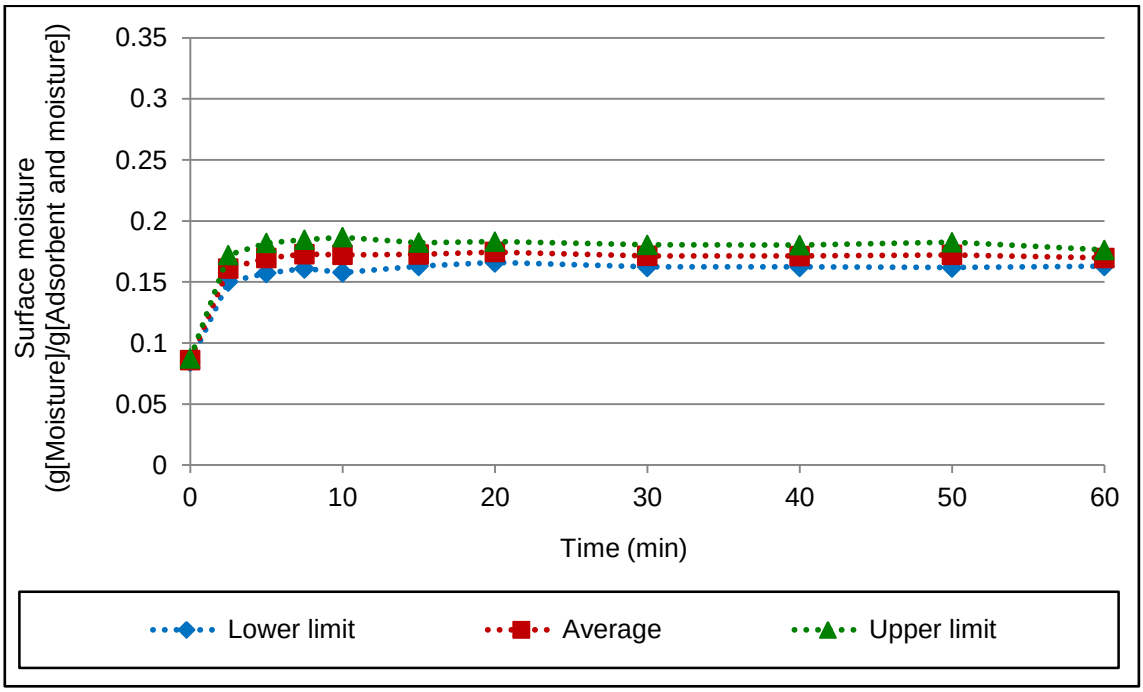

Figure A.3.1: Average and standard deviation of repeats for 5mm alumina-based adsorbents and -2mm+1mm coal

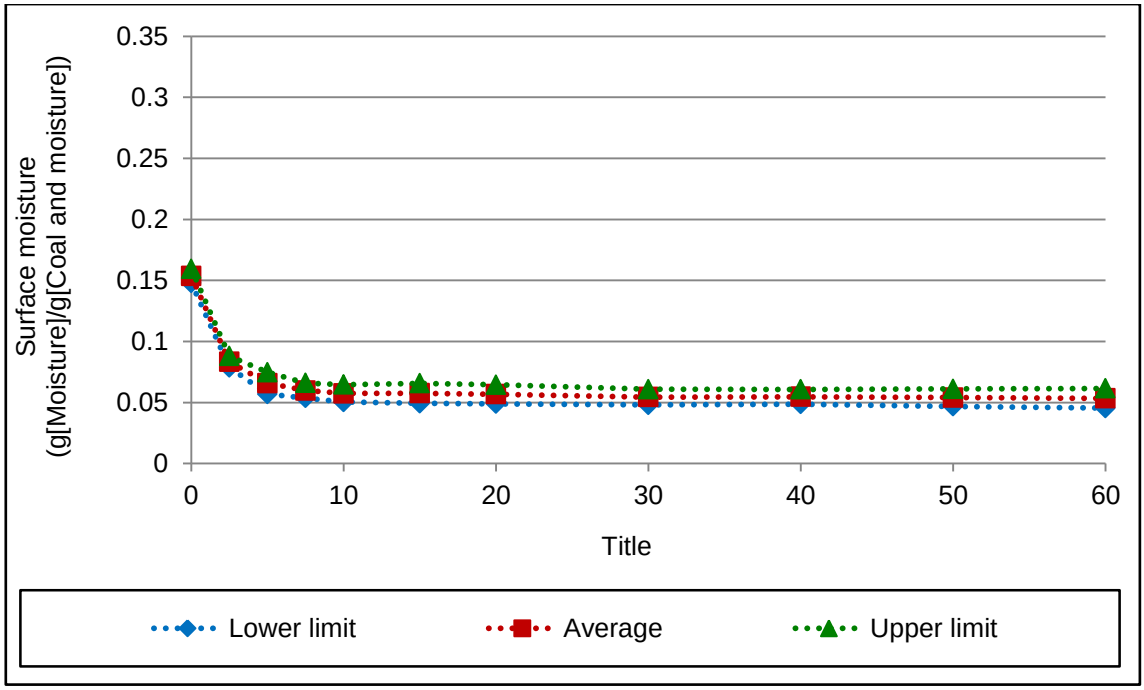

Figure A.3.2: Average and standard deviation of repeats for -2mm+1mm coal and 5mm alumina-based adsorbents

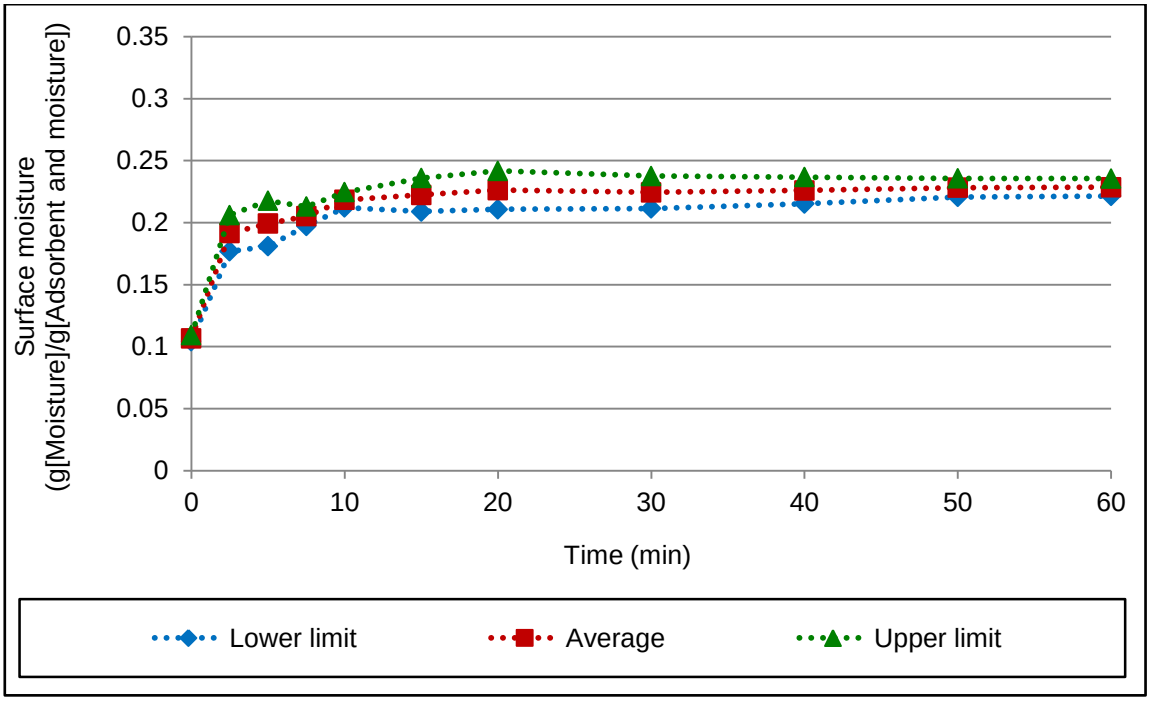

Figure A.3.3: Average and standard deviation of repeats for 5mm alumina-based adsorbents and -0.5mm+0.25mm coal

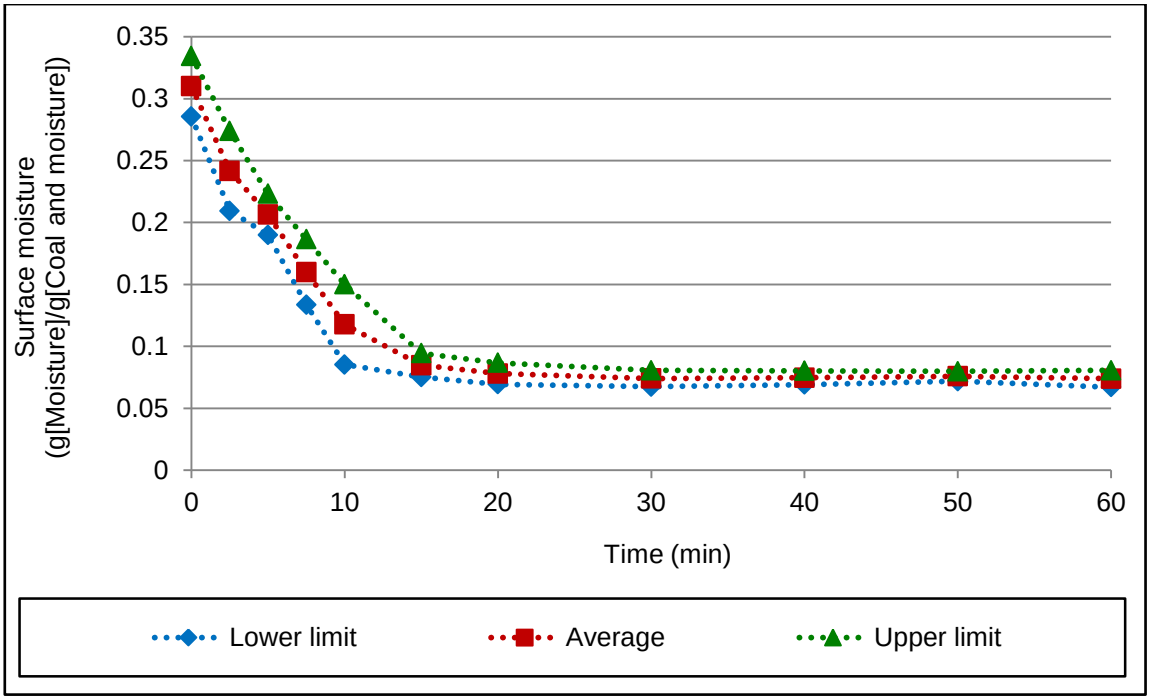

Figure A.3.4: Average and standard deviation of repeats for -0.5mm+0.25mm coal and 5mm alumina-based adsorbents

B

ANNEXURE

FIXED-BED DRYING TECHNIQUE

Added fixed-bed drying experimental results is summarised in Annexure B.

- B.1 General adsorption and desorption curves
- B.2 Adsorption rate
- B.3 Operating conditions
  - B.3.1 Influence of adsorbent to coal mass ratio
  - B.3.2 Influence of adsorbent type
  - B.3.3 Influence of adsorbent size
  - B.3.4 Influence of coal particle size range

B.1 General adsorption-desorption curves

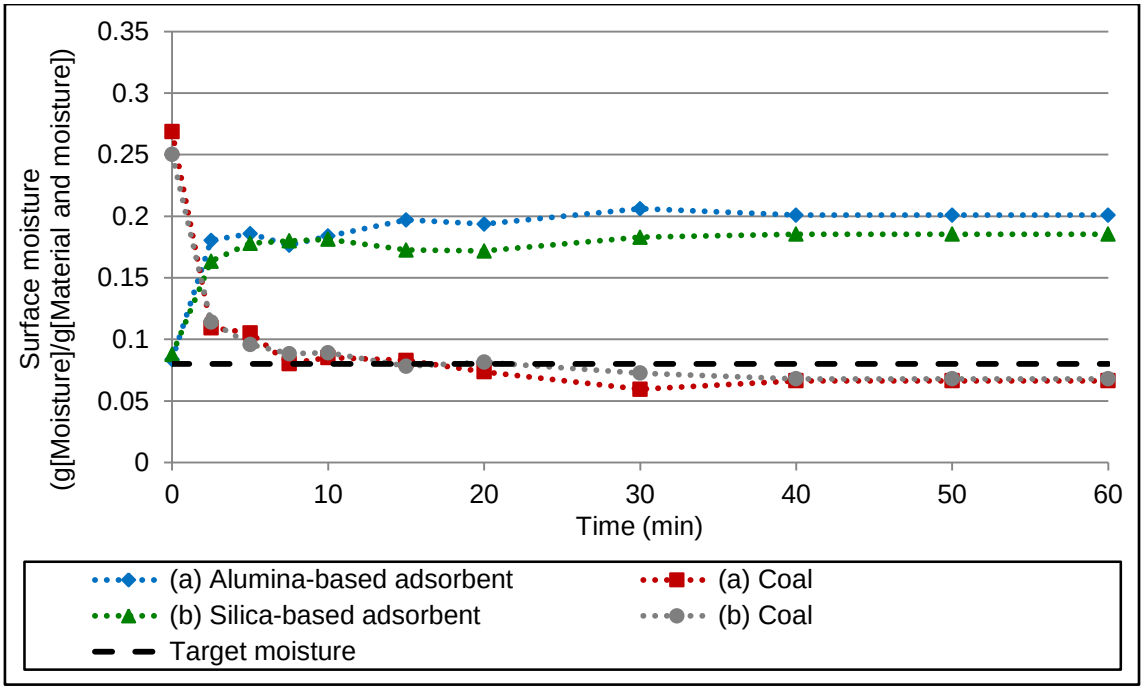

Figure B.1.1: Adsorption-desorption curves of -1mm+0.5mm coal and 3mm adsorbents at an adsorbent to coal mass ratio of 2:1

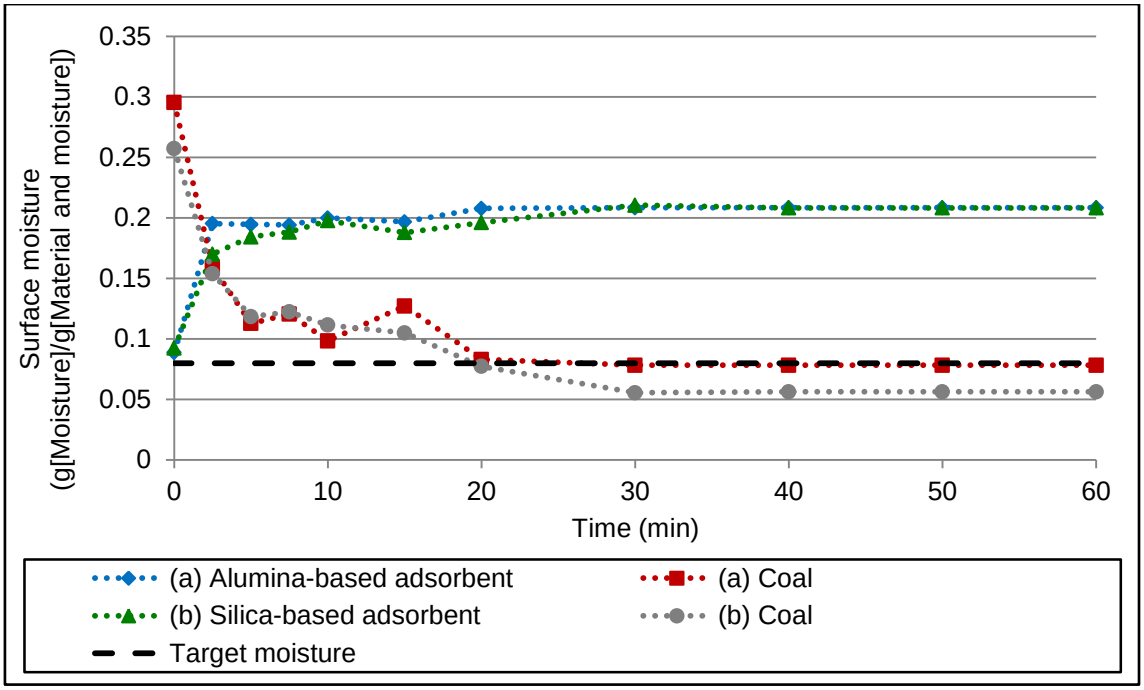

Figure B.1.2: Adsorption-desorption curves of -0.5mm+0.25mm coal and 3mm adsorbents at an adsorbent to coal mass ratio of 2:1

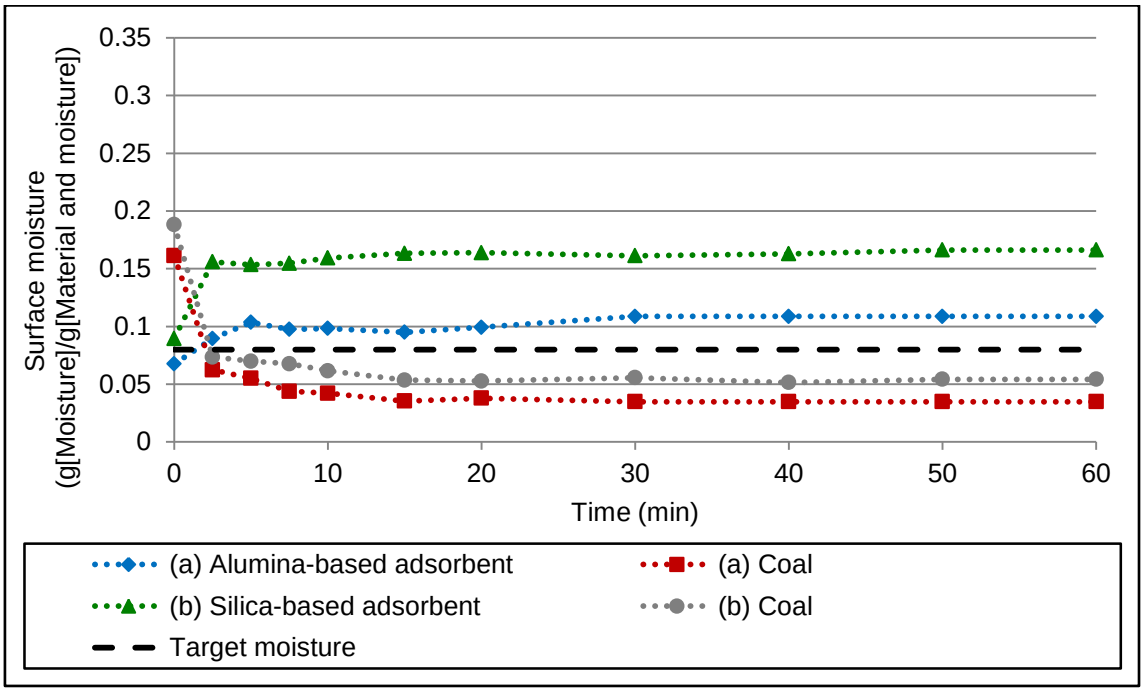

Figure B.1.3: Adsorption-desorption curves of -2mm+1mm coal and 5mm adsorbents at an adsorbent to coal mass ratio of 2:1

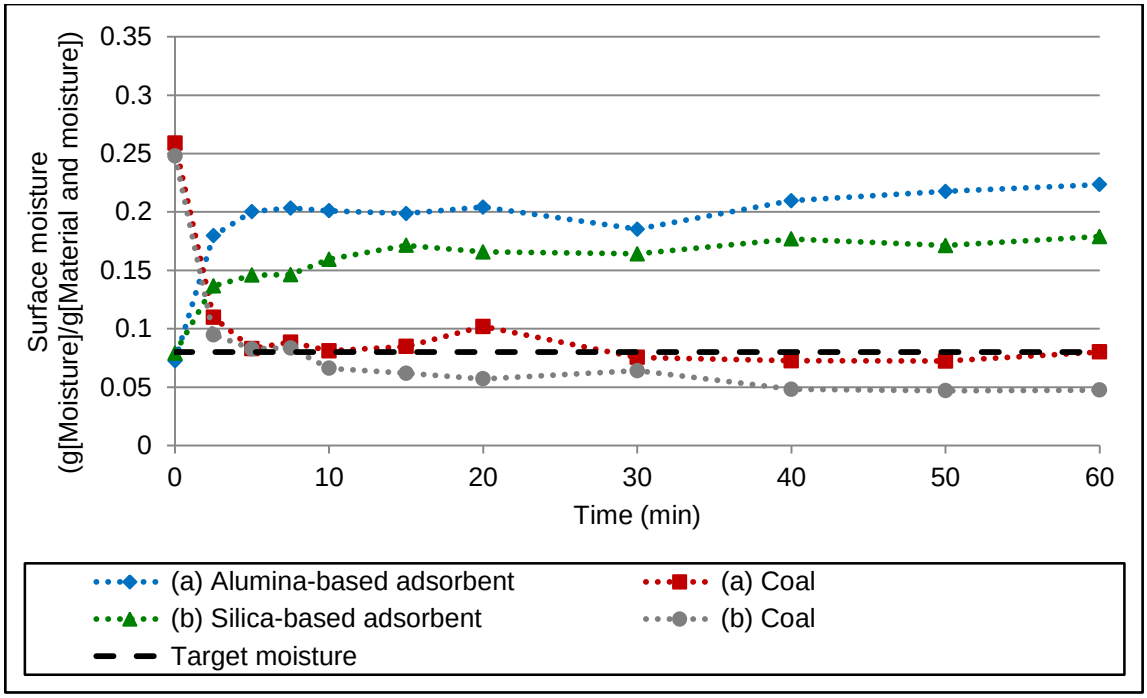

Figure B.1.4: Adsorption-desorption curves of -1mm+0.5mm coal and 5mm adsorbents at an adsorbent to coal mass ratio of 2:1

B.2 Adsorption rate

The adsorption curves in Figure 4.2.1, of Chapter 4, were plotted in Figure B.2.1 to demonstrate the characteristic adsorption curve. Three distinct adsorption phases were recognised from the adsorption curves as indicated in Figure B.2.1 by A, B and C.

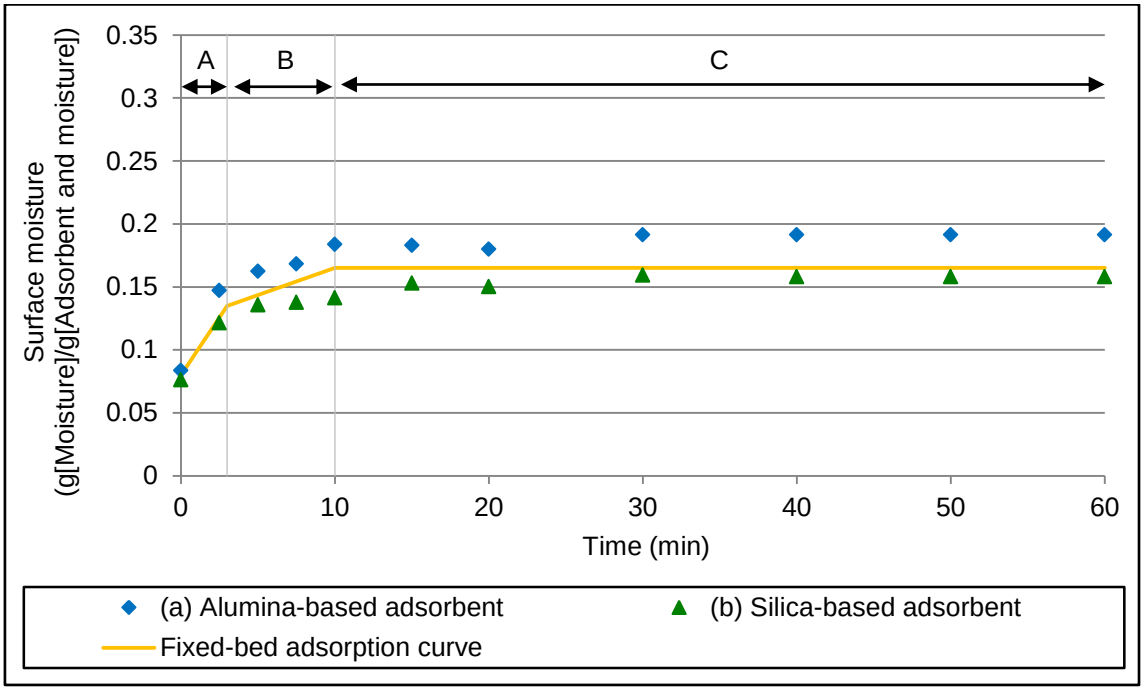

Figure B.2.1: Characteristic adsorption curve of adsorbents

The section of the adsorption curve labelled A, B and C in Figure B.2.1, represents the initial adsorption rate, secondary adsorption rate and final moisture load, respectively. The initial adsorption rate is defined as the load of moisture adsorbed by the adsorbent per unit mass of adsorbent over time (Knaebel, 2006). Equation B.2.1 was employed to calculate the initial adsorption rate:

$$Initial\ adsorption\ rate = \frac{Initial\ moisture\ load\ gain}{\Delta time}$$

Equation B.2.1

where the initial moisture load gain refers to the moisture adsorbed during A and is measured in g(Moisture)/g(Adsorbent and moisture) and the time recorded in minutes.

B.3 Operating conditions

B.3.1 Influence of adsorbent to coal mass ratio

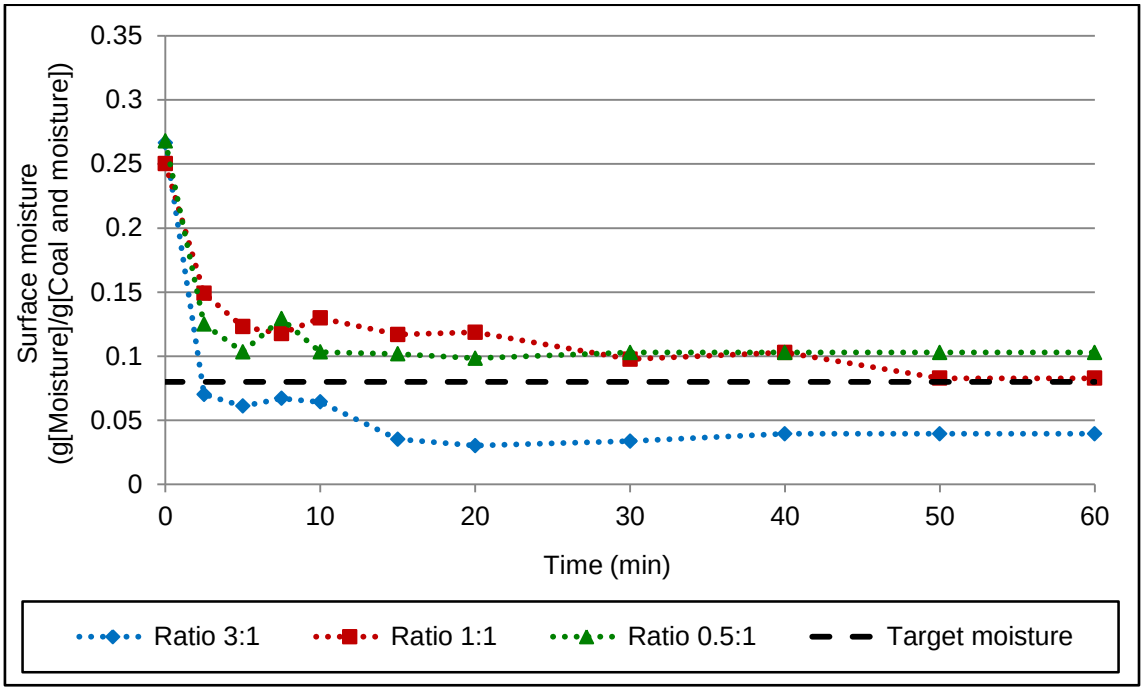

Figure B.3.1: Desorption curves of -1mm+0.5mm coal and 3mm alumina-based adsorbents

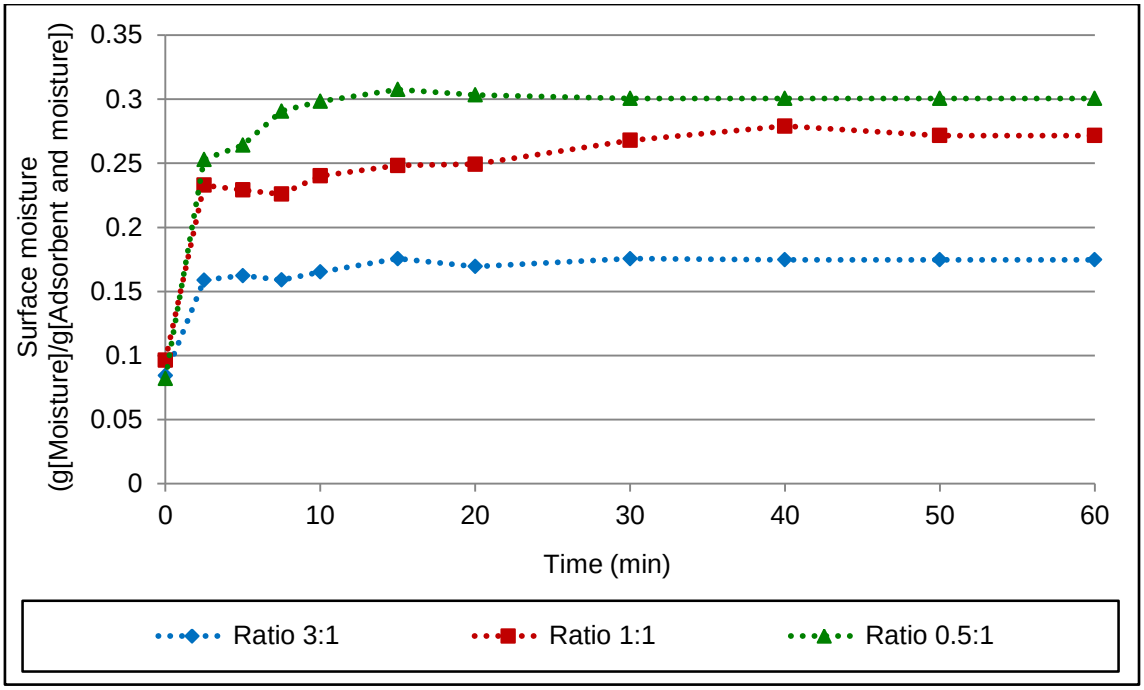

Figure B.3.2: Adsorption curves of 3mm alumina-based adsorbents and -1mm+0.5mm coal

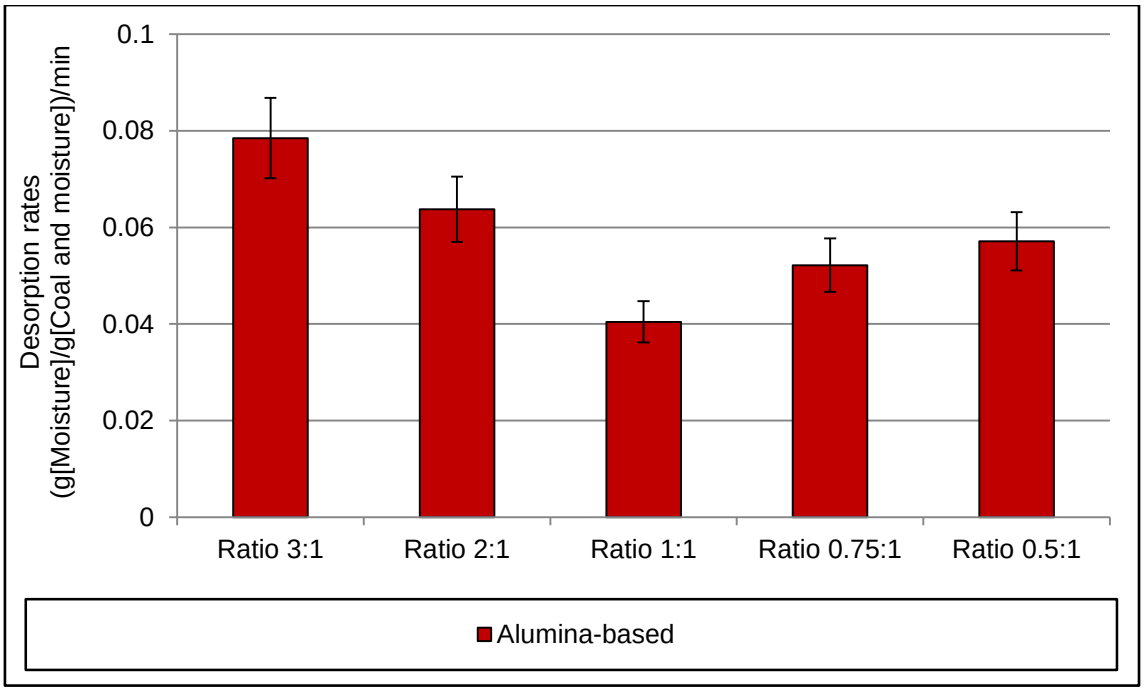

Figure B.3.3: Initial desorption rates of -1mm+0.5mm coal and 3mm alumina-based adsorbents

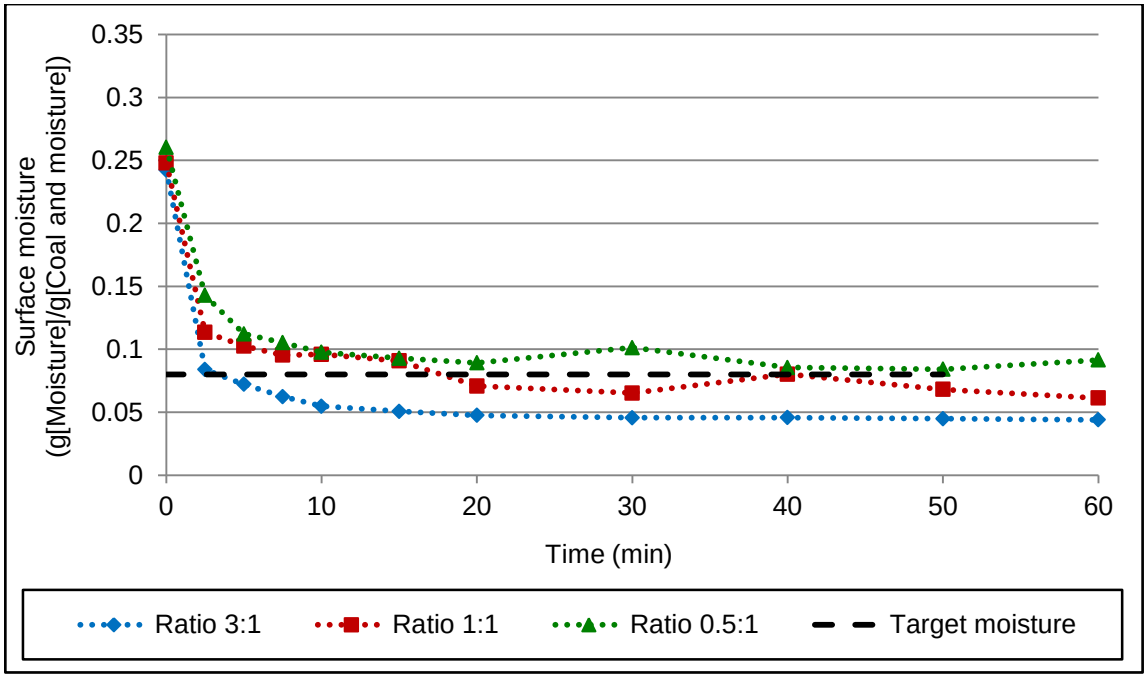

Figure B.3.4: Desorption curves of -1mm+0.5mm coal and 5mm silica-based adsorbents

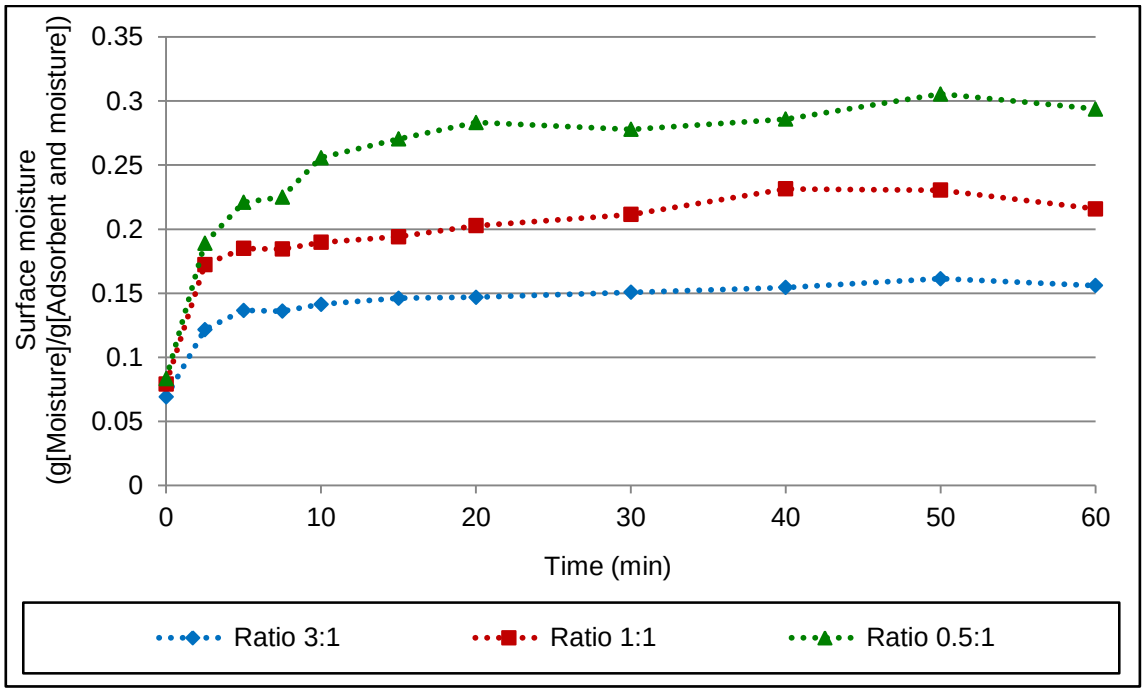

Figure B.3.5: Adsorption curves of 5mm silica-based adsorbents and -1mm+0.5mm coal

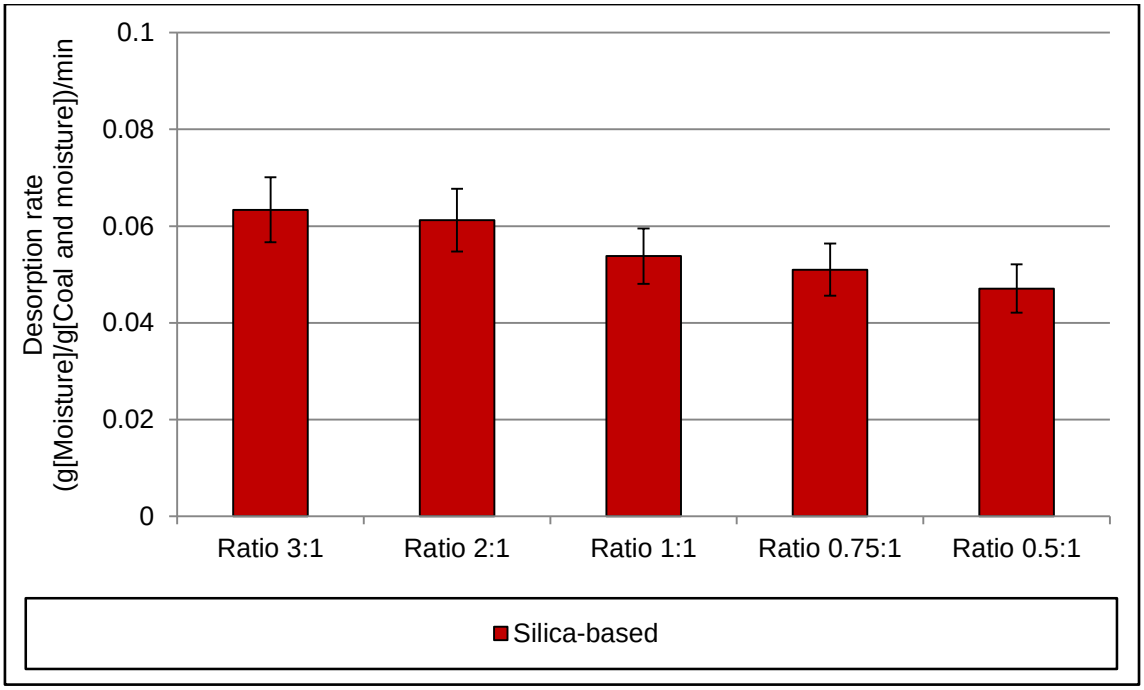

Figure B.3.6: Initial desorption rates of -1mm+0.5mm coal and 5mm silica-based adsorbents

B.3.2 Influence of adsorbent type

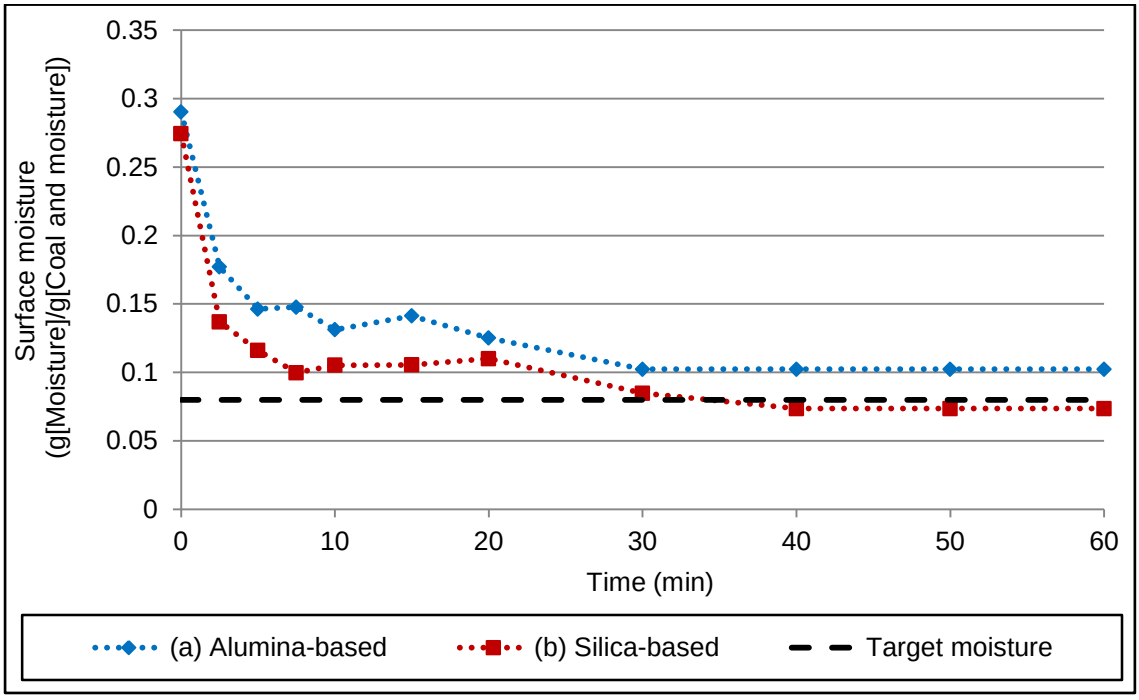

Figure B.3.7: Desorption curves of -0.5mm+0.25mm coal and 3mm adsorbents at an adsorbent to coal mass ratio of 1:1

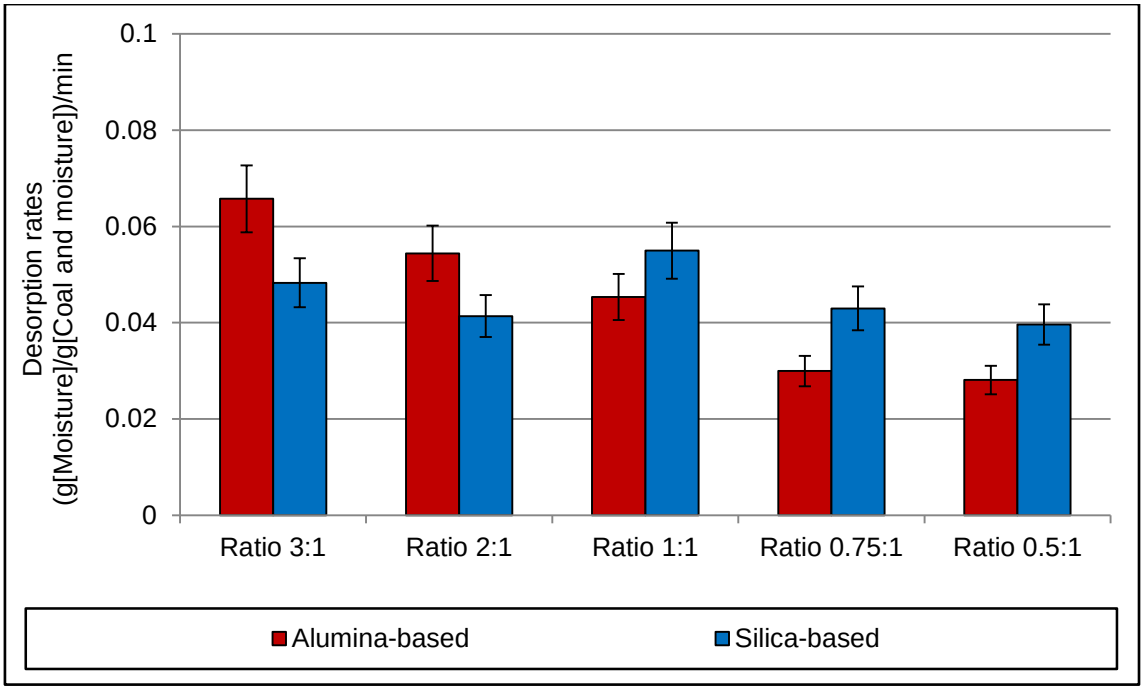

Figure B.3.8: Initial desorption rates of -0.5mm+0.25mm coal and 3mm adsorbents

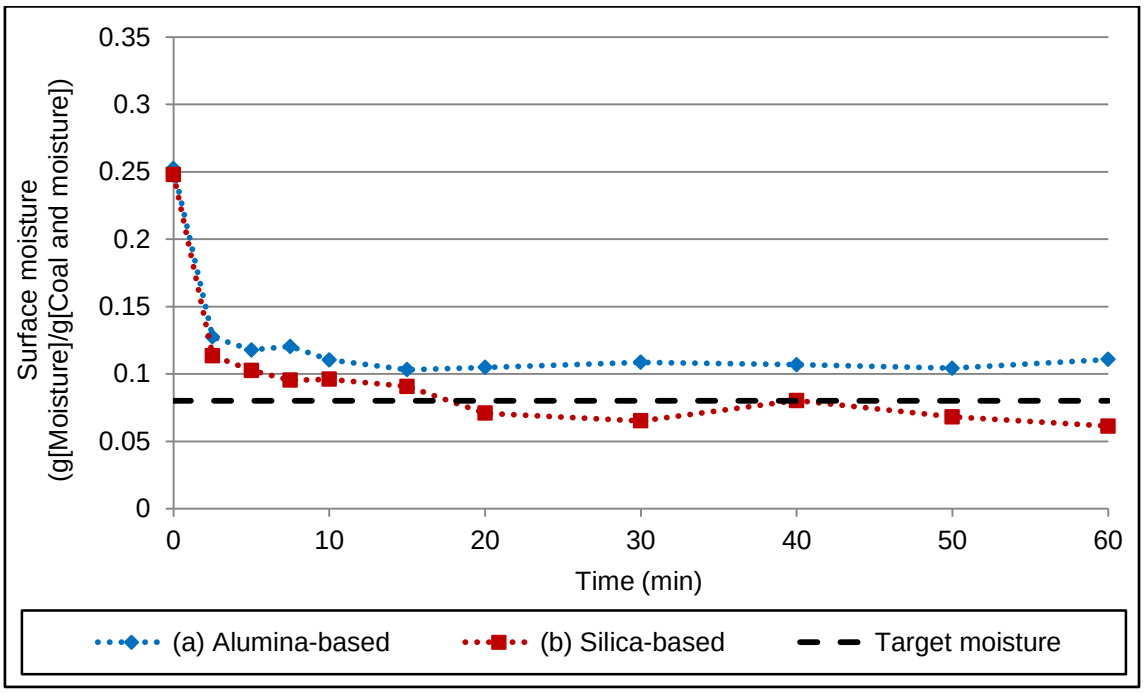

Figure B.3.9: Desorption curves of -1mm+0.5mm coal and 5mm adsorbents at an adsorbent to coal mass ratio of 1:1

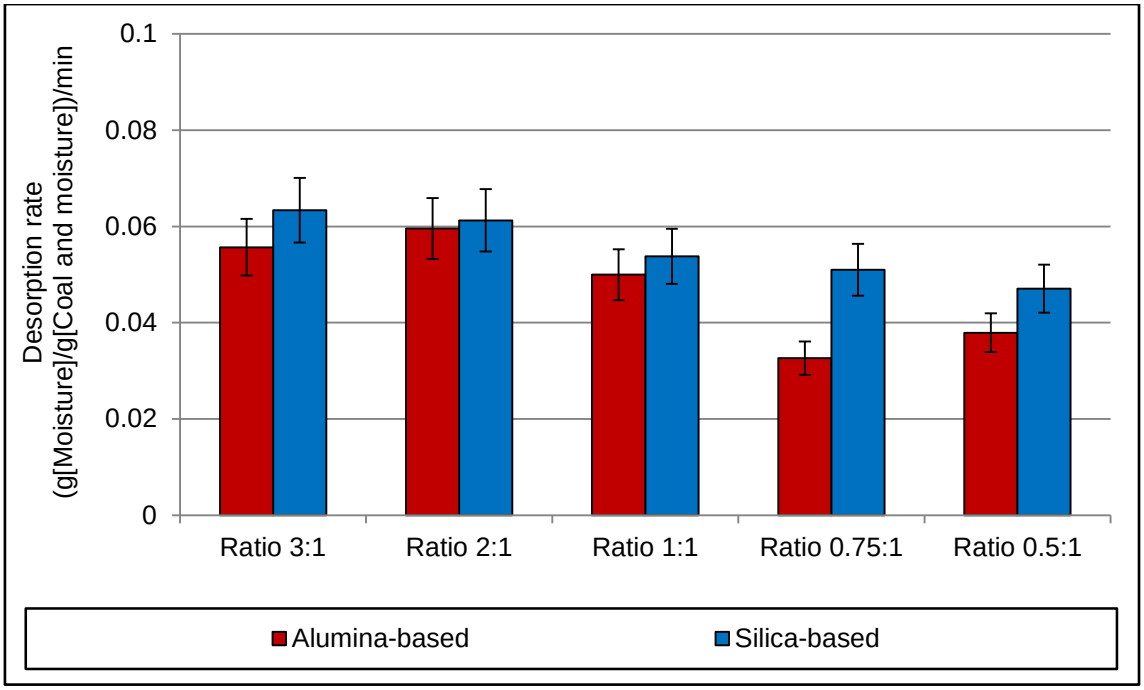

Figure B.3.10: Initial desorption rates of -1mm+0.5mm coal and 5mm adsorbents

B.3.3 Influence of adsorbent size

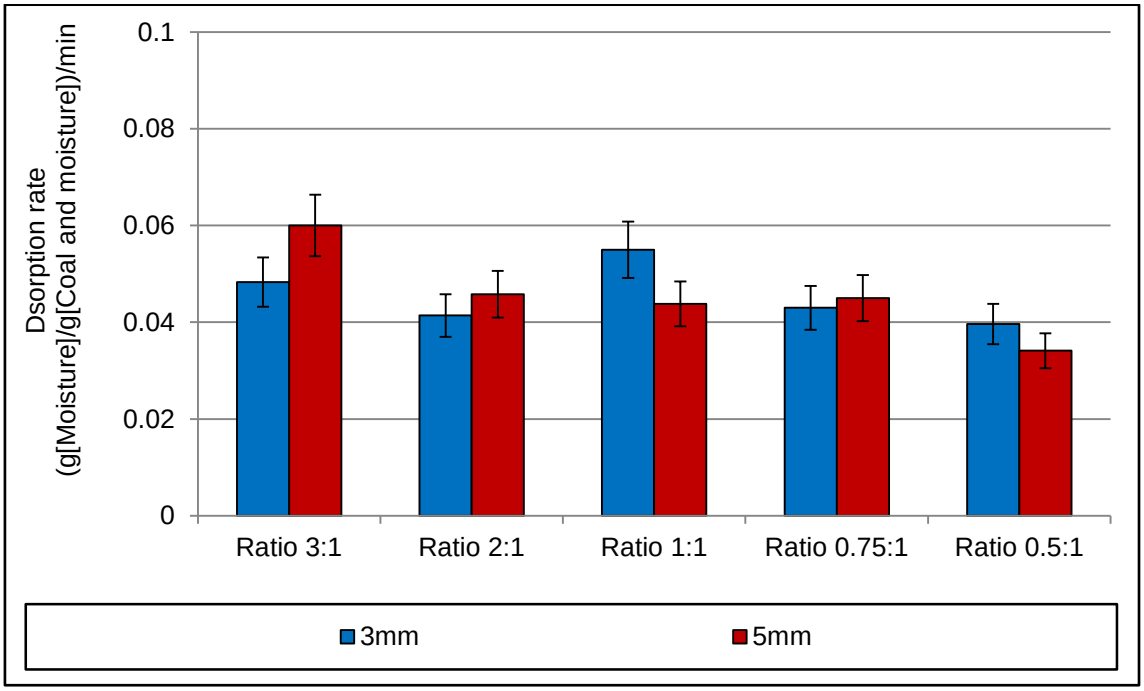

Figure B.3.11: Desorption rates of -0.5mm+0.25mm coal and silica-based adsorbents

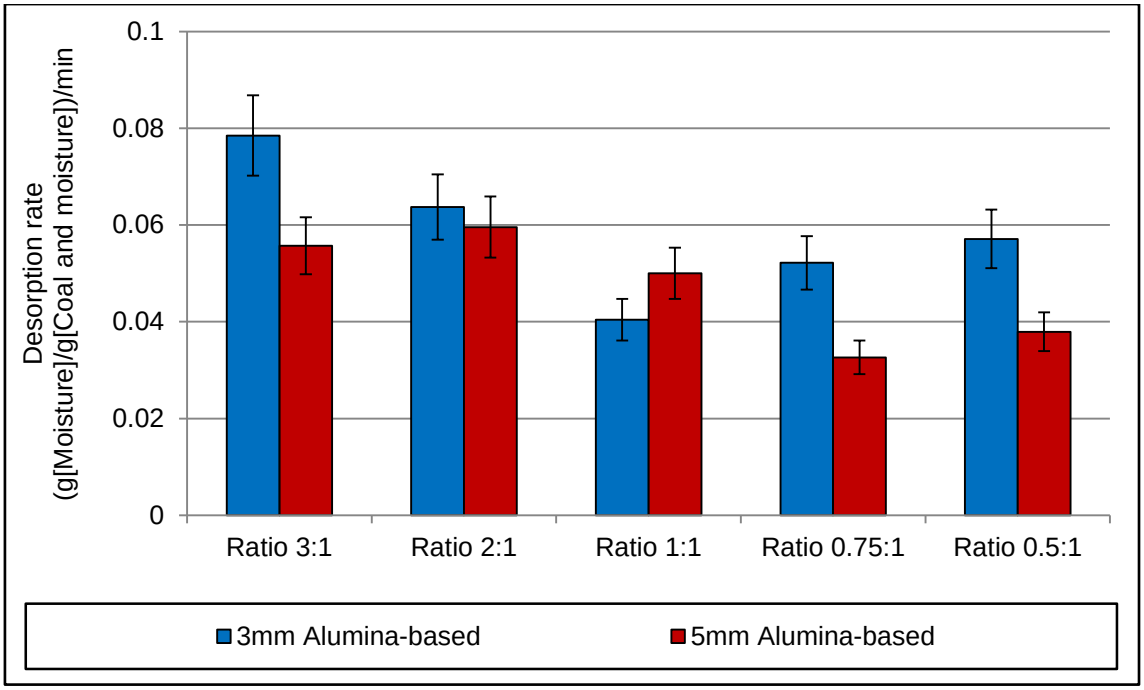

Figure B.3.12: Desorption rates of -1mm+0.5mm coal and alumina-based adsorbents

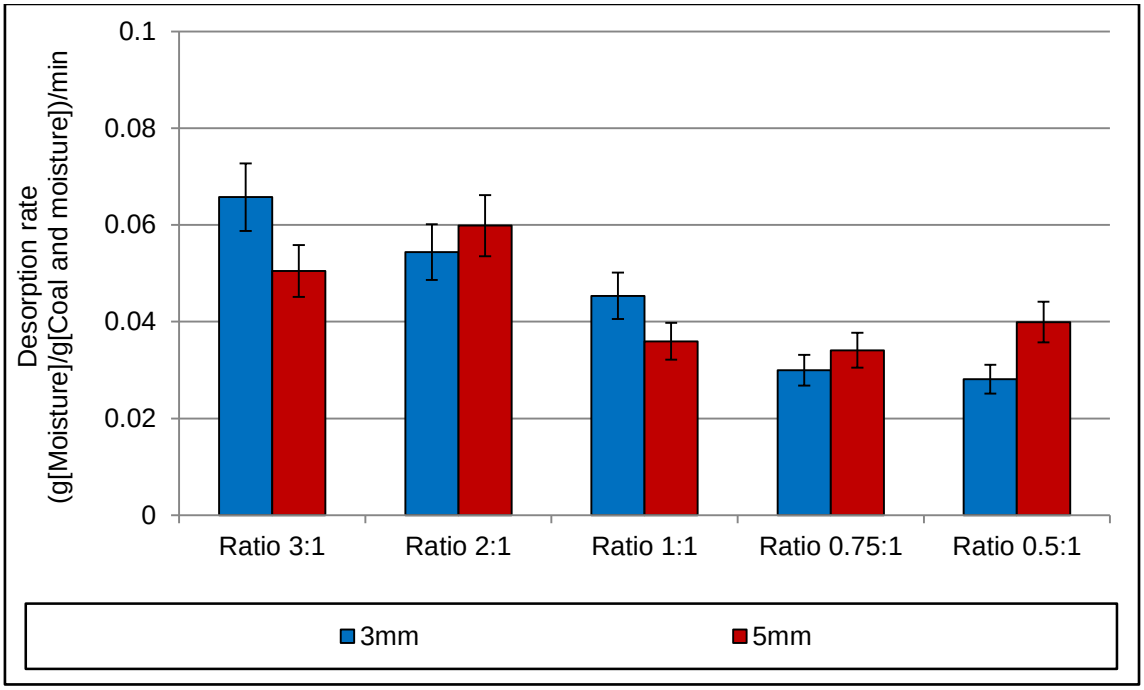

Figure B.3.13: Desorption rates of -0.5mm+0.25mm coal and alumina-based adsorbents

B.3.4 Influence of coal particle size range

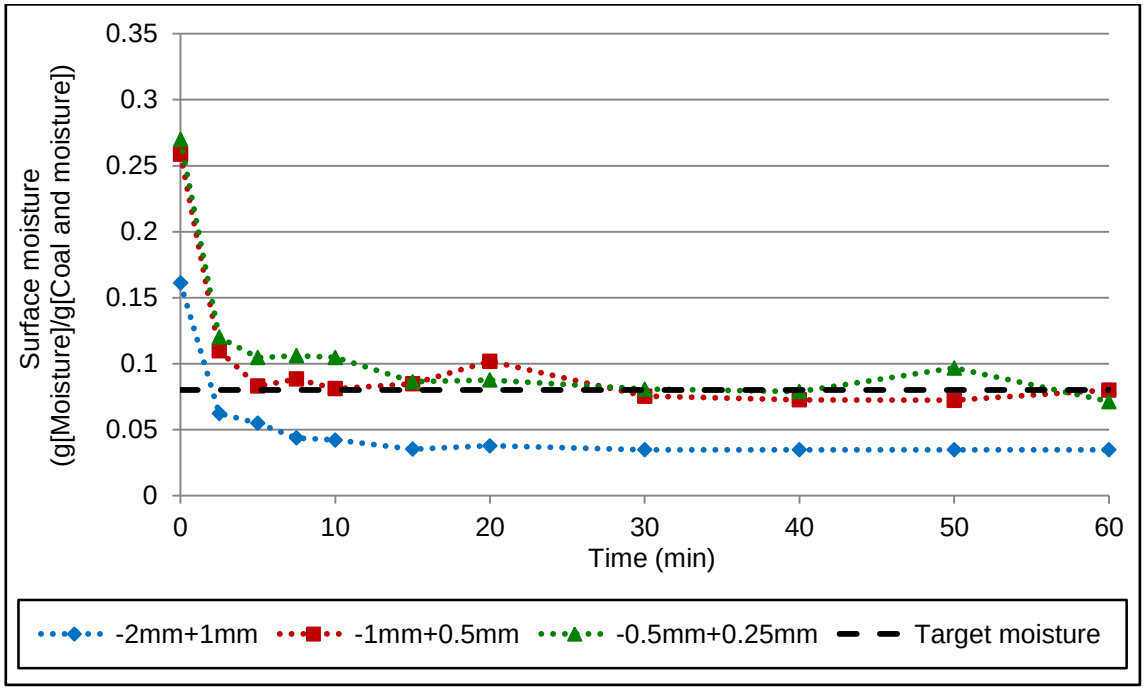

Figure B.3.14: Desorption curves of coal and 5mm alumina-based adsorbents at an adsorbent to coal mass ratio of 2:1

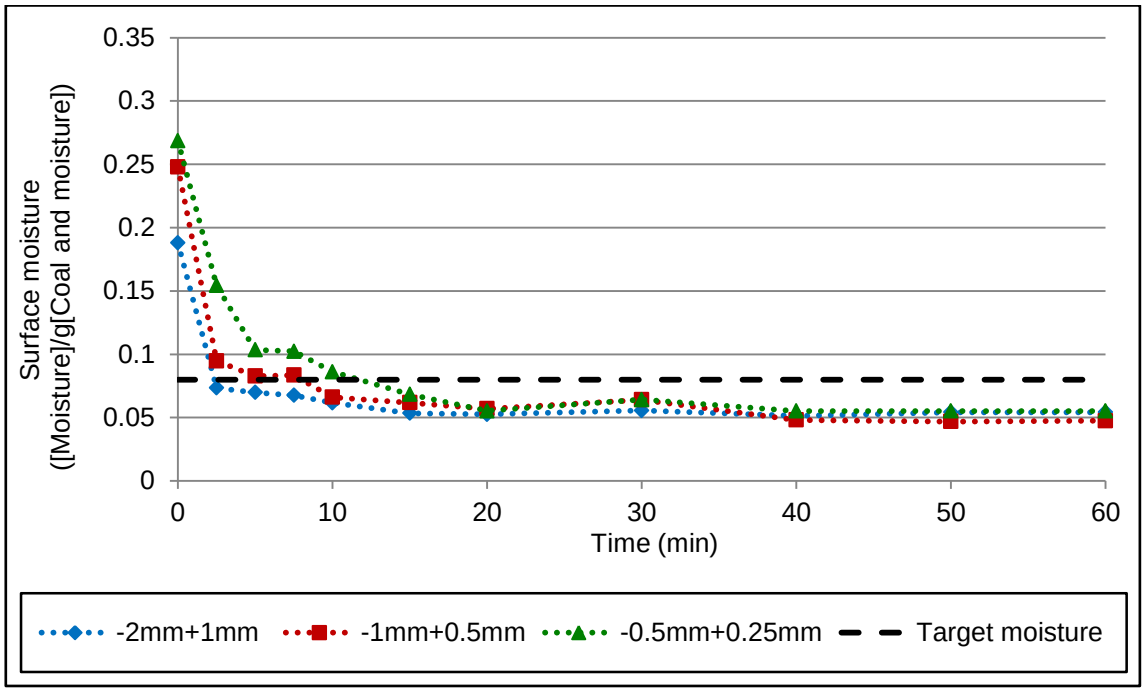

Figure B.3.15: Desorption curves of coal and 5mm silica-based adsorbents at an adsorbent to coal mass ratio of 2:1

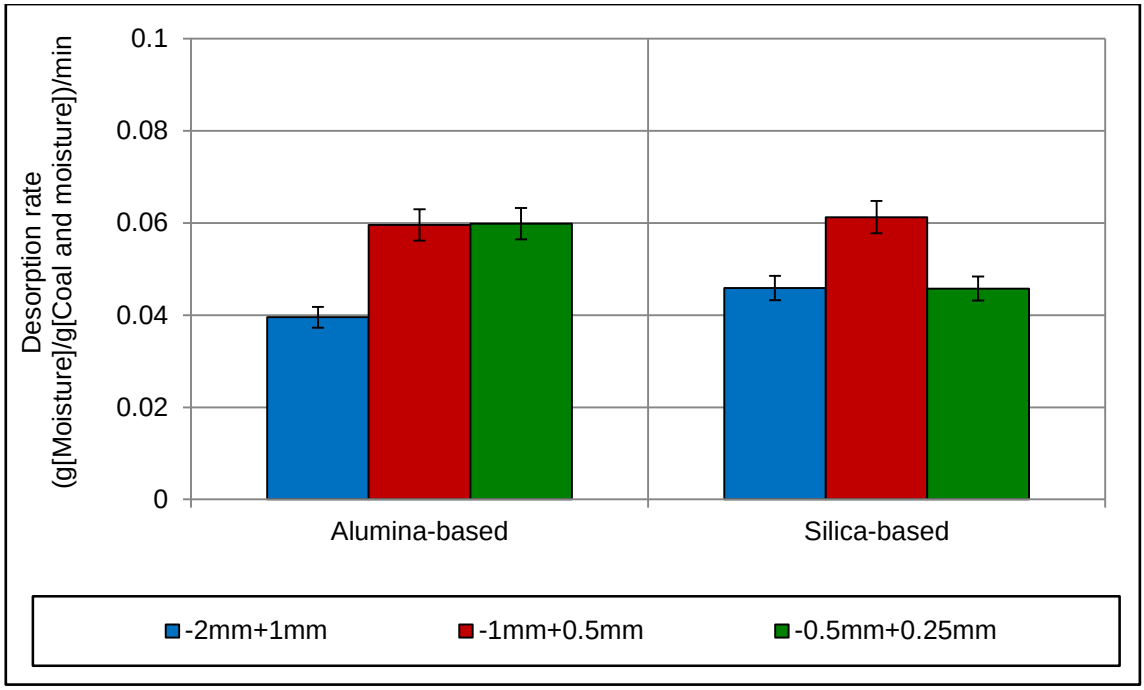

Figure B.3.16: Initial desorption rates of coal and 5mm adsorbents at an adsorbent to coal mass ratio of 2:1

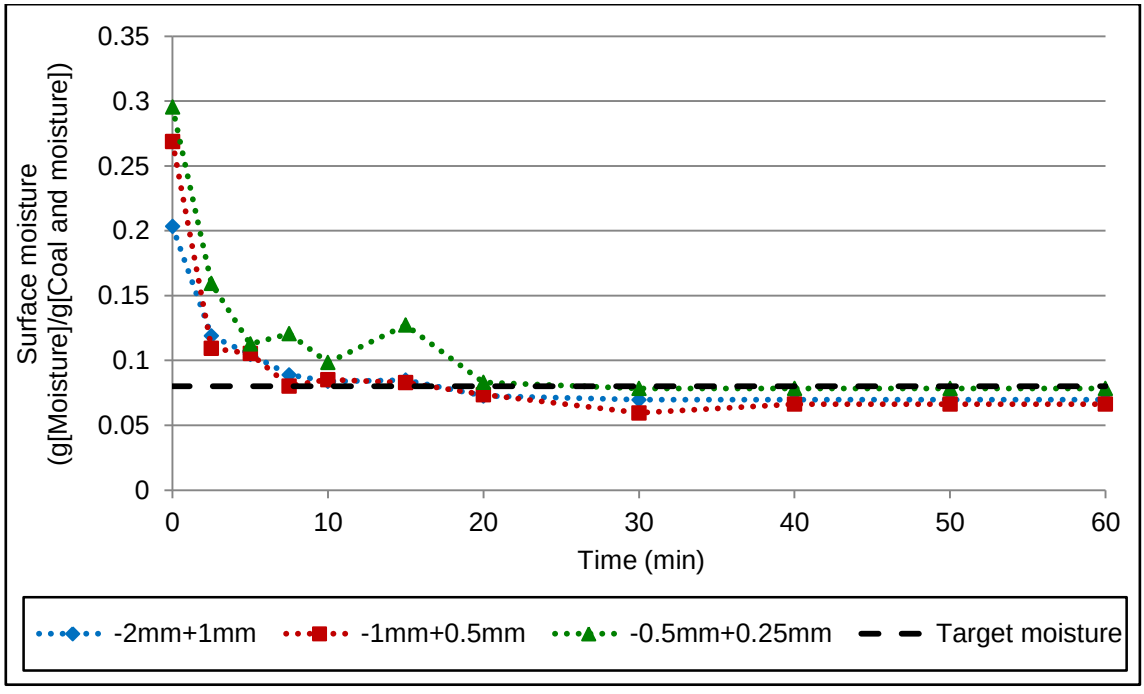

Figure B.3.17: Desorption curves of coal and 3mm alumina-based adsorbents at an adsorbent to coal mass ratio of 2:1

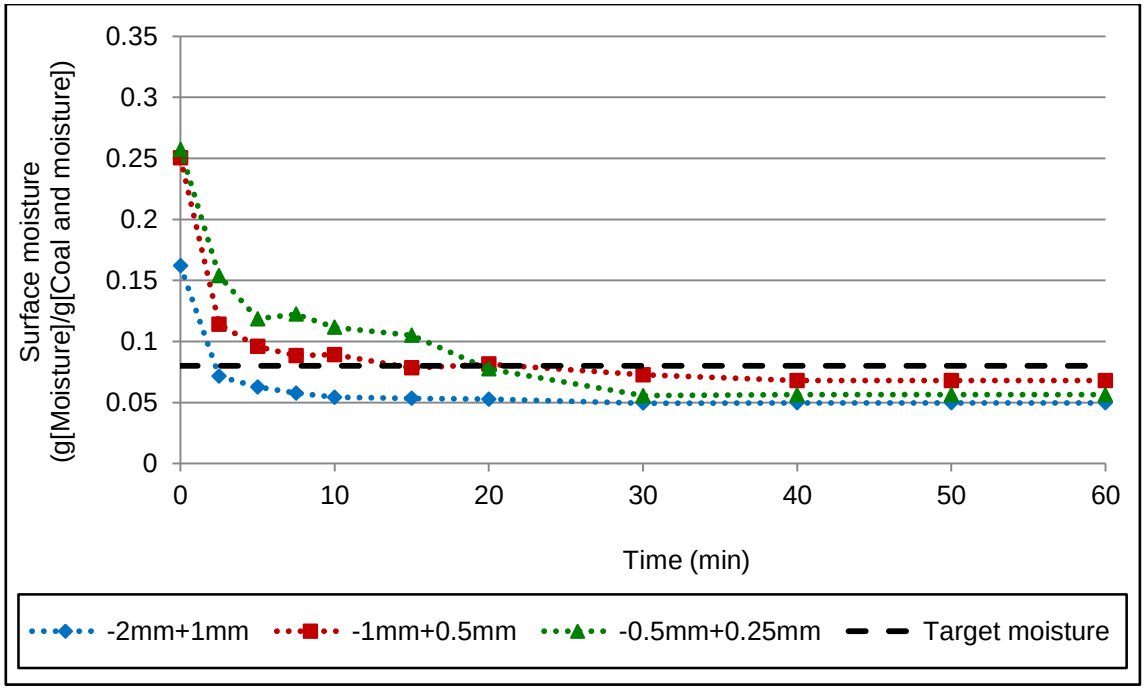

Figure B.3.18: Desorption curves of coal and 3mm silica-based adsorbents at an adsorbent to coal mass ratio of 2:1

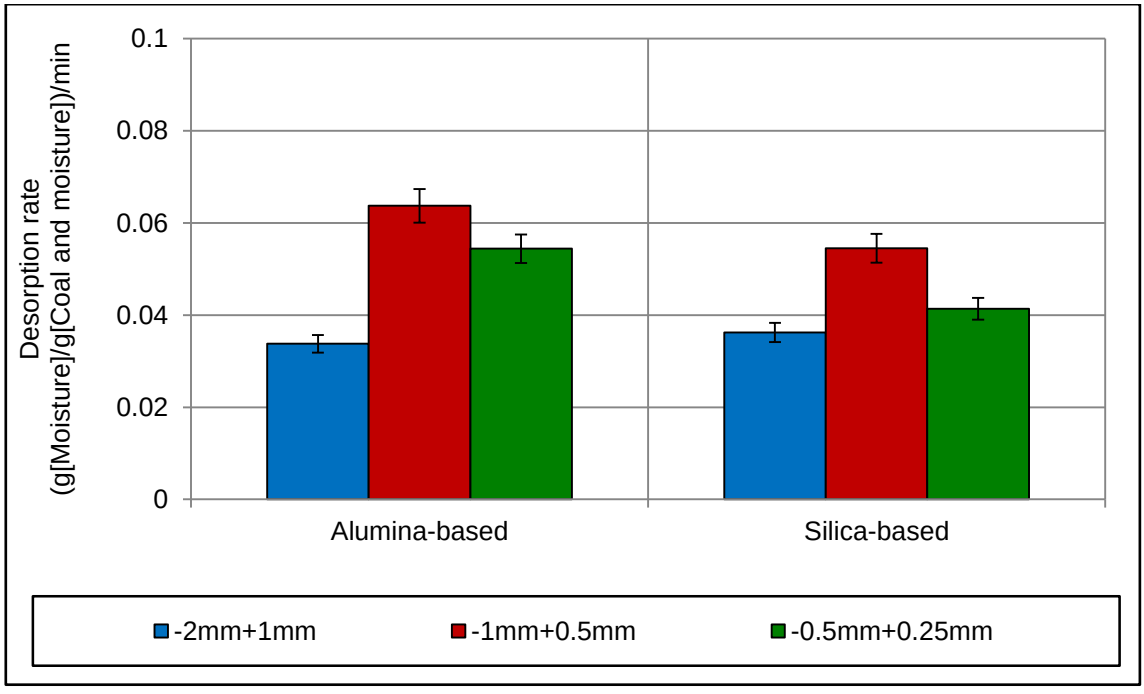

Figure B.3.19: Initial desorption rates of coal and 3mm adsorbents at an adsorbent to coal mass ratio of 2:1

C

ANNEXURE

CASCADING-BED DRYING TECHNIQUE

Annexure C holds the results of the cascading-bed drying experiments.

- C.1 General adsorption and desorption curves
- C.2 Operating conditions
  - C.2.1 Influence of adsorbent to coal mass ratio
  - C.2.2 Influence of adsorbent type
  - C.2.3 Adsorbent size influence
  - C.2.4 Coal size influence
- C.3 Influence of motion
  - C.3.1 General desorption curves
  - C.3.2 Surface moisture and contact time

C.1 General adsorption and desorption curves

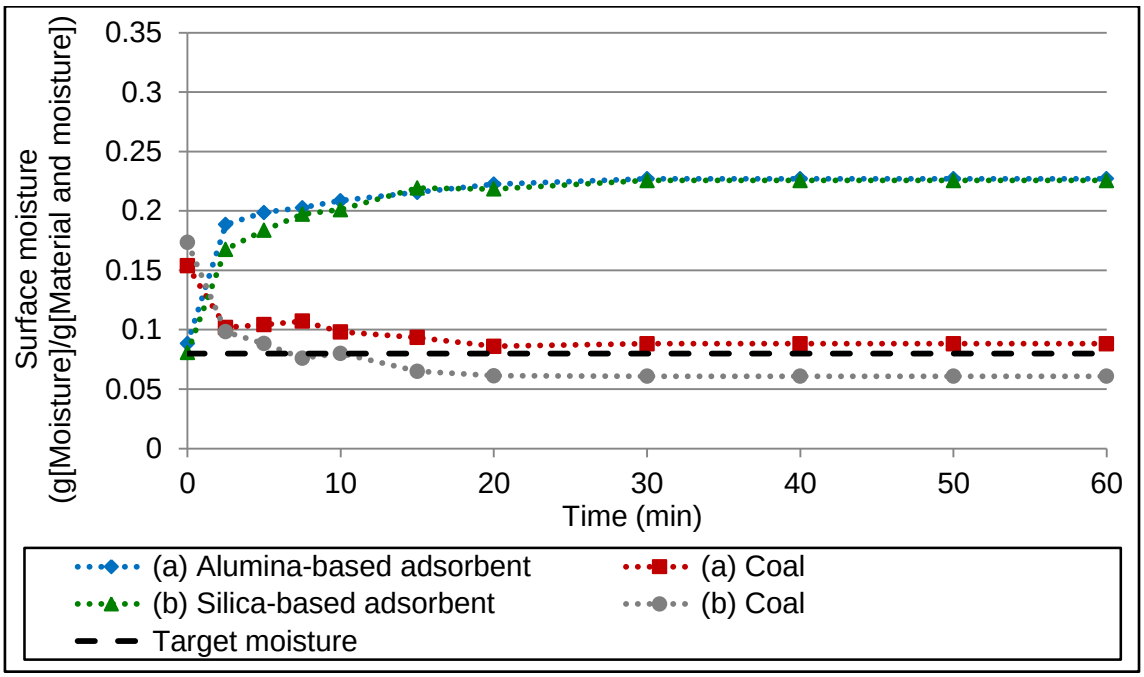

Figure C.1.1: Adsorption-desorption curves of -2mm+1mm coal and 5mm adsorbents at an adsorbent to coal mass ratio of 0.5:1

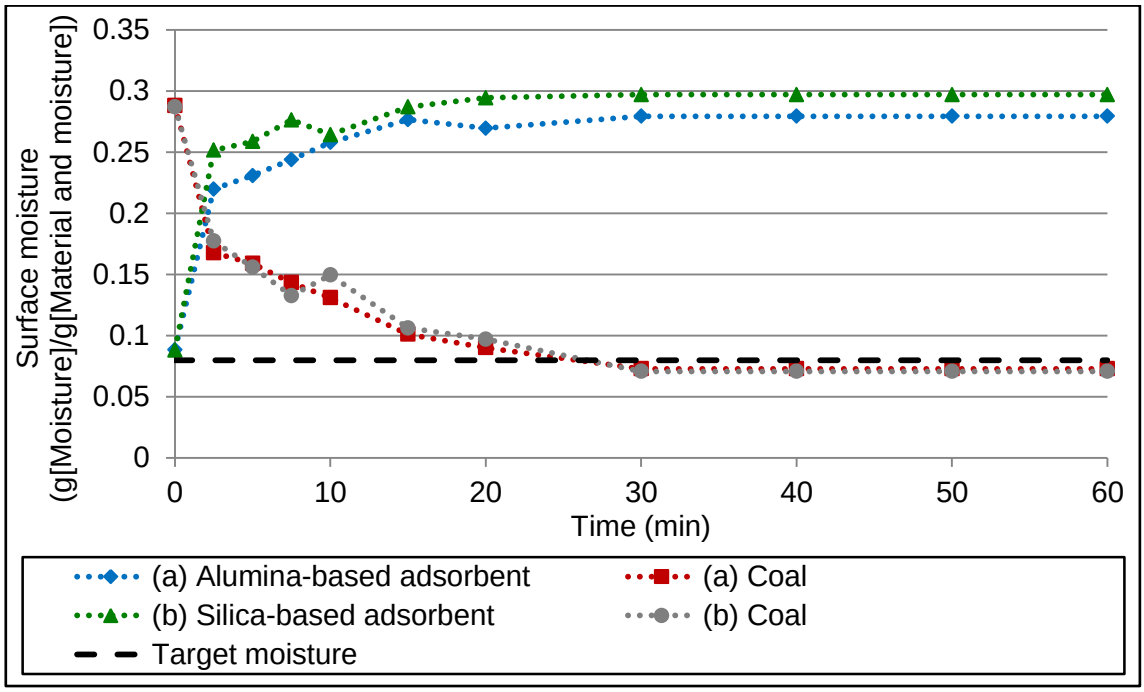

Figure C.1.2: Adsorption-desorption curves of -0.5mm+0.25mm coal and 5mm adsorbents at an adsorbent to coal mass ratio of 1:1

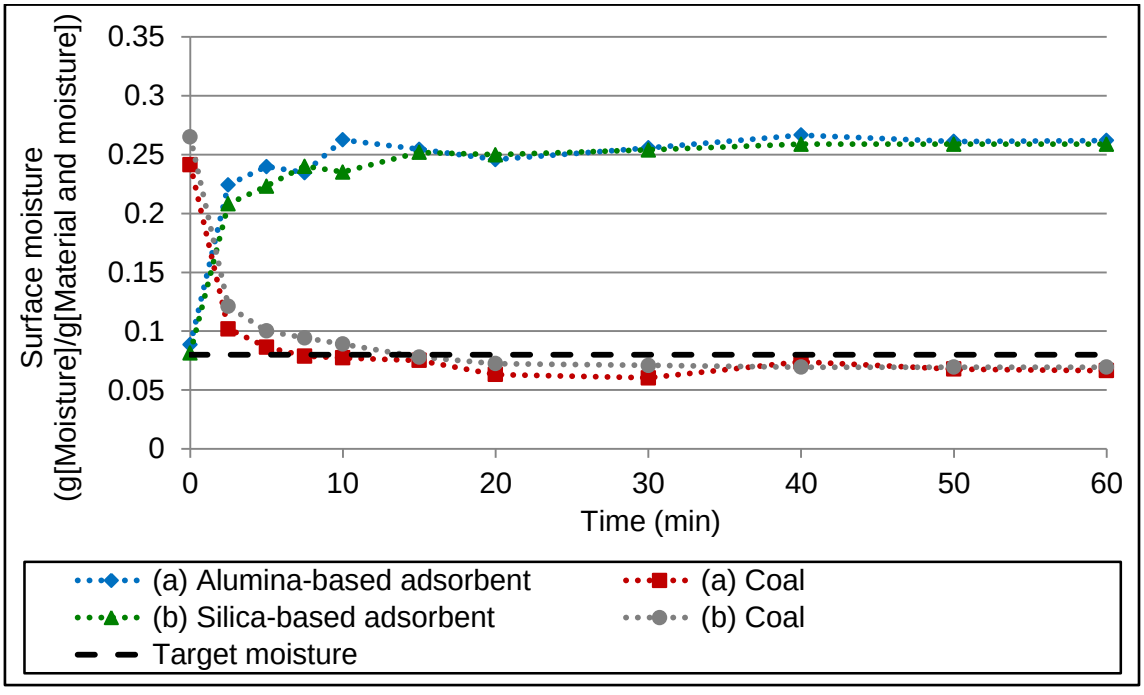

Figure C.1.3: Adsorption-desorption curves of -1mm+0.5mm coal and 3mm adsorbents at an adsorbent to coal mass ratio of 1:1

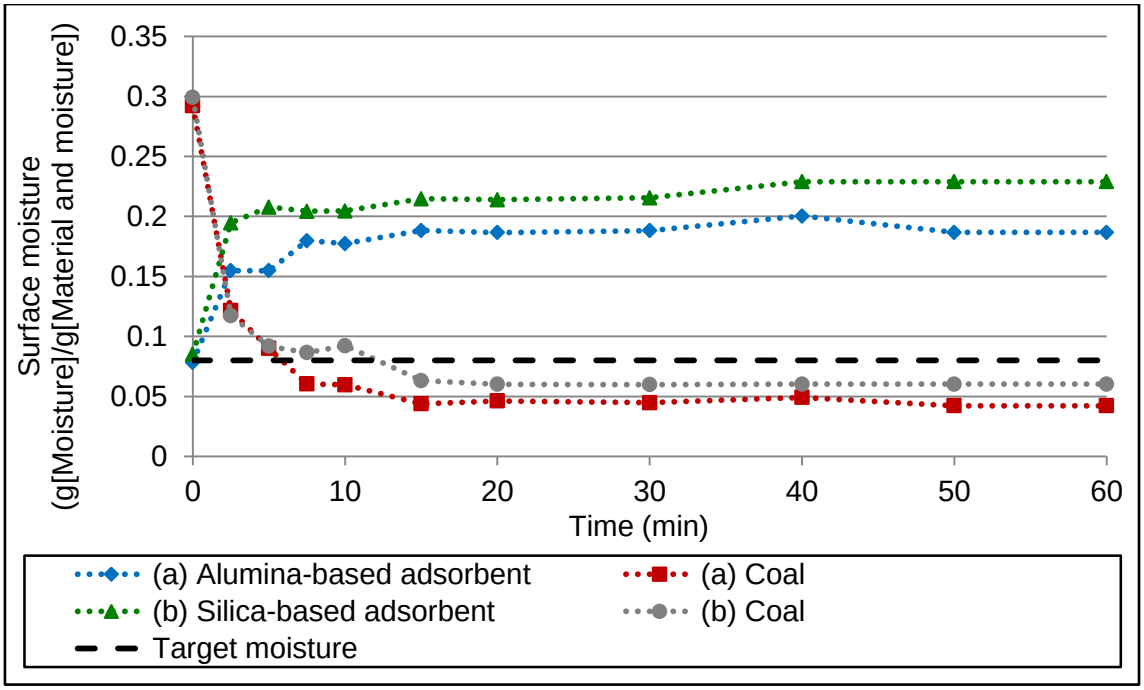

Figure C.1.4: Adsorption-desorption curves of -0.5mm+0.25mm coal and 3mm adsorbents at an adsorbent to coal mass ratio of 2:1

C.2 Operating conditions

C.2.1 Influence of adsorbent to coal mass ratio

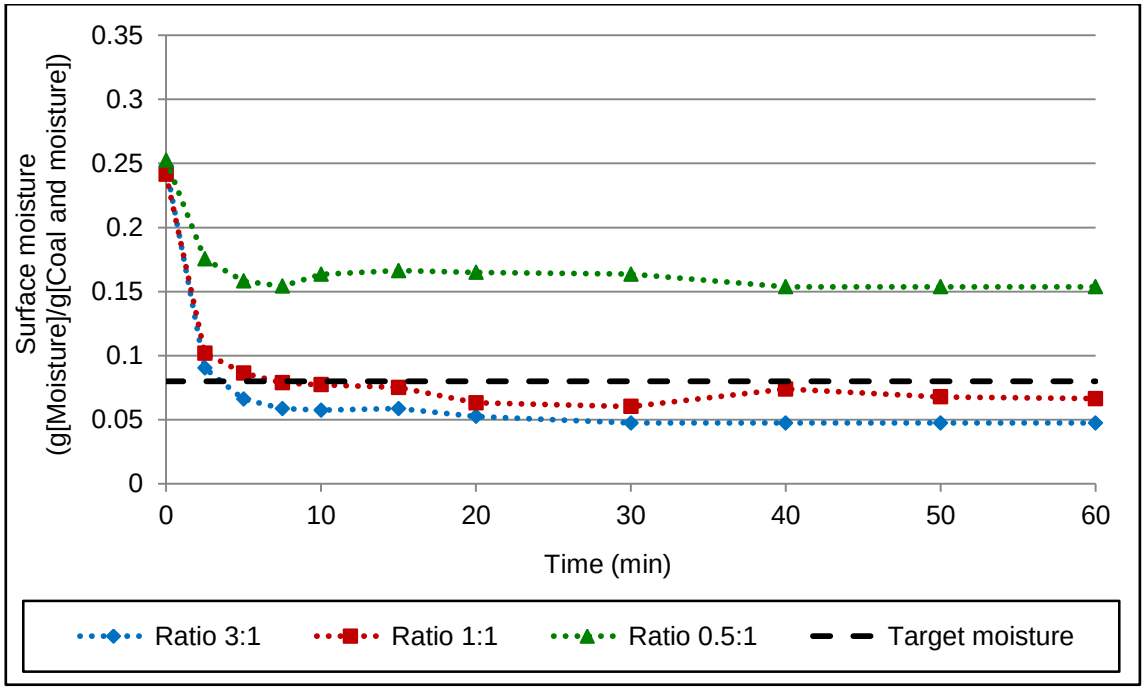

Figure C.2.1: Desorption curves of -1mm+0.5mm coal and 3mm alumina-based adsorbents

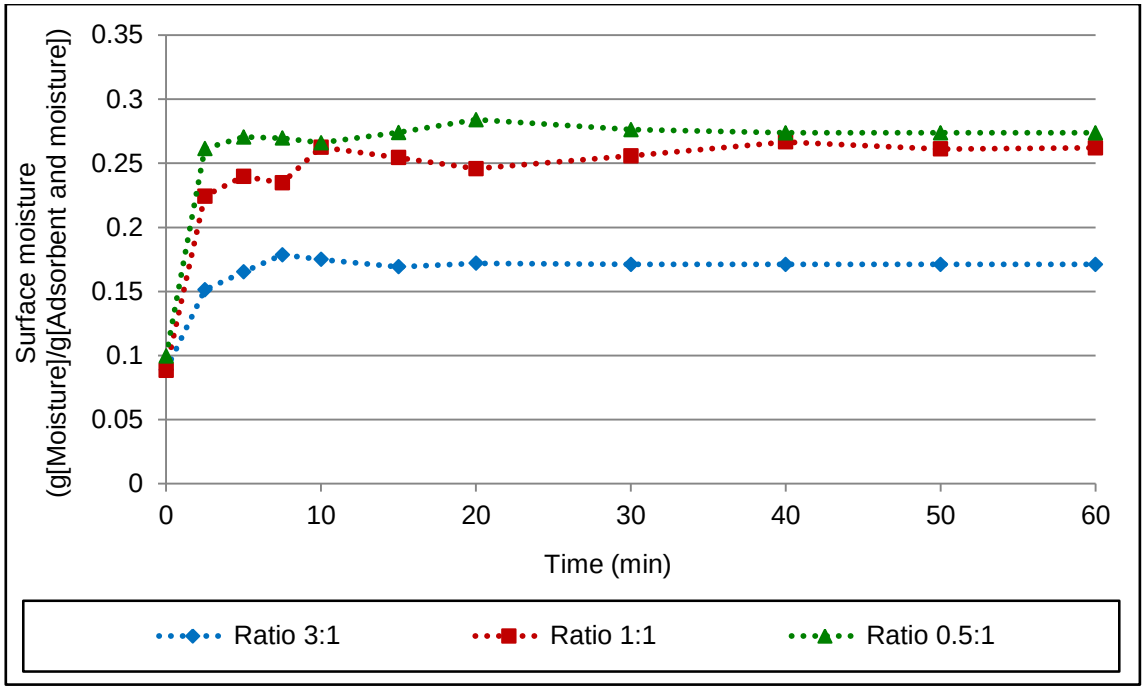

Figure C.2.2: Adsorption curves of 3mm alumina-based adsorbents and -1mm+0.5mm coal

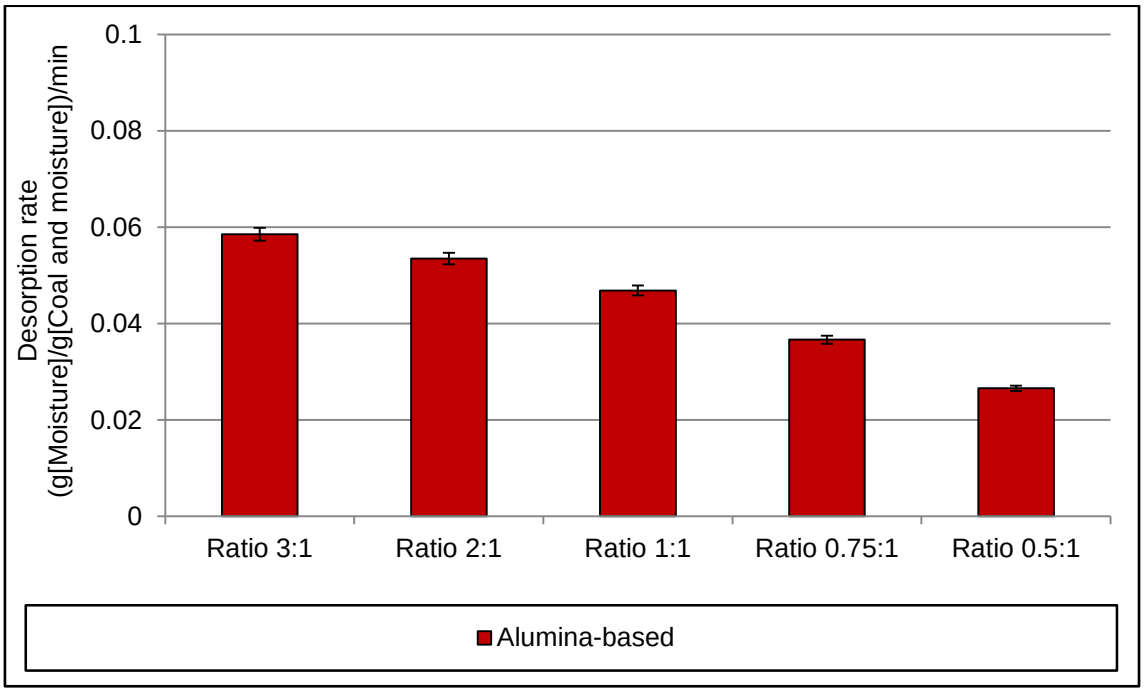

Figure C.2.3: Initial desorption rates of -1mm+0.5mm coal and 3mm alumina-based adsorbent

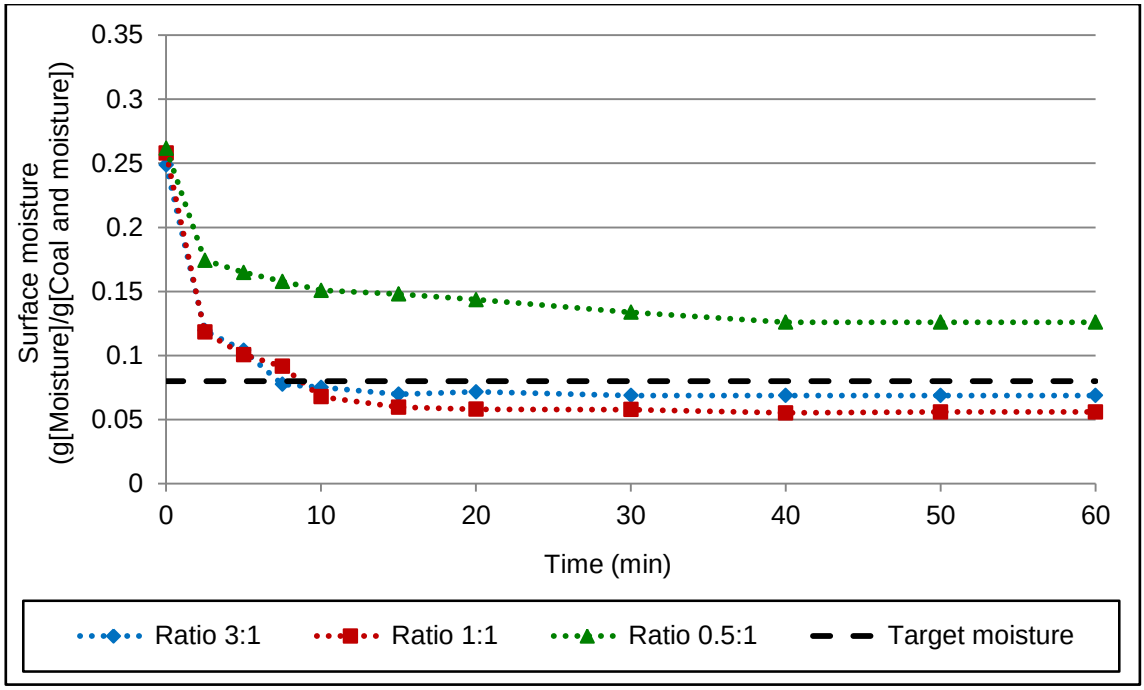

Figure C.2.4: Desorption curves of -1mm+0.5mm coal and 5mm silica-based adsorbents

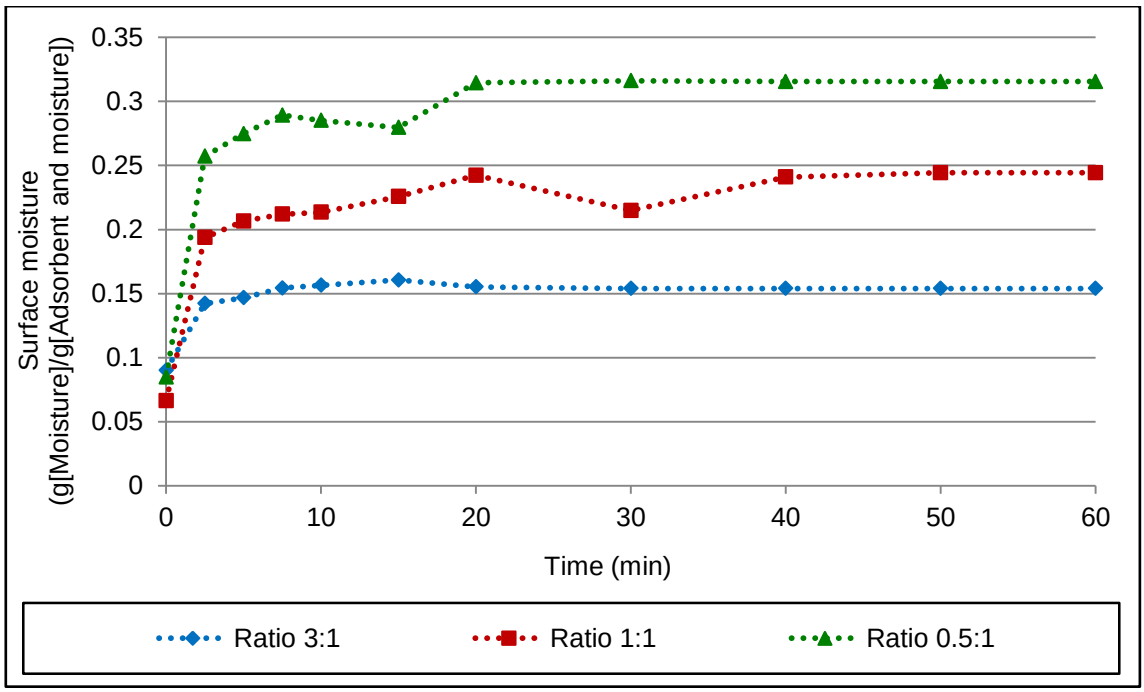

Figure C.2.5: Adsorption curves of 5mm silica-based adsorbents and -1mm+0.5mm coal

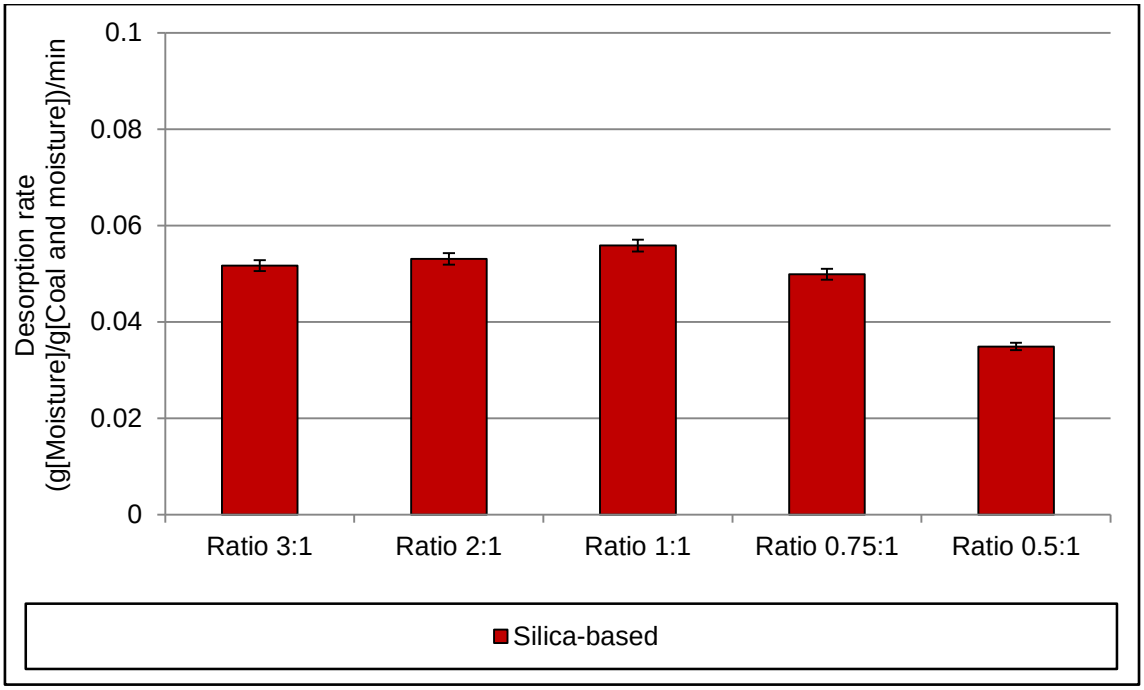

Figure C.2.6: Initial desorption rates of -1mm+0.5mm coal and 5mm silica-based adsorbent

C.2.2 Influence of adsorbent type

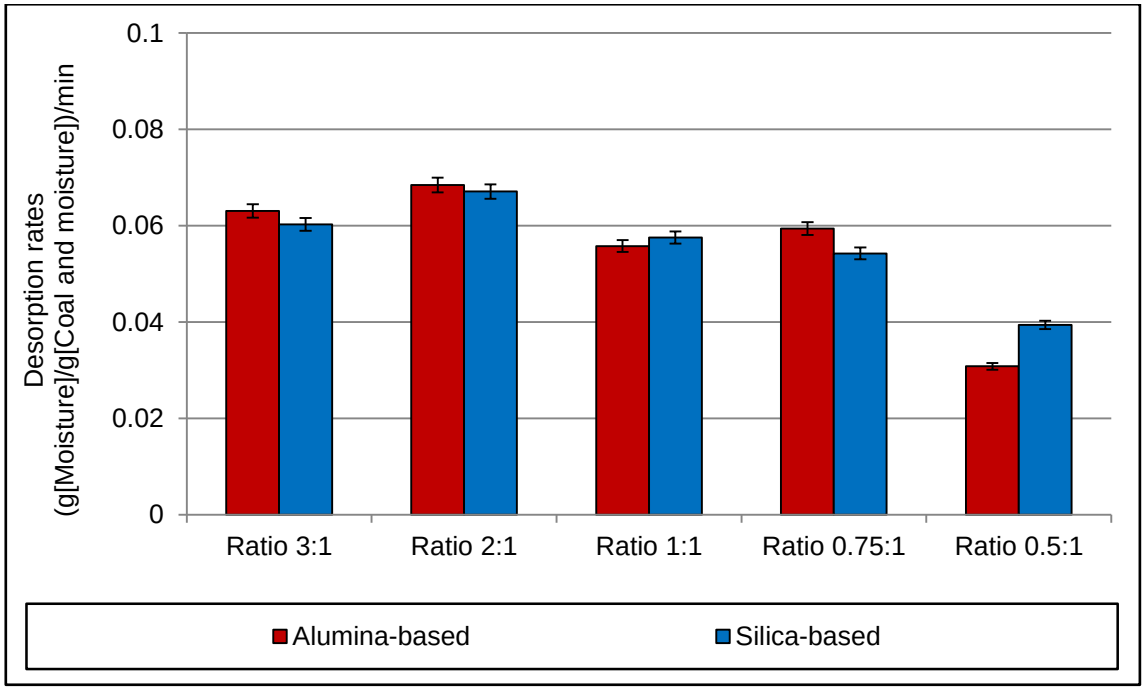

Figure C.2.7: Initial desorption rates of -1mm+0.5mm coal and 3mm adsorbents

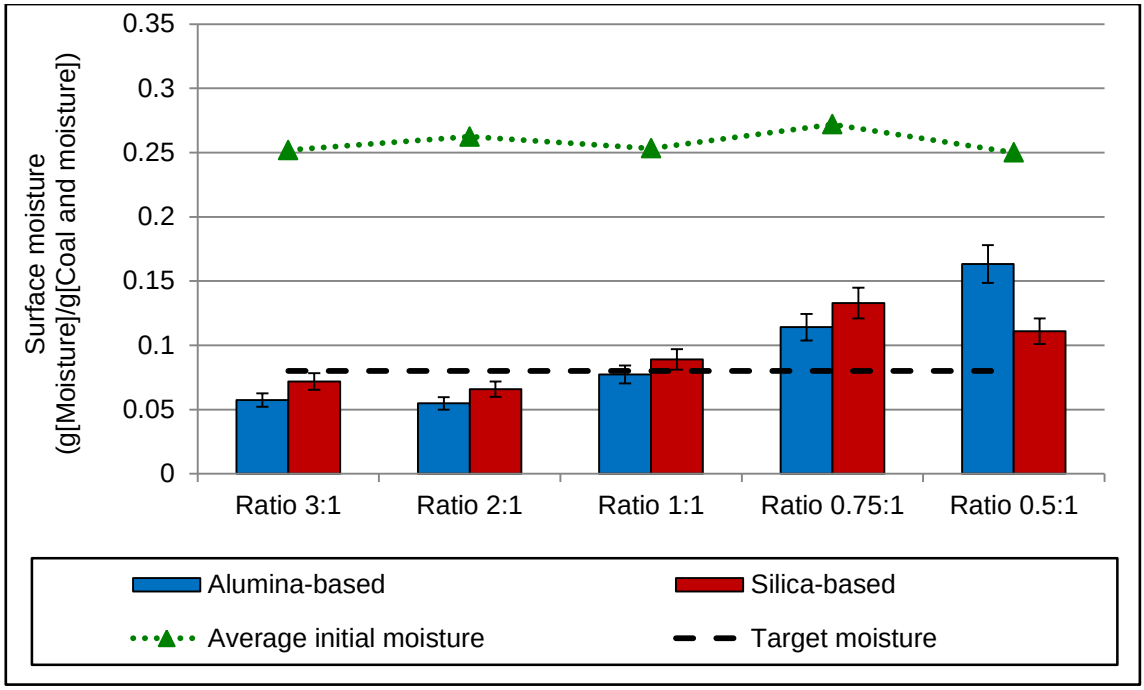

Figure C.2.8: Effect of 3mm adsorbent type on the final moisture loads of -1mm+0.5mm coal

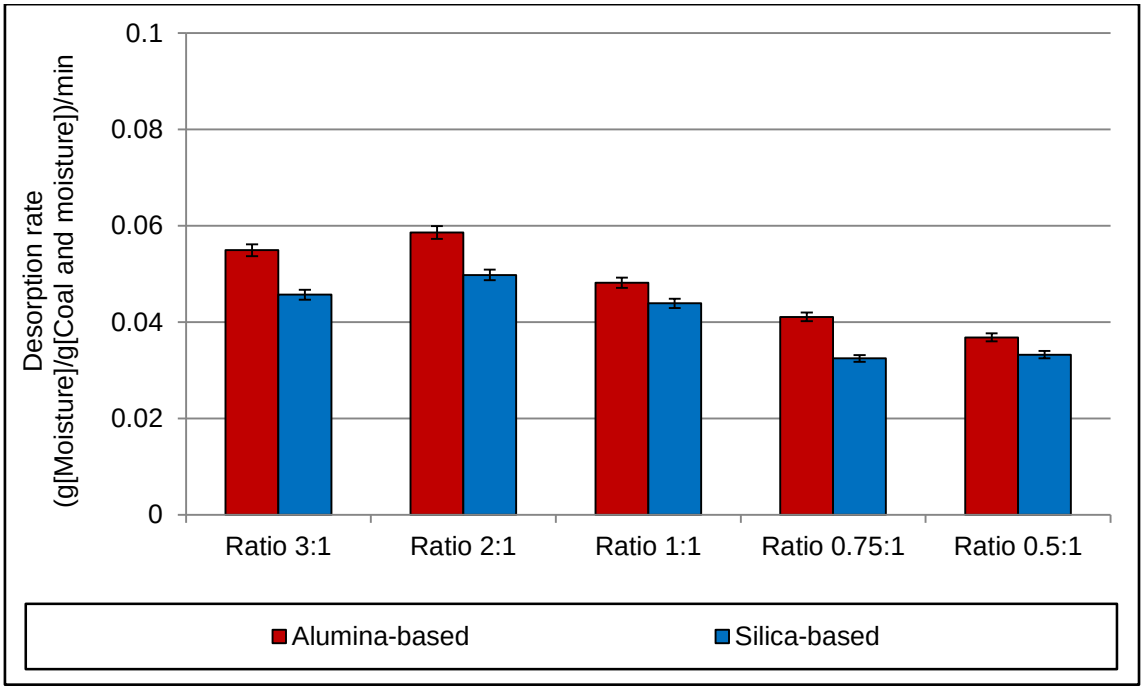

Figure C.2.9: Initial desorption rates of -0.5mm+0.25mm coal and 5mm adsorbents

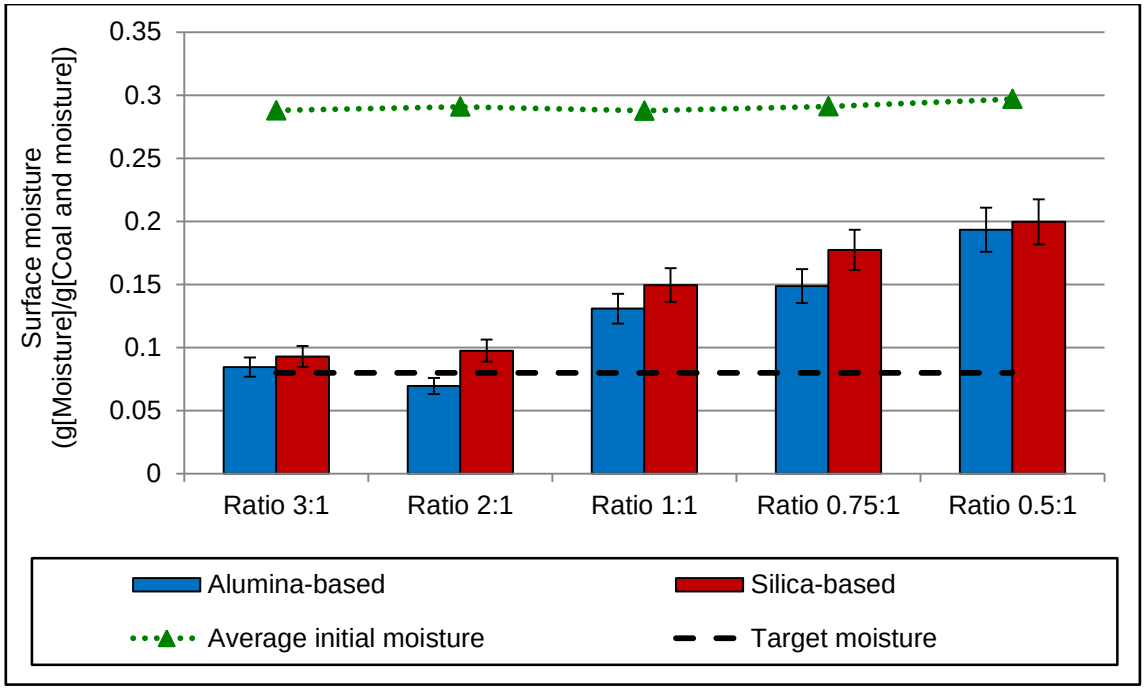

Figure C.2.10: Effect of 5mm adsorbent type on the final moisture loads of -0.5mm+0.25mm coal

C.2.3 Influence of adsorbent size

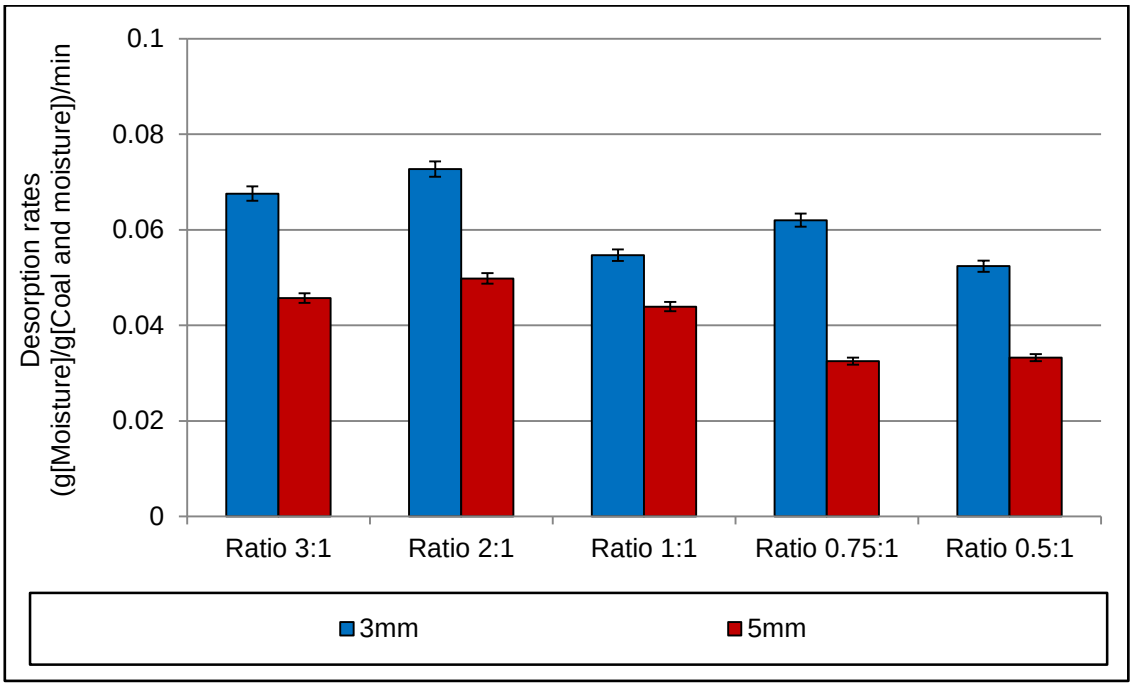

Figure C.2.11: Initial desorption rates of -0.5mm+0.25mm coal and silica-based adsorbents

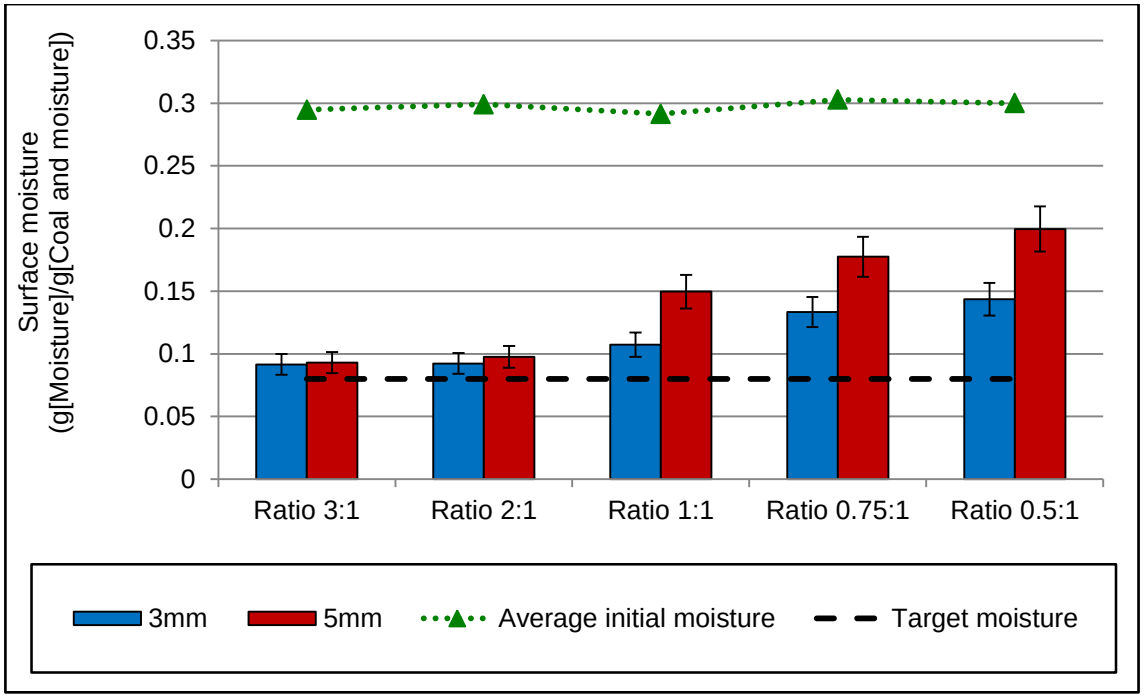

Figure C.2.12: Effect of silica-based adsorbent size on final surface moisture content of -0.5mm+0.25mm coal

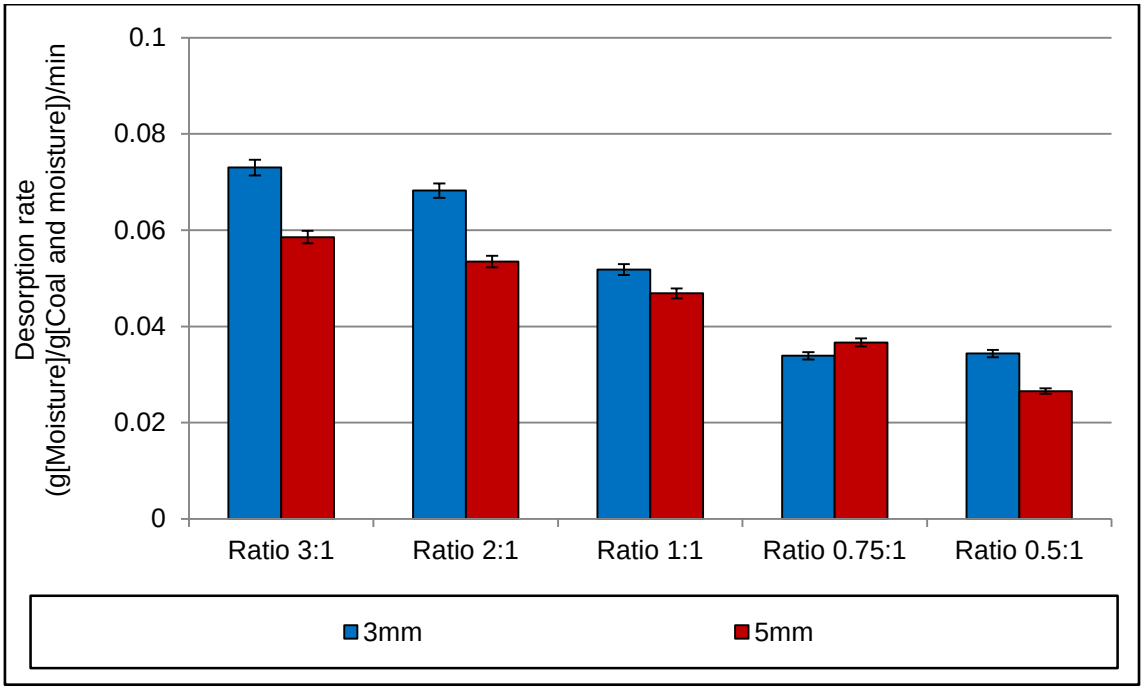

Figure C.2.13: Initial desorption rates of -0.5mm+0.25mm coal and alumina-based adsorbents

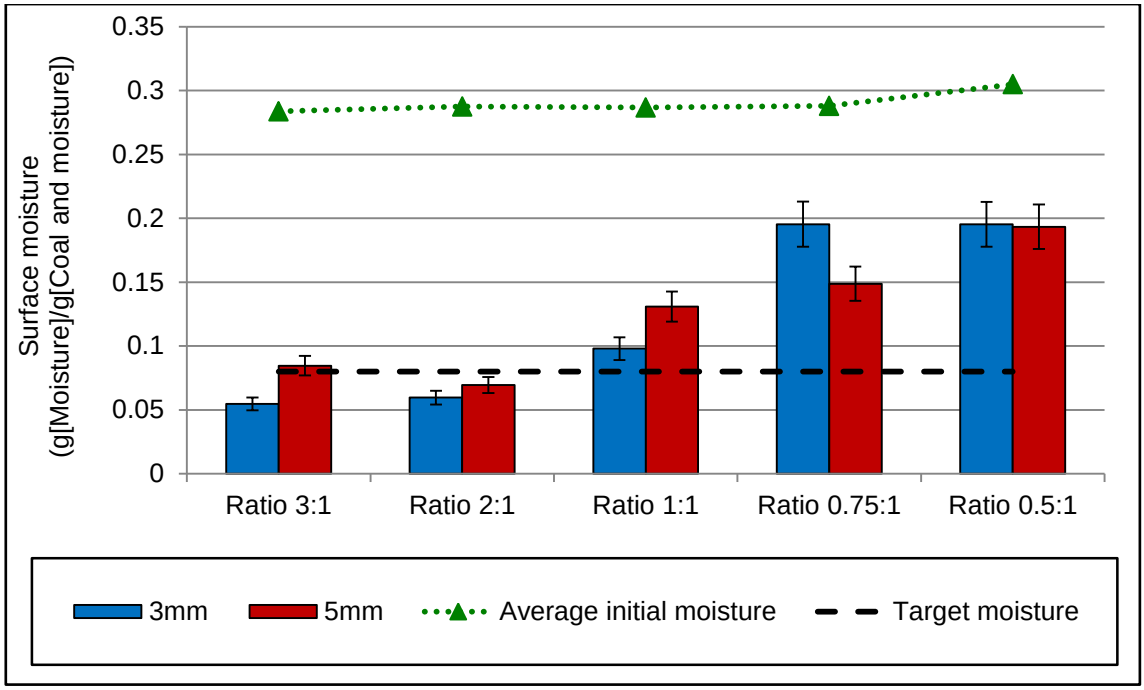

Figure C.2.14: Effect of alumina-based adsorbent size on final surface moisture content of -0.5mm+0.25mm coal

C.2.4 Influence of coal particle size

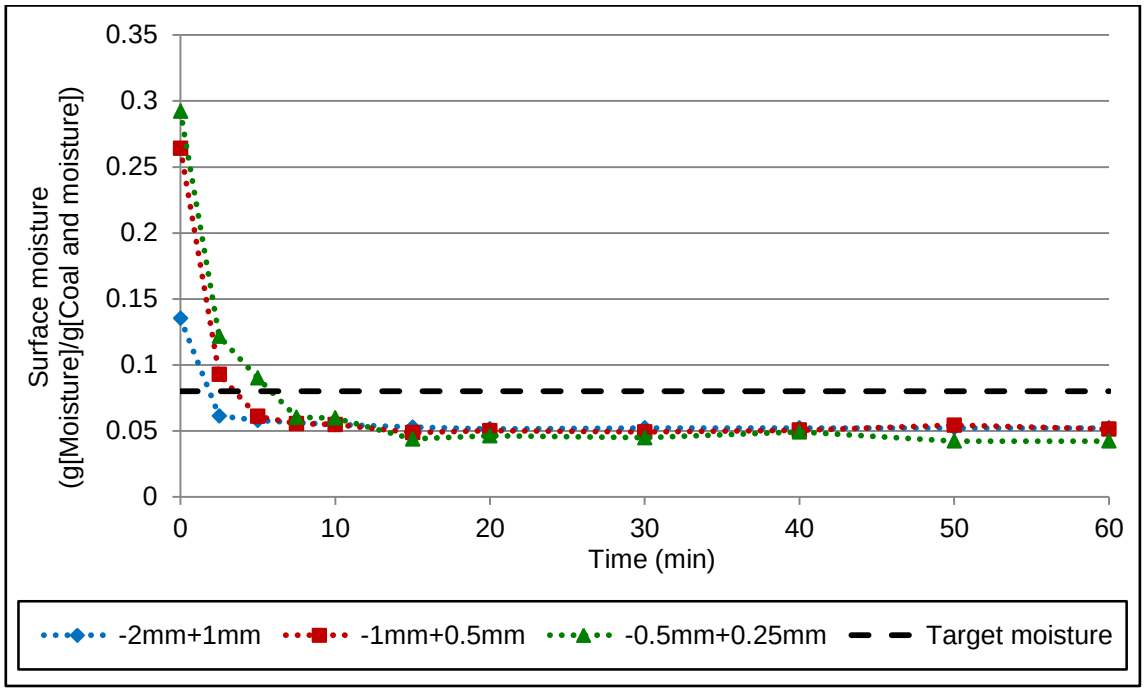

Figure C.2.15: Desorption curves of coal and 3mm alumina-based adsorbents at an adsorbent to coal mass ratio of 2:1

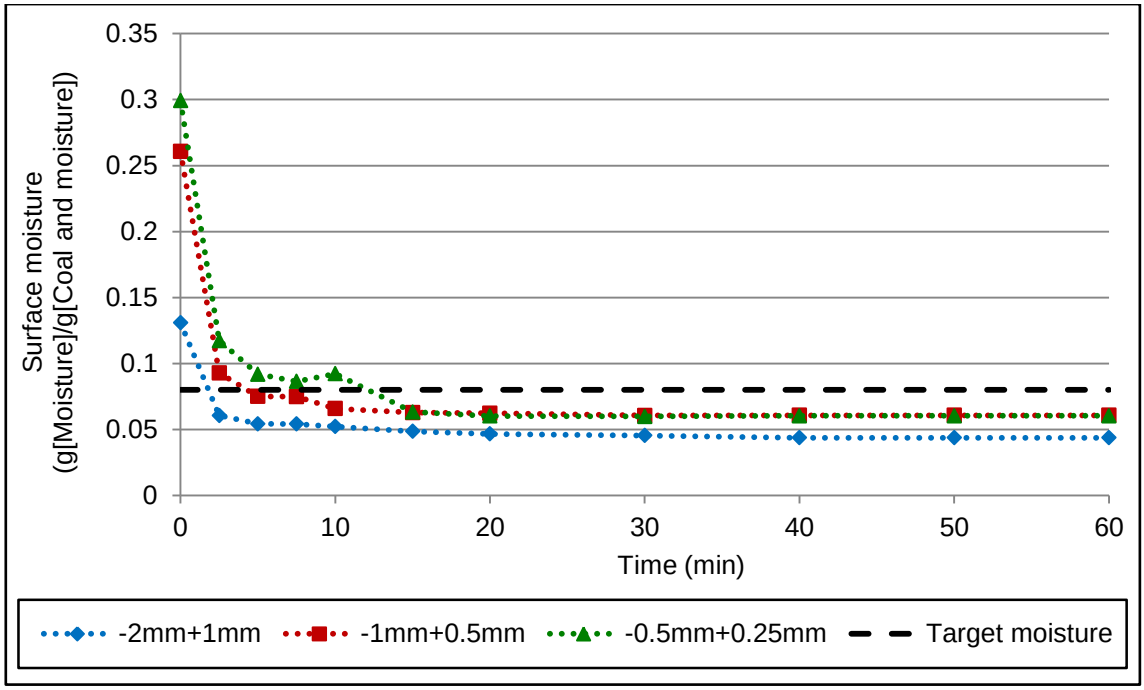

Figure C.2.16: Desorption curves of coal and 3mm silica-based adsorbents at an adsorbent to coal mass ratio of 2:1

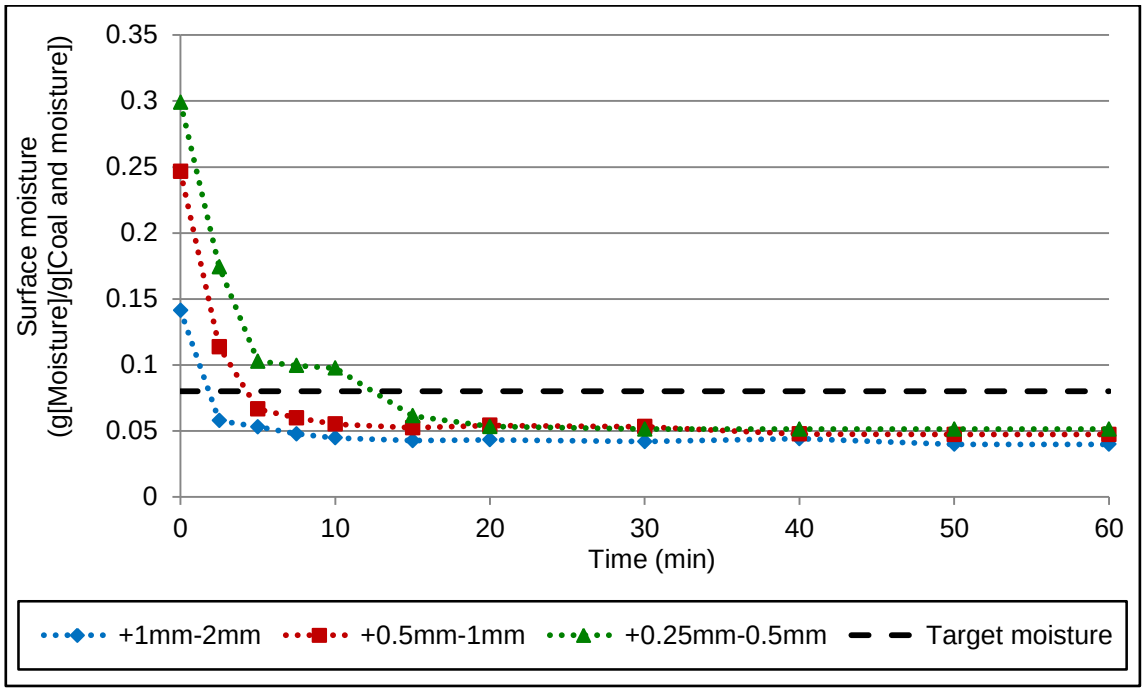

Figure C.2.17: Desorption curves of coal and 5mm silica-based adsorbents at an adsorbent to coal mass ratio of 2:1

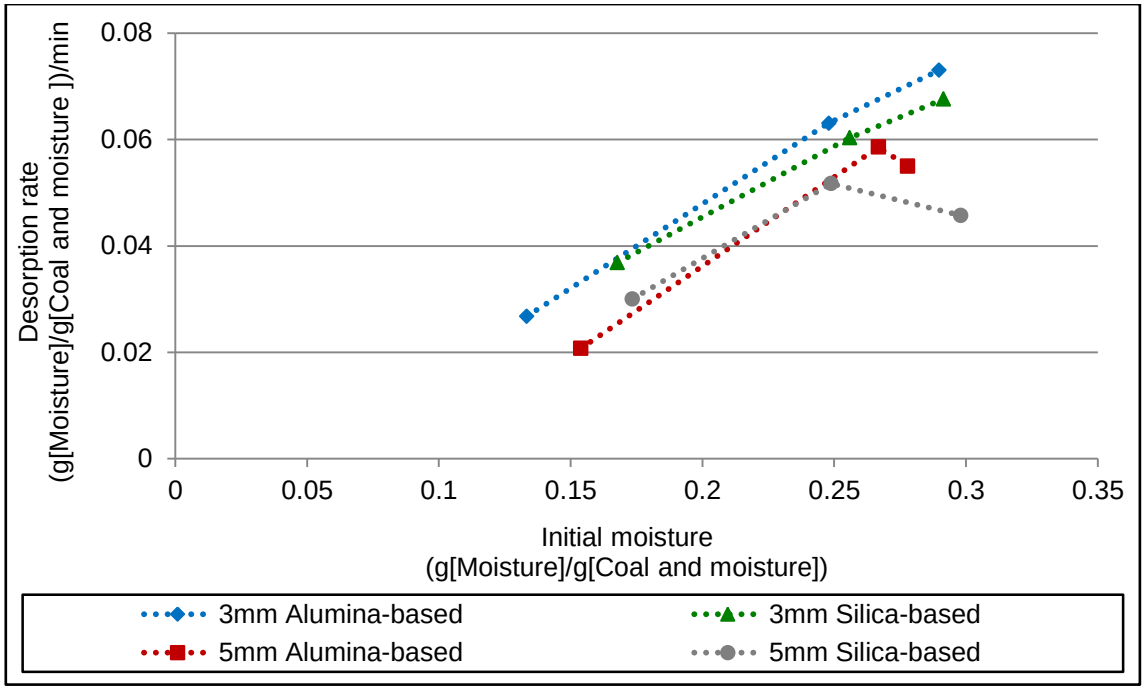

Figure C.2.18: Initial desorption rates of coal at an adsorbent to coal mass ratio of 3:1

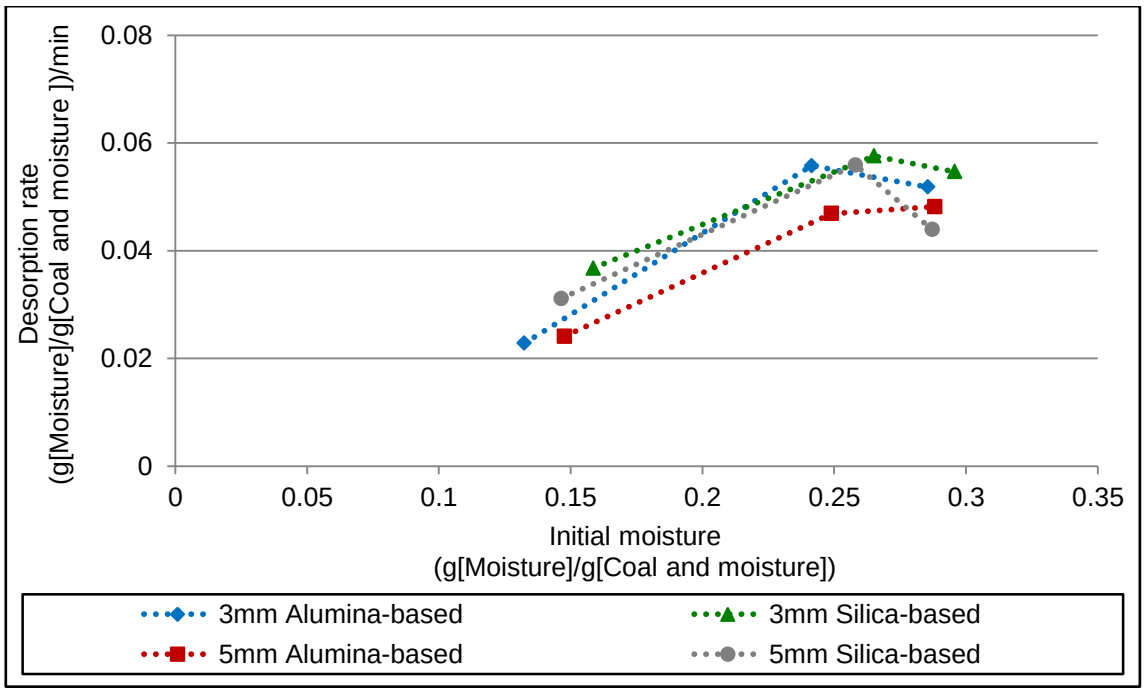

Figure C.2.19: Initial desorption rates of coal at an adsorbent to coal mass ratio of 1:1

C.3 Influence of motion

C.3.1 General desorption curves

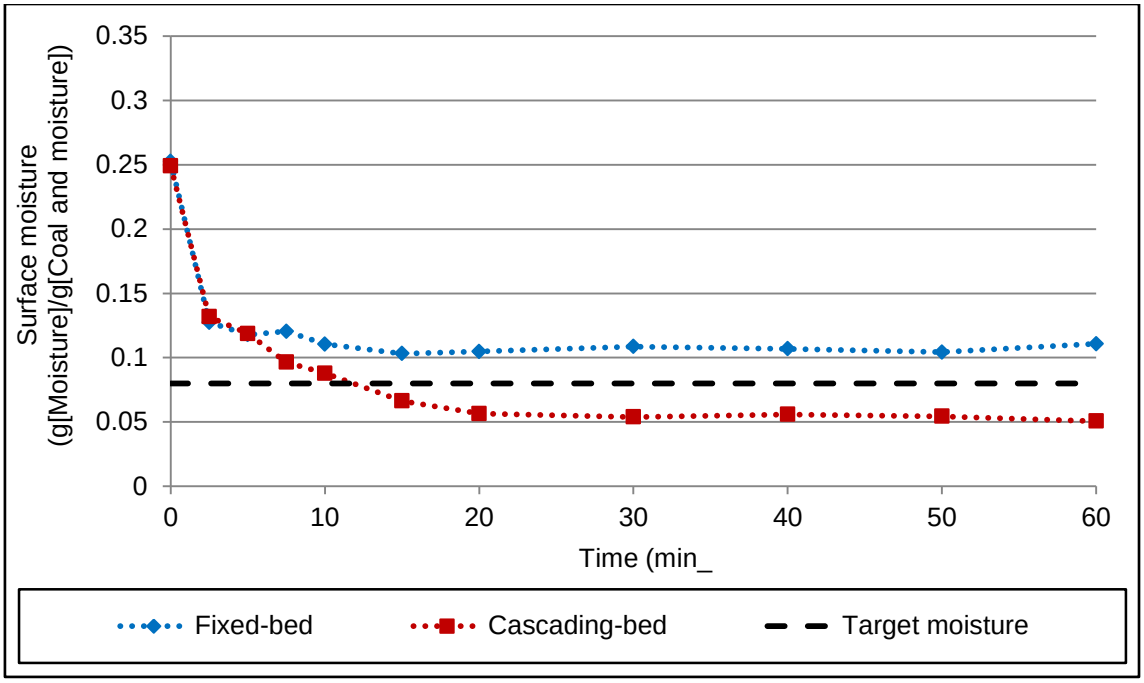

Figure C.3.1: Desorption curves of -1mm+0.5mm coal and 5mm alumina-based adsorbents at an adsorbent to coal mass ratio of 1:1

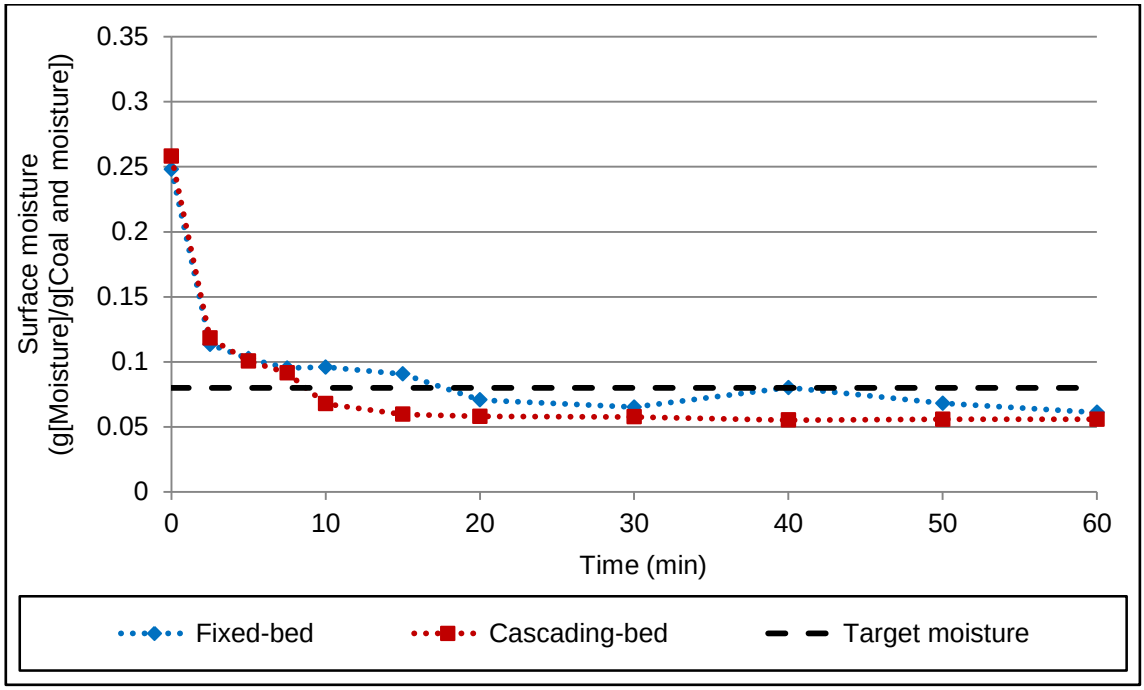

Figure C.3.2: Desorption curves of -1mm+0.5mm coal and 5mm silica-based adsorbents at an adsorbent to coal mass ratio of 1:1

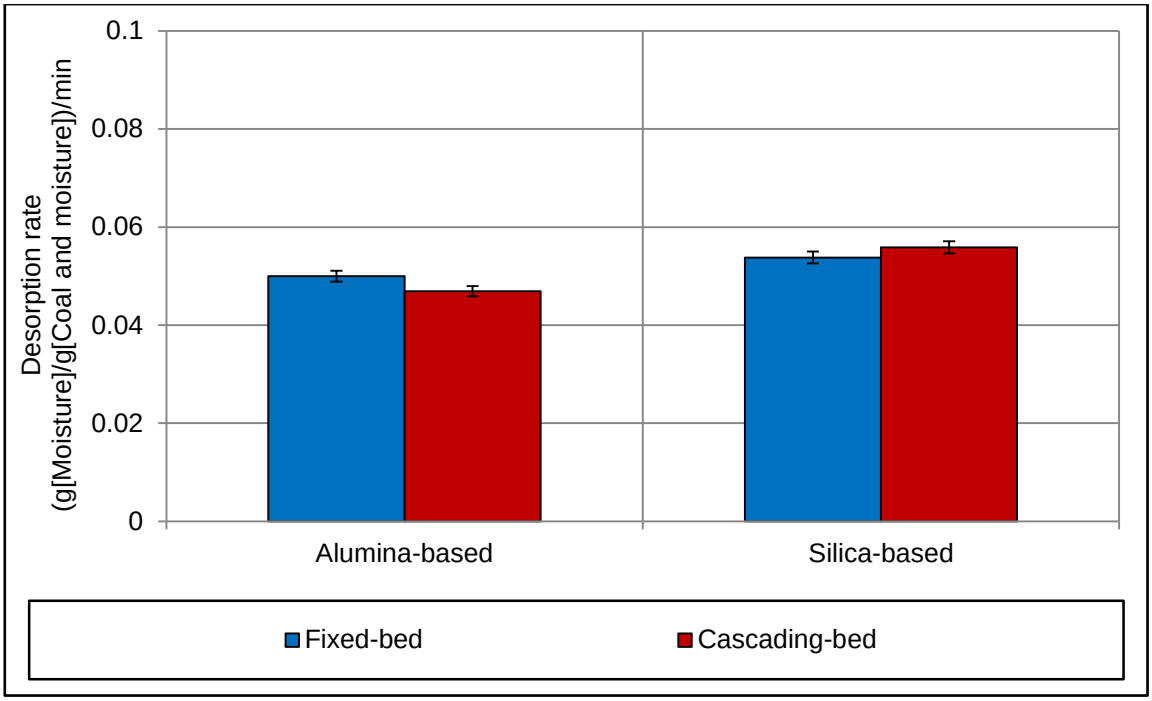

Figure C.3.3: Initial desorption rates of -1mm+0.5mm coal and 5mm adsorbents at an adsorbent to coal mass ratio of 1:1

C.3.2 Surface moisture and contact time

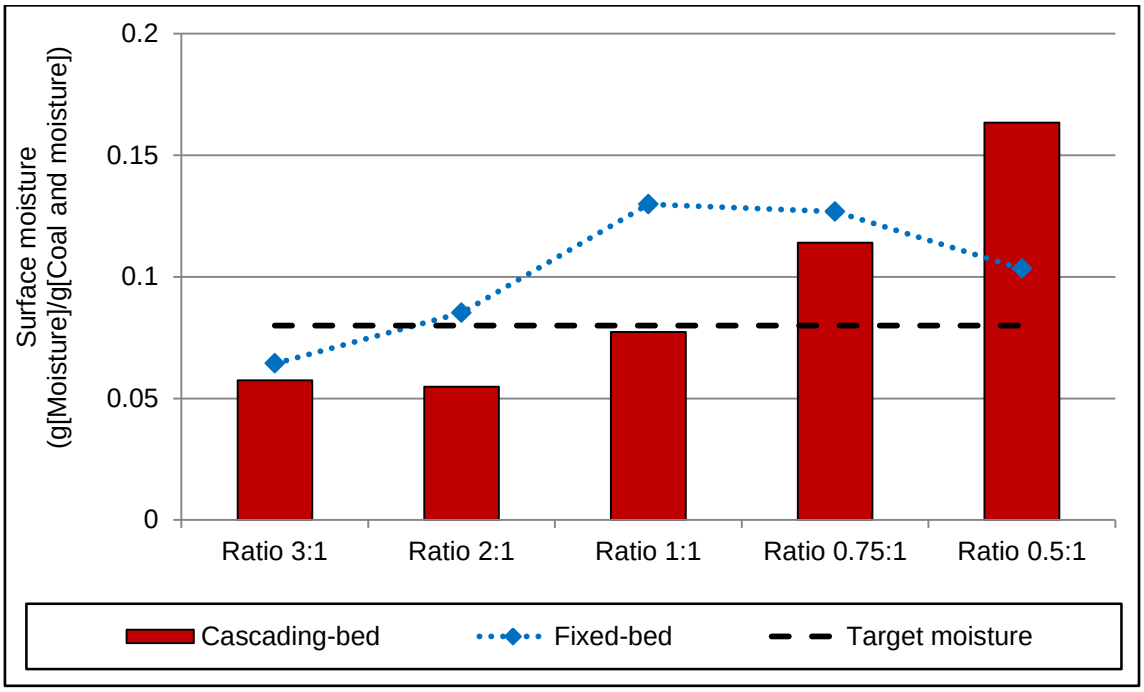

Figure C.3.4: Final moisture load of -1mm+0.5mm coal and 3mm alumina-based adsorbent

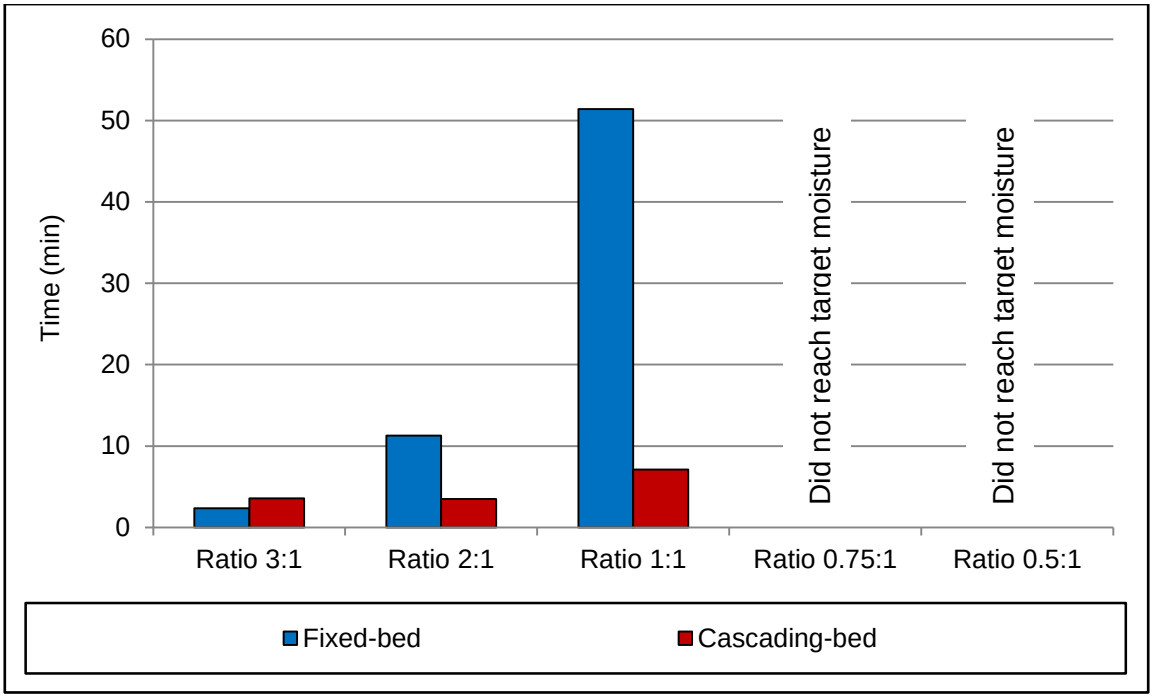

Figure C.3.5: 3mm alumina-based: Time required to dry -0.5mm+1mm coal to 0.08 g(moisture)/g(coal and moisture)

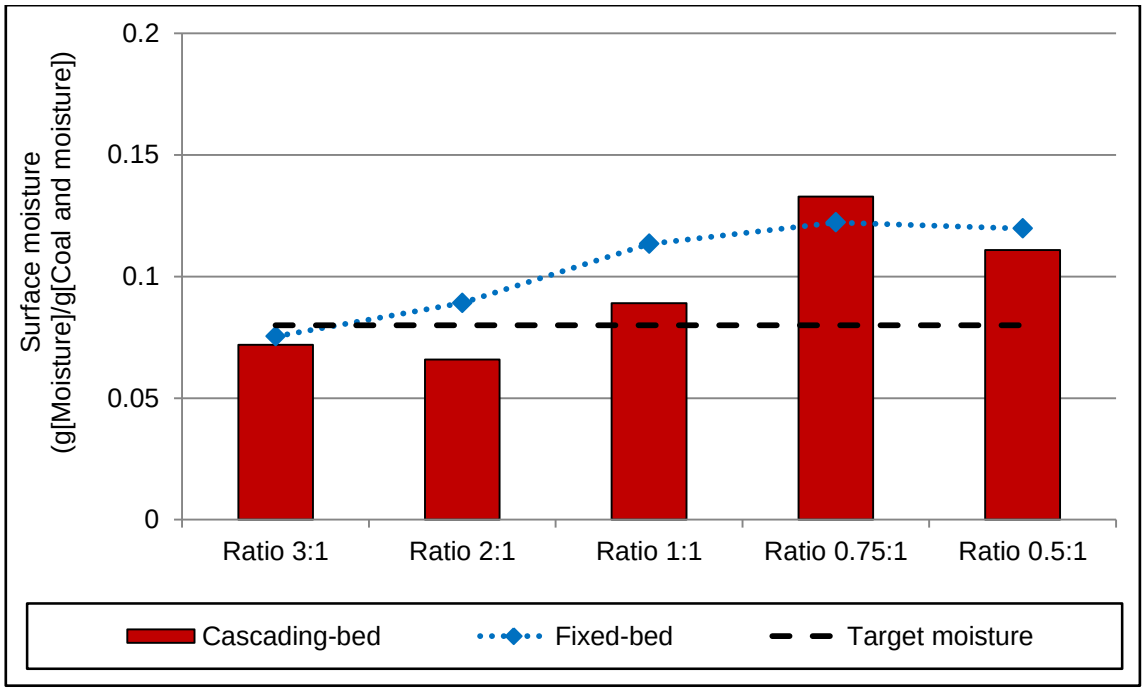

Figure C.3.6: Final moisture load of -1mm+0.5mm coal and 3mm silica-based adsorbent

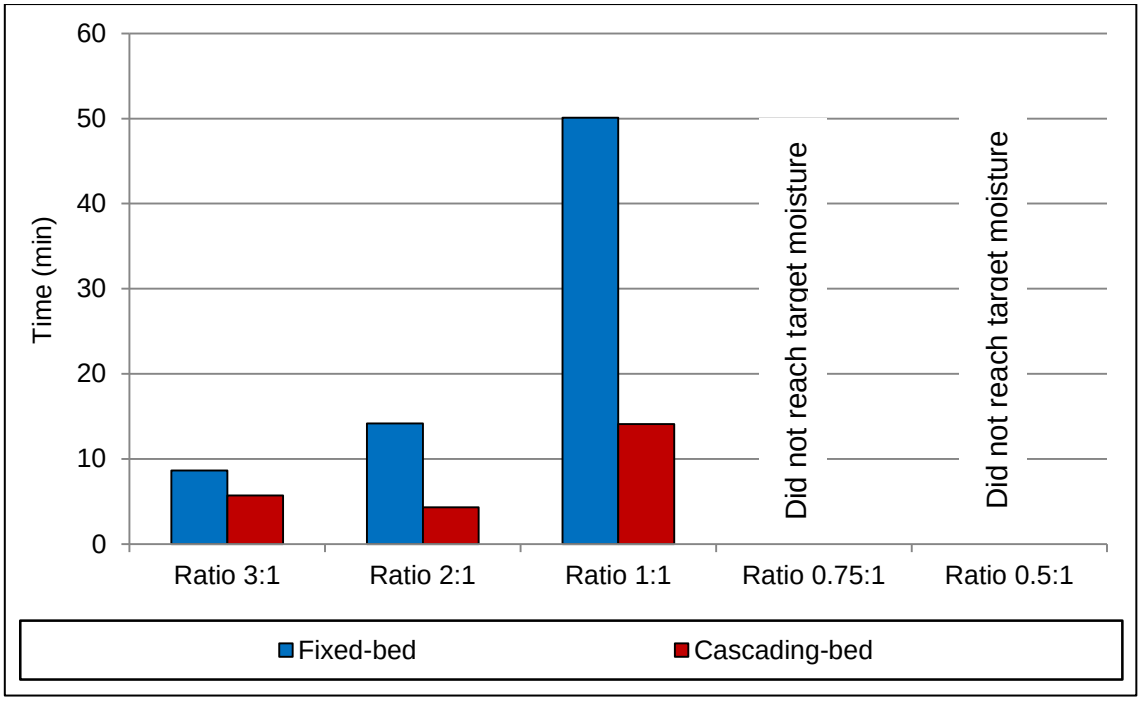

Figure C.3.7: 3mm silica-based: Time required to dry -0.5mm+1mm coal to 0.08 g(moisture)/g(coal and moisture)

D

ANNEXURE

INDUSTRIAL APPLICATION AND ENERGY CONSIDERATIONS

Annexure D holds additional results of industrial application and energy considerations

- D.1 Industrial application
  - D.1.1 Reuse of adsorbents
  - D.1.2 Adsorbent regeneration
- D.2. Energy considerations
  - D.2.1 Energy consumption
  - D.2.2 Total energy required
  - D.2.3 Coal drying technologies

D.1 Industrial application

D.1.1 Reuse of adsorbents

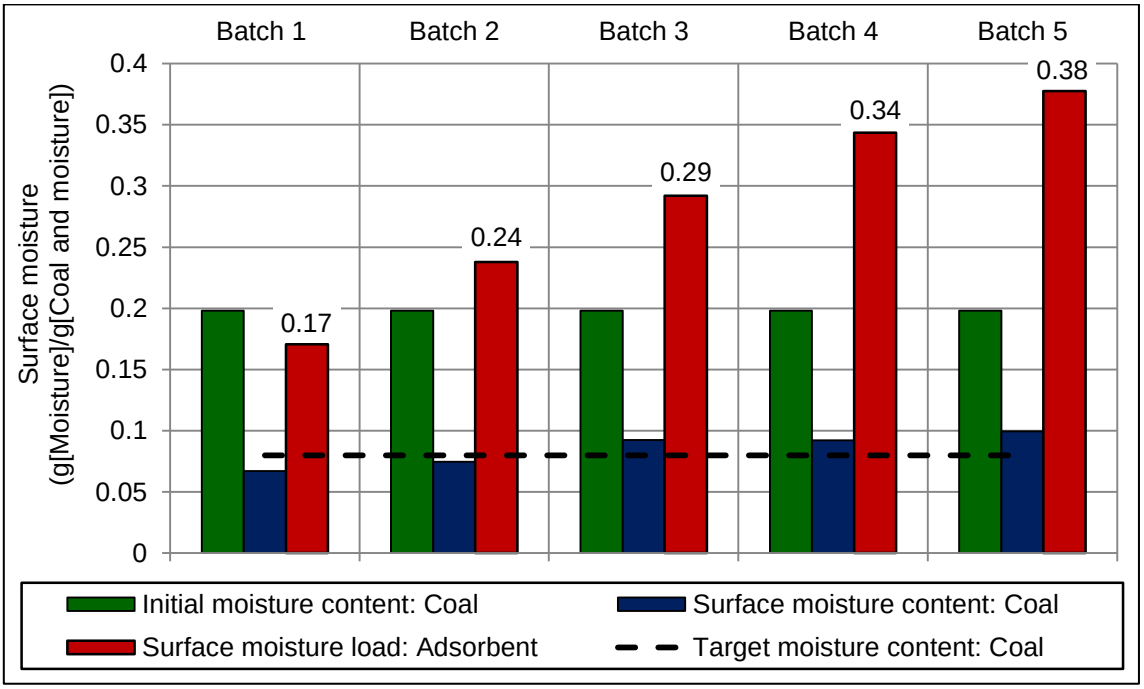

Figure D.1.1: Surface moisture content of -2mm+1mm coal and 5mm alumina-based adsorbent at an adsorbent to coal mass ratio of 2:1

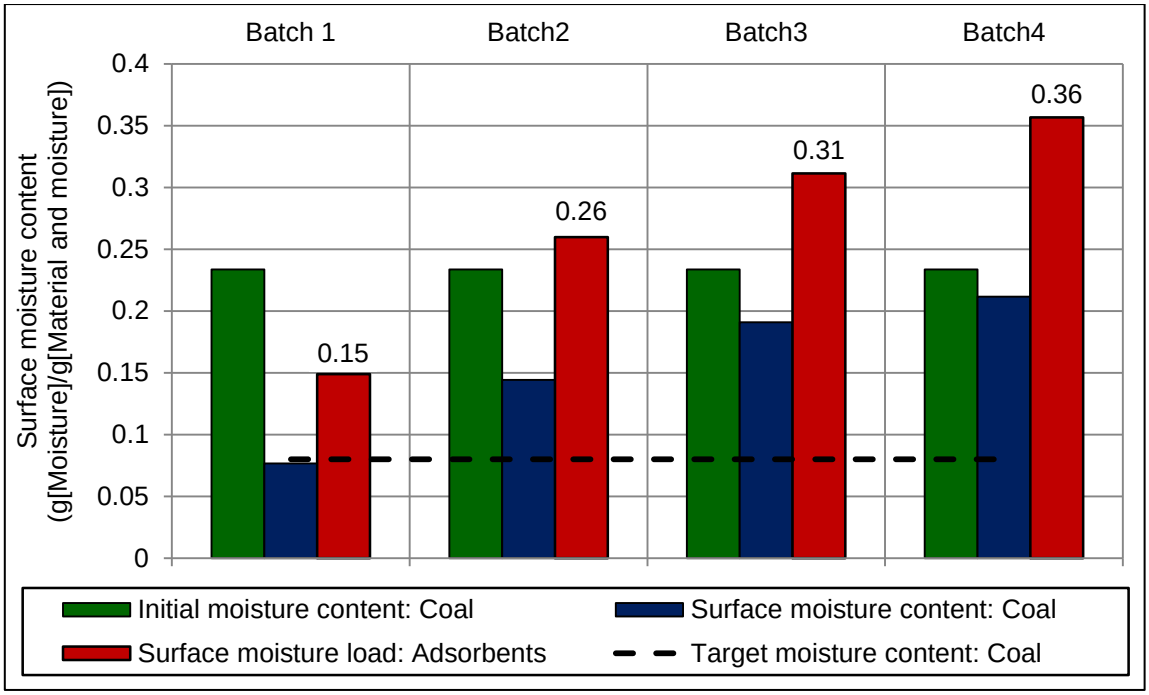

Figure D.1.2: Surface moisture content of -2mm+0.25mm coal and 3mm alumina-based adsorbent at an adsorbent to coal mass ratio of 1:1

D.1.2 Adsorbent regeneration

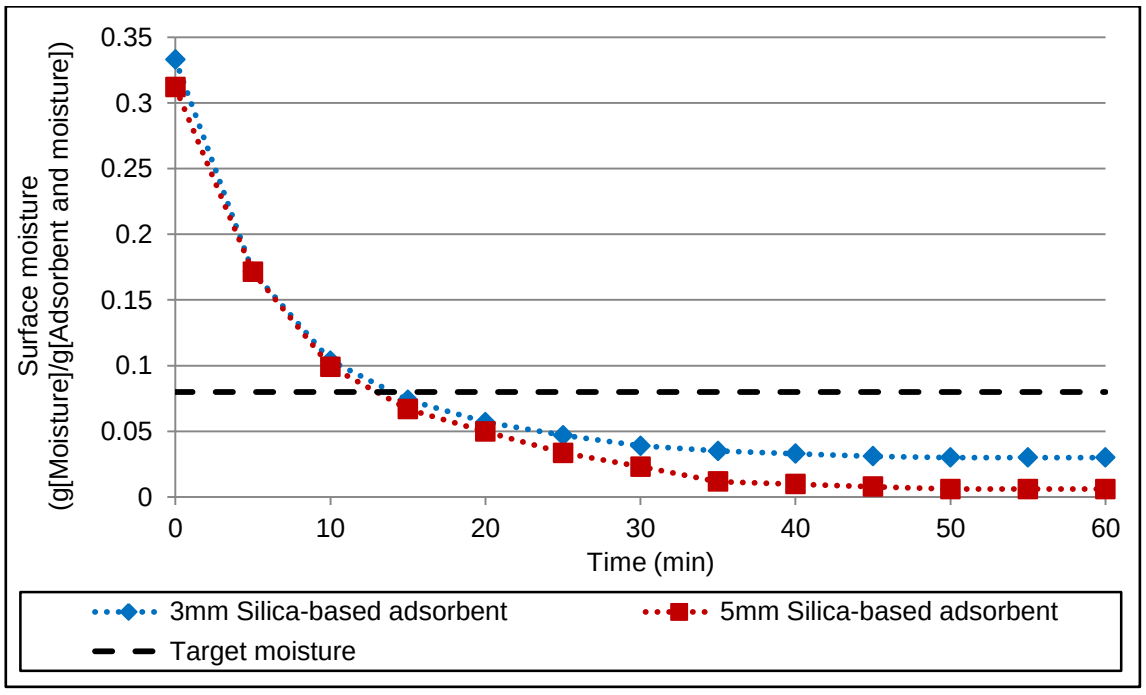

Figure D.1.3: Regeneration curves of silica-based adsorbents

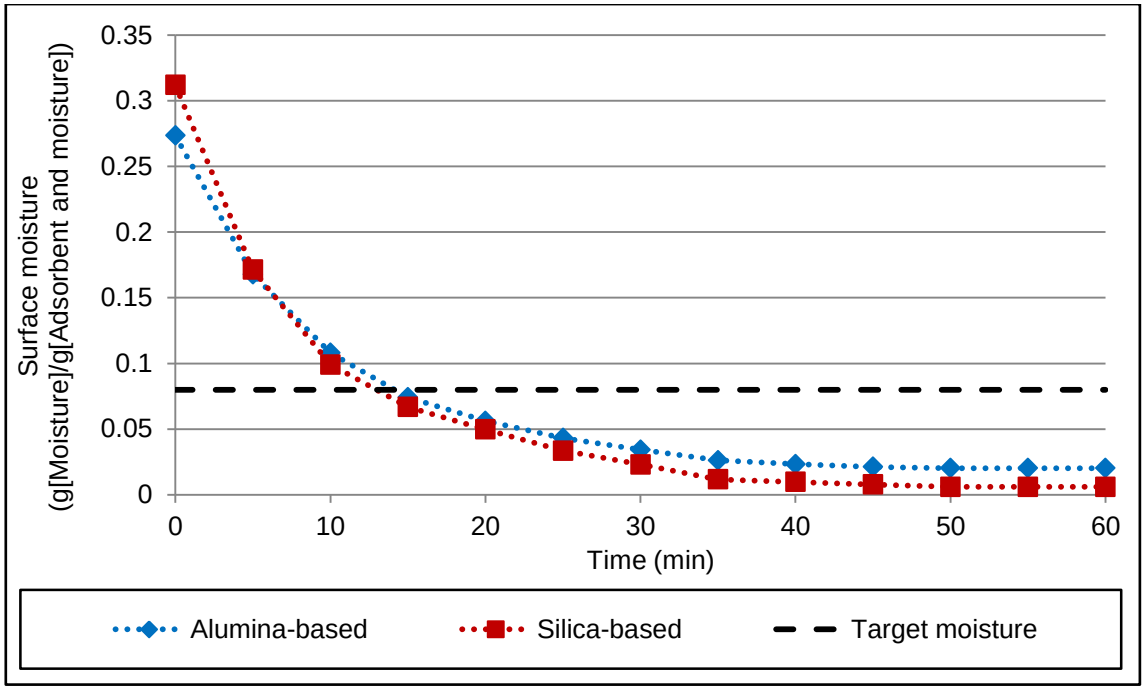

Figure D.1.4: Regeneration curves of 5mm adsorbents

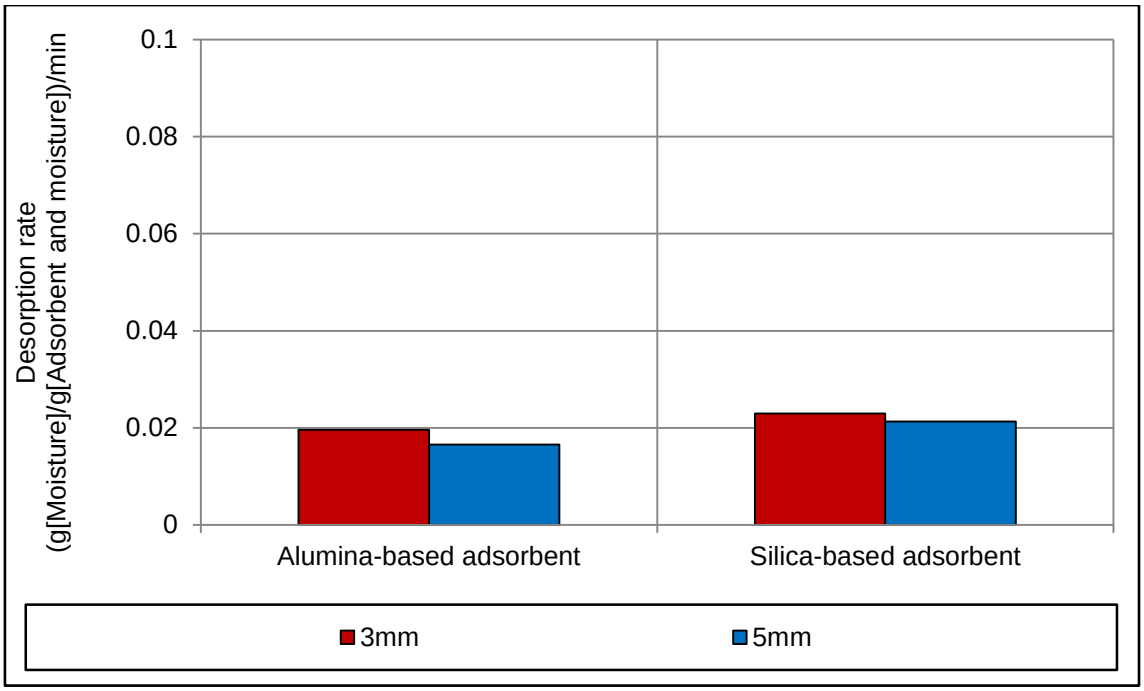

Figure D.1.5: Desorption rates of silica-based and alumina-based adsorbents

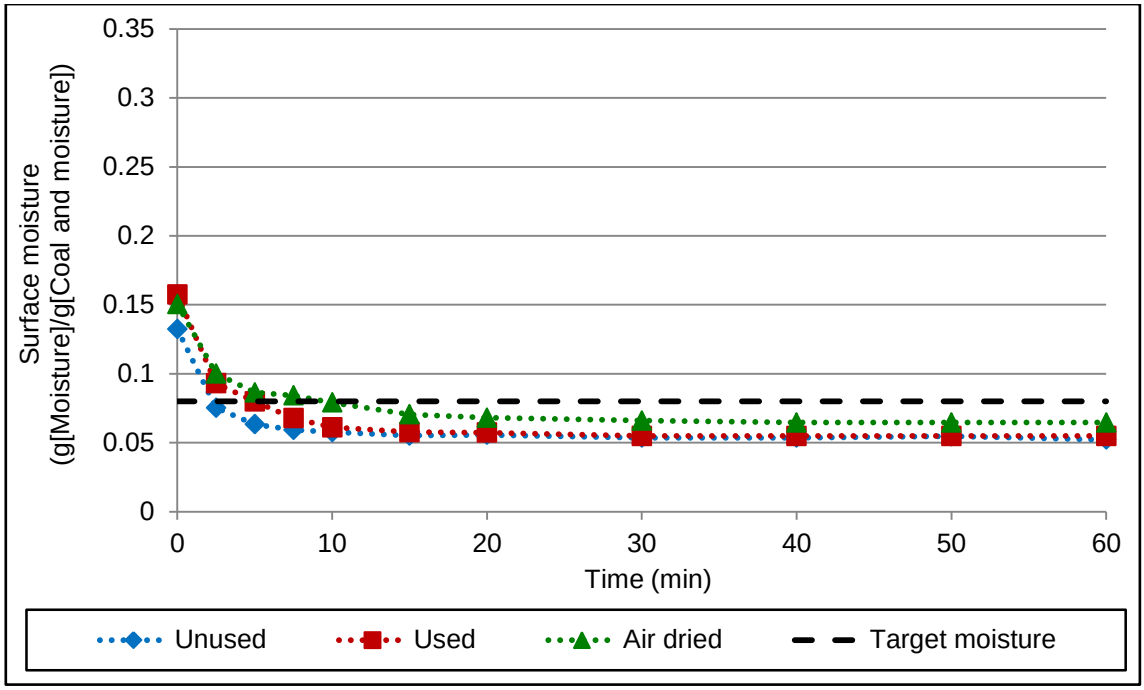

Figure D.1.6: Desorption curves of -2mm+1mm coal and 3mm alumina-based adsorbents at an adsorbent to coal mass ratio of 1:1

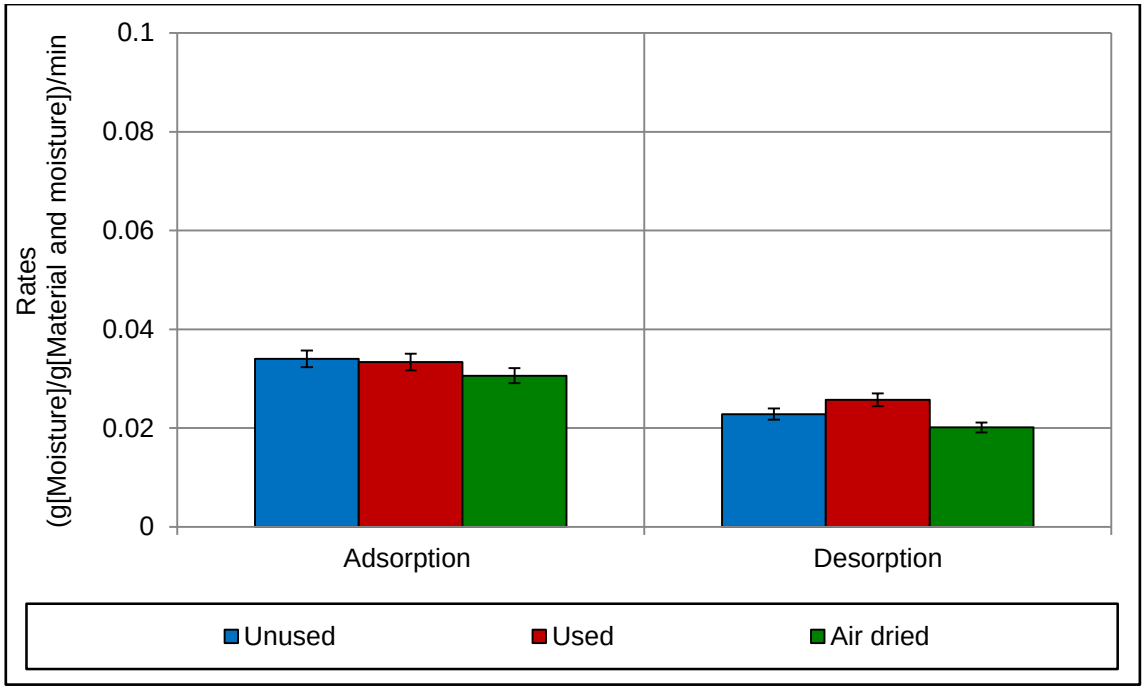

Figure D.1.7: Desorption and adsorption rates of -2mm+1mm coal and 3mm alumina-based adsorbents at an adsorbent to coal mass ratio of 1:1

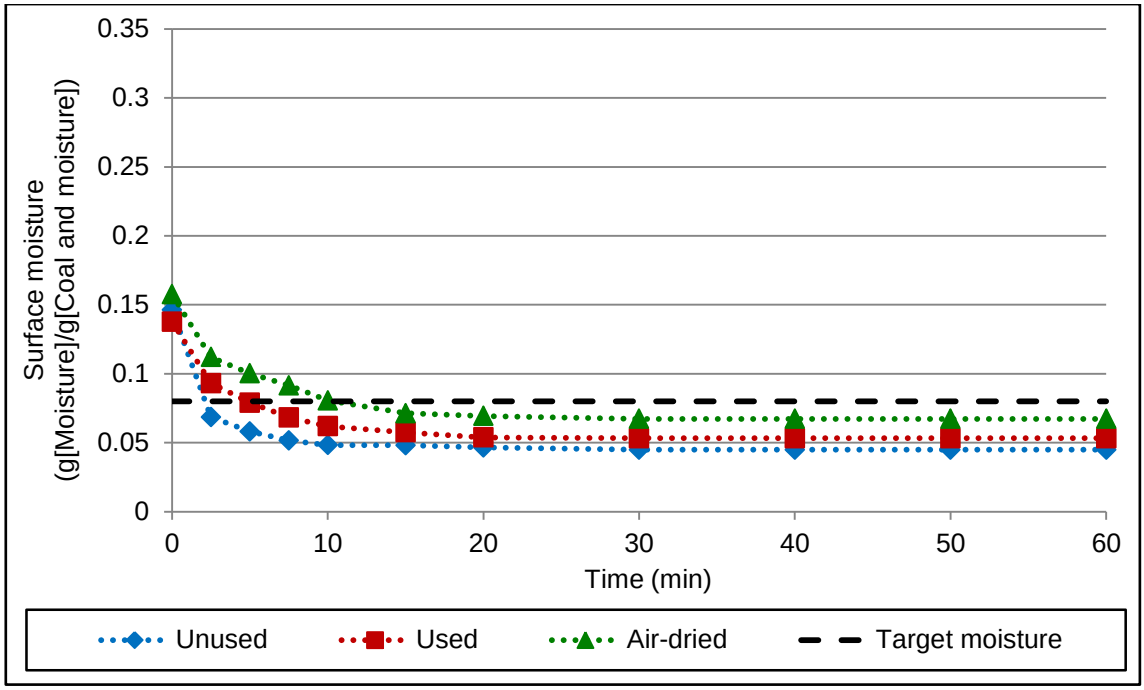

Figure D.1.8: Desorption curves of -2mm+1mm coal and 5mm silica-based adsorbents at an adsorbent to coal mass ratio of 1:1

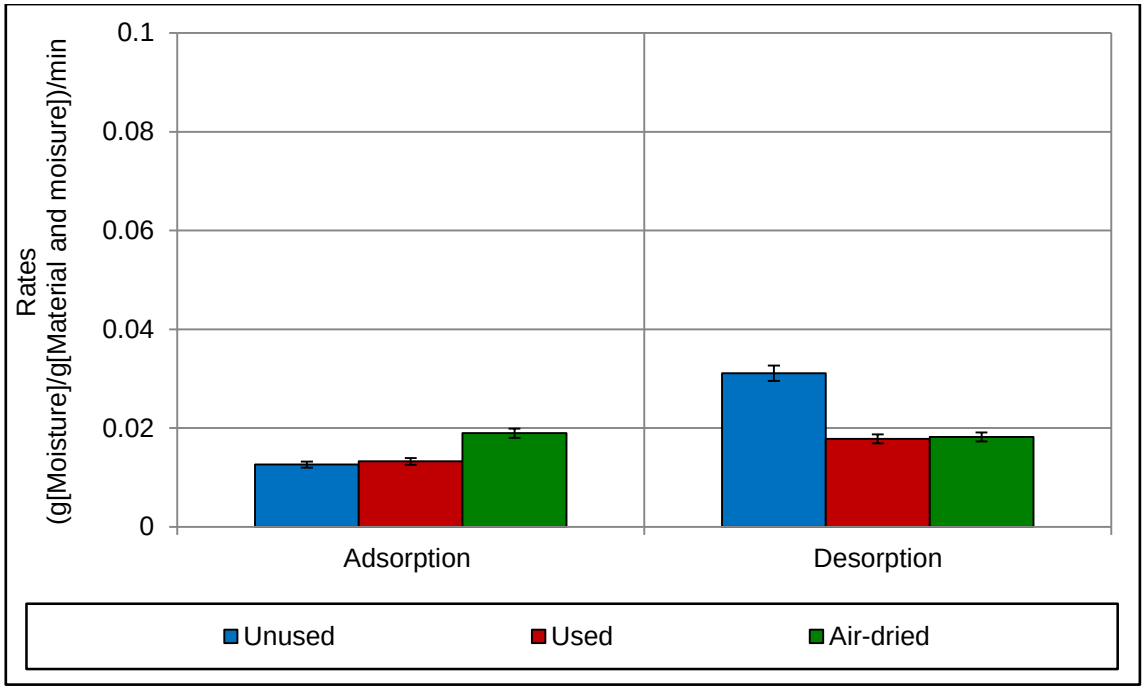

Figure D.1.9: Desorption and adsorption rates of -2mm+1mm coal and 5mm silica-based adsorbents at an adsorbent to coal mass ratio of 1:1

D.2 Energy considerations

D.2.1 Energy consumption

D.2.1.3 Cascading-bed rotary dryer

The cascading-bed experiments was completed by employing a rotary dryer. The rotary dryer induced a cascading motion, which enhances the contact area between the adsorbent and the coal particles. The rotary dryer operated at 3 rpm and required 40 Watts to operate. The contact time required in the rotary dryer, at an adsorbent to coal mass ratio of 1:1, to reduce the coal moisture load to 0.08 g(moisture)/g(coal and moisture) is summarised in Table D.2.1.

Table D.2.1: Contact time in rotary dryer (min)

Contact time in rotary dryer (min)							
Adsorbent type	**Coal size**	**-2mm+1mm**		**-1mm+0.5mm**		**-0.5mm+0.25mm**	
	Adsorbent size	**3mm**	**5mm**	**3mm**	**5mm**	**3mm**	**5mm**
Alumina-based		2.29	8.22	7.10	11.82	44.59	25.89
Silica-based		2.14	2.13	14.10	8.72	16.87	26.51

From the data in Table D.2.1, it is apparent that the contact time required decrease with increasing coal particle size. Equation 6.6 was used to calculate the energy required to operate the rotary dryer:

$$E_{Shaft\ work} = W_{Rotary\ dryer} t$$

Equation D.2.1

$W_{Rotary\ dryer}$ is the power required by the rotary dryer in J/s and t is the contact time in the rotary dryer in seconds. The energy consumed by the rotary dryer while drying the +0.5mm1mm coal in the presence of the alumina-based adsorbents are shown in Table D.2.2.

Table D.2.2: Energy consumed by rotary dryer (kJ)

Cascading-bed rotary dryer (kJ)							
Adsorbent type	**Coal size**	**-2mm+1mm**		**-1mm+0.5mm**		**-0.5mm+0.25mm**	
	Adsorbent size	**3mm**	**5mm**	**3mm**	**5mm**	**3mm**	**5mm**
Alumina-based		5.50	19.72	17.04	28.36	107.02	62.14
Silica-based		5.13	5.12	33.83	20.92	40.48	63.62

The energy consumed by the rotary dryer in Table D.2.2 increases as the adsorbent to coal mass ratio decreases. The coal needed more contact time to dry to the desired coal moisture loads at an adsorbent to coal mass ratios of 1:1, hence the elevated energy consumption. It was also marked that the 3mm alumina-based adsorbent and coal sample required less energy by the rotary dryer than the 5mm alumina-based adsorbent and coal sample. The 3mm adsorbents required less contact time within the cylindrical vessels on the rotary dryer. This is due to the larger number of individual 3mm adsorbent particles, which is dispersed better throughout the coal mass than the 5mm adsorbents.

D.2.1.4 Energy required for regeneration

After the adsorbents were reused for a given number of cycles, the adsorbents were removed from the drying process and regenerated. As mentioned previously, the technical viability of this drying process depends largely on the ability to regenerate the adsorbents successfully. One must bear in mind that the regeneration process is an energy demanding process and it is important to include this energy consumption to the total energy used. The regeneration process employs the climate chamber and blower to introduce conditioned air into the bottom of a packed-bed vessel containing the washed adsorbents.

The average room temperature and pressure range recorded for South Africa in the summer are 25°C and 30-80%RH. The enthalpies of 41.5-and 66.5kJ/kg were obtained from the psychometric chart for the minimum and maximum relative humidity values of 30-and 80%RH, respectively. The room temperature and pressure of the regeneration drying air was 25°C and 40%RH, which differs from the average room temperature and pressure conditions recorded for South Africa. The enthalpy of the air at 25°C and 40%RH was 45.50 kJ/kg. Therefore, the change in enthalpy that was required to condition the air to these conditions was determined. By using the change in enthalpy, the energy needed to

condition the drying air from the average room temperature and pressure range to 25°C and 40%RH was calculated.

In order to condition the air to 25°C and 40%RH, the change in enthalpy at saturation was calculated by using Equation D.2.2.

$$\Delta\widehat{H} = \widehat{H}_2 - \widehat{H}_1$$

Equation D.2.2

The change in enthalpy at saturation was -4.80kJ/kg dry air. This means -4.80kJ/kg dry air is required to condition the air from average room temperature and pressure to 25°C and 40%RH.

The humid volume was also determined at the hand of a psychometric chart. The volume of the humid air is defined as the volume occupied by 1kg of dry air and water vapour. The volume of the humid air ($\widehat{V}_{Humid\ air}$) was 0.86 m^3/kg dry air at 25°C and 40%RH. In order to obtain uniform air conditions throughout the drying system, the air contained in the climate chamber area was conditioned to 25°C and 40%RH. The volume of the climate chamber ($V_{Climate\ chamber}$) is 100 litres or 0.1m^3.

The mass of the dry air ($M_{Dry\ air}$) in the system was calculated as well as the energy ($E_{Condition\ air}$) required to condition the mass of dry air present. Equation D.2.3 and D.2.4 was used to calculate the mass of dry air and energy expenditure, respectively.

$$M_{Dry\ air} = \frac{1}{\widehat{V}_{Humid\ air}} \times V_{Climate\ chamber}$$

Equation D.2.3

$$E_{Condition\ air} = M_{Dry\ air} \times \Delta\widehat{H}$$

Equation D.2.4

The energy required to condition 0.116 kg of dry air to 25°C and 40%RH was -0.558kJ.

The climate chamber was able to reach the prescribed temperature and relative humidity of 25°C and 40%RH within 10 minutes. Relative humidity is a function of temperature; therefore, the climate chamber adjusts the relative humidity is according to the temperature. The climate chamber does not require lengthy conditioning to adjust the air conditions to the prescribed temperature and relative humidity conditions. The climate chamber was operated for the duration of the experimental run to ensure homogeneous air conditions were maintained.

The blower was run for approximately 10 minutes to reach the appropriate adsorbent moisture load. The blower was operated at an airflow rate of about 1.5-1.7m/s which consumed about 700 Watts. The blower was activated after the climate chamber conditioned the drying air to 25°C and 40%RH. Therefore, only the time required for drying the adsorbents were used to determine the energy usage of the blower. Equation 6.7 was used to calculate the energy (E_{Blower}) required by the blower during operation.

$$E_{Blower\ operation} = W_{Blower\ operation} t$$

Equation D.2.5

W_{Blower} is the work done by the blower in Watts and t is the time the blower was functioning in seconds. The total energy consumed during regeneration was 420kJ.

D.2.2 Total energy required

The total energy requirement was calculated for the cascading-bed drying process. The total energy consumed by the cascading-bed drying process included the energy expended by the air-water system, the climate chamber, the rotary dryer and the energy required by the blower during regeneration. Equation D.2.6 was used to determine the total energy required by the cascading-bed drying process.

$$E_{Cascading-bed} = E_{Condition\ air} + E_{Climate\ chamber} + E_{Shaft\ work} + E_{Blower\ operation}$$

Equation D.2.6

The total energy consumed by the cascading-bed drying technique for -1mm+0.5mm coal in the presence of 3mm alumina-based and 3mm silica-based adsorbents was gathered and is presented in Table D.2.3.

Table D.2.3: Total energy consumed (kJ/kg load) for -1mm+0.5mm coal and 3mm adsorbents

Total energy consumed (kJ/kg load)			
	Adsorbent type	**30%RH**	**80%RH**
Cascading-bed	**Alumina-based**	1637.75	1633.33
	Silica-based	1654.54	1650.12

The results in Table D.2.3 showed that relative humidity has a small effect on the total energy consumed when employing the cascading-bed drying technique. For instance, the alumina-based adsorbent, the total energy consumed by the 30%RH was 1637.75kJ, while

1633.33kJ was consumed at 80%RH. This indicated that relative humidity does have a significant effect on the drying process.

D.2.3 Coal drying technologies

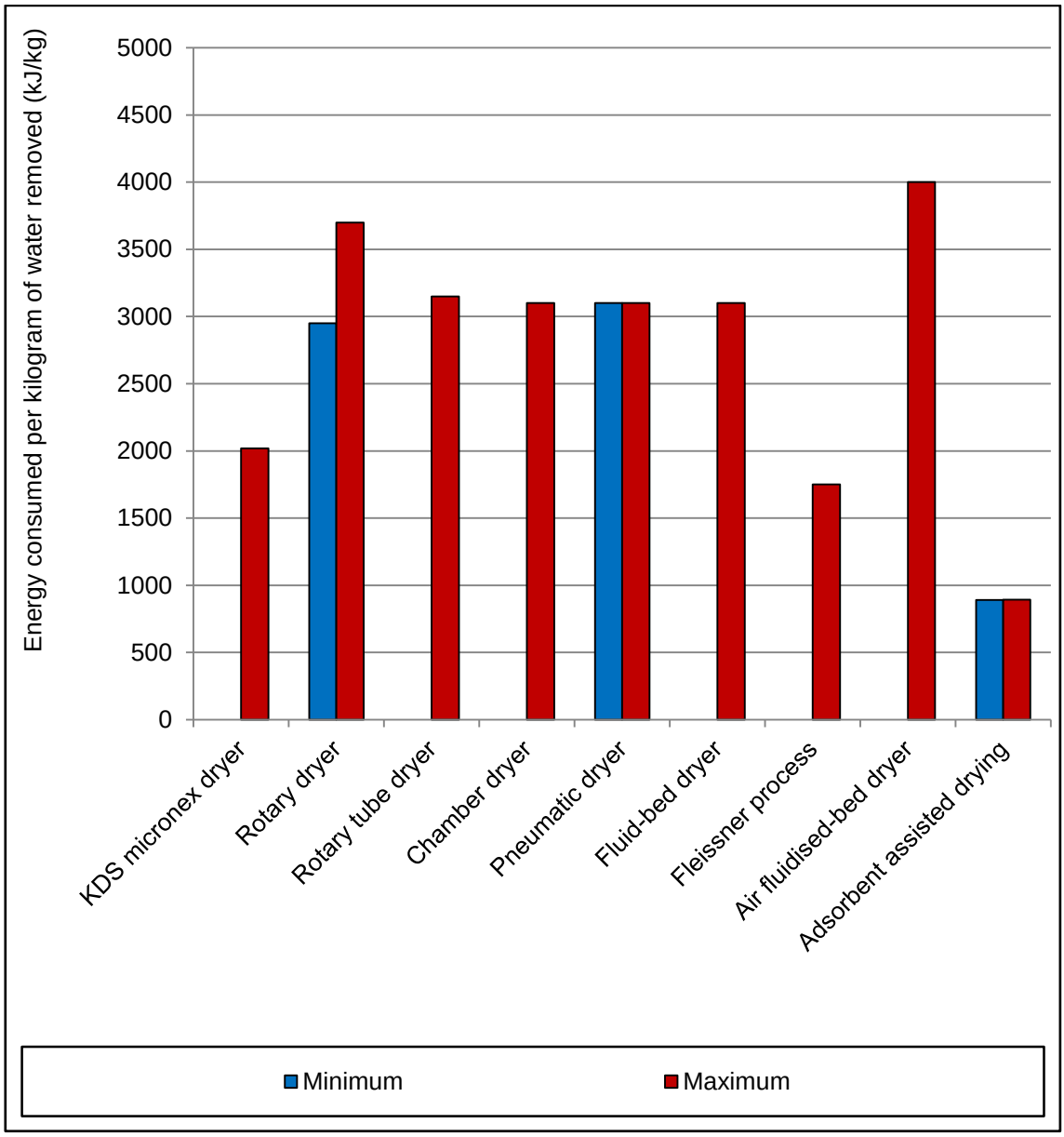

Figure D.2.1: Energy gain of -1mm+0.5mm coal and silica-based adsorbents at an adsorbent to coal mass ratio of 1:1